SAFETY IN MINES RESEARCH ADVISORY COMMITTEE

SIMRAC

Final Project Report

Title: ROCK MASS CONDITION, BEHAVIOUR AND SEISMICITY IN MINES OF THE BUSHVELD IGNEOUS COMPLEX

Author/s: A T Haile and A J Jager

Research Agency: CSIR: Division of Mining Technology

Project No: GAP 027

Date: Dececember 1995

Contents

Rock mass condition, behaviour and seismicity in mines of the Bushveld Igneous Complex

AT Haile and AJ Jager
Rock Engineering
CSIR Division of Mining Technology

Executive summary

The GAP027 project was initiated to give an overall view of the rock mass environment of the Bushveld Complex and its influence on the mine design practices. The main focus of the project was to survey the currently available data and conduct further analysis in order to obtain a picture of the current state of knowledge with regard to aspects of rock mechanics and geology relevant to the stability of mines in the Bushveld Complex.

An overall assessment of the geology of the Bushveld Complex indicates the importance that this plays in the rock mechanics considerations for design. The variability in the rock types and properties means that design practices may change significantly from one mining district to another. It is thus considered important that these geological regions be defined and an assessment of the impact on rock mechanics design be established in order to improve design procedures.

Preliminary joint mapping within platinum mines of the Bushveld Complex has indicated that the joint orientation is generally associated with the strike of the reef horizon and the major geological structures of the area. Also of interest was the observation that the presence of rogue joint orientations within footwall development may be indicative of the presence of a pothole on the reef horizon.

A survey of the current pillar design practices within the mines of the Bushveld Complex indicated that the empirically derived design procedures cater well for the majority of the rock mass environments. However there is concern that the design principles, which are primarily based on coal mining experience, may not cater well for the variability of the rock mass environment within the Bushveld Complex. Thus current pillar design may not be optimal with regard to ore extraction due to over design or more importantly with regard to safety may not be adequately designed to maintain stability. The requirement of a rational design procedure that caters for the critical rock mass parameters within the Bushveld Complex is thus highlighted.

A significant aspect of the project was to examine the seismicity associated with the current mining activities in order to assess future seismic potential. Initial analysis was carried out on data recorded by GENTEL systems that had been in operation on the mines for several years and was analysed using PSS software. This analysis indicated a significant variation in seismic potential between the mining districts that were investigated. This was considered to be primarily associated with differences in the geotechnical environment. Areas that are highly jointed or with weak partings in the immediate hanging or footwall were found to exhibit lower seismicity than the more competent rock mass environments. It is considered that in these 'soft' areas more of the deformation associated with the mining activities is accommodated by movement on these discontinuities, where as in more competent rock it is manifested as seismicity. Analysis also indicated that the design of the pillar system relative to the rock mass environment may result in changes in the seismic potential.

A Portable Seismic System (PSS) was installed around one stope to monitor the seismicity in greater detail. This data allowed the evaluation of a range of seismic parameters for the analysis of seismicity in order to determine the source mechanisms of events. A definition of the seismic source mechanisms

will allow the determination of seismic potential in new mining districts and design of mining strategies. The application of these techniques may allow the identification of different rock mass environments. At the investigation site most larger events were associated with pillar failure in the stope back areas and the majority of face events were relatively small and initiated during the blasting period. A significant number of events located on stope abutments where pillars were scheduled to be left.

Due to the variability in the rock properties of the Bushveld Complex, as indicated in the geological investigation, a data base for rock testing results was established. In future, with the growth of the database, this will allow an improved understanding of the parameters that influence the variability of the rock behaviour. The database will allow searches of specific rock type parameters to be conducted and analysed. Outputs can be obtained that indicate the average value and variability of the rock properties and also derive parameters for non-linear numerical modelling applications.

This project has indicated the important rock mass parameters that should be taken into consideration in design procedures for the Bushveld mining environment. However due to the variability in this rock mass environment it is important that these parameters be derived locally for design applications. Further important work with regard to the rock mass environment of the Bushveld Complex would be to define the different geotechnical areas and their characteristic behaviour in order to apply the correct design procedures to ensure safe and productive mining practices.

1 Introduction

This project was established in order to gain an insight into the fundamental characteristics of the rock mass environment of the Bushveld Complex to enable improved layout and support design. Areas of investigation included:

Variation in the virgin stress field.

Variation in the strength of rock types in the vicinity of the mining horizons.

The geology of the rock mass in the vicinity of the mining horizons.

A basic understanding of the seismicity of the Bushveld Complex.

Study of the current design practices for pillar supported mines.

This overview of the primary characteristics of the rock mass of the Bushveld Complex has enabled identification of the important parameters which influence the stability of underground excavations.

As a basis for research into solving practical rock engineering problems in the mines of the Bushveld Complex it is essential that an overall quantified picture of the rock mass conditions , which vary significantly across the mining areas, be produced. The investigation of these aspects provided exposure of the researchers, who have primarily worked in the gold mines, to the problems of mining in the Bushveld Complex. This information can thus be used by the research engineers in the application of this knowledge to the more detailed design projects.

The Bushveld Complex is located in the North West, Northern and Mpumalanga provinces of South Africa covering an area of approximately 66

000 sq. km. The primary mining activities of the Bushveld Complex are platinum and chrome mining. The ore bodies occur as tabular deposits, varying in depth from surface to a current maximum mining depth of approximately 2000 metres below surface. The general dip of the ore bodies is approximately 15° and the average stoping width is approximately 1 metre. The ore bodies and general rock mass environment are of igneous origin creating a layered suite in which the ore bodies are hosted. High horizontal stresses occur in segments of the Bushveld Complex. These lead to specific mining problems which require particular attention. This environment means that the general mining conditions of the Bushveld Complex are quite different from those of the gold mining industry where much of the previous research work has been based. Thus the mining rock mass environment and design procedures were considered to be sufficiently different to the previous gold mine research projects to warrant an overview of these practices in the Bushveld Complex.

2. General Geology of the Bushveld Complex

This aspect of the project addresses work conducted as part of enabling output 2.

This summary is an extract from a more detailed geological report compiled within the GAP027 project and may be referenced in appendix A

The Rustenburg Layered Suite of the Bushveld Igneous Complex is of major economic importance. The chief orebodies are the platinum bearing Merensky Reef and the UG2, and the chromitite bodies of the lower and middle chromitite groups. All of these deposits are located in the critical zone of the Rustenburg Layered Suite.

The report (Appendix A) first depicts the regional setting of the Bushveld Igneous Complex, which is also considered to regionally impact on rock mechanic issues. After briefly outlining the various components of the Bushveld Igneous Complex, also viewed in the light of their genesis, i.e. meteorite impact versus plume model, focus is placed on the mafic rocks of the Rustenburg Layered Suite. These host the chromitite and platinum deposits. An overview is also provided of the major mineral components that constitute the mafic rocks of the Rustenburg Layered Suite. Mineral properties are summarised and the potential usage of sophisticated mineralogical techniques to establish mineral assemblages and rock textures is highlighted.

The characteristics of the rocks associated with the chromitite and platinum orebodies are highly variable, which is also expressed by pronounced variations in grain sizes (from about 1 mm to over 30 mm). The application of mineralogical techniques is proposed to be of immediate rock engineering significance, implying that the microcosm may also contribute to the understanding of the macrocosm, i.e. the rockmass behaviour of the different rock types may differ while mining the various orebodies. Attention is then given to the chromitite and platinum orebodies and associated strata of the critical zone. Geological features of rock engineering significance are highlighted (Chapter 5, Appendix A). The investigation reveals that tremendous scope exists for combining the various rock engineering and geological disciplines, also expressed in the identification of potential, combined future studies, which are emphasised throughout the report and highlighted in Chapter 7 of appendix A.

The geological features of rock engineering significance are grouped into primary and secondary features. However, some overlap exists between the two groups.

Primary Geological Features: Primary geological features of significance are: rock type, reef geometry (thickness, rolling reef, potholes), dip, lithological contact relationships (identifying partings), and grade distribution.

Different rock types, characterised by distinct textures and composition, are suggested to respond differently to the mining induced stresses. The analyses reveal that the rock assemblages encountered within the various chromitite and platinum orebodies are variable. More important, footwall and hangingwall lithologies of the orebodies are regionally variable. This suggests that the compilation of geotechnical areas, defined by different footwall/hangingwall assemblages, could be attempted for the major economic horizons contained within the Rustenburg Layered Suite. The vertically and laterally changing nature of the footwall and hangingwall rock types may also be reflected in the highly variable, recorded rock stresses.

Thicknesses of the orebodies are similarly variable, with these also being controlled by the rolling and potholing. Different pothole types are defined, and the mine geology departments are contributing to the identification of the appropriate mining method, which varies according to pothole types. This reinforces the need for a combined rock engineering/geology effort. The geological setting associated with potholes is complex, where varying inclination of the strata is encountered. Pegmatoids, pegmatites and structural features are also responsible for a change in the stress field.

Lithological contact relationships are variable and range from sharp to transitional. Sharp contact relationships are associated with all the orebodies and their contact characteristics (i.e. mineralogical characteristics, thickness etc.) and distance to the orebody may be delineated in the future.

Grade is variably distributed within the orebodies under consideration, vertically and laterally. The prediction of grade into the unmined area therefore

facilitates the selective mining of economically most viable orebodies. This may result in the implementation of specific mining methods.

Secondary Geological Features: These are: Faults, dykes and sills, joints, hydrothermal veinlets, alteration (metamorphism), and the various secondary geological features (all of the aforementioned, but also magma bodies that intruded the Rustenburg Layered Suite) that impact on the regional stress field.

Faults are commonly associated with the chromitite and platinum orebodies, however not on the scale encountered in the Witwatersrand Basin. The stress field has been shown to be changed in the vicinity of certain faults. Both, compressional and extensional faults are present. This is expressed in faults at an angle to the orebodies and faults that are parallel to the reef plane. Future scope exists for the identification and delineation of distinct fault phases that occurred at discrete times. This will facilitate the grouping of faults into populations that are likely to be characterised by different orientations to the excavation, and distinct fault plane characteristics, exhibiting distinct excess shear stresses and hence propensity for generating seismic events. The same holds true for the dykes and sills. However, dyke and sill compositions, and their related host rock contact relationships, may be considered as an additional item of rock engineering significance. Different compositions are reflected in different competencies which are probably expressed in varying tendencies to burst.

The rock engineering importance of joints and hydrothermal veinlets is stressed. Joints have been shown to impact on hangingwall conditions, and the identification and delineation of various joint populations, and their associated features, may facilitate the prediction of these hazards ahead of the mining area. The rock engineering significance of hydrothermal veinlets has not been considered yet. However, it is proposed that these are of major importance, and their attitude, frequency and secondary mineral assemblage may vary from rock type to rock type.

Alteration, or metamorphism, will influence the rock engineering properties of the rock. It may be encountered on a local scale, in the vicinity of geological structures, but also regionally (e.g. close to most post-Bushveld intrusions). Degrees of alteration are variable throughout the Rustenburg Layered Suite and may also be delineated employing sophisticated microscopic techniques. Hydrothermal veinlets may, in addition, be more prominent in regions that are strongly altered.

Intrusion of the granites belonging to the Lebowa Granite Suite, and the intrusion of the Pilansberg Alkaline Complex are suggested to have impacted on the regional stress field. However, no studies trying to establish a relationship between these features and the pertaining stresses have been undertaken to date.

In summary it is concluded that both, primary and secondary geological characteristics should be considered in any rock engineering investigation.

3. Joint Mapping in Bushveld Complex Platinum Mines

A preliminary investigation of the jointing associated with the platinum mines of the Bushveld Complex was conducted over a two month period. This area of the project addresses work conducted under enabling output 2. A report containing a summary of the joint data is attached under appendix B.

Joint mapping sites were selected at various mines to be representative of the variation in joint intensity experienced by the mining operations. Surveys were conducted within off reef haulages and crosscuts and on reef dip and strike excavations to obtain a three dimensional picture of the jointing. Discontinuities were mapped with regard to their dip, orientation, persistence, roughness, infilling, rock type boundaries, and structure.

In general it was concluded that the primary joint orientation was sub parallel to the major geological features within the area and often a joint set would be orientated sub parallel to the strike of the reef horizon and dip steeply primarily in a down dip direction. A regular joint frequency was rarely observed and joint sets tended to occur in swarms, that is with joint intensity varying from less than 1 joint per metre to over 50 joints per metre within the same set. Often joints would be associated with infilling from either serpentinization, calcite or other clay type minerals further reducing the stability of the joints.

At some of the joint mapping sites, within the footwall development, unusual or rogue joint orientations could be correlated with the presence of potholes on the reef plane. If this observation is of more general application then this may serve as a method of predicting the presence of potholes on the reef horizon prior to mining operations. A knowledge of the location of a potential pothole would allow suitable planning to either avoid or take suitable support measures to minimise the hazard of these features to mining operations, or hangingwall instability. Further work in this area is however required to validate these initial observations.

4. Survey of Current Design of Pillar Systems in Tabular Hard Rock Mines.

This aspect of the project addresses work conducted as part of enabling out 2.

A report was compiled on this aspect of the project by Ozbay, Ryder and Jager (1994), a summary of which is given here. More detailed references can be made to the published SIMRAC interim report.

The application of pillar support systems in shallow mining environments can be ascribed to the requirement to support large zones of potentially unstable hangingwall rock due to the presence of vertical tensile stresses in the stope

hangingwall. The conventional support systems are not able to generate the required support resistance's necessary to ensure stability under these conditions.

The survey highlighted the considerable experience accumulated in pillar design over the years. The design of hard rock pillars has primarily been derived from procedures developed in coal mining operations and have generally been successfully applied to the hard rock mining environments. However pillar failures and stope collapses still occur with the resultant potential for casualties and production losses. The empirically derived design procedures adequately accommodate the general mining conditions however in an extremely variable rock mass environment such as the Bushveld Complex the design procedures fail to accommodate the detailed characteristics of the rock mass environment.

The behaviour of the rock mass around a stope is primarily a function of the mining depth in relation to the stope span and the relationship between the vertical and horizontal stress field (K ratio). The tensile zone above a stope excavation increases with increasing span / depth ratio and decreases with increasing k ratio, figure 1. The prominent features on which falls of ground occur within the platinum mines of the Bushveld complex have been identified as a weak pyroxenite layer approximately 2 - 4 metres in the hangingwall of the Merensky reef and the 'Bastard Merensky" reef parting approximately 15 metres above the Merensky reef. Even with the high k ratios experienced in the Bushveld Complex the predominance of failure and movement on these planes of weakness are indicative that they are primarily controlled by the dead weight tension in the immediate stope hangingwall.

At shallow depths the tensile zone in the hangingwall of the stope excavation may extend to surface. Under these conditions it may be critical to prevent or limit surface subsidence due to mining and thus the pillars must be designed to carry the full overburden load without yielding. Design procedures

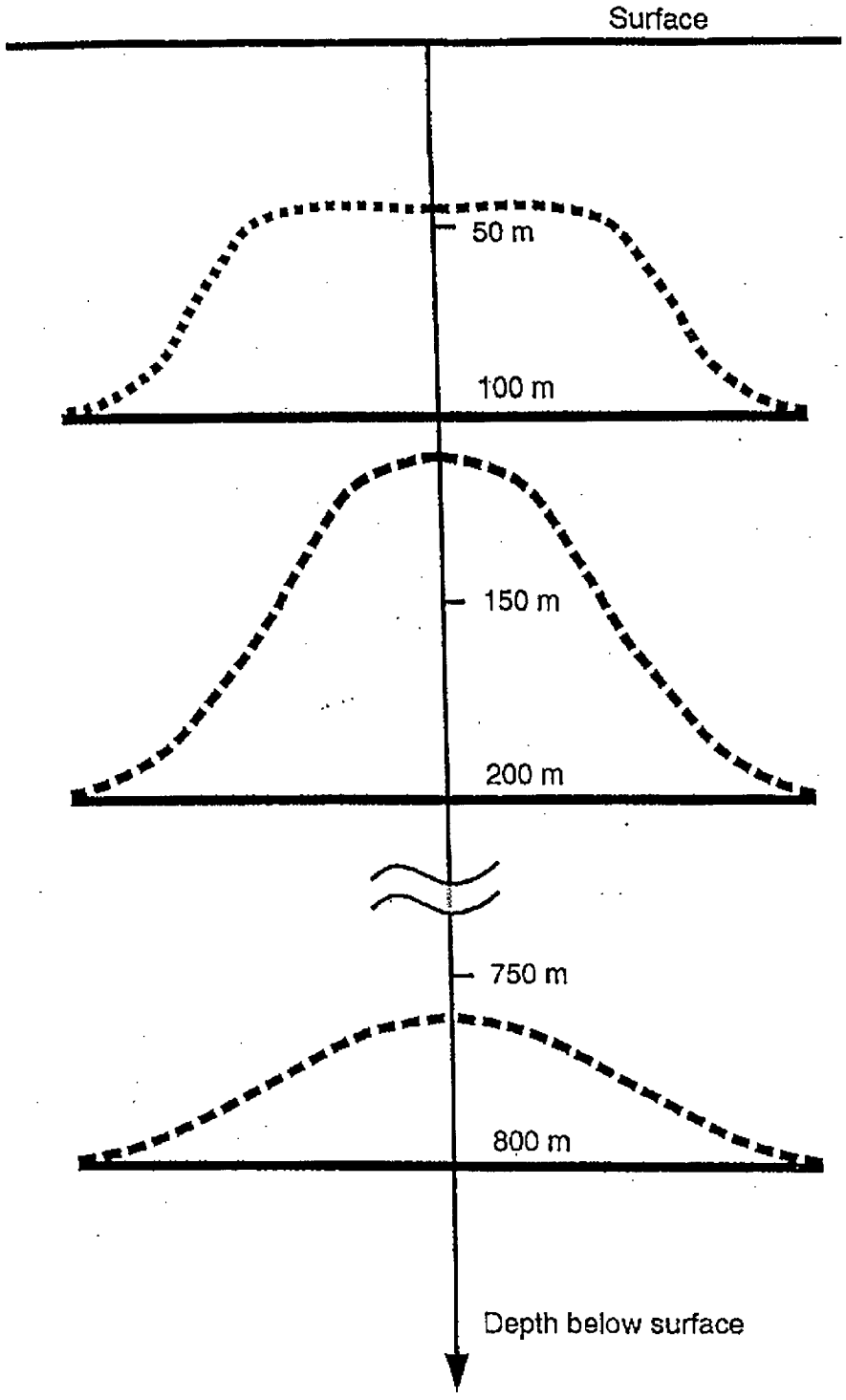

Figure 1. Tensile zone above 200m span stopes. Virgin horizontal stress field includes a fixed component of 10 - 30 MPa.

developed under coal mining operations are generally applicable for these conditions and the pillar characteristic is defined by the elastic properties of the rock. However as the depth of mining increases the size of the pillars may become prohibitively large with regard to practical mining and economic extraction and the necessity to support to surface no longer of consideration. The consideration for pillar design is then to control hangingwall stability up to the highest potential plane of failure. This may only necessitate support resistance as low as 1 MPa, which can be obtained from the residual strength of the pillar material. Thus the use of crush pillars are economically more viable to be incorporated into the stope support system design. In order to avoid the potential for violent failure of the pillar in the stoping excavation the pillar material should be in the post failure state when it is cut from the mining face. In the transitional area between non yield pillar and crush pillar design strategy the use of pillars which are initially solid but subsequently 'fail' as mining progresses may be necessary. The behaviour of these pillars should be such that their post failure characteristic is stable and the pillar yields in a controlled manner. It is generally very difficult to obtain this design characteristic for the hard rock pillars as it is both a function of the consistency of the pillar rock mass characteristic and the stiffness of the loading system. To ensure the viability of a mine it is often necessary to divide the mine into separate operational units by the use of indestructible pillars called barrier pillars. These pillars may be designed for several reasons including the provision of regional stability in case of a potential stope pillar failure and pillar run, or for ventilation, fire or water control. Traditional characteristic pillar load deformation curves are indicated in figure 2. However research under project GAP024 has indicated that significant variations in pillar behaviour, at variance with the pillar behaviour depicted by the curves, does occur. For example 5:1 pillars are known to fail and on occasions burst rather than deform in a ductile manner.

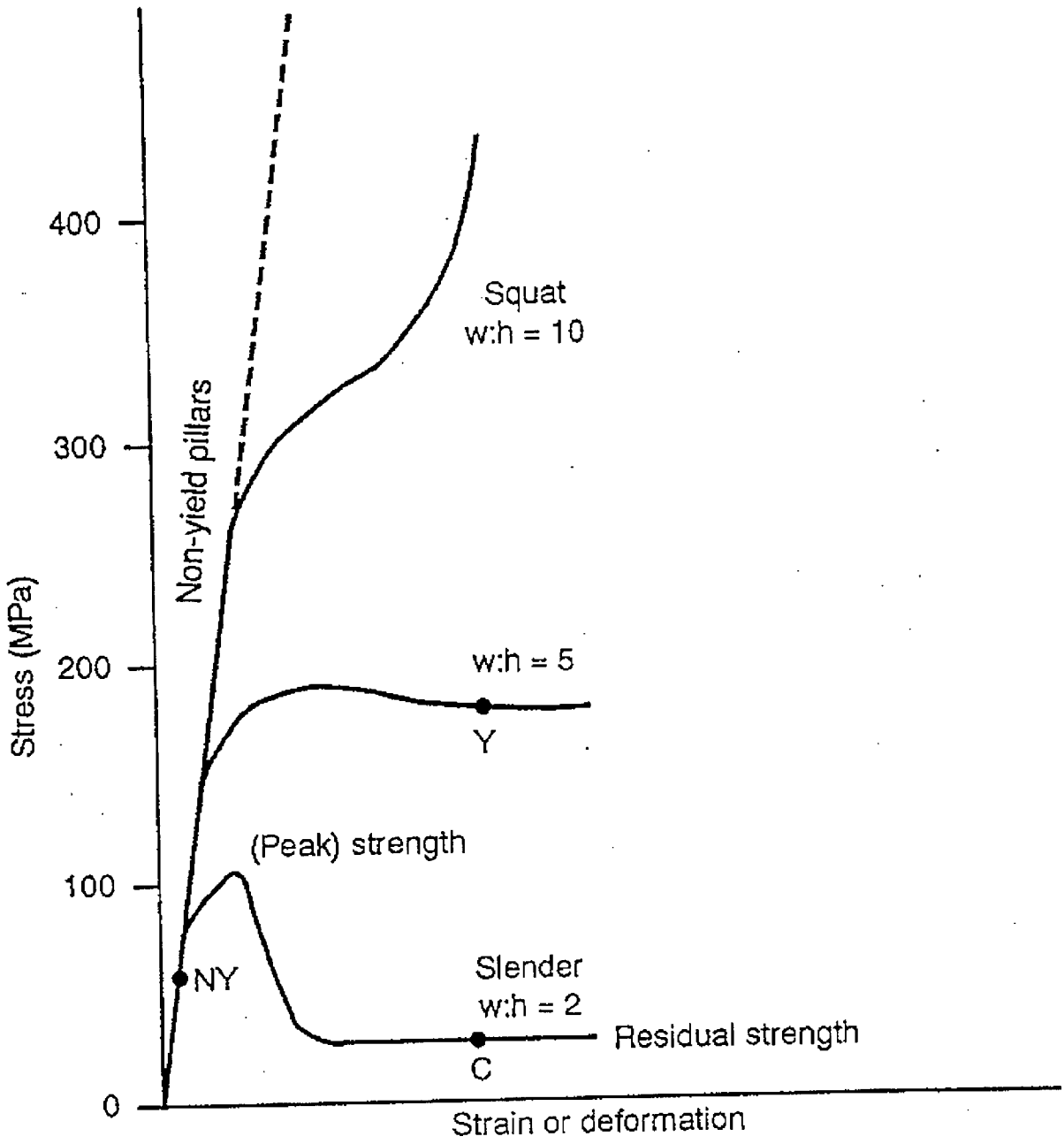

Figure 2. Typical stress strain behaviour of hard rock pillars of different width / height ratios

The design of pillars is primarily classified on the basis of width to height ratio (w/h). The approximate relationship to the defined pillar categories are as follows:

Non-yield pillars	w/h > 5
Crush pillars	w/h typically 1.7 to 2.5
Yield pillars	w/h 3 to 5 with a safety factor of approximately 1
Barrier pillars	w/h > 10

The characteristics of the pillar may be defined by 4 regions of behaviour as indicated in figure 3. The elastic modulus of the pillar is the main pre-peak characteristic. The stiffness of the pillar material in relation to the surrounding host rock mass will govern the loading of the pillar in relation to the adjacent mining abutments or barrier pillars. If the pillar material is soft in relation to the surrounding rock mass then the load will be shed to neighbouring abutments, however if the pillar material is equal to the stiffness of the host rock mass and close to surface then loading will be uniform and tributary area may be applied. Determination of the effective pillar modulus may be estimated from laboratory testing of the intact pillar material. Pillars are generally under a relatively high confinement stress environment and thus the influence of discontinuities within the pillar on the material modulus is considered to be minimal.

The influence of the volume of material being considered for design purposes is known as the size effect. The criteria for selection of a suitable material strength for pillar design is highly variable. Examples of material strength selection vary from the uniaxial compressive strength (UCS) of the material to $^{2}/_{3}$ reduction in strength have been noted. Laboratory experimentation has indicated a significant reduction in material strength with change in sample size from approximately 25mm to 300mm with a general trend towards consistent strength at a sample size of $1m^3$. This highly variable parameter

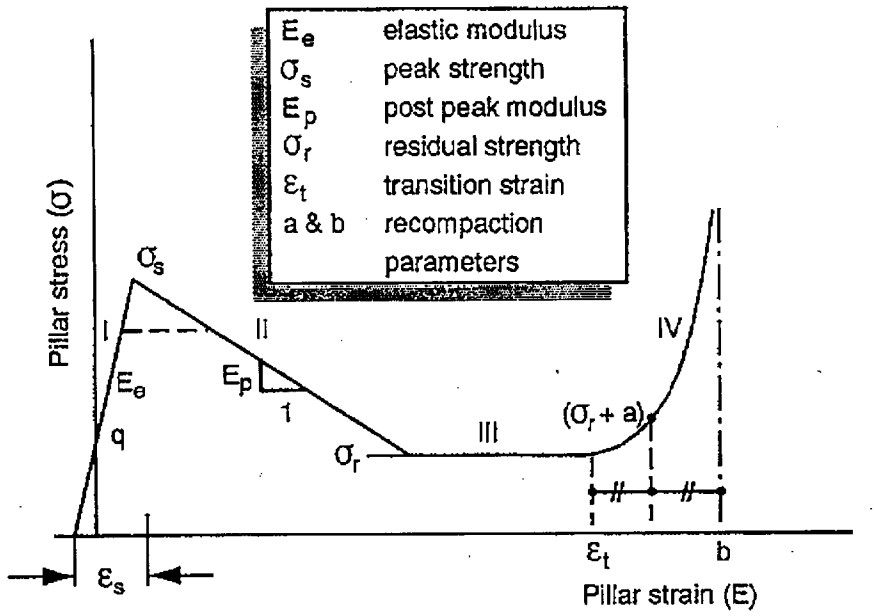

Figure 3. Idealised complete stress - strain behaviour of a slender pillar.

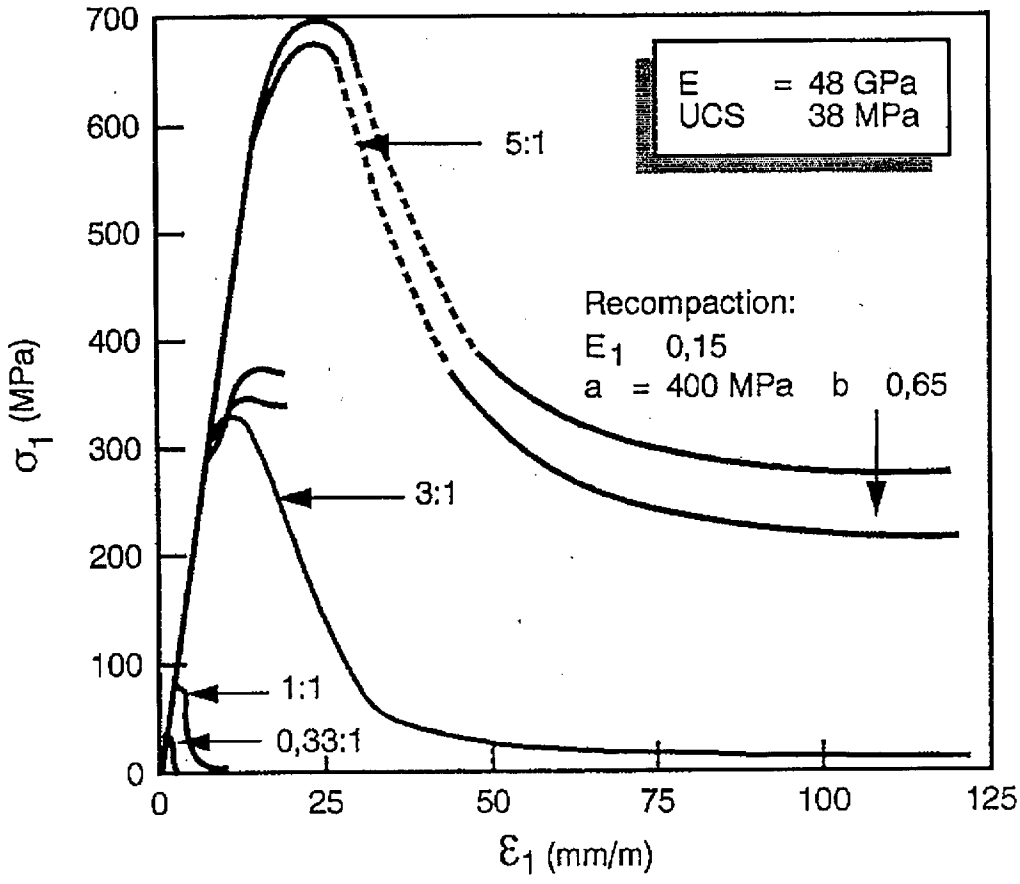

Figure 4. The strengthening effect of increasing width to height ratio on chromite tested in laboratory

selection indicates that careful consideration is required for each mining or rock mass environment.

The influence of the width to height ratio of the pillar is considered to be primarily a function of Poisson's effect, indentation effect and foundation confinement. These parameters contribute to the increased confinement of the core of the pillar with an associated triaxial increase in the rock mass strength of the pillar material. Of these factors the influence of Poisson's effect is considered to be the most significant. The strengthening effect is due to the friction and cohesion condition of the footwall and hangingwall pillar contacts limiting the dilation of the pillar due to loading as a function of Poisson's ratio. Indentation and foundation confinement similarly limit pillar dilation under loading. The behaviour of the pillar material under confinement will thus influence the ultimate strength of the pillar. The behaviour of rock under confinement is primarily a function of the angle of internal friction of the rock type and in general this is much higher for hard rock then soft rock such as coal for which most of the pillar design formulae are based. Also of importance but of limited understanding is the contact condition between the pillar and the host strata. Within the Bushveld Complex the lack of knowledge of the behaviour of the chrome and platinum seams under high confinement and the condition of the contact with the country rock limit the fully rational design of pillars.

The above discussions have generally been based on the consideration of square pillars, however the shape of the pillar will also influence its strength. The use of rectangular pillars will generally enhance the strength of the pillar compared to a square pillar due to the increased confinement provided by the increased pillar dimension. The factor of strength increase is considered to vary from 1.0 for a square pillar to 1.3 for an infinitely long pillar. However the influence of pillar shape is still governed by the pillar width to height ratio and pillar material and contact frictional conditions.

The stability of the foundations of pillars may influence the behaviour of the pillar system. The behaviour of the pillar foundation may result in the premature failure of the pillar due to plastic foundation deformation resulting in induced tensile loads within the pillar, stable pillar punching with the resultant yield of the pillar system, or unstable foundation failure of brittle foundations with associated seismic activity. Within the Bushveld Complex the occurrence of the first two mechanisms have been clearly recorded and in some instances the third mechanism has been inferred. Limited work has been conducted on the stability of pillar foundations but some laboratory testing and numerical modelling indicate a limiting stress level of approximately 2,5 x the average pillar stress to prevent violent foundation failure. Important factors in the analysis of pillar foundation behaviour are considered to be the pillar area, foundation moduli and contact friction condition.

Other areas of potential importance with regard to factors that influence the peak strength of the pillar are the creep behaviour of the rock type and the presence of discontinuities and inhomogeneity of the pillar material.

If the peak strength of the pillar is exceeded then the post failure modulus is crucial for governing the stability of the pillar system. It has been shown for laboratory test samples that the post failure modulus of a pillar may be strongly controlled by its width to height ratio. This has been shown to vary from approximately the pre failure modulus for narrow pillars to strength hardening at w/h ratio of approximately 5:1, figure 2. However this does not hold true for all rock types and some chromite rock types have indicated brittle failure under high confinement environments, figure 4. These properties may indicate the potential for pillar bursting with increased stope deformation.

With depth and in relatively high closure environments where crush pillars are to be implemented then the residual strength of the pillar is its important characteristic. Little is generally known of the residual strength of a pillar but estimates have been made that for a w/h of 2:1 it is of the order of 5 to 10%

of the peak strength. However this will be greatly influenced by factors such as the geometry of the pillar (w/h), friction angle of the pillar material or confinement applied to the pillar. At very large stope closures re-compaction of the pillar material at a strain of approximately 40% may be evident. This work again has primarily been based on laboratory experimentation and some underground observations and has not been fully quantified.

The spacing of the in-stope pillars will influence the load exerted on an individual pillar. The spacing of the pillars will also determine the panel span between regular pillars and thus influence the bord stability. In practice hangingwall stability at shallow to moderate depth becomes increasingly difficult at pillar spacing in excess of 35 metres but this is generally considered to be a function of joint density. In most cases bord failure extends up to approximately 2 - 3 metres into the hangingwall of the panel. The design of panel spans have generally been based on experience but attempts have been made to analyse their stability with regard to beam analysis or numerical modelling.

The design of non yield or rigid pillars are based on maintaining the operational life of the pillar in an un-failed state by ensuring that the pillar strength σ_s exceeds the average pillar stress (APS) by a suitable factor of safety. Pillar design is currently based on a modified form of Salamon and Munro's formula of the form

$$\sigma_s = K\, h^{\alpha}\, w^{\beta}$$

Where h and w are the height and width of the pillar and K is the unit strength of the pillar rock mass based on a $1m^3$ sample size. In hard rock mining the value of K in design practice has been found to vary from the UCS of the rock to $^1/_3$ of the UCS, also estimates have been based on the application of the Hoek and Brown rock mass strength criterion:

$$\sigma_1 = \sigma_3 + (m\sigma_c\sigma_3 + \sigma_c^2 s)^{1/2}$$

Where σ_1 would represent the unconfined rock mass strength (K) when $s = 0.1$ and $\sigma_3 = 0$ for good quality rock would realise a value of $0.32\sigma_c$.

For hard rock pillar design the exponents of α and β are generally taken as - 0.75 and 0.5 respectively based on the work of Hedley and Grant from back analysis of pillar workings at the Quirke Mine, Elliot Lake, Canada. This environment however was only representative of a limited range of w/h ratio's (0.7 to 1.5) and in a stratified conglomerate ore body. No work of this nature has been undertaken on South African hard rock mines.

The loading of the pillars is generally based on the assumption of tributary area theory (TAT) which accounts for full cover load applied to the pillars (APS).

$$APS = q / (1-e)$$

Where q is the vertical stress component and e is the areal extraction ratio. This calculation of the pillar loading assumes that the lateral extent of mining is extensive in relation to its depth so that the load is evenly distributed across the pillars. The proximity of mining abutments or large barrier pillars will tend to reduce the loading of adjacent in stope pillars. This however will tend to make the design considerations conservative and thus err on the side of safety. Computer programs may be used to estimate the stress acting on a pillar, but for a regular grid of pillars this will generally be more onerous than the application of TAT. In general a factor of safety (FS) will be applied to the design criterion to ensure stability of the system within the variability of the rock mass strength and loading conditions. The standard value of FS 1.6 as applied in coal pillar design is generally used for hard rock pillar design and any local adjustment is recommended not to be less than 1.3 on an individual basis. Factors of safety should not be applied in the design of crush pillars.

Pillar design may be based on back analysis to determine the in-situ strength of the rock mass (Kersten) based on the failure state of the pillar under TAT assumptions. This methodology is relatively simple and easy to use but it may be difficult and relatively subjective to decide on the failure state of the pillar without detailed internal pillar observations.

As the depth of mining increases the use of non yield pillars becomes less favourable due to limitations in extraction ratios. Under these conditions yield pillars may be implemented. When they are cut from the mining face they are intact but as mining progresses the pillar load exceeds the pillar strength, if the post failure stiffness characteristic of the pillar is less than the stiffness of the host rock then the pillars will yield in a stable manner. If the post peak pillar modulus is positive then stable pillar behaviour is assured. Pillar system yielding may be achieved with relatively intact pillars by yielding of softer layers in the pillar foundations.

The design of crush pillars is generally based on experience and trial and error to ensure that the pillar material has failed and reached its residual strength when the pillar is cut from the mining face.

The results of the mines survey indicated that in general pillar systems used in the South African mines perform satisfactorily on the basis of empirical design. However it was highlighted that mines in similar mining environments developed quite different design guidelines. This may be an indication of either inefficient extraction in some areas or a possibility of deficient pillar design with potential safety risk. This also indicates a potential risk in pillar and strata control design with a change in mining environment such as new mining lease areas or an increase in mining depth.

5. Summary of re-analysed virgin stress measurements

This aspect of the project address work as part of enabling output 1.

A report was compiled on this aspect of the project by Ryder (1994), a summary of the main conclusions of which is given here. More detailed references can be made to the published SIMRAC interim report.

Relatively few stress measurements have been conducted within the Bushveld Complex on which a detailed re-analysis could be conducted. The available test data was evaluated for its self consistency in order to sift out spurious data which may greatly influence such a small data base. This exercise involved the review of the stress measurement results and rock test data. It was noted that many of the Bushveld rock types indicated a non linear characteristic within the defined elastic region of their behavioural characteristic. This thus made the assignment of an elastic modulus difficult and interpretation of the strain relief results suspect. Particular concern was with regard to the indicated vertical stress being less than the overburden load for the shallower results.

Analysis of the accepted results still indicated the phenomenon of lower vertical stress than the overburden load to a depth of approximately 800 metres below surface, after which the vertical stress was in accordance with the overburden load of about 0.0275 x H, figure 5. With regard to the horizontal stress regime there is a general trend for the k-ratio to decline from values of approximately 2 at depths down to 500 metres towards a k-ratio of 1 at about 1000 metres. But still there are anomalous areas where high horizontal stresses are experienced at depth, figure 6.

In conclusion it was considered that there is a discernible trend in the stress regime of the Bushveld Complex, but within this areas can experience great

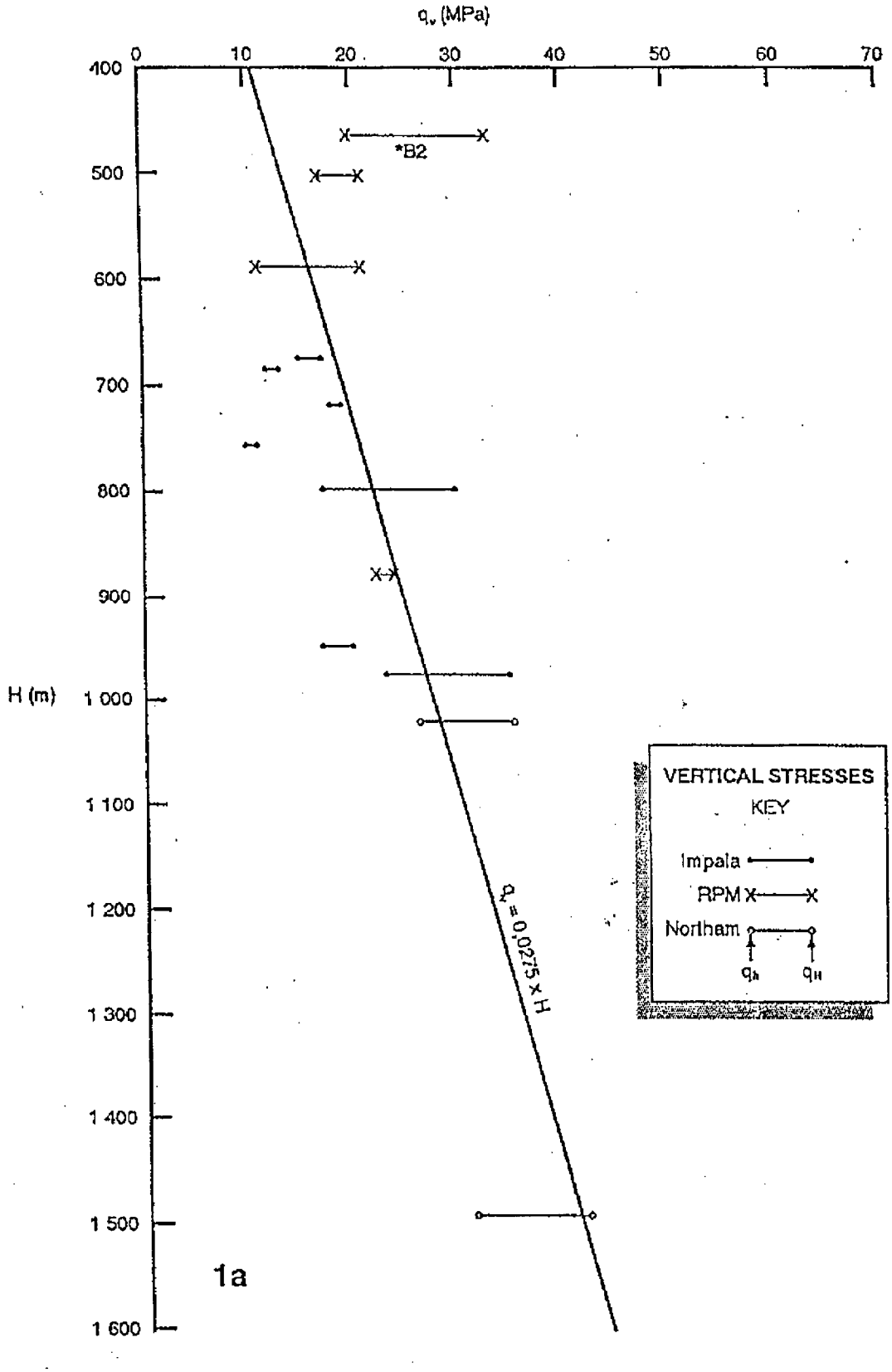

Figure 5. Measured virgin stresses in Bushveld Complex vertical component

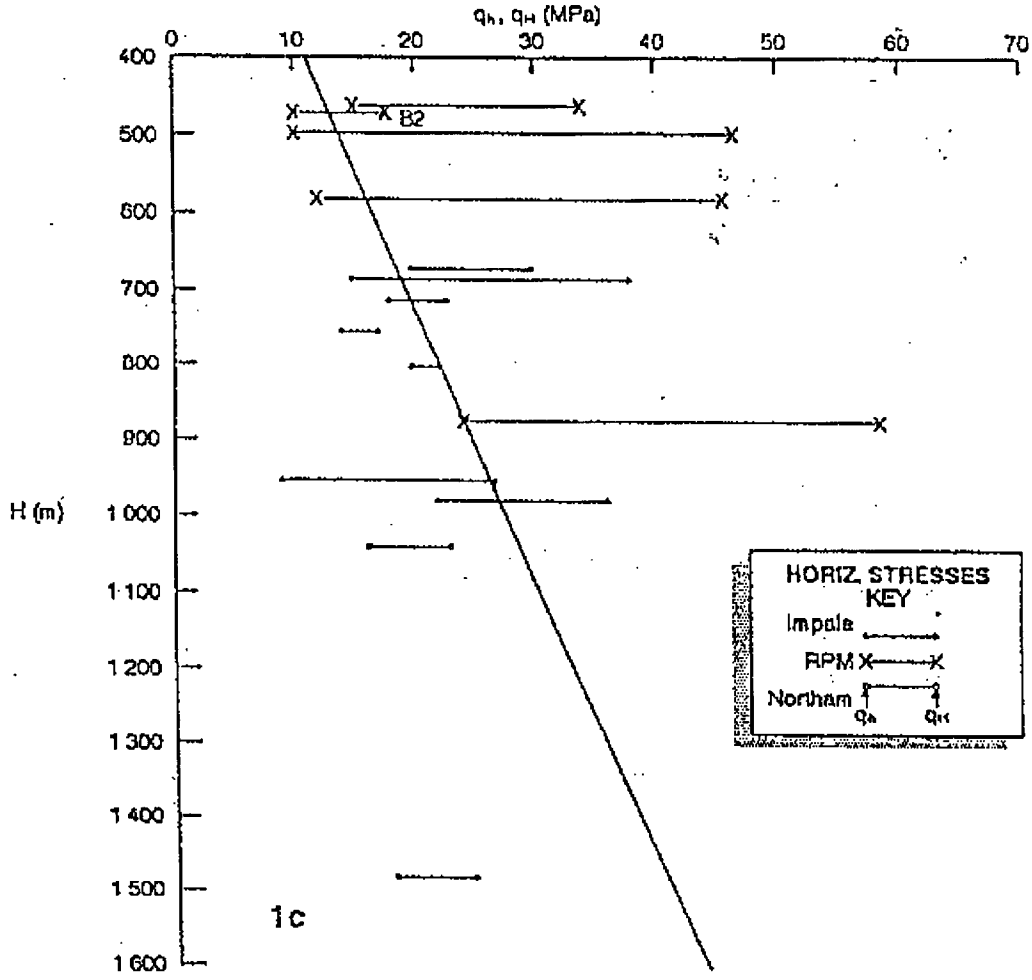

Figure 6. Major and minor horizontal stresses as measured

variability. Although analysis of the results is difficult due to the non linear elastic modulus of the Bushveld rock types and their relatively large grain size in relation to the measurement techniques, the variability of the stress environment is considered to be valid based on underground observations.

In order to improve the knowledge of the Bushveld stress environment it is recommended that a much larger data base of stress measurements or even estimates of k-ratios be established for analysis. This may require investigation of more applicable and mine worthy stress measurement techniques for the Bushveld Complex.

A further mine survey of the variability of the stress environment within the mines of the Bushveld Complex indicated some association with the proximity of major geological structures. The presence of potholes and replacement pegmatoid structures can be associated with abnormally high vertical and horizontal stresses respectively. The presence of very high horizontal stresses have been associated with low angle thrust faulting. These stresses are confined to approximately 50 metres either side of the feature and result in intense failure of the excavation hangingwall.

6. An assessment of seismicity at Wilderbeestfontein North Mine and Frank Shaft

This part of the project addresses work conducted under enabling output 3

A report was compiled on this aspect of the project by Aref, Jager and Spottiswoode (1994), a summary of which is given here. More detailed references can be made to the published SIMRAC interim report.

Due to the increasing strike extent of the current mining operations and the increase in mining depth the incidence of seismicity on the Bushveld mines is

increasing. Although relatively few rockburst incidents have occurred it is envisaged that this will become more significant as mining progresses and thus the ability to categorise the seismic potential and rockburst hazard will become more critical.

The initial work on investigating seismicity within the Bushveld Complex was based on the analysis of seismic data as recorded by GENTEL sites at Wildebeestfontein North mine of Impala Platinum Mines and at Frank shaft of Rustenburg Platinum Mines. These sites were selected to evaluate the differences in seismic potential based on the different mining environments at the two sites. The principle difference in the mining environments was initially considered to be the pillar design criteria. Wildebeestfontein utilises a 'yield' pillar system where as Frank shaft uses crush pillars.

The GENTEL data is based on a single triaxial geophone located in a 50 metre borehole from surface. The sensitivity of the system allowed only for analysis of events with magnitudes greater than 0 because of interference from background noise. In general the system was designed and used for obtaining event magnitude and location and further analysis of the GENTEL data is limited. The data was thus transferred and analysed with PSS software. The seismograms indicated a lot of interference from reflected surface seismic waveforms, especially from seismic events outside of an incidence angle of 40° from the vertical. Therefore reliable data analysis was limited to events within a cone of incidence with an apex angle of 80° from the geophone location. Analysis was conducted on data over the period January 1992 to December 1992.

Analysis of the general seismicity of the two shaft areas indicated fairly marked differences in their seismic characteristics. General analysis of the validity of the seismic data for the 1992 period for the two shaft areas however was also markedly different with 70% of events at Wildebeestfontein falling within the 40° incidence angle but only 5% for Frank shaft. This is also

a function of the relative distance of the geophone location from the reef plane being much closer at Frank shaft and that mining was taking place at a greater distance from the geophone site. However some conclusions of the general seismicity in these areas could be made. Both areas indicated non uniform distribution of seismicity with mining activity, some areas showed close correlation between seismicity and the mining rate while other areas of the shafts indicated aseismic mining activity. It is provisionally considered that this phenomenon may be due to differences in the geotechnical environment influencing the areas seismic potential. However overall comparison of the differences in the seismicity of the active areas of the two shafts indicated that the Wildebeestfontein area has a higher potential for large seismic events (b value) and also a larger rate of seismic energy release with mining as indicated in table 1.

Table 1. Comparison of seismic characteristics of WN and FS

Mine	Total Energy (J)	Area Mined (m^2)	Energy (kJ/m^2)
WN	23 E+8	3,5 E+5	6,6
FS	8 E+8	6 E+5	1,3

The seismic data of the two mines was also analysed by means of the volume change method. This methodology enables categorisation of the rock mass on the basis of the potential for seismicity (γ_c = 0 to 1) as a function of the volume change in the rock mass due to mining. At Wildebeestfontein North the seismically active mining blocks were analysed on an individual basis and the seismic potential, as expressed by γ_c, varied from 0,2 to 1 with a mine average of 0,4. This indicates that 40% of the mining induced deformation may be associated with seismicity and was considered to be unexpectedly high for the Bushveld Complex. Analysis of the Frank Shaft data was conducted for the whole mining area due to the wide distribution of seismic data and a significant proportion of the data falling outside of the geophone

incidence angle. This analysis indicated the seismic potential expressed as γ_c to be 0.04 for the whole of the mine area indicating that only 4% of the mining induced deformation may potentially be due to seismicity.

Comparison of the two mining areas on the basis of the volume change method would verify the overall analysis of seismicity in indicating that the Widebeestfontein mine has a far higher potential for seismicity as a function of mining than Frank shaft. However this may be a function of the selection of parameters for the calculation of the seismic parameters especially the overall stope closure which were estimated as 50mm and 250mm for WN and FS respectively, based on mine estimates of the performance of the pillar systems. Comparison of the seismic potential of the shafts to that of the Klerksdorp gold field indicate that WN has a comparable seismic potential. It was thus considered that the continued use of the yield pillar system at depth as opposed to the crush pillars as used at FS may result in significantly larger seismic events. Overall it is considered that a 'softer' mining environment , whether a function of the pillar system or geotechnical environment results in a lower potential for stope deformation to result in seismicity.

The data sets were also analysed with regard to the static stress drop of the mines seismic data set. Static stress drop has been used to differentiate between seismic events of similar magnitude with regard to their rock mass environment. A high static stress drop may be indicative of a high stress environment or high rock mass strength which is conducive to high stress loading and hence more damaging seismic events. The stress drop data for the two mines is indicated in the following table:

Name	$0 < \Delta\sigma <$ 1 (MPa)	$1 < \Delta\sigma <$ 2 (MPa)	$2 < \Delta\sigma <$ 8 (MPa)	$8 < \Delta\sigma <$ 16 (MPa)	$\Delta\sigma >$ 16 (MPa)
WN	46 (20%)	34 (15%)	93 (41%)	38 (17%)	17 (8%)
FS	645 (81%)	87 (11%)	65 (8%)	4 (0,5%)	3 (0,4%)

Analysis of the results indicates that the Wildebeestfontein mine has an overall higher percentage of high stress drop events and thus is considered to have a higher stress and rock mass strength environment and damaging seismic potential than the Frank Shaft area. The crush pillar system and rock mass characteristics at FS create a softer mining environment where potentially hazardous stress concentrations are not apparent from the seismic data. Analysis of individual areas within the Wildebeestfontein North mine indicated a significant difference in the stress drop characteristic, and is considered to be indicative of different geotechnical areas within the mine.

The data sets were also analysed with regard to the characteristic of the seismic waveform expressed as a ratio of the P and S wave seismic moment and radius to define the seismic event mechanism. In brief a high P wave component would be indicative of a crush type event or pillar failure expressed as a high compressional component. A high S wave component will be indicative of the more classically assumed shear type event.

Analysis of the data from WN indicates an overall tendency for events to have a higher P wave component and thus be indicative of crush type events such as pillar failure. Underground observations as reported by the mine rock mechanics support the mechanism of pillar failure or footwall foundation failure, with a generally more competent hangingwall strata. Thus a significant proportion of the stope closure may be attributed to these failure

mechanisms. However the data again indicates that there is significant variation in event mechanisms across the mine which may be indicative of different geotechnical areas. Analysis of the FS data indicates that the majority of events have a higher component of shear. Comparison against underground observations of failure mechanisms indicate the FS rock mass to be more discontinuous and that stope and off reef excavation damage is generally associated with suspected movement on these features.

It has been stressed that these seismic mechanisms are conceptual and thus require qualification with a significantly larger data set and with corroborating underground observations of movements on geological structures and excavation damage.

An assessment of rockburst damage indicated that at current depths this phenomenon is not critical, although it is anticipated that as mining progresses and moves deeper, this will change. Current damage mechanisms at WN are the violent failure of pillars in the stope back areas, but this may be expected to progress closer to the operating face as indicated above. At FS the problem is generally associated with damage to the off reef excavations due to strain bursting or slip on a predominant sub-horizontal feature.

7. Analysis of mining induced seismicity related to the platinum mines of the Bushveld Complex : No.10 shaft Wildebeestfontein North Mine

This aspect of the project addresses work conducted under enabling outputs 4 and 5. This work may be referenced in more detail in the accompanying document under appendix C.

Subsequent to the GENTEL analysis conducted at Wildebeestfontein North mine it was decided to install a PSS system at the No.10 shaft due to the indicated high level of seismicity as recorded by the GENTEL system. The

PSS system utilised 5 triaxial geophones delineating an area of approximately 200 metres x 200 metres on the Merensky reef horizon which was to be the focus of the investigation. The use of calibration blasts indicated the Primary and Secondary seismic wave velocities for these rock types to be 6600 m/s and 3600 m/s respectively, and indicated a location accuracy of approximately 3 metres within an area of 400 m x 400 m. A total of 254 seismic events were recorded by the system over the period September 1993 to August 1994.

Initial analysis of the seismicity of the area as recorded by the GENTEL system was re-evaluated with the PSS software. This analysis and subsequent events recorded on both systems indicated a calculated magnitude discrepancy of 1 between the two systems with the same waveforms. This difference was only finally resolved when a large event was recorded by the GENTEL system and the national seismic system of the Council for Geoscience. This also indicated the GENTEL system to overestimate magnitude by a factor of 1. Thus it was concluded that the PSS analysis was comparable to the national standard and the excepted correct magnitude.

The spatial distribution of events for the period of analysis are indicated in Figure 7. Analysis of the spatial distribution of events indicated the following characteristics

1) The majority of events located in close proximity to pillars in the stope back areas. These events in some cases could be correlated with pillar damage or foundation failure.

2) 35.5% of the recorded events were located close to the active mining faces. These events were generally of lower order magnitude.

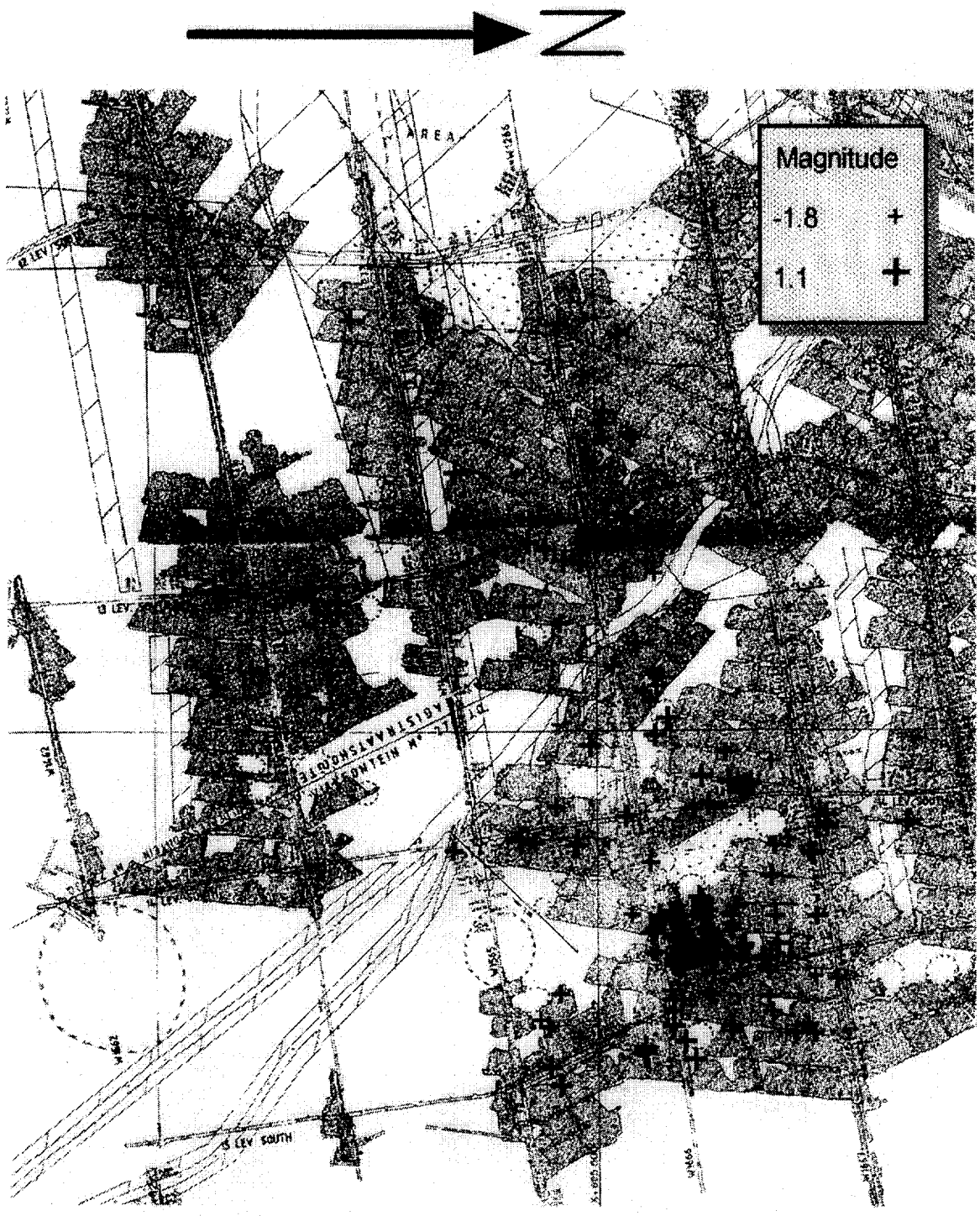

Figure 7. Spatial distribution of seismic events recorded at 10 shaft Wildebeestfontein North mine

3) The updip panels between W1566 and W1567 (central area) adjacent to a major fault which ran on dip experienced higher levels of seismicity associated with their strike abutments in the immediate vicinity of the face.

4) Most of the seismicity was associated with the reef plane and only one event could be correlated with a major geological structure off the reef plane.

Analysis of the temporal distribution of seismicity over the period of analysis indicates a uniform rate of seismicity with time and mining. However analysis of the temporal distribution of seismic moment indicates an increase in the energy release due to seismicity over the period of analysis (Sept. 1993 - Aug. 1994). This is considered to reflect an increase in the seismic hazard and thus seismic damage potential with increasing maturity of mining. The daily distribution of seismicity indicates the expected peak associated with blasting is evident between 14h00 and 16h00 with an approximately 3 hour tail off period.

Analysis of the magnitude distribution of events was considered not to be conclusive due to the relative small time frame and area of the investigation. However it was considered that the potential for events larger than 1.1 within this area was limited. The spatial and temporal distribution of events with regard to magnitude indicated that the smaller magnitude events were associated with blasting time and the active mining faces, where as the larger events generally occurred out of this time window and were associated with the stope back areas.

Analysis of seismic source parameters considered the stress drop and energy index of the seismic events recorded. The application of the stress drop as an analysis tool has been discussed previously. Within the immediate area of investigation it was generally found that all events indicated a similar stress drop, however comparison with some large events located in an extensively mined out area indicated the active mining area to have a high average stress

drop associated with the seismic events than the larger magnitude events located in the mined out areas. This may be interpreted as the events occurring in the mined out area are associated with a lower overall stress environment due to the destressing as a result of mining. Analysis of the seismic data was also conducted by means of event energy index. The energy index is the ratio of the seismic energy of an individual event to the average energy of events of similar seismic moment within the area of analysis. A linear relationship exists between the stress drop and the energy index parameters, this is considered to be a function of the higher level of energy radiated from a potentially high stress rock mass environment. Examination of the area of analysis indicates that events with higher energy index are associated with seismic events on pillars in the stope back areas and the abutments of larger 'regional' pillars.

The examination of seismic source mechanisms such as the ratio of the P and S-wave moment and energy, and moment tensor inversion techniques were also conducted on the seismic data set. The application of the P and S wave ratio technique has been described previously for the analysis of the GENTEL data for Wildebeestfontein North and Frank shaft. Analysis of the PSS data from this site indicated that the majority of the events located in the 'transition' zone between crush types events and shear type events and thus the seismic mechanism is inconclusive. A few of the events did indicate high P or S components and were correlated to face bursts and pillar failure or foundation failure of a pillar respectively.

Moment tensor inversion analysis was conducted on the full seismic database inclusive of events defined as production blasts previously. This analysis examines the magnitude and direction of the stresses at the source of the seismic event by analysis of the recorded waveforms for a pre-determined rock mass response. The analysis of the data indicated that all events with positive volumetric moment (explosional) could be correlated with the production blasts, events with small moment traces of shear component were

associated with events away from the reef plane, and the majority of events, which had implosional components (closure), could be correlated with pillar failure and hangingwall collapses. Comparison of this analysis of the data against the P and S wave ratio analysis indicates a much clearer indication of the source mechanisms of the majority of the events which previously plotted in the 'transitional' zone. With further development and confidence it is considered that this could represent a significant tool in the analysis of seismic mechanisms within the Bushveld Complex with the proviso that good quality seismograms are recorded.

Conclusion of this analysis indicated that for this geotechnical environment the majority of the seismic energy was associated with the failure of pillars in the stope back area as mining became more extensive. Seismicity associated with the active mining faces was generally of smaller magnitude and initiated with blasting activities. Anomalous seismicity was experienced on the updip mining area which may be a function of the proximity of a fault which necessitated the change in the conventional mining direction. The application of seismic source analysis gave a reasonable indication of the mechanisms of the seismic events and thus the controlling environmental factors. In conclusion it was recommended that this work be extended to different mining environments in order to principally determine the influence of geotechnical structure on seismicity.

It was planned to expand the Wildebeestfontein seismic network in order to cover a larger area inclusive of further mining operations, and in addition install an second PSS at Rustenburg Platinum Mines Rustenburg Section Frank 2 shaft. However although site selection and planning had been completed in 1994, delays in obtaining permission from the mines for installation and assistance with infrastructure meant these systems have not become operational. The system at RPM Rustenburg Section Frank 2 shaft was being installed at the time of project termination. The future application of this system must now be considered.

8. Analysis of mining induced seismicity related to the platinum mines of the Bushveld Complex : No.12 shaft Bafokeng North mine

This aspect of the project addresses work conducted under enabling output 3. A more detailed report of this area of investigation may be referenced under appendix D.

The analysis of Bafokeng North mine No.12 shaft was conducted to investigate the reported lower incidence of seismicity in comparison to equivalent mining operations at Wildebeestfontein North mine, and also to examine the influence of a change in the pillar system on seismic potential. In 1991 the mine utilised a system of 5 x 5 metre (elastic / yield) pillars on a diamond pattern at 30 metre spacing, in 1992 the pillar system was changed to 6 x 3 metre (yield / crush) pillars spaced 8 metres on strike and 31 metres on dip. The seismic analysis was conducted using data derived from the GENTEL system over the periods 1991 and 1993 (1992 omitted due to transitional phase) and processed with the PSS analysis software. The area of investigation was quite distant from the GENTEL installation and thus location accuracy would be relatively poor, however comparative analysis of the seismic parameters was considered to be valid.

The spatial distribution of events generally indicated that the majority were associated with the active mining areas, however a difference in seismic event distribution was noted between 1991 and 1993 with the change in the pillar system. In 1991 with the larger pillars the seismicity was relatively uniformly distributed over the mining area, figure 8, while in 1993 the seismicity was concentrated on regional pillars, figure 9. This may be indicative of the smaller pillars shedding more load to the regional pillars which become more highly stressed.

The magnitude distribution of events over the period of analysis indicates a change to larger magnitude events in 1993 compared to 1991. In 1991 the

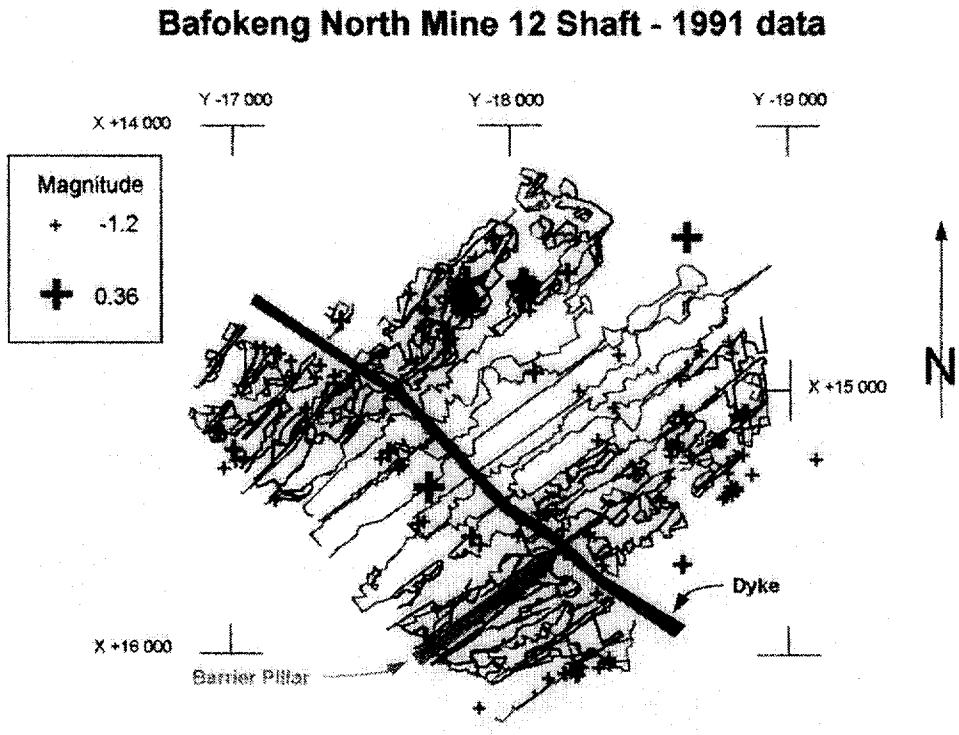

Figure 8. Spatial distribution of seismicity at Bafokeng North 12 shaft for the period late 1991

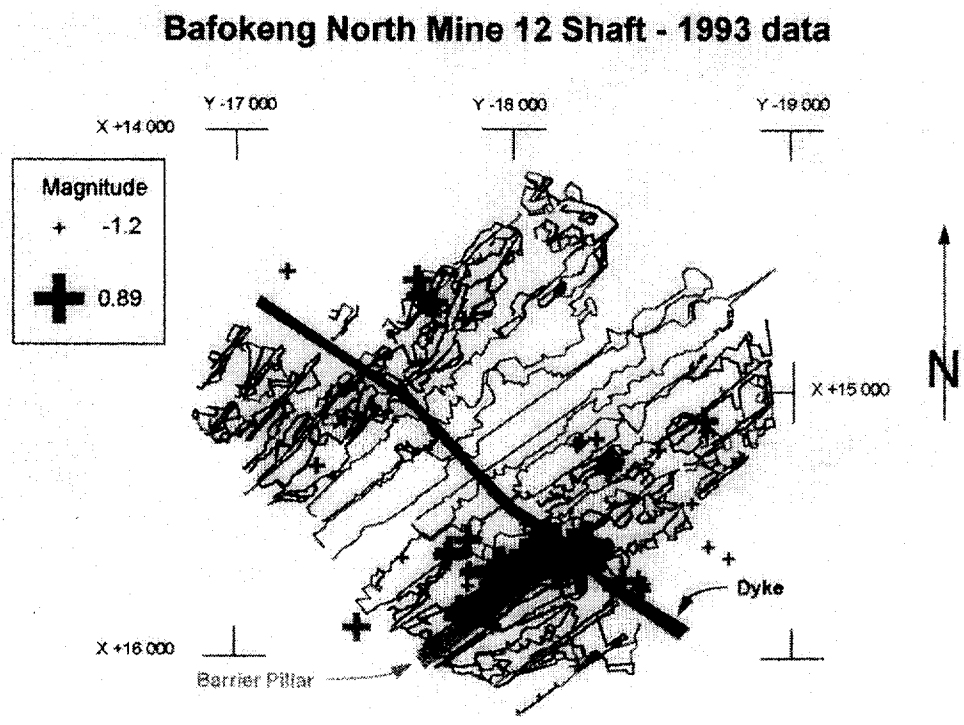

Figure 9. Spatial distribution of seismicity at Bafokeng North 12 shaft for the period early 1993

larger magnitude events were generally associated with a regional barrier pillar to the south of the mining area, figure 9.

The seismic event database was also evaluated with regard to seismic parameters. Analysis of the static stress drop indicated little variation between 1991 and 1993 and this is considered to be indicative of a fairly constant rock mass and general stress environment over these periods. Analysis of the seismic energy released over the two periods shows an increase in seismic energy during 1993 with the smaller pillar design. Analysis of the volume change associated with seismicity (γ_c)in comparison to the overall mining deformation also indicates increased volumetric moment associated with seismicity for the 1993 period. Together these factors tend to demonstrate the 5 x 5 metre pillars have a greater capacity to store the potential seismic energy and limit overall mining deformation.

A comparison was conducted of the seismic parameters associated with the mining of the No.12 shaft Bafokeng North mine with the previous analysis of the data from Wildebeestfontein mine and RPM Frank shaft in order to evaluate the influence of the geotechnical environment on seismicity. Comparison on this basis was considered valid due to the comparable mining methods and depths of the operations. This analysis is summarised in table 2.

Table 2. Comparison of seismic parameters for mines of the Bushveld Complex.

Mine	Energy Released per area (J/m^2)	Gamma γ_c
Frank Shaft	1300	0.04
Wildebeestftn 10 shaft	6600	0.4
Bafokeng 12 shaft 1991	9	0.02
Bafokeng 12 shaft 1993	156	0.13

The comparison indicates a significantly lower overall degree of seismic energy released for the mining operations of Bafokeng 12 shaft, and this is considered to be indicative of a difference in the geotechnical environment. Comparison of the pillar systems employed at No.12 shaft Bafokeng North mine indicate that a far greater degree of the energy within the rock mass associated with the mining operations is released as seismicity with the smaller (6 x 3 metre) pillar system. The general magnitude level of the seismicity is still low, and thus it is considered that with increasing mining depth the controlled release of seismic energy through crush / yield pillars is more favourable than the potential violent failure of a highly stressed larger pillar.

In conclusion the geotechnical environment appears to play a significant role in the seismic potential and thus rockburst hazard of a mining district. However a much greater understanding of the interaction of the rock mass structure on the seismic potential is required to develop a useful tool for planning mining strategies. This analysis does however indicate the potential of seismic monitoring as a tool for the evaluation of rock engineering strategies to develop safe mining practices.

9. Variation in the strength of rock types in the vicinity of the mining horizons / Rock Strength Database

This aspect of the project addresses work conducted under enabling output 2.

As part of the investigation into the variation in the strength of the rock types of the Bushveld Complex mining horizons it was considered necessary to establish a database of the laboratory test results for ease of analysis. This had previously been considered as a project under COMRO funding but at the time, the selected database format was considered to be too complex for on-mine usage. Work on this aspect of the project is detailed in appendix E by Dr. J A Ryder, and a brief summary of this report is given here.

Under this project the database format was chosen to be MS-ACCESS® due to its wide acceptance as a small to intermediate database platform, thus providing a relatively stable database environment in the foreseeable future. Additional graphics for the presentation of the database outputs has been developed on MS-Visual Basic® due to its compatibility within the MS® suite of software.

The data base is set up to accommodate and process primarily uniaxial and triaxial test data, but it will accommodate the future addition of Brazilian tests, point load or any other type of test data. The organisation of the data base is designed to minimise data inconsistencies by the application of data selection tables and data warning flags. The data selection tables cover areas such as mining district, formation description, rock type description, failure mode and test centre, where the user must select from a pre-defined listing. If the user is unsure of any of the required inputs the field is either designated 'unknown' or left blank, unless it is a critical field such as peak sample strength, confining stress and test reference. The primary unit of data storage is defined as a 'Batch' and would consist of a series of uniaxial, triaxial and any other mechanical tests conducted on a rock type or section of core which could be defined as homogeneous. The stress / strain behaviour of the test is input into the database as a series of characteristic points defining the end of the sample bedding in period, the yield point, the peak strength, the point of termination of unstable failure and the point of commencement of the post failure residual strength, figure 10. The location of these characteristic points allows a reasonable definition of the behavioural characteristic of the sample while achieving efficient data capture and storage. In addition to these points other material properties as defined by the testing programme may be entered into the database as required.

Analysis of the test data allows the user to attach reliability flags to data which is considered not to be valid. This highlights the relevant data point as

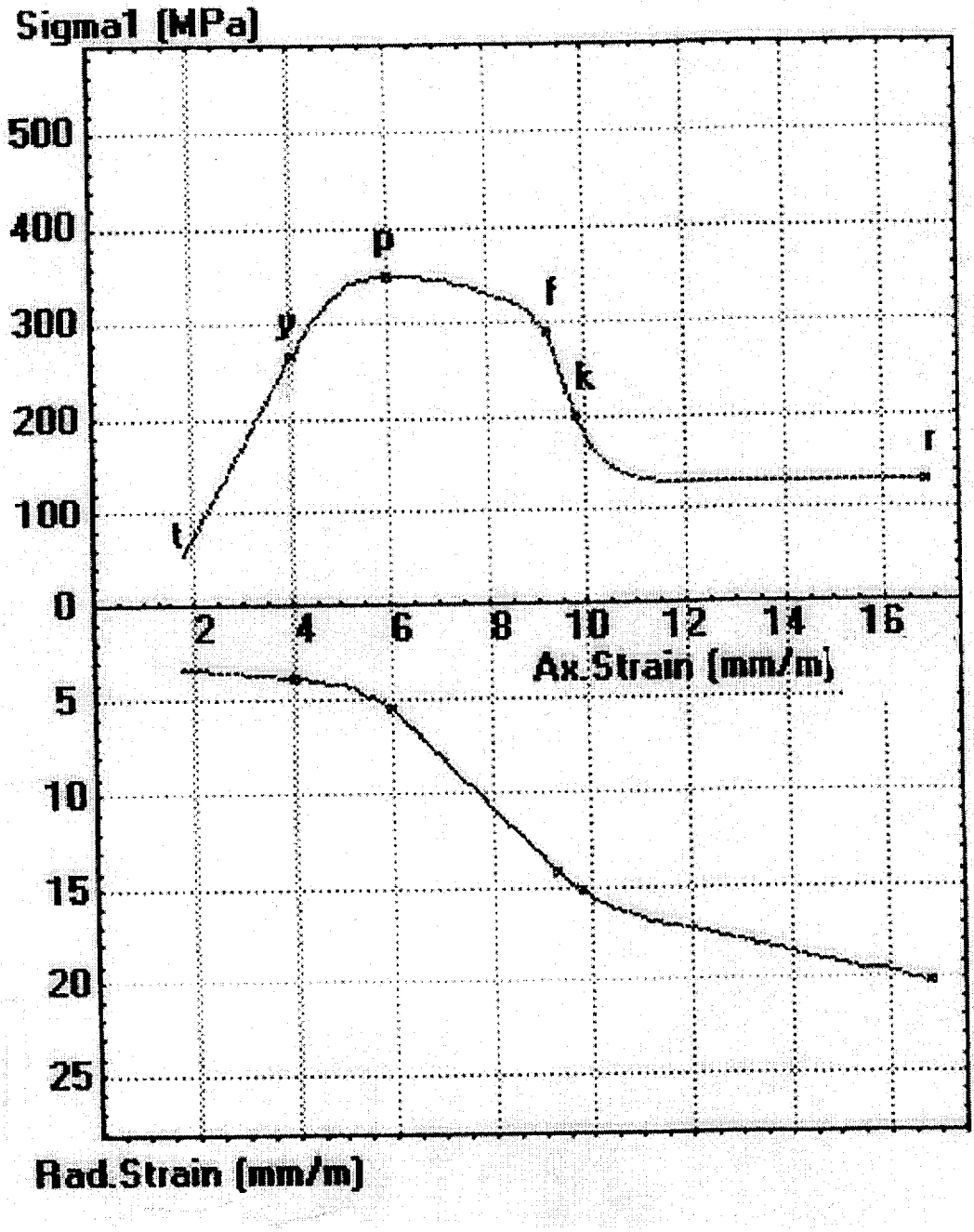

Figure 10. Typical stress - strain curve indicating characteristic points

red in the graphical displays for ease of identification, but the data does not take part in any further data calculation or manipulation. The output of the database is currently displayed under the Visual Basic® program. Generated outputs are graphical representations of the evolution of the rock modulus (E) and Poisson's ratio (nu) with confining stress, and the evolution of cohesion, friction and dilation with plastic strain. The later parameters are the required inputs for FLAC strain softening modelling, which may be adjusted for rock mass conditions, that allow non-linear modelling of mine excavations.

As the database stands currently it is available for manual data input of uniaxial and triaxial test data and the graphical representation of the batch data as indicated above. However the manual input of the data is quite time consuming and is estimated to take approximately 10 minutes per test; it is thus proposed that data capture from the Miningtek test machine be automated in future and that software be developed to capture data from the current database and data forms.

It is envisaged that this facility, if further developed, will become a major asset of the South African mining industry to enable data searches on rock types for different mining district for utilisation in better and more confident mine design.

With regard to Bushveld rock types initial rock testing programmes have been initiated from mines of the Bushveld Complex. These primarily are derived from the rock mass in the vicinity of the Merensky and UG2 mining horizons. The detailed test results are given in appendix 3 to appendix D and are analysed briefly here.

Detailed testing has been conducted on the rock types of the Merensky reef from a site at Richard shaft Union Section of Rustenburg Platinum Mines. The following rock types were tested and results indicated.

Rock type	Avg. UCS (MPa)	Modulus E (GPa)	Poisson's Ratio
Anorthosite (mottled)	196	80	0,20
Anorthosite (spotted)	180	74	0,23
Leuconorite	189	81	0,23
Melanorite	137	74	0,23
Norite	209	96	
Pyroxenite (Bastard Reef)	167	104	0,21
Pyroxenite (Merensky)	133	104	0,20

Triaxial testing was also conducted and these results are presented in the appendix.

Analysis of the results indicated some variation in the rock type properties. The mottled anorthosite was sourced from two different stratigraphic horizons at approximately 25 and 50 metres in the hangingwall of the Merensky horizon. Analysis of the individual strengths from these horizons indicated the UCS to be 175 and 233 MPa respectively. The modulus of the two horizons indicated the upper horizon to have a slightly higher average modulus at 85 GPa. Analysis of the triaxial test data indicates a significant increase in the modulus of the material with confinement. This was found to be generally the case for all the rock types tested, which however may only be a function of the internal damage to the specimen with the recovery and preparation process.

Rock type uniaxial strength have also been derived from tests conducted on samples collected from Karee mine of Lonrho Platinum Mines as indicated below.

Rock Type	Average UCS (MPa)
Anorthosite	239
Pyroxenite (Merensky)	105
Norite	169
Leuconorite	194

Comparison of these results to those as tested from RPM Union Section indicate some variance although this is not consistent throughout the rock types tested. However the comparison is based on a very limited database and thus conclusions on material behaviour are premature.

10. Conclusions

Although the major emphasis of the project was to gain an overview of the rock mass behaviour of the Bushveld Complex the following points are considered to be of immediate application to the mines for implementation in rock mechanics design considerations.

1) Variations in the geology of the rock mass may result in significantly different rock mass behavioural characteristics and thus of prime consideration in excavation design.

2) Joint sets of the Bushveld Complex are generally associated with the strike of the reef horizon and the major geological features of the area.

3) The presence of rogue joint sets within footwall development may be indicative of the presence of a pothole on the reef horizon.

4) Variability in the stress environment of the Bushveld Complex would indicate the importance of establishing the local stress environment prior to the development of critical long term excavations. In addition it may be

anticipated that significant stress concentrations may be experienced in the vicinity of potholes, replacement structures and reverse fault, or thrust structures.

5) The application of seismic monitoring has been demonstrated to be a useful mine design tool with regard to the performance of pillar systems and definition of the rock mass environment. Preliminary results of seismic analysis indicate:

5.1. The geotechnical environment has a significant influence of the seismic potential of a mining district. A relatively soft (discontinuous) rock mass environment results in low seismic potential whereas a competent rock mass environment is indicated to have a higher seismic potential.

5.2. Stiffer pillar / mining systems may have a higher potential for damaging seismicity then softer mining systems (crush pillars) especially with applications at increasing depths.

5.3. Most seismicity is associated with active mining faces, abutments and pillars, and limited seismicity has been indicated on major geological structures.

5.4. The use of crush pillars or elimination of internal stope pillars may result in an increase in seismicity associated with regional pillars and potholes. This may necessitate consideration of additional support measures for off reef excavations in these vicinities.

6. A rock properties data base has been established for the collection and analysis of rock testing data. This may be utilised for the analysis of anticipated rock properties for detailed rock mechanics design work in the future.

11. Recommendations

The aim of this project was to provide an overview of the rock mass environment and the rock mechanics design implications for mines of the Bushveld Complex. As such the scope of the project was not formulated to resolve problems in these areas and thus the following recommendations are made with regard to future research areas.

1) It is considered that the establishment of geotechnical areas within the Bushveld Complex with regard to rock mechanics parameters is of primary importance. This will allow the definition of mining districts based on the characteristic geotechnical parameters and associated behavioural characteristics. This will allow the application of site specific regional and local support design to ensure safe and productive mining activities.

2) The continued monitoring of seismicity, particularly in identified contrasting geotechnical areas in order to define the influence of the rock mass environment on seismic potential. This will allow an assessment of the potential seismicity of a new mining area prior to extensive mining activities and thus the design and implementation of correct local and regional support design.

3) Definition of the regional variation in the stress environment of the Bushveld complex in order that improved estimates of the stress field on a regional basis can be made for initial planning and numerical modelling applications.

4) Further development of the rock properties data base as a tool of the South African mining industry for improved application of rock property characteristic in rock mechanics design. This work would require automation of data capture directly from testing machines.

5) Requirement for a rational design procedure for pillars and strata control in a shallow and intermediate mining environment.

12. SIMRAC interim report references

Ozbay, M U et al. "A literature survey on the design of pillar systems in tabular hardrock mines." Miningtek report, Project GAP027, January 1994

Ryder, J A. "A summary of virgin stress measurements carried out in mines of the BIC." Miningtek report, Project GAP027, January 1994

Aref, K. "An assessment of seismicity at Wildebeestfontein North Mine and Frank Shaft." - (Analysis of waveforms recorded with the GENTEL seismic system.) Miningtek Final Report, Project GAP027, February 1994.

Aref, K., Jager, A., Spottiswoode, S M. "An assessment of seismicity in the Bushveld Igneous Complex." The 1994 ISRM International Symposium and IV South American Congress on Rock Mechanics, Santiago, Chile, February 1994.

Aref, K., Jager, A., Spottiswoode, S M. "Observations and failure mechanisms at Impala Mines - A case study." The First North American Rock Mechanics Symposium, Texas, USA, February 1994.

Appendix A

Geological Controls on Rock Mass Behaviour

GEOLOGICAL CONTROLS ON ROCKMASS BEHAVIOUR ASSOCIATED WITH PLATINUM AND CHROMITITE EXCAVATIONS, RUSTENBURG LAYERED SUITE, BUSHVELD IGNEOUS COMPLEX: A PILOT STUDY

BY

JOCHEN SCHWEITZER AND JOACHIM BERLENBACH

CSIR - MINING TECHNOLOGY

DECEMBER 1995

GEOLOGICAL CONTROLS ON ROCKMASS BEHAVIOUR ASSOCIATED WITH PLATINUM AND CHROMITITE EXCAVATIONS, RUSTENBURG LAYERED SUITE, BUSHVELD IGNEOUS COMPLEX: A PILOT STUDY

0 EXECUTIVE SUMMARY

The regional geological setting of the Bushveld Igneous Complex is established, discussed and its potential impact on rock engineering aspects is evaluated. The body of the report concentrates on the relevant geological features of the critical zone of the Rustenburg Layered Suite, which contains the chromitite and platinum bearing orebodies. These orebodies are located in a complex geological environment. Primary and secondary geological features of potential rock engineering significance are identified:

Primary geological features are: rock type, reef geometry (thickness, rolling reef, potholes), dip, lithological contact relationships (including partings), and grade distribution.

Secondary geological features are: faults, dykes/sills, joints, hydrothermal veinlets, alteration (metamorphism), and the various secondary geological features (all of the aforementioned, but also magma bodies that intruded the Rustenburg Layered Suite) that impact on the regional stress field.

It is concluded that both, primary and secondary geological features are of rock engineering significance. These may be qualitatively and quantitatively assessed in future studies. It is also concluded that, to date, no serious attempt has been made to evaluate rockmass behaviour associated with chromitite and platinum mines in a team effort, considering the various rock engineering and geological disciplines.

GEOLOGICAL CONTROLS ON ROCKMASS BEHAVIOUR ASSOCIATED WITH PLATINUM AND CHROMITITE EXCAVATIONS, RUSTENBURG LAYERED SUITE, BUSHVELD IGNEOUS COMPLEX: A PILOT STUDY

1 INTRODUCTION

This report provides an overview of the Bushveld Igneous event. The geological setting, including a regional and structural overview, is described. In order to evaluate rockmass behaviour on the platinum and chromitite mines of the Bushveld Complex, an intimate knowledge of the geological aspects of these orebodies is necessary. Composition of rocks, structural deformation and the intrusion of dykes and sills, degree of alteration, the width of reef horizons and the depth at which mining occurs are all known to influence rockmass behaviour in other orebodies and must therefore also be considered in the analysis of rockmass behaviour in the Bushveld mines. The most recent advancements in the understanding of the genesis of the worlds' biggest intrusive orebody (Fig. 1) are summarised for completeness.

In this investigation we concentrate on the geological characteristics of the mafic rocks of the Rustenburg Layered Suite, which host the economically important chromitite and platinum deposits. Firstly, the stratigraphy of this suite is established, with special reference to the stratigraphic intervals containing the orebodies. We then proceed to highlight the geological features that could have an impact on the rockmass behaviour around the excavations.

2 GENERAL GEOLOGY

2.1 Bushveld Complex: Geological Setting and Overview

The Bushveld Igneous Complex intruded into the sedimentary rocks of the Transvaal Supergroup. It is the world's largest chromitite and platinum depository. An area of approximately 300 000 km^2 is occupied by rocks of the Bushveld Complex with the total sequence having a thickness of about 15 km. Four units are defined: the Rustenburg Layered Suite, the Rashoop Granophyre Suite, the Lebowa Granite Suite (SACS, 1980), and the volcanic suite of the Rooiberg Group (Schweitzer and Hatton, 1995a; Hatton and Schweitzer, 1995). Fluorspar and tin are the chief orebodies contained in the Rooiberg Group and the Lebowa Granite Suite (see Crocker and Callaghan, 1979; Crocker et al., 1976; and Schweitzer et al., 1995a for descriptions of various ore deposits).

The acid rocks of the Lebowa Granite Suite and the Rashoop Granophyre Suite are centrally placed within the outcrop pattern of the Rustenburg Layered Suite (Fig. 2). In the past, some workers (e.g. Daly, 1928; Truter, 1949; Lenthall and Hunter, 1977) have suggested that the granites are genetically linked to the Rooiberg Group, but more recent field and isotopic work suggests that different sources for the granites and felsites must be invoked (e.g. Twist and Harmer, 1987).

The relationship between the granophyres and the Rooiberg Felsite is also debated. In the Tauteshoogte/Paardekop area, von Gruenewaldt (1972) proposed that rocks of the granophyre suite had resulted from shallow level melting of felsites, caused by the emplacement of the Rustenburg Layered Suite. In contrast, Walraven (1979) interpreted most of the granophyres as the shallow intrusive equivalents of the Rooiberg lavas. This is supported by Schweitzer and Hatton (1995a) and Hatton and Schweitzer (1995).

The three main commodities mined from the layered mafic rocks of the Rustenburg Layered Suite, in order of importance, are the Platinum Group Elements (PGE), chromitite, and vanadiferous magnetite. The Rustenburg Layered Suite, the major concern of this study, is estimated to contain 80% of the world's PGE reserves (Morrissey, 1988). It is conveniently separated into five major sectors, or limbs:

i) the Western Limb
ii) the Eastern Limb
iii) the Potgietersrus (northern) Limb
iv) the Bethal (southern) Limb and
v) the Far Western Limb.

Currently platinum mining is predominantly located in the Western Limb of the Complex (Rustenburg, Union and Amandelbult in the Amplats stable, Impala and Western Platinum in the Genmin stable, and Gold Field's Northam Mine), the exception being Amplats Atok Mine in the northern sector of the Eastern Limb. Platinum mining has historically been based on the Merensky Reef, but several mines currently also exploit the UG 2 Reef.

The general stratigraphy of the Bushveld Complex is summarized in Fig. 3 and a detailed discussion of the stratigraphy of both, chromitite and platinum mines, is given in Chapters 3 and 4. Although Fig. 3 shows a composite section, the substance of the stratigraphy is amazingly similar throughout the Rustenbug Layered Suite. Individual layers of mafic rock may be followed for over 120 km along strike but, in general, lateral discontinuities and thickness variations are common. Both, the Eastern and Western Limbs can be subdivided into proximal and distal facies, the tenor of the PGE and chromitite ores being superior in the proximal facies (Scoon and Teigler, 1994 and 1995).

Stratigraphically, the Rustenburg Layered Sequence is subdivided into six zones, from the base up the marginal zone, the lower zone, the lower critical zone, the upper critical zone, the main zone, and the upper zone (Fig. 3). An overview of the Complex, including a brief summary of available geophysical data, is presented by Eales et al. (1993). Magnetite seams are confined to the upper zone. These are mined on surface and are therefore not considered in this study.

The appearance of different cumulus mineral phases marks the base of each zone (Fig. 3). The lower zone is orthopyroxene-rich; cumulus chromitite and plagioclase are indicative of the critical zone; cumulus clinopyroxene appears at the base of the main zone and magnetite, Fe-rich olivine and apatite appear in the upper zone. The most primitive rocks are preserved in the lowest part of the Rustenburg Layered Suite (i.e., the lower zone).

The thickness of many lithological units, in particular the anorthositic layers, increases significantly southwards towards the so-called *distal facies* (Leeb-Du Toit, 1986; Viljoen and Hieber, 1986; Farquhar, 1986). The reader is referred to the aforementioned and other studies, all in Anhaeusser and Maske (1986) for detailed descriptions of the various platinum and chromitite mines of the Bushveld Complex. These are easy to read, well illustrated, and carry a wealth of information and introduce mine-specific terminology.

2.2 Genesis of the Bushveld Igneous Complex

The Bushveld Igneous Complex has received, due to its "uniqueness", major scientific attention, with studies commencing at the turn of the century. Genetic interpretations also considered the subduction of a mid-oceanic spreading centre, a multiple meteorite impact, and a mantle plume.

The following needs to be accommodated in a genetic model: U/Pb and whole rock Rb/Sr dating reveals that the Bushveld Igneous event occurred over a relatively short time period, not exceeding 7 Ma. The granophyres, volcanic rocks of the Rooiberg Group, and the mafic rocks of the Rustenburg Layered Suite (2061 $\pm$ 2 Ma; Walraven, 1995) simultaneously intruded and extruded into and onto the sedimentary rocks of the Transvaal Supergroup. The sequence of events was terminated by the intrusion of granites (2054 Ma; Walraven, op. cit.). It is the short-lived duration and the synchronous nature of events that leads present-day scientists to favour two genetic models for the origin of the Bushveld Igneous Complex, both relating its origin to one event, i.e. the impact and plume models. These models will briefly be described in the following:

2.2.1 The Bushveld Impact Model

Several previous workers have related the Bushveld Complex to a major astrobleme impact event. Diets (1961, 1963) suggested that the Rooiberg Felsite may represent a fallback breccia, which was deposited after crater excavation by a meteorite. Large quartzite xenoliths are often present in the Rooiberg Felsite at distinct stratigraphic levels (Schweitzer et al., 1995b), and these have been interpreted as relict fragments of almost completely melted crater-floor rocks (Rhodes, 1975). Some studies have failed to identify any unequivocal shock-metamorphic features (such as shatter cones, pseudotachylites, meggabreccias or high pressure minerals) in rocks associated with the Bushveld Complex (French and Hargraves, 1971; Twist and French, 1983). The major element concentrations, REE pattern and Ti and Zr concentrations of some volcanic flows are similar to Proterozoic, upper crustal sediments. This led Elston (1995) to suggest that these volcanic flows represent an impact melt. Alternatively, this rock type could be the result of very high degrees of melting of subducted sediment (Hatton and Sharpe, 1988), or melting of crust (Hatton and Schweitzer, 1995). The absence of volcanic detritus in sedimentary rocks of the lower Rooiberg Group, above the

Rustenburg Layered Suite, was interpreted as evidence of an impact origin of these rocks by Eriksson et al. (1994).

2.2.2 The Bushveld Plume Model

The link of the Bushveld Igneous Complex to a mantle plume was originally proposed by Davies et al. (1980), and subsequently reinforced by several workers (Sharpe, 1982; Sawkins, 1984; Campbell et al., 1989). First detailed evidence for the plume origin of the Bushveld Igneous event was provided by Hatton (1994 and 1995), Hatton and Schweitzer (1995), Schweitzer et al. (1995a), and Schweitzer and Hatton (1995a), (Fig. 4).

The argument against the impact origin of the Bushveld Igneous Complex mainly revolves around the predominantly volcanic Rooiberg Group. Beside the absence of shock metamorphic features (Twist and French, 1983) several other features argue against the impact origin of the Bushveld event, and the reader is referred to Hatton (1994 and 1995), Hatton and Schweitzer (1995), Schweitzer et al. (1995a), and Schweitzer and Hatton (1995a) for more detail.

Idealised plumes consist of plume heads, responsible for short-lived, voluminous igneous events (e.g. Anderson 1994, Kerr 1994). Petrogenetic modelling indicates that the Bushveld plume was shallow (Hatton 1994, 1995) and ascended continuously into higher crustal levels.

The plume model proposes that initially the most primitive lower zone magma intruded peripherally, accompanied by the peripheral extrusion of the initial, mafic volcanic rocks of the Rooiberg Group. The mafic Bushveld rocks are confined to the periphery of the Complex due to a ceiling silica cap above the mantle plume (Fig. 4), as is commonly

observed in plume settings. This phenomenon also explains why the siliceous rocks of the Complex, i.e. the granites, granophyres and the majority of the Rooiberg Group, are occupying the central portion of the Bushveld Complex.

Through time the plume head expanded and flattened, resulting in continuously increasing intrusive and extrusive magma volumes. Increasing intrusive volumes are therefore encountered from the lower-, to the critical- and finally the main zone. The upper zone was "pushed" towards the top of the magma chamber by the intruding main zone magma (due to density differences), and originally represented the uppermost portion of the critical zone. Areal extents and eruptive volumes of the different pulses are, similarly, increasing from the bottom to the top in the synchronous Rooiberg Group. The Bushveld plume intruded into the crust, resulting in increased crustal contamination in younger Bushveld magmas. This is also reflected in the addition of new magma types into the shallow magma chamber (Sharpe, 1985).

Workers favouring the plume model advocate that the Bushveld Complex is not a unique phenomenon. Amazing compositional and spatial similarities between the Bushveld and the Yellowstone plume have been documented (Hatton and Schweitzer, 1995). The Bushveld Complex may therefore be regarded as a larger and older example of processes currently operating at Yellowstone (Hildreth et al., 1991) and that are recorded in various forms throughout the geological record (e.g. Anderson, 1994; Kerr, 1994).

2.3 Tectonic History

The Bushveld Complex was intruded into the upper Transvaal Sequence. This event resulted in significant deformation of the older sediments, for example intensive folding and faulting is documented in the eastern and western sectors of the Bushveld Complex (Walraven, 1974; Lee and Sharpe, 1983). The Transvaal basin depocenter was controlled

by older tectonic structures, most likely by the Ventersdorp rift architecture (see Carr et al. (1994) for a detailed discussion). Both, the Bushveld Complex and the Transvaal basin that hosts the former, are interpreted to have formed in an extending continental setting (Carr et al., 1994). The nature of the stress field and the resultant structures, which developed during syn-emplacement subsidence of the Bushveld Complex, were compared with the loading caused when newly constructed dams are filled with water, which induces lithological adjustments and maximum subsidence below the deepest part of the water body (Wepf and Wolf, 1989; Carr et al., 1994).

The late-stage granites intruded in the already lithified mafic sequence. Therefore the granite intrusions also resulted in deformation of the older rocks. The mechanisms of granite intrusions can be related to "ballooning", resulting in deformation and thinning of the outer part of the intrusive body and the country rock (Fig. 5; Ramsay, 1991). To date, no work has been done addressing the potential link between the granite intrusions and the regional stress pattern.

Following the intrusions of the Bushveld Complex, the Pilanesberg Alkaline Complex intruded into the rocks of the Rustenburg Layered Suite and probably had a significant control on its deformation. In particular, it had an influence on the horizontal stress field (De Maar and Holder, 1994). The volcanic activity associated with the Pilanesberg event is complex and was accompanied by the formation of a dyke swarm which radiates outwards, "pushing aside" the country rock of the Rustenburg Layered Suite. Fig. 6a shows the orientation of dykes associated with the Pilanesberg Complex. The stress field associated with the intrusion of a magma body is well known (e.g. Park, 1983) and is summarised in Fig. 6b. The stress field exerted by dykes of the Pilanesberg Complex should be considered when analysing stress values and structural deformation. Many structures and alteration patterns observed in the western Bushveld mines are probably related to the intrusion mechanisms of the Pilanesberg magmas.

2.4 Petrologic Terminology

Since the layered mafic rocks of the Rustenburg Layered Suite have been stratigraphically subdivided on the basis of petrology (rock types), it is appropriate to give a brief overview of the rock types encountered in the Rustenburg Layered Suite, and of the minerals of which they are constituted. The rock mechanic properties will directly be influenced by the composition and texture of the rock and a detailed knowledge of these parameters is of rock engineering significance and may lead to a better understanding of rockmass behaviour.

2.4.1 Major Mineral Components of the Rustenburg Layered Suite

Each of the main rock-forming minerals, and its principal physical properties, are listed below. Hardness is measured on the Mohs scale, on which talc has a value of 1, and diamond a value of 10. SG is specific gravity:

a) **Olivine:** is a solid solution (mixture) between two end members, **forsterite** (Mg_2SiO_4) and **fayalite** (Fe_2SiO_4). Olivine in the lower, lower critical and upper critical zones is the Mg-rich variety, whilst that in the upper zone is Fe-rich. Olivine has a hardness of 6½ - 7, and SG 3.27 - 4.37, both these parameters increasing with Fe content. Colour is olive green. Magnesian olivine alters readily to serpentine [$MgSi_4O_{10}(OH)_8$], with a consequent substantial reduction in hardness, strength and SG. This can have a significant influence on rock mechanic properties (see discussion below).

b) **Orthopyroxene:** [$(Mg, Fe)SiO_3$] is a solid solution between magnesian and ferroan end members, and has an orthorhombic crystal structure. Orthopyroxene is Mg-rich up to the base of the main zone, and then becomes progressively more Fe-rich through the main zone and into the upper zone. In the upper part of the main zone and in the upper zone,

orthopyroxene has inverted from the pigeonite structure, with the consequent exsolution of blebs of augite. Orthopyroxene has a hardness of 5½ - 6, and a SG of 3.2 - 3.6. Its colour is brown, sometimes with a bronze-like sub-metallic lustre, hence the name 'bronzite' for relatively Mg-rich orthopyroxene. The name **hypersthene,** given to the most commonly occurring variety of orthopyroxene (somewhat more Fe-rich than bronzite), is a reference to its strength. Orthopyroxene is relatively resistant to alteration.

c) **Augite:** [$Ca(Mg, Fe)Si_2O_6$] is a clinopyroxene, distinguished from orthopyroxene by its monoclinic crystal structure. It is relatively rare in the lower, lower critical and upper critical zones, but becomes an important component of the rocks of the main and upper zones. Augite has a hardness of 5 - 6, and an SG 3.2 to 3.3 In hand specimen, it is usually dark grey-green in colour.

d) **Plagioclase:** a solid solution between **anorthite** ($CaAl_2Si_2O_8$) and **albite** ($NaAlSi_3O_8$), is a feldspar. It is relatively rare in the lower and lower critical zones, but becomes a significant component of the rocks in the upper critical, main and upper zones. It has a hardness of 6, SG of 2.62 to 2.76, and is white to pale grey in colour. Under certain conditions, it may alter partially to **sericite,** a fine-grained form of mica, with a consequent reduction in hardness and strength.

e) **Chromite:** ($FeCr_2O_4$) has a hardness of 5½ and SG of 4.6 It is black in colour, with a metallic lustre. The ratio of Cr to Fe is variable, and is the main control on grade of chromite ore. Chromite is the diagnostic mineral of the lower and upper critical zones, and does not occur in any of the other zones.

f) **Magnetite:** (Fe_3O_4) has a hardness of 6 and SG of 5.18 It is black, with a submetallic lustre, but may be slightly reddened by oxidation. Its most distinctive property is its strongly magnetic character. Cumulus magnetite occurs in significant quantities only in

the upper zone, but it may occur in late-stage iron-rich ultramafic pegmatites in the upper critical and main zones.

Apart from these minerals, **K-feldspar** ($KalSi_3O_8$), **apatite** [$Ca_5(PO_4)_3$], **quartz** (SiO_2), **biotite mica,** various **sulphides** and the **platinum group minerals** occur in minor amounts, usually only interstitially.

The analyses of rocks, their compositions and fabrics is, for example, facilitated by optic microscopy (Fig. 7) and scanning electron microscopy (SEM; Fig. 8). An example of fabric analysis with the aid of SEM is shown in Fig. 8: Various chemical compositions and interstitial phases in anorthosites can be semi-quantitatively analysed in a short time. In Fig. 8, X-ray maps for phosphorous of a mottled anorthosite of the main zone, showing apatite (Fig. 8a) can be compared with a backscattered electron image (BSE; Fig. 8b); or an X-ray map for potassium, indicating sericitization of plagioclase (Fig. 8c) can be compared with an X-ray map for Si, showing interstitial quartz and apatite (Fig. 8d).

2.4.2 Definition of Rock Types Encountered in the Rustenburg Layered Suite

The rocks that make up the Rustenburg Layered Suite and other similar layered igneous complexes throughout the world, are referred to as **cumulate rocks,** having originally been regarded as igneous 'sediments' (see Wager and Brown (1968) for details). Although the interpretation of these rocks as products of igneous sedimentation has been shown in recent years to be invalid in many cases (McBirney and Hunter, 1995), the cumulate terminology developed by Wager and co-workers still provides a logical basis for describing most of the rocks of the Rustenburg Layered Suite, at least at a fundamental level.

In the simplest terms, cumulate rocks consist of:

a) **cumulus minerals,** which are the earliest minerals to crystallize from the melt, and which form discrete, recognizable grains, and:

b) **intercumulus minerals,** which are late-crystallizing, and form something akin to what sedimentologists would refer to as matrix or cement around the cumulus minerals.

c) It might sometimes be necessary to refer to very late-stage minerals filling cavities in cumulate rocks as **interstitial minerals,** as distinct from cumulus or intercumulus.

The rocks of the Rustenburg Layered Suite are named using the IUGS recommendations (Streckeisen, 1976) as a basis, the following being the main rock-types encountered.

a) **Dunite** is a rock consisting of more than 90% cumulus olivine with minor intercumulus orthopyroxene. Dunite is most common in the lower zone.

b) **Harzburgite** is a rock consisting of 40-90% cumulus olivine, the remainder of the rock consisting of cumulus or intercumulus orthopyroxene. In general "Bushveld" usage, harzburgite is referred to as 'granular' if the orthopyroxene is cumulus, and 'poikilitic' if the orthopyroxene is intercumulus.

c) **Pyroxenite** usually refers, in the "Bushveld" context, to a rock which contains more than 60% cumulus orthopyroxene, and less than 10% felsic minerals (plagioclase, k-feldspar and quartz). The common intercumulus minerals are plagioclase and/or augite. Where

the content of intercumulus plagioclase is high, the term 'feldspathic pyroxenite' may be used. The term 'bronzitite' may sometimes be used as a synonym for orthopyroxenite.

d) **Norite** is a rock consisting almost exclusively of orthopyroxene and plagioclase in various proportions. Both minerals may be either cumulus or intercumulus, and may be accompanied by up to 10% of either augite or olivine. If a norite contains more than 65% plagioclase, it is termed a leuconorite. If it contains less than 35% plagioclase, it is termed a melanorite.

e) **Gabbro** is a rock consisting almost exclusively of augite and plagioclase. There is very little true gabbro in the Rustenburg Layered Suite, and most of what is referred to as gabbro is, in fact, gabbronorite.

f) **Gabbronorite,** as its name suggests, is a hybrid between norite and gabbro. It contains more than 10% of each of plagioclase, orthopyroxene and augite. The prefixes leuco or mela may be applied to it as in the case of norite (see above).

g) **Anorthosite** is a rock consisting of 90% or more cumulus plagioclase, together with small amounts of orthopyroxene and/or augite. In Bushveld terminology, the term 'mottled anorthosite' refers to anorthosite in which large areas of intercumulus orthopyroxene and/or augite, from 10 mm diameter up to the diameter of tennis balls, form dark mottles in a matrix of almost pure white or pale grey anorthosite. 'Spotted' anorthosite is anorthosite in which a small percentage of cumulus orthopyroxene gives the effect of dark spots in the pale anorthosite matrix. Anorthosites do not occur below the upper critical zone.

Anorthosites can be regarded in many respects as residual material, accumulated after separation of the mafic mineral components (pyroxene, olivine) from the original magmatic melt. Apart from plagioclase, anorthosites contain relatively Fe-rich

intercumulus pyroxene, and often also contain small but significant quantities of quartz and apatite. It is not certain what the effect of these interstitial components is on the strength of the rocks, and some quantification is necessary. Apatite and quartz are both colourless in thin section, and are often difficult to distinguish from plagioclase by microscope. X-ray mapping by Scanning Electron Microscope (SEM; Fig. 8a to d), however, allows the distribution and proportions of these interstitial phases to be rapidly evaluated. X-ray mapping also allows the degree of sericitization of plagioclase to be quantified.

h) **Chromitite** is a rock consisting of more than 95% cumulus chromite. The main intercumulus minerals are plagioclase, orthopyroxene and, sometimes, olivine. Chromitites occur only in the lower and upper critical zones of the Rustenburg Layered Suite.

I) **Magnetitite** is a rock consisting of more than 95% cumulus magnetite with intercumulus plagioclase and/or pyroxene. Magnetites are restricted to the upper zone of the Rustenburg Layered Suite.

Some pre-nomen further describe the appearance of a rock:

Leuco describes a rock of light appearance. A **Leuconorite** is therefore a light coloured norite.

Melano describes a rock of dark appearance. A **Melanonorite** is therefore a dark coloured norite.

Mottled describes a rock which is irregularly marked with spots or patches of different colour, e.g. a **mottled anorthosite**, with brown patches.

Poikilitic is a texture of an igneous rock in which small grains of one mineral are irregularly scattered without common orientation in a typically anhedral larger crystal of another mineral. In hand specimen this texture produces lustrous patches (*luster mottling)* due to reflection from cleavage planes.

Under certain circumstances, some rocks in the Bushveld stratigraphy may be pegmatoidal, implying that they are coarser grained than other cumulates they are associated with. Pegmatoids are, however, by definition stratiform (i.e. they form part of the igneous layering, and do not cross-cut it). Typical examples of pegmatoids are the pyroxenite or harzburgite pegmatoids associated with the platiniferous UG 2 and Merensky Reefs. Whereas the grain size of most cumulate rocks is of the order of 1 mm to 5 mm, the grain size in pegmatoids like the Merensky pegmatoid can be in excess of 30 mm.

Another group of rocks, also coarse-grained, but distinct from the pegmatites, are the late-stage mafic and ultramafic pegmatites that cross-cut the igneous layering in various parts of the Complex. Perhaps the most famous of these are the carrot-shaped dunite pegmatite pipes of the eastern Bushveld (Driekop, Mooihoek, Onverwacht etc.), which were mined for platinum in the early part of the century (Wagner, 1929; Viljoen and Scoon, 1985). The most important pegmatites from the point of view of current mining operations, however, are the iron-rich ultramafic pegmatites (IRUP), which cross-cut and disrupt the igneous layering (Scoon and Mitchell, 1994), particularly in the upper critical zone, where the UG2 and Merensky Reefs are situated, and in the main zone.

Table 1 indicates the average major and selected trace element composition of strata associated with the Merensky Reef. The major compositional variations in elements such as Al_2O_3, FeO, MgO and the base metals are suggested to be also reflected in rock engineering properties.

3 GEOLOGICAL SETTING OF CHROMITITE MINES

The serially-positioned chromitite layers in the Bushveld Complex were grouped from the bottom upwards into a lower, middle, and upper series by Cousins (1964) and Cousins and Feringa (1964) and a detailed discussion of the economic significance of chromitite deposits in Southern Africa is given by Vermaak (1986). Some detailed descriptions of chromitite deposits of the Rustenburg Layered Suite are given in Worst (1986a,b), Gain (1986), and von Gruenewaldt and Worst (1986).

Chromite is mined at several places in both the Western (Fig. 9a) and the Eastern (Fig. 9b) Limbs of the Bushveld Complex. The main sources of chromitite are the LG6 chromitite layer and the MG1 and MG2 chromitites. The locations of these reef horizons are shown in the stratigraphic column in Fig. 10.

3.1 Lower Group Chromitite Layers

In broad terms, the *"LG"* or lower group chromitite layers which form the base of the critical zone, occur towards the top of the pyroxenite-dominated lower part of the Rustenburg Layered Suite (Fig. 11). Seven layers are recognised of which the so-called LG 6 is economically the most important. The LG 1 to LG 4 chromitites are never more than 0.3 m thick and are often associated with olivine, a feature distinguishing them from overlying chromitite layers which are invariably olivine free. The total thickness of the composite LG 5 is 0.8 m, but the amount of interlayered pyroxenite waste in the partings renders the layer uneconomic (Hatton and von Gruenewaldt, 1985).

The on average 0.8 m thick LG 6 chromitite layer is composite, with impersistent silicate partings being occasionally encountered. On Rustenburg Platinum Mines (RPM) it occurs 478 m below the Merensky Reef and is mined near surface at several localities

immediately south of the Rustenburg Section (Viljoen and Hieber, 1986). Typical thicknesses of the main layer in this area are close to 90 cm. The typical Cr_2O_3 content of the LG 6 is about 45 %. The 0.3 m thick LG 7 lies 110 m above the LG 6. Little is known about this layer and it is economically insignificant. A detailed discussion of lateral variations exhibited by the lower group chromitite layers is presented by Hatton and von Gruenewaldt (1985).

3.2 Middle Group Chromitite Layers

The middle group chromitites occur throughout the Bushveld Complex (Figs. 12 and 13). Chromitite layers of this group are developed over some 50 m, within which interval up to 8 m comprises chromitite with a fairly high degree of purity, indicating that conditions favourable to chromitite formation persisted longer in this interval than in any other comparable package in the Rustenburg Layered Suite of the Bushveld Complex (Hatton and von Gruenewaldt, 1985). The four chromitite horizons within this group are often developed as multiple chromitite layers. For example, MG 1 contains two thinner chromitite layers below a 1 m thick chromitite band.

The middle group straddles the boundary between the lower and upper critical zones with pyroxenite and a characteristically pure anorthosite in the footwall and hangingwall of the MG 2, respectively, and norite in the hangingwall of the MG 3.

The different lithologies associated with the middle group chromitite layers show significant variations in thickness and composition (Fig. 13). Both, footwall and hangingwall lithologies of the orebodies also change laterally. A detailed discussion of the lateral variations and the stratigraphy of the individual sections presented in Fig. 13 is given by Hatton and von Gruenewaldt (1985).

3.3 Upper Group Chromitite Layers

The upper group chromitites are, similar to the middle group, of great lateral extent (Fig. 1). It usually consists of two chromitite layers, UG 1 and UG 2, although in the central sector of the eastern Bushveld additional layers, UG 3 and UG 3a, are developed. In addition, thin chromitite layers, present in the overlying Merensky and Bastard Reefs have traditionally been included in discussions of the upper group. The stratigraphy, thicknesses and compositions of the upper group of chromitite layers show considerable variations throughout the Bushveld Complex (Figs. 14, 15; Table 2). The high degree of variability invites a detailed analysis of the different footwall and hangingwall lithologies throughout the Rustenburg Layered Suite and their associated rock mass behaviour, potentially resulting in the establishment of geotechnical areas.

Due to the high variability of footwall and hangingwall lithologies, the following discussion of the various assemblages can only be an example. The Rustenburg section on RPM (Figs. 12, 14) is chosen as the reference section.

The UG 1, the first of the upper group chromitite layers is one of the most distinctive and persistent chromitite layers within the Rustenburg Layered Suite (Viljoen and Hieber, 1986). On RPM, the main layer shows an average thickness of 70 cm, which can, again, vary considerably. The footwall of the UG 1 is anorthosite, followed by pyroxenite, both found within the multiple chromitite layers of the UG 1, and in the immediate hangingwall.

The fine- to medium-grained pyroxenite passes sharply upwards into an anorthositic norite. The norite continues up to the UG 2. Pyroxenite is again encountered above the UG 2 chromitite layer and again norite is present above the pyroxenite up to the next unit, the Merensky Reef. Two thin chromitite layers are developed above and below the

Merensky pegmatoid, a pegmatoidal pyroxenite in which the platinum-group elements are concentrated.

The UG 2 forms the uppermost of the substantial chromitite layers within the Rustenburg Layered Suite and on RPM it lies approximately 140 m below the Merensky Reef. It is in average 70 cm thick. The overlying 8 m of feldspathic pyroxenite, contains up to three chromitite layers, each several centimetres thick, within the first 1 m above the main layer. The UG 2 is of significant economical importance, due to its PGE content.

It is noted that lithological contact relationships of the various strata is variably ranging from sharp to transitional. Especially the sharp contacts are of rock engineering significance. These may be seismically active or contribute to different degrees to the hangingwall and footwall closure. However, bottom and top contacts of chromitite layers are commonly sharp.

3.4 Potholes

The so called "potholes" are known to occur, to a lesser or greater extent, on all platinum and chromitite mines of the Rustenburg Layered Suite. They are especially pronounced with the Merensky Reef, the UG 1 and the UG 2. They are also reported from the middle group and lower group chromitite layers. Potholes occur when the reef "slumps", crosscutting its own unlithified footwall, consequently resulting in the reef occurring unconformably at a lower horizon than normal. Potholes are roughly circular in shape and may vary from tens to hundreds of metres with depths up to 90 m (e.g. the Merensky Reef in the Frank I and Frank II mining complex (De Maar and Holder, 1994)). There is generally a close relationship between reef thickness and the abundance of potholes (Viljoen, 1994).

Numerous theories have been put forward for the origin of potholes; however, the generally accepted interpretation is that these structures developed where a density disequilibrium occurred, with a heavy pyroxenite or chromitite layer positioned above a lighter, partly-consolidated, anorthosite footwall. The lighter footwall rocks are locally mobilized and become buoyant, thereby "floating off" and mixing with the pyroxenitic liquid of the succeeding unit (Hahn and Ovendale, 1994).

Potholes are of rock mechanic significance, due to the sudden change of dip of the strata and the change in composition of hangingwall and footwall lithologies, as a result of the unconformable relationship of the strata. Mining of potholes should not result in the development of *brows*, because these will increase hazards and costs due to wear and tear on equipment. Invariably, the intersection of potholes necessitates detailed logging and observation by Geology and Survey Departments. The Geology Department plays an active and important role in instructing mining personnel in the recognition of potholes and in the identification of pothole types, so that the correct development strategy can be applied.

Hahn and Ovendale (1994) give a detailed discussion of three different pothole types associated with the UG 2 chromitite layer on the Wildebeestfonein North Mine, Impala Platinum, which is summarized below.

Some of the general characteristics of the three types of UG 2 potholes at Wildebeestfonein North Mine are shown in Figs. 16 a-c. The majority of Impala's shafts are designed to mine both, the Merensky Reef and the UG 2 chromitite layer, therefore the succession most commonly exposed ranges from below the UG 1 chromitite layer to the top of the critical zone (Fig.3).

Type 1 potholes (Fig. 16a)

The *Type 1* pothole is most common and is usually of the order of 10 to 25 m in diameter. This type of pothole is associated with steep slumping of the UG 2 chromitite layer on the margins of the pothole, with dips of 80 being not uncommon. The UG 2 chromitite layer cuts down through the UG 2 pegmatoid to rest directly on the underlying *Footwall 13* (note, that specific terms for the stratigraphic succession have been locally introduced on the various mines).

Type 2 potholes (Fig.16b)

Type 2 potholes occur less frequently and are characterised by an apparent gradual slumping of the UG 2 chromitite layer. The base of potholes of this type is characterised by a thickening of the UG 2 chromitite layer, however, a drop in the overall PGM grade may occur. *Type 2* potholes often exhibit slight "rolling" of the reef.

Type 3 potholes (Fig. 16c)

The margins of a *type 3* pothole show only minor slumping and thinning of the UG 2 chromitite layer and as such may resemble the margins of a *type 2* pothole. This is followed, however, by major slumping with the UG 2 chromitite layer potholing as much as 20 m below its normal position, and coming to rest on *Footwall 16*. These potholes can reach a diameter of 50 m at their base. *Type 3* potholes are not a viable mining proposition.

4 GEOLOGICAL SETTING OF PLATINUM MINES

Platinum Mines in the Bushveld Complex are mainly concentrated in the western half of the complex (Fig. 17). Although the UG 1 and 2 chromitite reefs are exploited at some mines for their platinum content, the Merensky Reef, located in the critical zone, is by far the most important platinum producer of all the reefs of the Bushveld Complex. Despite lateral variations of the critical zone, the Rustenburg Section of Rustenburg Platinum Mines (RPM) gives a good overview of the stratigraphical setting of this package. The wide variety of reef types of the Rustenburg Layered Suite, including different pothole facies are shown in Fig. 18. Similar to the UG 1 and 2 Reefs, considerable variations of the footwall and hangingwall lithologies occur and may have an influence on rockmass behaviour.

4.1 Footwall Anorthositic Markers of the Merensky Reef

A number of distinctive anorthositic marker horizons occur in the upper part of the UG 2 rhythmic unit and form part of the footwall succession of the Merensky Reef, which are summarised for the Rustenburg Facies (Fig. 19).

i) Between 35 and 90 m below the Merensky Reef is a medium-grained leuconorite containing a number of distinctive spotted-anorthosite layers as well as darker noritic layers.

ii) Of note, 90 m below the Merensky Reef, is the "Flame Bed", consisting of conical tongues of mottled anorthosite (not shown on Fig. 19).

iii) An anorthositic norite, containing a number of well-known remarkably distinctive and consistent anorthositic layers, which can be recognised throughout the mine area,

occurs in the 35 m immediately below the Merensky Reef. These are: *the Boulder Bed, the Pioneer Marker, the Brakspruit Marker* and *the Footwall Marker.* Lithological contact relationships of the above layers vary from sharp to transitional.

4.2 Merensky Reef

The Merensky Reef unit, which includes the Merensky Reef, is remarkably consistent in thickness across the whole of Rustenburg Section, varying between 9 and 10 m (Viljoen and Hieber, 1986), unless potholes are encountered (see below). The Merensky Reef unit commences with a pyroxenite layer with associated chromitite layers, and is overlain by a differentiated suite consisting of norite, anorthositic norite, spotted anorthosite and, finally mottled anorthosite (Fig.19).

The Merensky Reef forms the lowermost part of the basal pyroxenite/chromitite assemblage of the Merensky Reef unit (Fig.19). It commences with a thin, 1 cm thick chromitite layer which rests, in most instances, directly on underlying anorthositic norite (Fig. 19; the footwall relationships in potholes is described in section 4.4). The lower chromitite layer is well defined and is immediately overlain by a pegmatoidal feldspathic pyroxenite which, for large areas of the Rustenburg Section, averages 25 cm in thickness. A second chromitite band (1 cm thick), occurs at or close to the top of this coarse-grained unit and demarcates the top of the geological entity termed the Merensky Reef at Rustenburg Platinum Mines. The upper chromitite layer is overlain by a medium-grained poikilitic pyroxenite, the so-called "Merensky pyroxenite".

The dominant silicate in the pegmatoidal reef is bronzite which accounts for about 80 % by volume of the reef and occurs as closely packed, subhedral to euhedral crystals. The less abundant plagioclase feldspar is intercumulus. Biotite, hornblende and magnetite are accessory minerals. Base-metal sulphides and PGM form minor constituents in the

spotted anorthosite footwall for several centimetres below the reef in some areas. These tend not to be present in the mottled anorthosite footwall. In order of diminishing abundance, these ore minerals are: pyrrhotite, pentlandite, chalcopyrite, and pyrite (Viljoen and Hieber, 1986).

The PGE have their highest concentration in the pegmatoidal feldspathic pyroxenite, throughout Rustenburg Section where values account for about 70 % of the total PGE mined. As the greater portion is thinner than the minimum practical stoping width, it is necessary to extract material from above and below the reef during mining operations (Fig.20). This has also consequences for the evaluation of rockmass behaviour, since it requires knowledge of the hangingwall and footwall lithologies, their composition (which influences strength of the rock), fabric development (igneous and structural) and the formation of faults and joints in the hangingwall of mining areas, which may control potentially hazardous conditions.

Locally the PGE can show a tendency to become either enriched in the hangingwall pyroxenite or in the spotted anorthosite footwall. This may then result in different mining layouts. Examples of average value profiles, for different sections of the RPM, are shown in Fig. 21.

4.3 The Bastard Reef

The Bastard Reef unit shows a similar cyclicity as the Merensky Reef unit, viz. a basal pyroxenite grading upwards into a norite, spotted anorthosite and terminated by a very well-developed mottled anorthosite. The whole unit is, however, over 100 m thick, compared to 9 m for the Merensky Reef Unit. The lowermost poikilitic pyroxenite constituting the Bastard Reef is frequently marked by a chromitite layer or parting along its base, although this is not developed everywhere. Odd scattered patches of coarser

grained and pegmatoidal pyroxenite are developed immediately above the basal contact, and low PGE values are also sometimes encountered at or close to this contact. The unit culminates, as noted, in the mottled anorthosite which also demarcates the top of the critical zone of the Rustenburg Layered Suite.

4.4 Potholes associated with the Merensky Reef

Similar to the potholes associated with the chromitite layers, potholes associated with the Merensky Reef significantly influence reef distribution and thicknesses (Fig. 22) and result in variations in footwall relationships. Potholes on the Rustenburg Section vary in diameter from a few metres to almost half a kilometre. Figs. 23 and 24 show schematic sections of typical major potholes. The general features of these potholes compare with those described for the UG 2 chromitite layer. However, some special characteristics of potholes associated with the Merensky Reef are summarised below (after Barry, 1964):

1. Alteration of the normal spotted anorthosite footwall of the Merensky Reef into a mottled (poikilitic) anorthosite,
2. Inclusion of mottled anorthosite in the Merensky Reef,
3. The association, either directly or indirectly with potholes, of younger pegmatoid/pegmatite bodies which transgress the layering,
4. Partial or complete alteration of the Merensky pyroxenite to a coarse pegmatoidal variety.

Of special interest is the formation of the so-called "Rolling Reef" potholes. This term describes a structural condition of the Merensky Reef wherein occurs a high frequency of what might be termed small potholes. These features vary in diameter from 12 to 100 m and they are relatively shallow, generally 2 to 3 m below the elevation of normal reef. The continual variation in reef elevation has given rise to the term "Rolling Reef". These

potholes can be very frequent as, for example along the *Townlands* longwall, where the chromitite layer undulates gently and forms localised dimples containing thicker chromitite development. In places the anorthosite layer is truncated by small dimples of hangingwall pyroxenitic or pegmatoidal material. The term "contact-type" reef is used to describe this type of reef development.

5 GEOLOGICAL FEATURES OF ROCK ENGINEERING SIGNIFICANCE

5.1 Primary Geological Features

Primary geological features to be considered are: rock type (this includes composition, texture, mineral assemblage, and grain size, reef geometry and the geometry of the associated footwall and hangingwall strata (e.g. thickness, rolling, potholes), lithological contact relationships (including potential partings represented by igneous layering), and grade.

i) Rock Type

Significant variations in rock types associated with the chromitite and platinum bodies are encountered. These are the result of lateral variations of hangingwall and footwall lithologies. Varying grades are associated with these footwall and hangingwall lithologies. Reef horizons are, in addition, mined at varying stratigraphic levels. This will also result in specific footwall and hangingwall rock assemblages.

Rock type characteristics are also reflected in the rocks' texture (including grain size and mineral assemblage) and composition. Little is known about the influence of igneous texture on rockmass behaviour. The textures encountered in the igneous rocks of the Rustenburg Layered Suite are highly variable, and it is suggested, that they should be

studied, in order to evaluate their relevance on rock mechanic studies. For example, grain size, alteration and orientation of minerals in anorthosites may differ widely (Figs. 7a to d) and contribute to differing degrees to the strength of materials. The intergranular relationship between crystals, interstitial phases and fluid content may also affect the stability of a rock; all these are phenomena which are little investigated, due to the isolated nature of studies.

Textural analyses, and their relationship to rock engineering properties and rockmass behaviour, may also consider geochemical studies (e.g. Table 1) and petrographic analyses, such as thin section studies or the SEM analyses as presented in this report. This would enable the quantification of many geological parameters, enabling more confident across discipline communication.

In summary, major potential exists to establish geotechnical areas for the various regions of mining. The rockmass potentially behaves differently in the various areas.

ii) Reef Geometry

Reef geometry is commonly variable with the chromitite and platinum orebodies. Variable reef geometry is also reflected in pronounced thickness variations and irregular grade distribution. Reef geometry is also expressed by the undulating nature of the footwall strata, defining the various pothole types that are associated with the orebodies under consideration. The hangingwall and footwall rock assemblage is, again, modified in these areas. Reef geometry does not only consider the thicknesses of the orebody, and the undulating nature of the deposit, but is proposed to also include the rock assemblage that make up the orebody. It has been documented in previous chapters that this assemblage can be highly variable and this could impact on rockmass behaviour.

iii) Contact Relationships

Contact relationships varying from transitional to sharp have been documented. The sharp contacts are of special interest. These could potentially be seismically active, and/or contribute to the hangingwall and footwall closure. Sharp bottom and top contacts have been documented for chromitite bands. No reference, investigating into the parting characteristics (i.e. mineralogical features, with different mineral types parting with different ease) and their frequency and orientation above and beneath the excavation, could be found.

Igneous partings are also present, resulting from the flowage of the various Rustenburg Layered Suite magmas. Flowage resulted in the alignment of specific minerals. The type of aligned minerals will vary, depending on the nature and composition of the rock type.

In summary it is proposed that the primary geological features should significantly impact on rockmass behaviour. However, to date, no studies investigating into this potential link have been undertaken.

5.2 Secondary Geological Features

During the long geological history of the Bushveld Complex, the rocks of the Rustenburg Layered Suite were exposed to a variety of secondary processes, which are of rock mechanic significance. These include the intrusion of dykes/sills and the formation of secondary veinlets, degree of alteration of rocks, and faults and joints. Often, these smaller scale structures may be related to changes in the regional stress field as the result of tectonic process. A detailed knowledge of the tectonic history therefore facilitates the understanding of these secondary structures and consequently supports the analysis of rockmass behaviour. However, they may necessitate detailed field and

underground mapping. The major secondary processes which are of rock mechanic significance are summarised below.

i) Relationship between tectonic stresses and rockmass behaviour

Detailed measurements of rock stresses were undertaken on Frank I and Frank II Shaft and Paardekraal Shaft (De Maar and Holder, 1994). In this area the following relevant aspects of the rock-stress measurements were documented and these are at least partly the result of the long and complex tectonic history of the Bushveld Complex. Similar correlations to the ones described here will also be significant on other platinum and chromitite mines of the Bushveld Complex and should be considered in the analyses of rock mechanic properties:

- An exceptionally high east-west horizontal off-reef stress distribution is oriented approximately on strike;
- The off-reef vertical stress is less than the weight of the overburden;
- There is a large disparity between the off-reef horizontal stresses;
- The off-reef rock stress changes in the vicinity of a geological disturbances, often in the vicinity of potholes;
- At one locality (Panel 61) the measured on-reef vertical stress is slightly higher than the weight of the overburden, in contrast to the off-reef stress 35 m below this panel. The on-reef vertical stress is 1.6 times higher than the horizontal on-reef stress values (k-ratio of 0.63). This represents a radical change from the off-reef k ratio of 2.29;
- The on-reef east-west and north-south horizontal stresses are similar. This aspect is quite different from the off-reef horizontal stresses.
- A marked change in strike direction on Rustenburg Platinum Mines (Rustenburg Section) is attributed to buckling of the floor rocks, particularly in the central portion of

the mine. Folding of the underlying Pretoria beds in the Rustenburg district may also have influenced the magnitude and direction of stress.

In essence, there is a tremendous vertical and horizontal variation in rock stress throughout the geological succession which can at least partly be attributed to the tectonic history of the Bushveld Complex. The assessment of rock mechanic properties of the Bushveld lithologies should therefore go hand in hand with a detailed structural analysis and a common approach by rock engineers and geologists appears to be most promising in analysing the complex environments associated with the Bushveld mines.

ii) Structure

Little is known concerning the structural history that affected the Rustenburg Layered Suite. The establishment of the number of tectonic events that resulted in the structures associated with the orebodies would greatly contribute to the better understanding of "fault behaviour" during mining. Distinct fault populations possessing distinct fault plane characteristics may be identified and grouped, leading to a better prediction of, e.g., the seismic attitude of the various fault populations.

The structural setting of the upper and lower chromitite layers on the farms Grasvally and Zoetveld, south of Potgietersrus, where considerable structural complexities are encountered, is shown in Figs. 25 a and b. Here, extensive block faulting resulted in the displacement of the lower and the critical zones. The faulting is mostly compressional and may, possibly, be related to a nearby granite intrusion (see Fig. 25a, inset). The eastward-verging thrust faults are also shown in a cross section (Fig. 25b) where the displacement of the reef horizons by several tens of metres is emphasised. The possible reactivation (inversion) of one of the thrust faults may indicate a later tectonic event (double arrow with question-mark in Fig. 25b).

Steep dipping faults occur throughout the chromitite and platinum mines of the Bushveld Complex, and may result in considerable displacements, influencing mining operations (Fig. 26). Such steep dipping faults may also activate seismic slips. An example is a reverse fault with a displacement of 6 m on Frank II Shaft. This fault was several times seismically active when approached by mining.

Strata-parallel faulting is also common throughout the Bushveld succession and was partly related to "slumping", i.e. sliding of individual packages into the dip direction of the strata or strata-parallel. Such strata-parallel faults may step up in stratigraphy, resulting in the formation of "toe thrusts".

Examples of strata-parallel compressional faults also occur in the Boulder Bed, the Flame Bed, the Footwall Marker, and the Bastard Reef, all of which are in close proximity to the Merensky Reef (Fig. 27). Reactivation of these fault planes due to mining processes may result in the liberation of seismic energy measuring up to 2.0 on the Richter Scale.

iii) Dykes and Sills

There appears to be a close relationship between pothole distribution and dykes and faults (Viljoen and Hieber, 1986; Fig. 28). In fact, it is often observed that dykes cut across the centre of potholes. Where this occurs, a local variation of the stress field may occur. Although Pilanesberg Dykes appear to be the most dominant generation of dykes, younger, Karoo Dykes may also be considered. No further data of Karoo age Dykes are available at this stage.

Many of the relevant features elaborated upon for the faults hold also true for sills and dykes. However, dyke and sill compositions and textures, and the dyke/host rock contact relationships are additional features associated with these intrusive features.

iv) Joints and hydrothermal veinlets

Fluids migrated through the rocks of the Rustenburg Layered Suite, due to dehydration of the Transvaal floor rocks and fluids expelled during the crystallisation of the magma (Schiffries and Skinner, 1987; Schweitzer and Hatton, 1995b; Fig. 29). Migration of hydrothermal fluids occurred on a regional scale and the resulting hydrothermal veinlets are associated with all mining operations. Two episodes of fluid migration are distinguished (Schiffries and Skinner, 1987) characterised by distinct secondary mineral assemblages. We suggest that these regionally persistent veinlets could have a major impact on the rockmass behaviour associated with chromitite and platinum excavations, which needs to be confirmed via future studies.

In general, the presence of serpentinised and calcitised joints increase with mining depth, e.g. in the Frank I and II area. In the latter it was reported that joints in the hangingwall of the Merensky Reef significantly influence the stability of the hangingwall. Fig. 30 shows a schematic diagram of differently oriented joints resulting in so-called "dome structures", due to the intersection of different generations of joints. Clearly, an understanding of joint orientations appears necessary, so to predict hazardous areas of mining. Because both, faults and joints are the result of tectonic forces, and both have significant influence on rockmass behaviour, its is suggested that rock engineering analyses should be accompanied by a detailed structural analysis.

v) Degree of Alteration

Alteration of rocks may result in a reduction of competency. The often observed serpentinization of Bushveld rocks can, for example, results in a change of rock properties. The study of such alterations may be aided by petro-analytical techniques. Alteration of strata occurs on a local scale (e.g. close to faults and dykes) and on a regional scale, such as the above serpentinization. X-ray mapping also allows to determine the degree of sericitization of plagioclase to be quantified, which is an additional alteration feature.

The Merensky Reef has a thin stringer of chromitite (2 or 3 grains thick) at its base. Sericitization and the amount of interstitial material in the anorthosites has an effect on the mechanical properties of the rocks. An additional complicating factor as regards footwall conditions is that IRUP bodies of various shapes and sizes often intrude and replace the anorthosite footwall of the Merensky Reef, especially in the vicinity of potholes. The reef itself is often pegmatoidal in its basal parts. Its coarse grain size, coupled with the presence of interstitial biotite, mica, sulphides and other minor phases, needs to be evaluated regarding its rock engineering significance.

6 Summary and Discussion

The Rustenburg Layered Suite of the Bushveld Igneous Complex is of major economic importance. The chief orebodies are the platinum bearing Merensky Reef and the UG2, and the chromitite bodies of the lower and middle chromitite groups. All of these deposits are located in the critical zone of the Rustenburg Layered Suite.

This report first depicts the regional setting of the Bushveld Igneous Complex, which we also consider to regionally impact on rock mechanic issues. After briefly outlining the

various components of the Bushveld Igneous Complex, also viewed in the light of their genesis, i.e. meteorite impact versus plume model, we focus on the mafic rocks of the Rustenburg Layered Suite. These host the chromitite and platinum deposits. An overview is also provided of the major mineral components that constitute the mafic rocks of the Rustenburg Layered Suite. Mineral properties are summarized and the potential usage of sophisticated mineralogical techniques to establish mineral assemblages and rock textures is highlighted.

The characteristics of the rocks associated with the chromitite and platinum orebodies are highly variable, which is also expressed by pronounced variations in grain sizes (from about 1 mm to over 30 mm). The application of mineralogical techniques is proposed to be of immediate rock engineering significance, implying that the microcosm may also contribute to the understanding of the macrocosm, i.e. the rockmass behaviour of the different rock types may differ while mining the various orebodies. We then concentrated on the chromitite and platinum orebodies and associated strata of the critical zone. Geological features of rock engineering significance are highlighted (see Chapter 5). Our investigation reveals that tremendous scope exists for combining the various rock engineering and geological disciplines, also expressed in the identification of potential, combined future studies, which are emphasized throughout the report and highlighted in Chapter 7.

The geological features of rock engineering significance are grouped into primary and secondary features. However, some overlap exists between the two groups.

Primary Geological Features: Primary geological features of significance are: rock type, reef geometry (thickness, rolling reef, potholes), dip, lithological contact relationships (identifying partings), and grade distribution.

Different rock types, characterised by distinct textures and composition, are suggested to respond differently to the mining induced stresses. Our analyses reveals that the rock assemblages encountered within the various chromitite and platinum orebodies are variable. More important, footwall and hangingwall lithologies of the orebodies are regionally variable. This suggests that the compilation of geotechnical areas, defined by different footwall/hangingwall assemblages, could be attempted for the major economic horizons contained within the Rustenburg Layered Suite. The vertically and laterally changing nature of the footwall and hangingwall rock types may also be reflected in the highly variable, recorded rock stresses.

Thicknesses of the orebodies are similarly variable, with these also being controlled by the rolling and potholing. Different pothole types are defined, and the mine geology departments are contributing to the identification of the appropriate mining method, which varies according to pothole types. This reinforces the need for a combined rock engineering/geology effort. The geological setting associated with potholes is complex, where varying inclination of the strata is encountered. Pegmatoids, pegmatites and structural features are also responsible for a change in the stress field.

Lithological contact relationships are variable and range from sharp to transitional. Sharp contact relationships are associated with all the orebodies and their contact characteristics (i.e. mineralogical characteristics, thickness etc.) and distance to the orebody may be delineated in the future.

Grade is variably distributed within the orebodies under consideration, vertically and laterally. The prediction of grade into the unmined area therefore facilitates the selective mining of economically most viable orebodies. This may result in the implementation of specific mining methods.

Secondary Geological Features: These are: Faults, dykes and sills, joints, hydrothermal veinlets, alteration (metamorphism), and the various secondary geological features (all of the aforementioned, but also magma bodies that intruded the Rustenburg Layered Suite) that impact on the regional stress field.

Faults are commonly associated with the chromitite and platinum orebodies. The stress field has been shown to be changed in the vicinity of faults. Both, compressional and extensional faults are present. This is expressed in faults at an angle to the orebodies and faults that are parallel to the reef plane. Future scope exists for the identification and delineation of distinct fault phases that occurred at discrete times. This will facilitate the grouping of faults into populations that are likely to be characterised by different orientations to the excavation, and distinct fault plane characteristics, exhibiting distinct excess shear stresses. The same holds true for the dykes and sills. However, dyke and sill compositions, and their related host rock contact relationships, may be considered as an additional item of rock engineering significance. Different compositions are reflected in different competencies which are probably expressed in varying tendencies to burst.

The rock engineering importance of joints and hydrothermal veinlets is stressed. Joints have been shown to impact on hangingwall conditions, and the identification and delineation of various joint populations, and their associated features, may facilitate the prediction of these hazards ahead of the mining area. The rock engineering significance of hydrothermal veinlets has not been considered yet. However, we propose that these are of major importance, and their attitude, frequency and secondary mineral assemblage may vary from rock type to rock type.

Alteration, or metamorphism, will influence the rock engineering properties of the rock. It may be encountered on a local scale, in the vicinity of geological structures, but also regionally (e.g. close to most post-Bushveld intrusions). Degrees of alteration are variable throughout the Rustenburg Layered Suite and may also be delineated

employing sophisticated microscopic techniques. Hydrothermal veinlets may, in addition, be more prominent in regions that are strongly altered.

Intrusion of the granites belonging to the Lebowa Granite Suite, and the intrusion of the Pilansberg Alkaline Complex are suggested to have impacted on the regional stress field. However, no studies trying to establish a relationship between these features and the pertaining stresses have been undertaken to date.

In summary it is concluded that both, primary and secondary geological characteristics should be considered in any rock engineering investigation.

7 RECOMMENDATIONS FOR FUTURE WORK

Areas that could be addressed by future studies have been identified throughout this report. This section therefore attempts to highlight and summarise some of these identified areas. Most of these can be applied on a macro-, meso-, and micro-scale.

The variability of footwall and hangingwall rock types associated with the major orebodies, and their potential impact on rock mechanic issues clearly merits future attention. Petrographic investigations could also marry primary and secondary (e.g. alteration) features. The delineation of geotechnical areas could result in the identification of mining areas characterised by distinct rockmass behaviour. Parting characteristics and their distances to the excavations may also vary within distinct geotechnical areas. The potential of applying geological and geophysical methods in predicting rolls and potholes ahead of the face may also be proposed.

Potential also exists for relating events post-dating the Bushveld Complex to the pertaining regional and local stress fields. Future studies may attempt to group faults,

dykes and sills, joints, and hydrothermal veinlets into populations, via underground mapping and petrographic studies. The various populations could well be characterised by distinct orientations to the excavations, fault plane characteristics, dyke and sill compositions and their host rock contact relationships, and type of secondary mineral associated with joints. All these features are of rock engineering significance. Despite the regional existence of possibly two generations of hydrothermal veinlets, little is known about these features, and this should also be investigated in the future.

Acknowledgements

Andrew Mitchell contributed to the petrographic discussion of the rock types. Stephens Letlotla, Deborough Xhaba and Franz Seloane helped in the compilation of this report.

References

Anderson, D.L., 1994. Superplumes or supercontinents? Geology, **22**, 39-42.

Anhaeusser, C.R., and Maske, S. (Eds.), 1986. Mineral Deposits of Southern Africa, Vol. II, Geol.Soc.S.Afr, 1308 pp.

Barry, J.A., 1964. Pothole and koppie investigation at Rustenburg Platinum Mines. Intern. Rep. (Unpubl.). JCI, Johannesburg, 5 pp.

Barry, S.D., and Odendaal, N., 1993. Platinum-Group Metals produced in South Africa 1993. Minerals Bureau, Republic of South Africa, D6/93, 19 pp.

Campbell, I.H., Griffiths, R.W., and Hill, R.I., 1989. Melting in an Archaean mantle plume: Heads it's basalt, tails it's komatiites. Nature, **339**, 697-699.

Carr, H.W., Groves, D.I., and Cawthorne, R.G., 1994. The importance of synmagmatic deformation in the formation of Merensky Reef Potholes in the Bushveld Complex. Economic Geology, **89**, 1398-1410.

Crocker, I.T., Coetzee, G.L., and Mehliss, A.T.M., 1976. Tin. *In:* Coetzee, C.B., Ed. *The Mineral Resources of the Republic of South Africa.* Handb. Geol. Surv. S. Afr. 7: 213-220.

Crocker, I.T., and Callaghan, C.C., 1979. Tin resources of South Africa: classification and inventory. Geol. Surv. S.Afr.Bull., **66,** 28 pp.

Cousins, C.A., 1964. Additional notes on the chromitite deposits of the eastern part of the Bushveld Complex. *In:* Haughton, S.H., Ed., *The Geology of Some Ore Deposits in Southern Africa,* II. Geol.Soc.S.Afr.,169-182.

Cousins, C.A., and Feriga, G., 1964. The chromitite deposits of the western belt of the Bushveld Complex, *In:* Haughton, S.H., Ed., *The Geology of Some Ore Deposits in Southern Africa,* II. Geol.Soc.S.Afr., 183-202.

Daly, R.A., 1928. Bushveld Igneous Complex of the Transvaal. Bulletin of the Geological Society of America, **39**, 703-768.

Davies, G., Cawthorn, R.G., Barton, J.M., and Morton, M., 1980. Parental magma to the Bushveld Complex. Nature, **287**, 33-35.

De Klerk, W. J., 1982. The geology, geochemistry and silicate mineralogy of the Upper Critical Zone of the north-western Bushveld Complex at Rustenburg Platinum Mines, Union Section.MSc thesis, Rhodes University, Grahamstown, 210 pp, not published.

De Maar, W.J., and Holder, G., 1994. Strata control at Rustenburg Platinum Mines (Rustenburg Section). Xvth CMMI Congress. Johannesburg, SAIMM, **1**, 149-157.

Dietz, R.S., 1961. Astroblemes. Scientific America, **205**, 51-58.

Dietz, R.S., 1963. Cryptoexplosion sructures: A discussion. Annual Journal of Science, **261**, 650-664.

Eales, H.V., Botha, W.J., Hattingh, P.J., de Klerk, W.J., Maier, W.D., and Odgers, A.T.R., 1993. The mafic rocks of the Bushveld Complex: a review of their emplacement and crystallization history and mineralization in the light of recent data. J.Afr.EarthSci., **16**, 121-142.

Elston, W.E., 1995. Bushveld Complex and Vredefort Dome: Case for multiple impact origin (abstract). Geocongress '95, Geol.Soc.S.Afr., Johannesburg, 504-507.

Eriksson, P.G., Schreiber, U.M., Reczko, B.F.F., and Snyman, C.P., 1994. Petrography and geochemistry of sandstones interbedded with the Rooiberg Felsite Group (Transvaal Sequence, South Africa): implications for provenance and tectonic setting. Journal of Sedimentary Research, **A64**, 836-846.

Farquahr, J., 1986. The Western Platinum Mine. *In:* Anhaeuser, C.R., and Maske, S., Eds., Mineral Deposits of Southern Africa, Vol. II, Geol.Soc.S.Afr., 1135-1142.

French, B.M., and Hargraves, R.B., 1971. Bushveld Igneous Complex, South Africa: Absence of shock-metamorphic affects in a preliminary search. Journal of Geology, **79-5**, 616-620.

Gain, S.B., 1984. Distribution and Origin of the Platinum-Group Elements in the UG-2 Chromitite Layer on Maandagshoek, Eastern Bushveld Complex. Institute for Geological Research on the Bushveld Complex, University of Pretoria, Research Report, **47**, 37 pp.

Gain, S.B., 1986. The Upper Group Chromitite Layers at Maandagshoek, Eastern Bushveld Complex. *In:* Anhaeuser, C.R., and Maske, S., Eds., Mineral Deposits of Southern Africa, Vol. II, Geol.Soc.S.Afr., 1197-1208.

Hahn U.F., and Ovendale, B., 1994. UG 2 Chromitite Layer Potholes at Wildbeestfontein North Mine, Impala Platinum Limited. Xvth CMMI Congress. Johannesburg, SAIMM, 1994, **3**, 195-200.

Hatton, C.J., 1994. PGE and Cr mineralization in the Bushveld Complex - product of interaction among magmas derived from a mantle plume. Communication Geological Survey Namibia, in press.

Hatton, C.J., 1995. Mantle plume origin for the Bushveld and Ventersdorp magmatic provinces. Journal of African Earth Sciences, in press.

Hatton, C.J., and Von Gruenewaldt, G., 1985. The Geological Setting and Petrogenesis of the Bushveld Chromitite Layers. Institute for Geological Research on the Bushveld Complex, University of Pretoria, Research Report, **57**, 48 pp.

Hatton, C.J., and Sharpe, M.R., 1988. Significance and origin of boninite-like rocks associated with the Bushveld Complex. *In:* Crawford, A.J., Ed., *Boninites and related rocks*. Unwin Hyman, London, 299-311.

Hatton, C.J., and Schweitzer, J.K., 1995. Evidence for synchronous extrusive and intrusive Bushveld magmatism. Journal of African Earth Sciences, in press.

Hildreth, W., Halliday, A.N., and Christiansen, R.L., 1991. Isotope and chemical evidence concerning the genesis and contamination of basaltic and rhyolitic magma beneath the Yellestowne Plateau volcanic field. J.Petr., **32/1**, 63-138.

Irvine, T.N., Keith, D.W., and Todd, S.G., 1983. The J-M Platinum- Palladium Reef of the Stillwater Complex, Montana. II. Origin by double-difusive convective magma mixing and implications for implications for the Bushveld Complex. Institute for Geological Research on the Bushveld Complex, University of Pretoria, Research Report **43**, 93 pp.

Kerr, A.C., 1994. Lithospheric thinning during the evolution of continental large igneous provinces: a case study from the North Atlantic Tertiary province. Geology, **22**, 1027-1030.

Lee, C.A., and Sharpe, M.R., 1983. The structural setting of the Bushveld Complex - an assessment aided by Landsat Imagery. Institute for Geological Research on the Bushveld Complex, University of Pretoria, Research Report **36,** 21 pp.

Leeb-Du Toit, A., 1986. The Impala Platinum Mines. *In:* Anhaeuser, C.R., and Maske, S., Eds., *Mineral Deposits of Southern Africa, Vol. II, Geol.Soc.S.Afr.*, 1091-1106.

Lenthal, D.H., and Hunter, D.R., 1977. The geology, petrology, and geochemistry of the Bushveld granites and felsites in the Potgietersrus tin-field. Inf.Circ., Econ.Geol.Res.Unit, Univ. Witwatersrand, **110**, 91 pp.

McBirney, A.R., and Hunter, R H., 1995. The cumulate paradigm reconsidered. Journal of Geology, **103,** 114-122.

Morrissey, C.J., 1988. Exploration for platinum. *In:* Pritchard, P.J., Potts, P.J., Bowles, J.F.W., and Cribb, S.J., Eds., *Geo-platinum 87,* Elsevier, 1-12.

Mossom, R.J., 1986. The Atok Platinum Mine. *In:* Anhaeuser, C.R., and Maske, S., Eds., *Mineral Deposits of Southern Africa, Vol. II, Geol.Soc.S.Afr.,* 1143-1154.

Park, R.G., 1983. Foundations of Structural Geology. Blackie, London, 135 pp.

Ramsay, J.G., 1991. Emplacement kinematics of a granite diapir: the Chindamora batholith, Zimbabwe. J.Struct.Geol., **11**, 1/2, 191-209.

Rhodes, R.C., 1975. New evidence for impact origin of the Bushveld Complex, South Africa. Geology, **3,** 549-554.

Sawkins, F.J., 1984. Metal deposits in relation to plate tectonics. Berlin: Springer Verlag, 322 pp.

Schiffries, C.M., and Skinner, B.J., 1987. The Bushveld hydrothermal system: Field and petrologic evidence. Am. J. Sci., **287**, 566-595

Schweitzer, J.K., and Hatton, C.J., 1995a. Synchronous emplacement of the felsites, granophyres, granites and mafic intrusives of the Bushveld Complex (abstract). Geocongress '95, Centennial, Geological Society of South Africa, Johannesburg, April 3-7, 532-535.

Schweitzer, J.K., and Hatton, C.J., 1995b. Chemical alteration within the volcanic roof rocks of the Bushveld Complex. Economic Geology, in press.

Schweitzer, J.K., Hatton, C.J., and de Waal, S. A., 1995a. Economic potential of the Rooiberg Group - volcanic rocks in the floor and roof of the Bushveld Complex. Mineralium Deposita **30,** 168-177.

Schweitzer, J.K., Hatton, C.J., and de Waal, S.A., 1995b. Regional lithochemical stratigraphy of the Rooiberg Group: a proposed new subdivision. South African Journal of Geology, **98/3**, 245-255.

Scoon, R.S., and Mitchell, A.A., 1994. Discordant Iron-Rich Ultramafic Pegmatites in the Bushveld Complex and their Relationship to Iron-Rich Intercumulus and Residual Liquids. J.Petr., **35/4**, 881-917.

Scoon, R.N., and Teigler, B., 1994. Platinum-group element mineralization in the Critical Zone of the western Bushveld Complex: I. Sulfide-poor chromitites below the UG-2. Economic Geology, **89**, 1094-1121.

Scoon, R.N., and Teigler, B., 1995. A new LG-6 chromitite reserve at Eerste Geluk in the boundary zone between the central and southern sectors of the Eastern Bushveld Complex: I. Sulfide-poor chromitites below the UG-2. Economic Geology, **90**, in press.

Sharpe, M.R., 1982. Noble metals in the marginal rocks of the Bushveld Complex. Economic Geology, **77**, 1286-1295.

Sharpe, M.R., 1985. Strontium isotope evidence for preserved density stratification in the main zone of the Bushveld Complex, South Africa. Nature, **316/11**, 119-126.

South African Committee for Stratigraphy (SACS), 1980. Lithostratigraphy of the Republic of South Africa, South West Africa/Namibia, and the Republic of Bophuthatswana, Transkei and Venda. Handbook of the Geological Survey of South Africa, **8**, 633 pp.

Streckeisen, A., 1976. To each plutonic rock its proper name. Earth Science Reviews, **12**, 1-33.

Truter, F.C., 1949. A review of volcanism in the geological history of South Africa. Trans.Geol.Soc.S.Afr., **52**, XXXIX-IXXXIX.

Twist, D., and Harmer, R.E., 1987. Geochemistry of contrasting siliceous magmatic suites in the Bushveld Complex: genetic aspects and implications for tectonic discrimination diagrams. J.Volcanol.Res, **32**, 83-98.

Twist, D., and French, B.M., 1983. Voluminous acid volcanism in the Bushveld Complex: a review of the Rooiberg Felsite. Bull.Volcanol., **46**, 225-242.

Vermaak, C.F., 1986. Summary Aspects of the Economics of Chromium with special Reference to Southern Africa. *In:* Anhaeuser, C.R., and Maske, S., Eds., *Mineral Deposits of Southern Africa, Vol. II, Geol.Soc.S.Afr.*, 1155-1181.

Viljoen, M.J., 1994. A Review of Regional Variations in Facies and Grade Distribution of the Merensky Reef, Western Bushveld Complex with some Mining Implications. XVth CMMI Congress, Johannesburg, SAIMM, **3**, 183-194.

Viljoen, M.J., and Hieber, R., 1986. The Rustenberg Section of Rustenberg Platinum Mines Limited, with Reference to the Mersensky Reef. *In:* Anhaeuser, C.R., and Maske, S., Eds., *Mineral Deposits of Southern Africa, Vol. II, Geol.Soc.S.Afr.,* 1107-1134.

Viljoen, M. J., and Scoon, R.N., 1985. The distribution and main geologic features of discordant bodies of iron-rich ultramafic pegmatite in the Bushveld Complex. Economic Geology, **80**, 1109-1128.

Von Gruenewaldt, G., 1972. The origin of the roof-rocks of the Bushveld Complex between Tauteshoogte and Paardekop in the eastern Transvaal. Trans.Geol.Soc.S.Afr., **75**, 121-134.

Von Gruenewaldt, G., and Worst, B.G., 1986. Chromitite Deposits at Zwartkop Mine, Western Bushveld Complex.*In:* Anhaeuser, C.R., and Maske, S., Eds., *Mineral Deposits of Southern Africa, Vol. II, Geol.Soc.S.Afr.,* 1217-1227.

Wagner, P.A., 1929. The platinum deposits and mines of South Africa. Oliver & Boyd, Edinburgh, 588pp.

Wager, L.R., and Brown, G.M., 1968. Layered Igneous Rocks. Oliver & Boyd, Edinburgh, 588pp.

Walraven, F., 1974. Tectonism during the Emplacement of the Bushveld Complex and the resulting Fold Structures. Trans.Geol.Soc.S.Afr., **77**, 323-328.

Walraven, F., 1979. Granophyre - lava relations in the Bushveld Complex. Annals Geological Survey South Africa, **13**, 59-80.

Walraven, F., 1995. Geochronology of the Rooiberg Group, Transvaal Supergroup, South Africa. Chemical Geology and Isotope Geosciences, in press.

Walraven, F., Armstrong, R.A., and Kruger, F.J., 1990. A chronostratigraphic framework for the north-central Kaapval Craton, the Bushveld Complex and the Vredefort structure. Tectonophysics, **171,** 23-48.

Wepf, D.T., and Wolf, J.P., 1989. Time domain dam-reservoir-interaction analysis based on boundary elements. *In:* Clough, R.W., and Zhang, G., Eds., *Earthquake behaviour of an arch dam.* China-U.S. Workshop, Proceedings, Oxford, International Academic Publishers, 130-147.

Worst, B.G., 1986a. The Chromitite Deposits of the Montrose and Groothoek Mines, Eastern Bushveld Complex. *In:* Anhaeuser, C.R., and Maske, S., Eds., *Mineral Deposits of Southern Africa, Vol. II, Geol.Soc.S.Afr.,* 1189-1195.

Worst, B.G., 1986b. The Chromitite Deposits at Kroondaal Chrome Mine, Western Bushveld Complex. *In:* Anhaeuser, C.R., and Maske, S., Eds., *Mineral Deposits of Southern Africa, Vol. II, Geol.Soc.S.Afr.,* 1209-1215.

Appendix: Figures and Tables

TABLE 1: Whole-rock analyses of Bushveld Complex cumulates from Amplats Union Section (de Klerk, 1982)

	1	2	3	4
SiO_2	48.10	42.10	48.70	48.90
TiO_2	0.08	0.15	0.09	0.08
Al_2O_3	30.00	4.10	26.30	27.00
Fe_2O_3	0.36	2.41	0.52	0.37
FeO	1.82	12.05	2.61	1.83
MnO	0.02	0.19	0.06	0.03
MgO	1.70	28.10	4.90	4.60
CaO	14.60	2.62	13.20	13.50
Na_2O	2.20	0.40	1.90	2.10
K_2O	0.14	0.09	0.15	0.14
P_2O_5	0.03	0	0.03	0
LOI	0.13	6.02	0.91	0.33
TOTAL	99.18	98.23	99.37	98.88
Sr	470	58	52	337
Rb	nd	4	5	nd
Y	nd	nd	7	4
Zr	6	14	20	7
Nb	nd	nd	nd	nd
Co	9	182	107	21
Cr	66	3503	2856	560
V	17	68	130	32
Cu	16	1100	350	60
Ni	80	4700	1540	280

1 = Mottled anorthosite footwall to Merensky Reef

2 = Merensky Reef pegmatoidal harzburgite

3 = Merensky unit feldspathic pyroxenite

4 = Merensky unit norite

Table 1: Average major and selected trace element composition of strata associated with the Merensky Reef. Note the significant variations in Al_2O_3, FeO, MgO and base metal (Co, Cr, V, Cu, and Ni) concentrations. These compositional variations are likely to also be reflected in the rock engineering properties.

AREA	LAYER	AVE THICK.	% Cr_2O_3	% FeO	% Al_2O_3	% MgO	% SiO_2	% TiO_2	% V_2O_5	Cr/Fe	MgO/FeO	Cr/Al
South of Steelpoort River	UG2	1,29	43,70	28,28	17,74	7,36	0,02	1,63	-	1,36	0,26	2,46
	UG1	1,68	44,67	30,42	14,99	7,64	0,11	-	-	1,29	0,25	2,98
	MG	6,55t	37,80	25,55	15,95	7,50	-	-	-	1,30	0,29	2,37
	Main (F)	1,56	45,94	25,79	16,18	9,07	1,41	1,29	-	1,57	0,35	2,84
Eastern Belt	UG2	0,77	42,60	27,50	17,10	8,00	0,50	0,90	-	1,36	0,29	2,49
	UG1	1,13	42,87	30,27	15,70	8,74	-	0,76	-	1,25	0,29	2,73
	MG	0,27	43,68	29,86	15,94	8,36	0,06	0,87	0,57	1,29	0,28	2,74
	LG7	0,39	42,78	28,21	17,40	9,88	0,06	0,67	0,36	1,33	0,35	2,46
	LG6 Ldr	0,34	47,12	27,22	12,77	9,58	0,17	0,56	0,45	1,52	0,35	3,69
	LG6 (Steelp)	1,05	47,36	25,26	14,49	10,85	0,09	0,51	0,45	1,65	0,43	3,27
	LG6 Lwr	0,22	47,80	24,72	15,32	11,00	0,03	0,74	0,30	1,70	0,44	3,12
	LG5	Thin*	48,95	24,50	14,83	10,49	0,08	0,63	0,30	1,76	0,43	3,30
	LG3	0,38	49,10	24,58	14,34	10,30	0,02	0,56	0,30	1,76	0,42	3,42
	LG2	0,48	48,94	22,19	14,44	11,25	0,06	0,57	0,30	1,94	0,51	3,39
Western Belt	UG2	1,22	43,67	28,50	16,67	9,50	-	-	-	1,35	0,33	2,62
	UG1	1,14	43,83	30,42	14,33	8,08	-	-	-	1,27	0,26	3,06
	MG4	1,78	44,17	28,33	16,92	8,58	-	-	-	1,37	0,30	2,61
	MG3	0,95	43,50	27,17	17,17	9,00	-	-	-	1,41	0,33	2,53
	MG2	1,78	45,25	26,13	17,00	9,12	-	-	-	1,52	0,35	2,66
	MG1	0,76	45,10	27,50	16,40	9,00	-	-	-	1,44	0,33	2,75
	MGt	5,27	44,56	27,42	16,83	8,89	-	-	-	1,43	0,32	2,65
	LG7	0,28	45,67	27,00	16,00	9,17	-	-	-	1,49	0,34	2,85
	LG6	0,87	46,30	25,75	15,55	10,00	-	-	-	1,58	0,39	2,98
	LG5	0,58	47,50	25,75	14,50	10,37	-	-	-	1,62	0,40	3,27
	LG4	0,34	51,25	21,25	11,75	13,50	-	-	-	2,12	0,63	4,36
	LG3	0,18*	51,67	22,67	12,00	12,30	-	-	-	2,01	0,54	4,30
	LG2	0,19*	51,00	24,00	12,67	11,00	-	-	-	1,87	0,46	4,02
	LG1	0,31	50,17	23,66	14,67	9,67	-	-	-	1,87	0,41	3,42
Marico	Upper	0,46	43,3	18,9	-	-	-	-	-	2,02	-	-
	Middle	0,38	48,13	23,07	12,85	12,13	-	0,90	-	1,84	0,52	3,74
	Lower	0,84	45,45	19,49	16,66	13,06	-	2,83	-	2,05	0,67	2,73
Potgietersrus	Grasv-L	0,41	55,29	20,36	10,15	11,97	0,17	0,21	-	2,39	-	-
	Grasv-U	0,38	56,29	18,82	10,26	12,19	0,31	0,21	-	2,63	-	-
	Zufin L	0,32	52,43	20,75	13,15	9,62	-	0,39	-	2,22	-	-
	Zufin U	0,30	-	-	-	-	-	-	-	-	-	-

* Omitted from calculation Ldr = Leader Lwr = Lower

Table 2: Orebody thicknesses, element concentrations and ratios for selected elements for chromitite layers contained in the lower, middle and upper group chromitites.

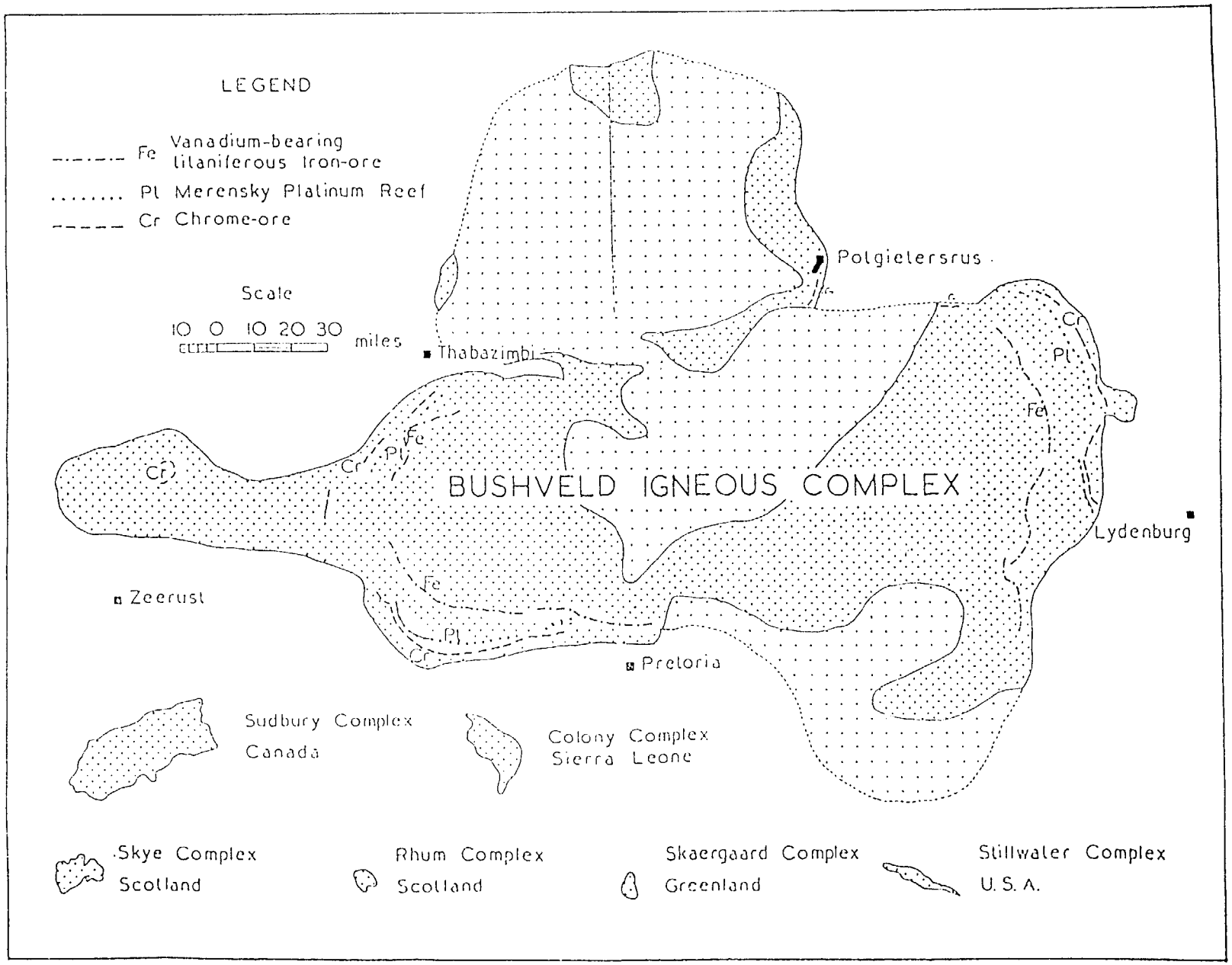

Figure 1: Schematic outline of the Bushveld Igneous Complex, also showing the distribution of the major chromitite and platinum bearing horizons. The real size of other, major intrusions are compared to the size of the Bushveld Igneous event.

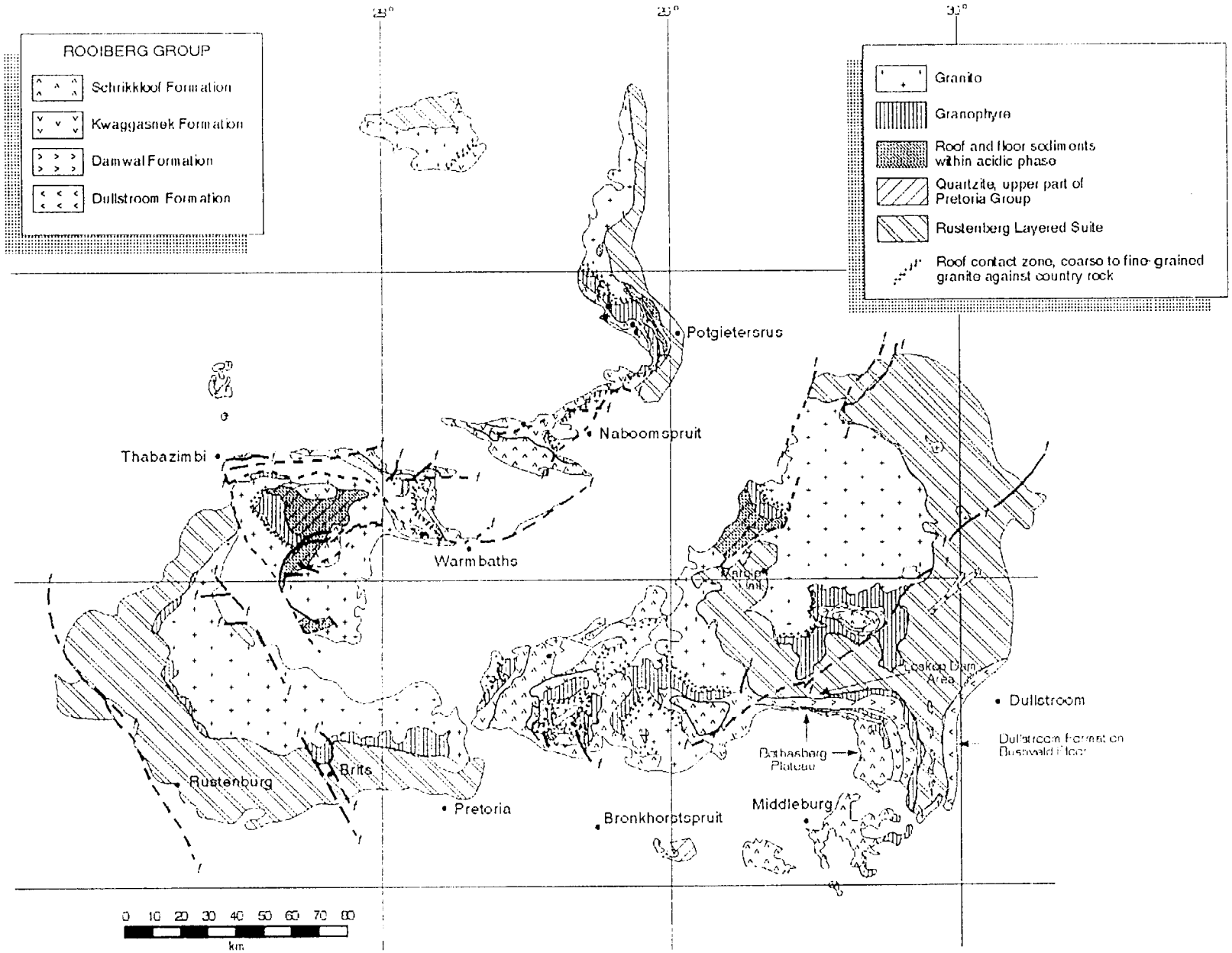

Figure 2: Geological map of the Bushveld Igneous event delineating the distribution of the Rustenburg Layered Suite, Rashoop Granophyre Suite, the Rooiberg Group, and the Lebowa Granite Suite (modified after Schweitzer et al., 1995b). The platinum and chromitite orebodies, the major concern of this study, are confined to the mafic intrusives of the Rustenburg Layered Suite.

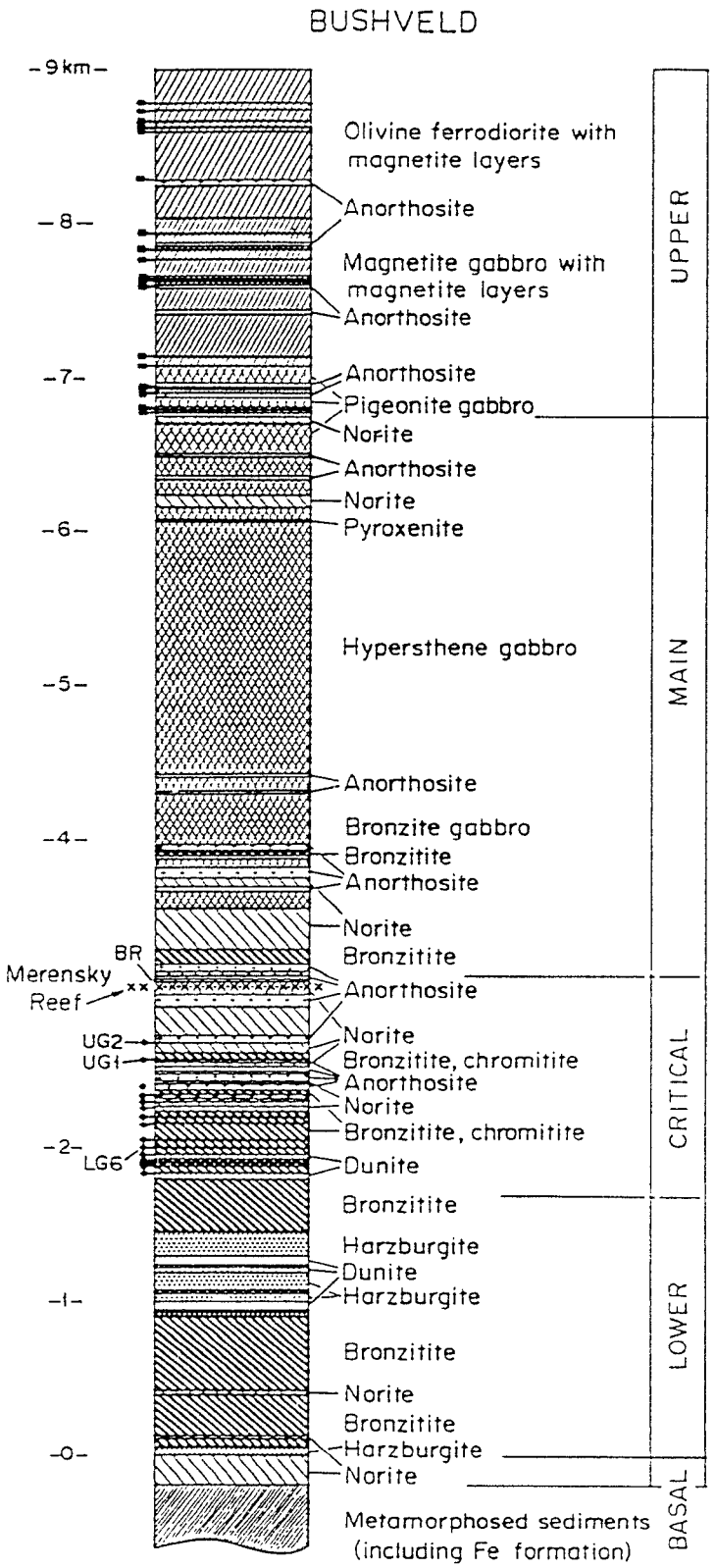

Figure 3: Generalised stratigraphic section through the mafic rocks of the Rustenburg Layered Suite, identifying the lower-, critical-, main-, and upper zones (modified after Irvine et al., 1983). The approximate positions of the lower, middle, and upper chromitite layers, and the Merensky and Bastard (BR) reefs are also identified.

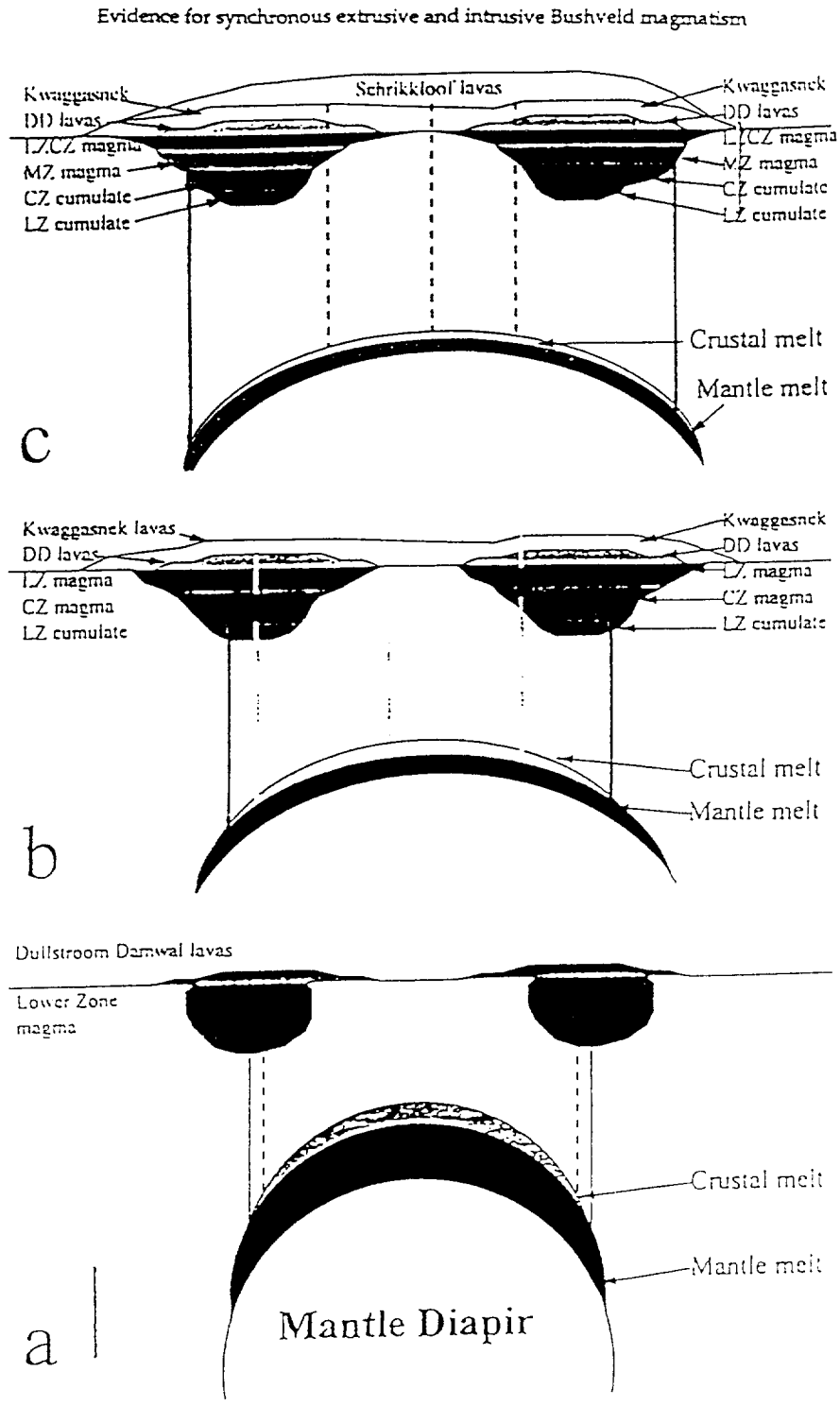

Figure 4: Schematic diagram depicting the proposed mantle plume origin of the Bushveld Igneous Complex (modified after Hatton and Schweitzer, 1995). Considered is the contemporaneous development of the Rustenburg Layered Suite and the volcanic rocks of the Rooiberg Group.

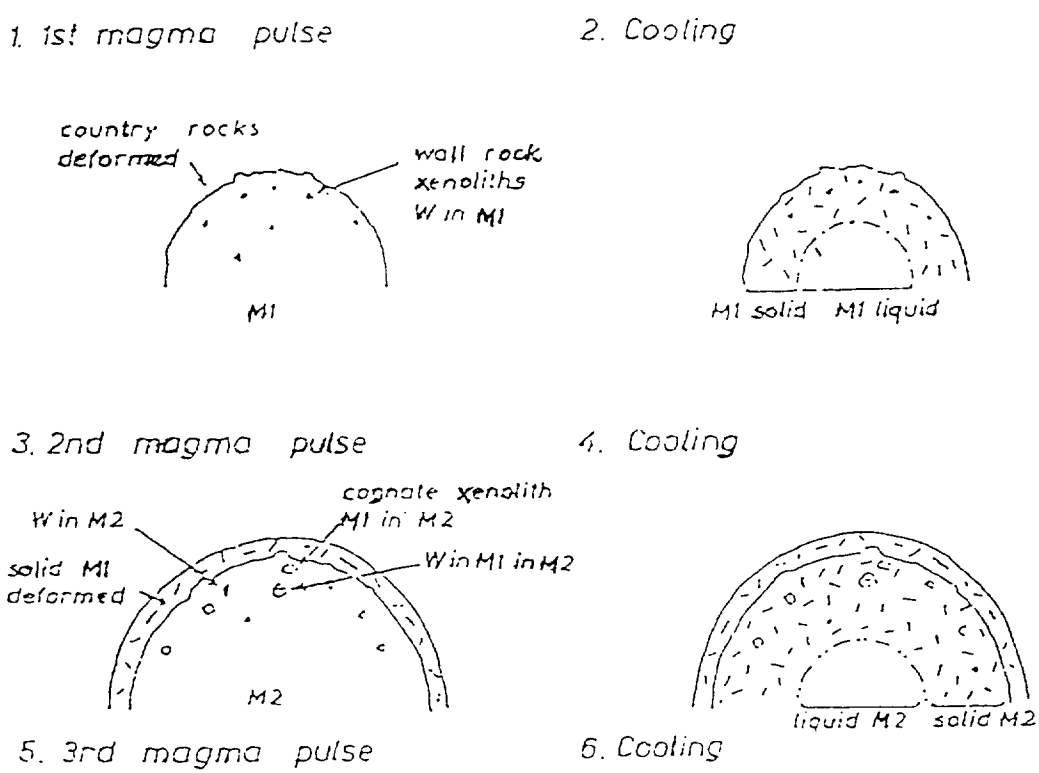

Figure 5: Suggested scheme for the intrusion of a granite body (modified after Ramsay, 1991). Granite bodies are the most prominent rocks in the central portion of the Bushveld Igneous Complex (see Figure 2). These intrusion are therefore suggested to have influenced the regional stress pattern.

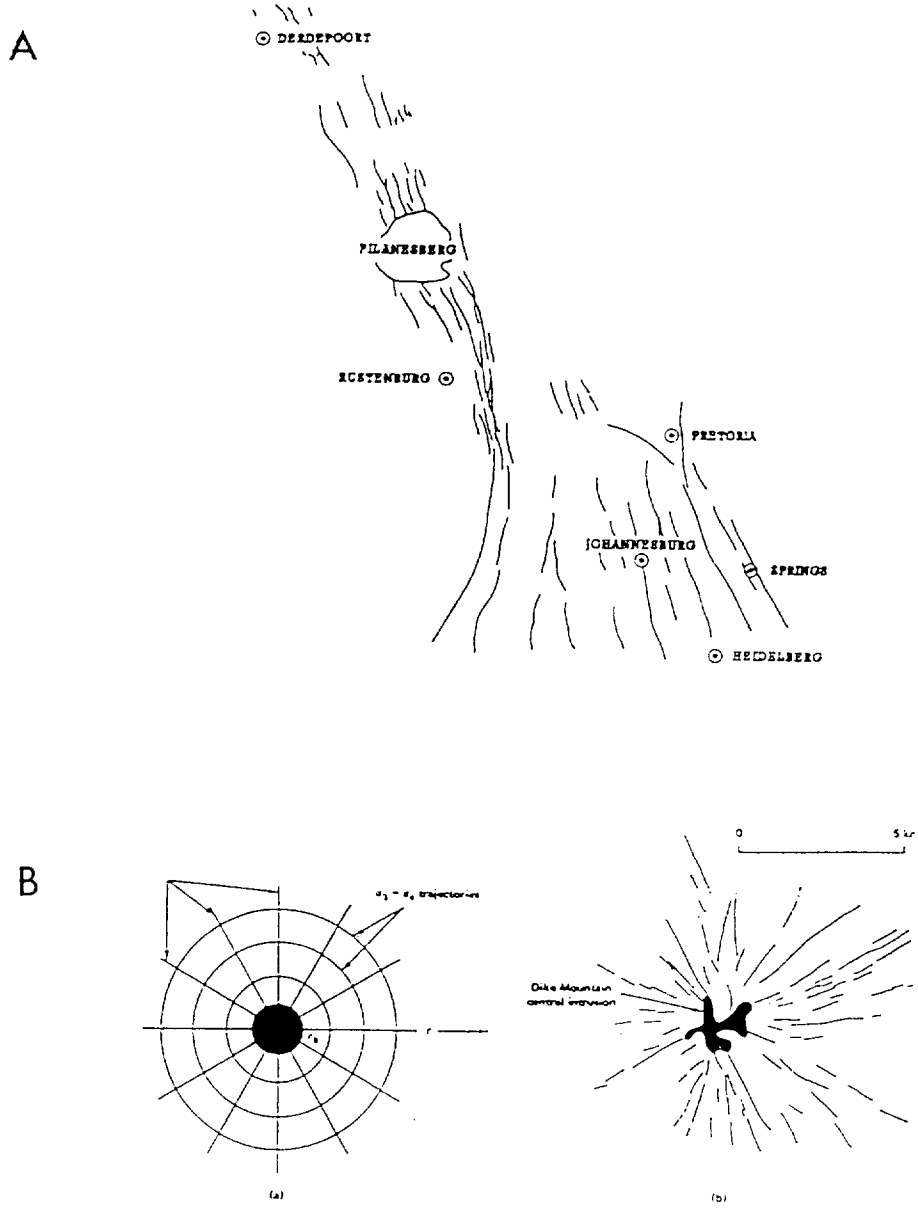

Figures 6a and b: Dyke swarm related to the Pilansberg Complex, in the western portion of the Bushveld Complex (Fig. 6a; after De Maar and Holder, 1994). These dykes also intruded the strata associated with the platinum and chromitite deposits. The Pilansberg dyke orientation is compared to the dyke pattern as observed around the Dyke Mountain Intrusion, Colorado (after Park, 1983).

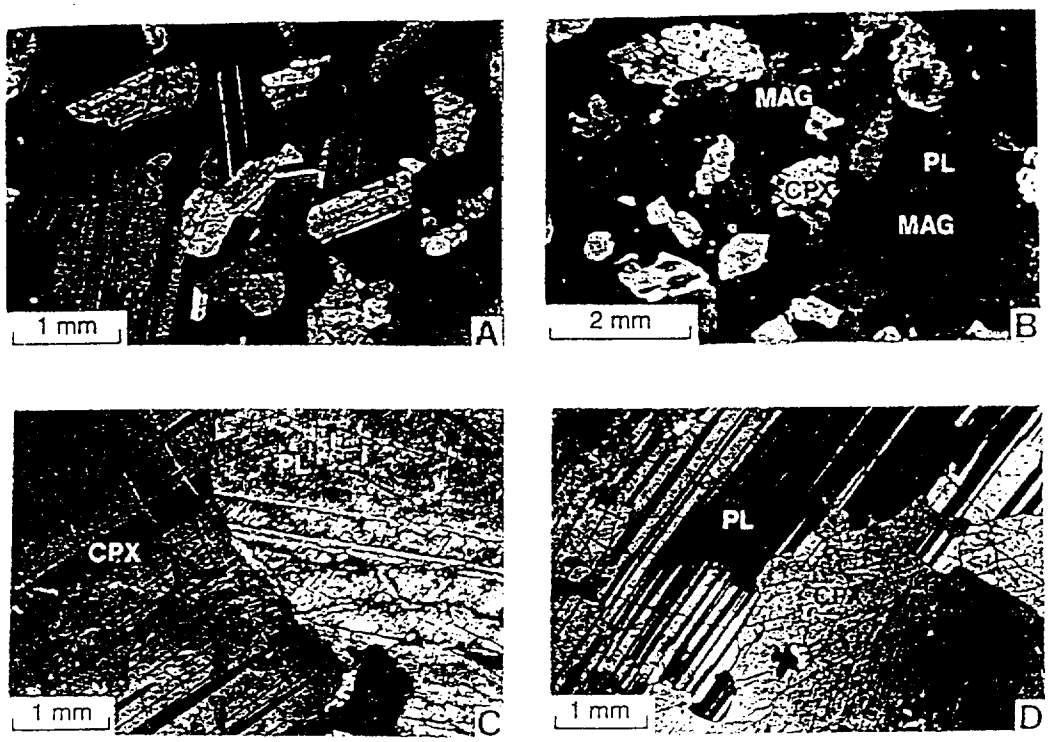

Figures 7a to d: Textures encountered in anorthosite and pegmatoid from the upper critical zone (after Scoon and Mitchell, 1994). Predominantly straight grain boundaries of twinned plagioclase and pyroxene (a), plagioclase enclosing clinopyroxen exhibiting irregular grain boundaries (b), and intergrowths of plagioclase and clinopyroxene with regular and irregular contact relationships (c and d) are encountered. Also note the distinct variations in grain sizes.

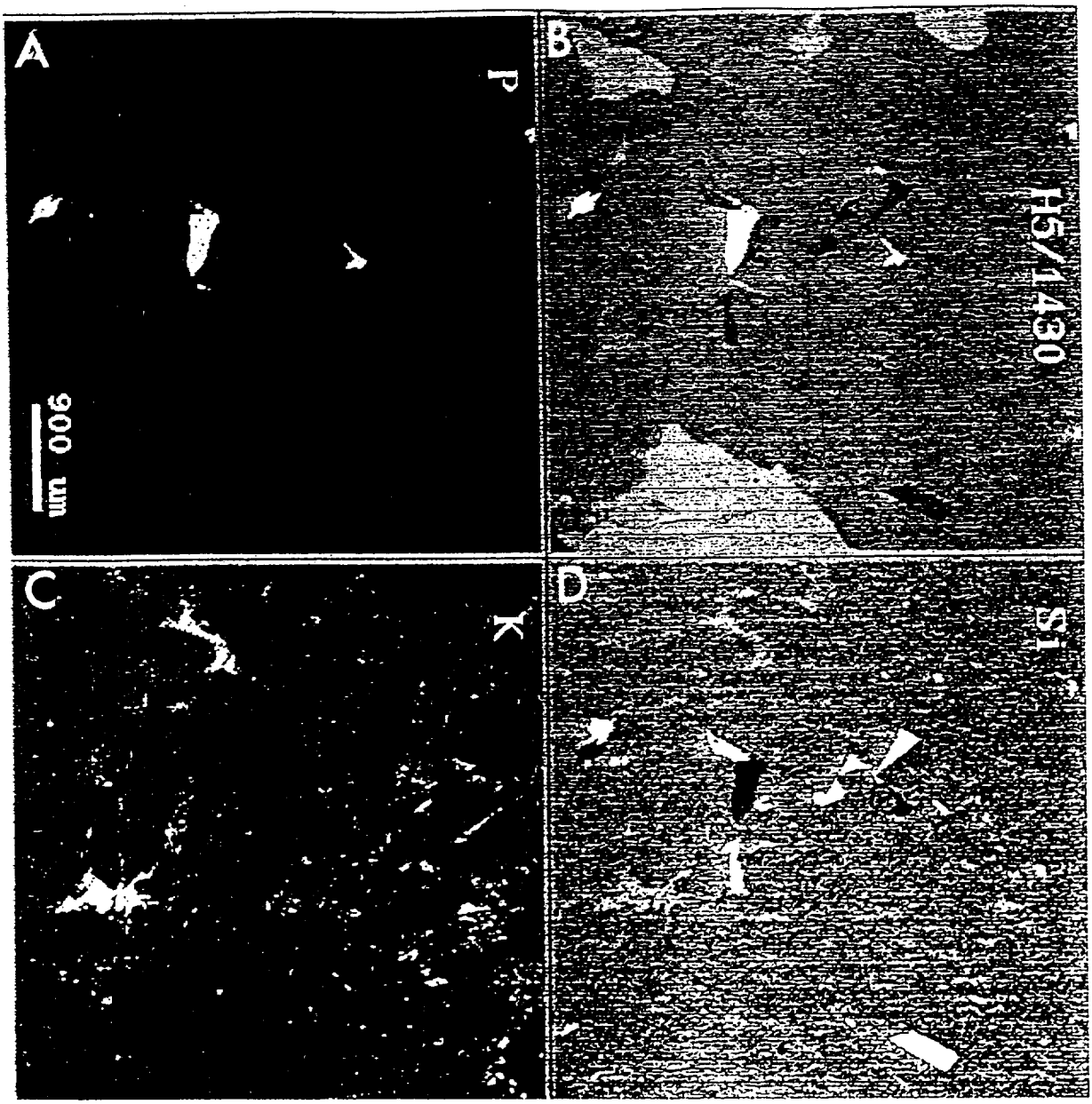

Figures 8a to d: Scanning electron microscope images of a mottled anorthosite from the main zone of the Rustenburg Layered Suite in the vicinity of Brits. Clockwise from top left: a) X-ray map for phosphorous, showing interstitial apatite (white) b) Backscattered electron (BSE) image showing apatite (very pale grey), augite (pale grey), plagioclase (large areas of dark grey) and quartz (very dark grey) c) X-ray map for potassium (K), indicating extensive, but patchy sericitization of plagioclase d) Energy dispersive (EDS) x-ray map for silica (Si), clearly showing interstitial quartz (white) and apatite (black).

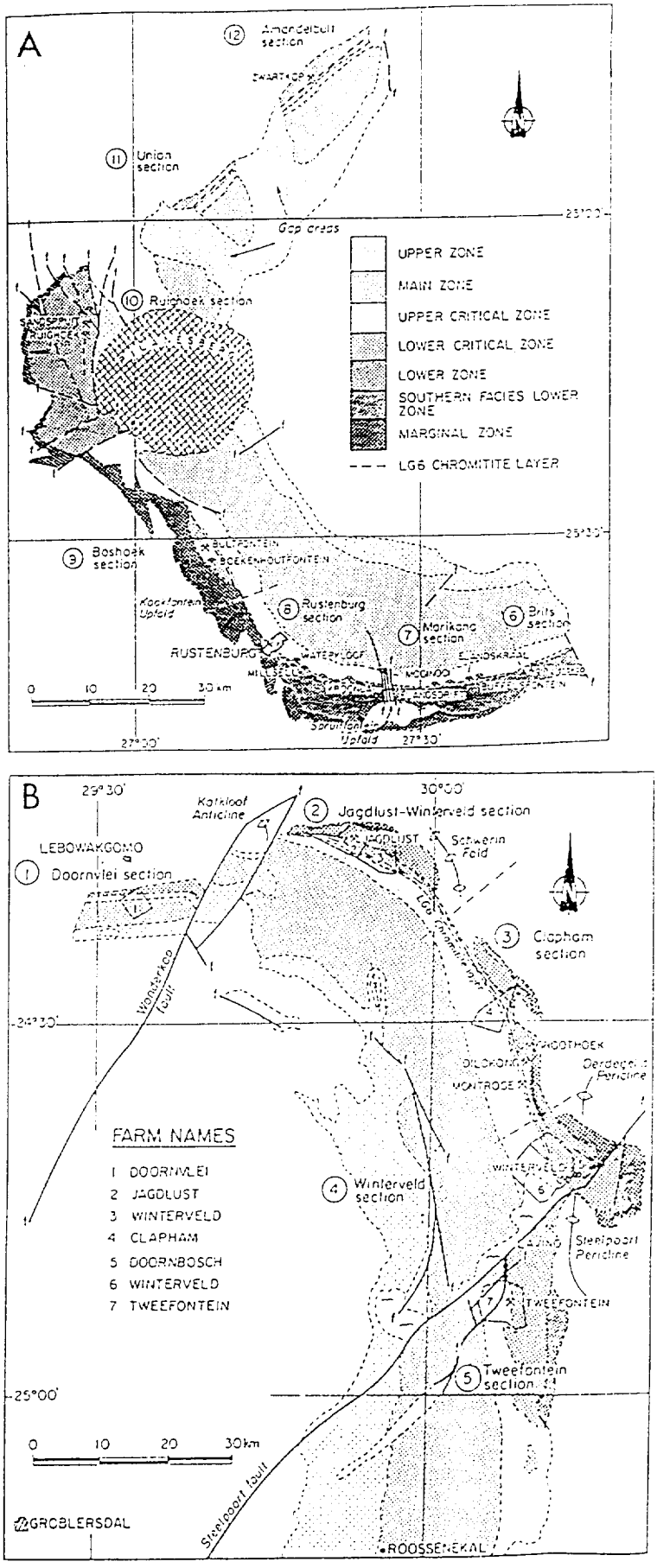

Figures 9a and b: Geographic position of the chromitite mines in the western and far western (a) and eastern (b) compartments of the Bushveld Complex (modified after Hatton and von Gruenewaldt, 1985). Crossed hammers indicate the positions of chrome mines.

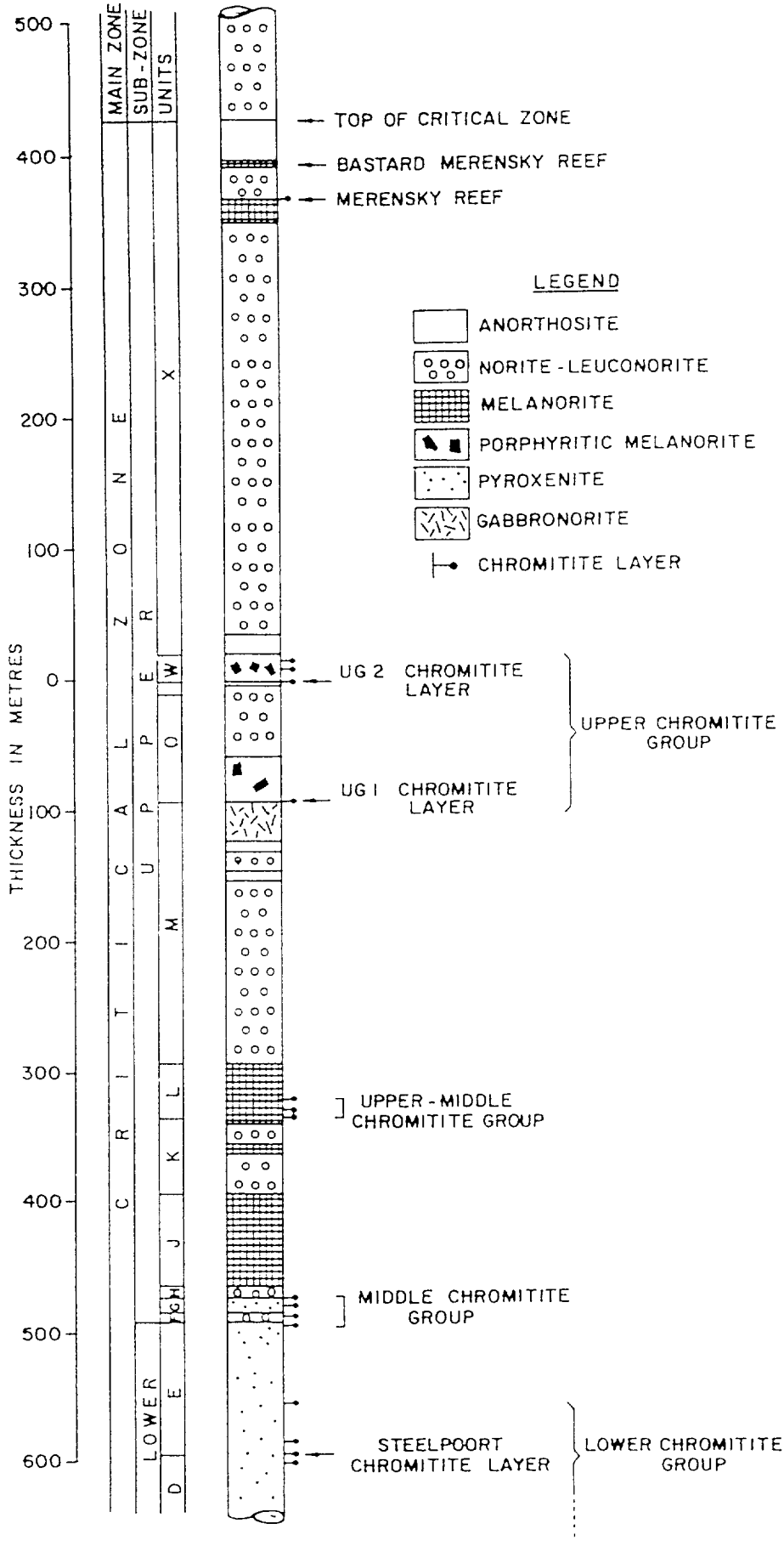

Figure 10: Generalised stratigraphic column identifying the stratigraphic position of the lower, middle and upper chromitite groups, with each group containing several chromitite layers (after Gain, 1984).

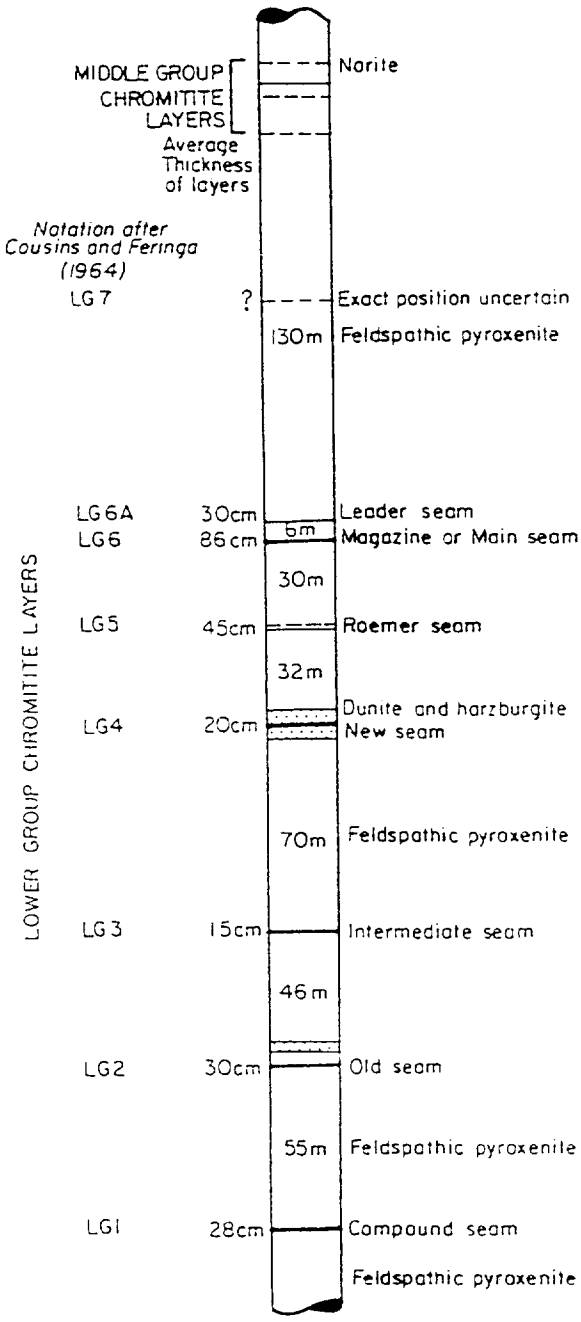

Figure 11: Stratigraphic section delineating the stratigraphic position of the lower group (LG) chromitite layers as observed at Zwartkop (after Hatton and von Gruenewaldt, 1984).

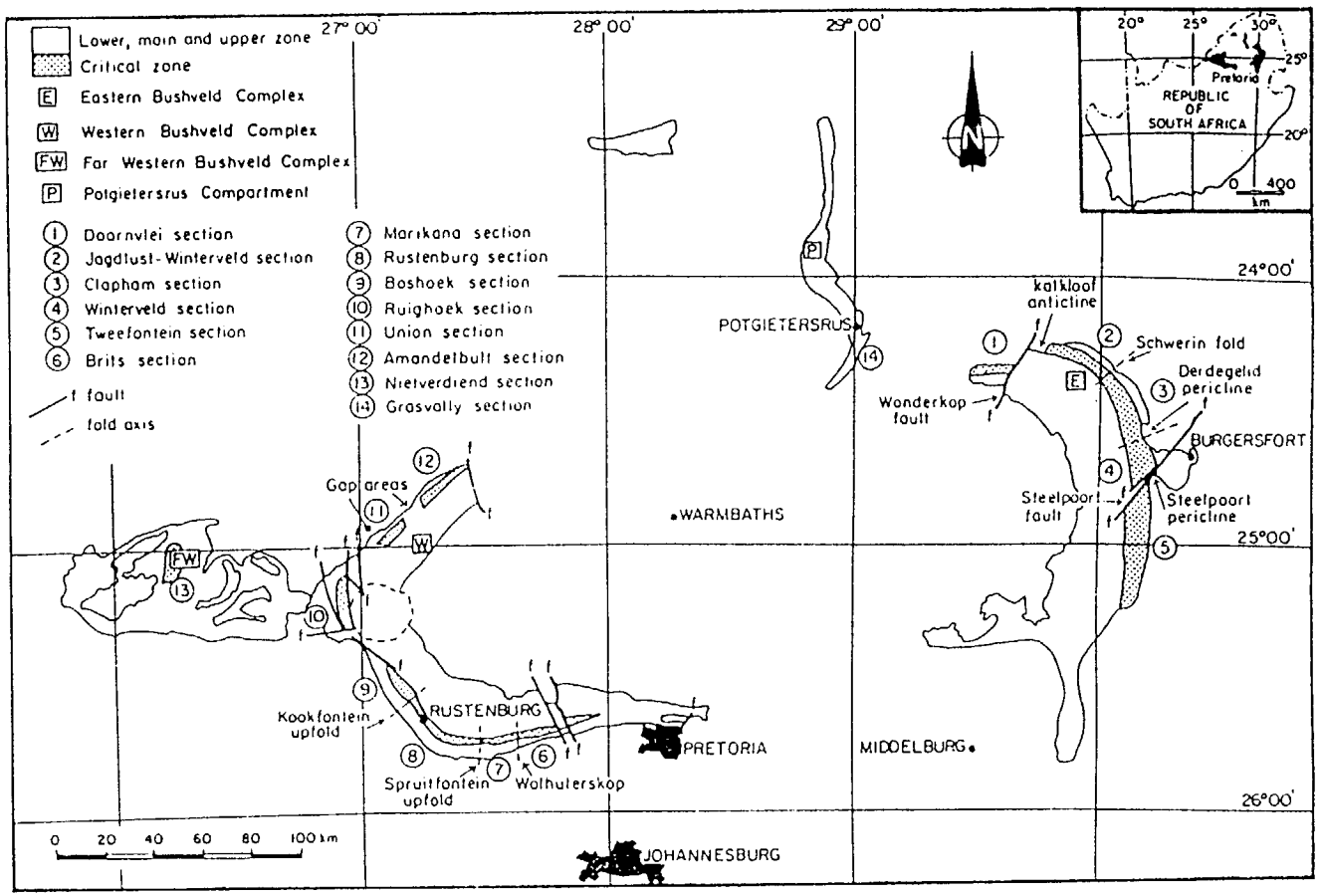

Figure 12: Map of the Bushveld Complex identifying the section lines along which the stratigraphic sections for the middle and upper chromitite groups were drawn (after Hatton and von Gruenewaldt, 1985; see Figures 13 and 14).

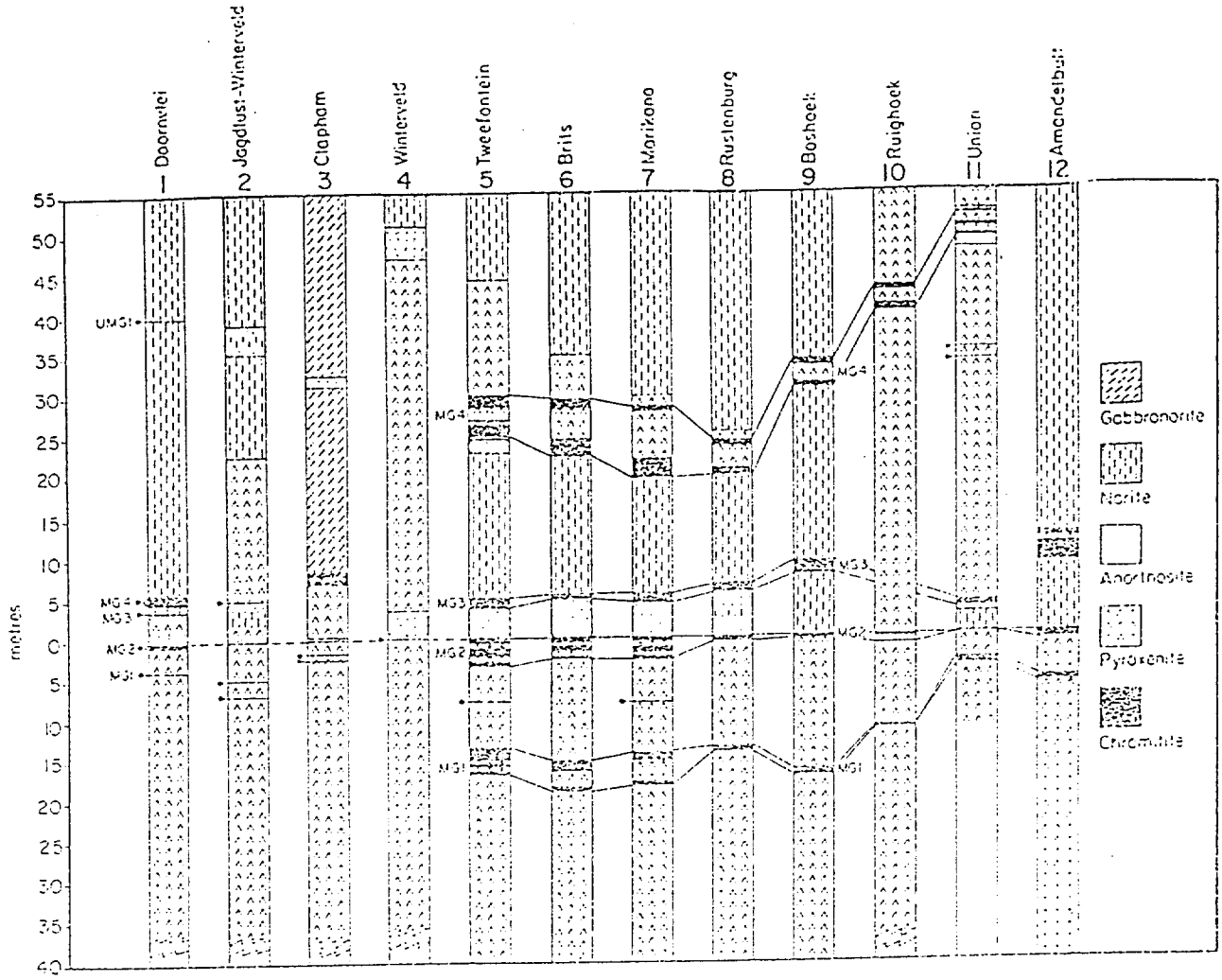

Figure 13: Stratigraphic position and rock assemblages of the middle group chromitite layers. Note the distinct footwall/hangingwall assemblages for the sections (after Hatton and von Gruenewaldt, 1985). Refer to Figure 12 for the position of the various stratigraphic columns.

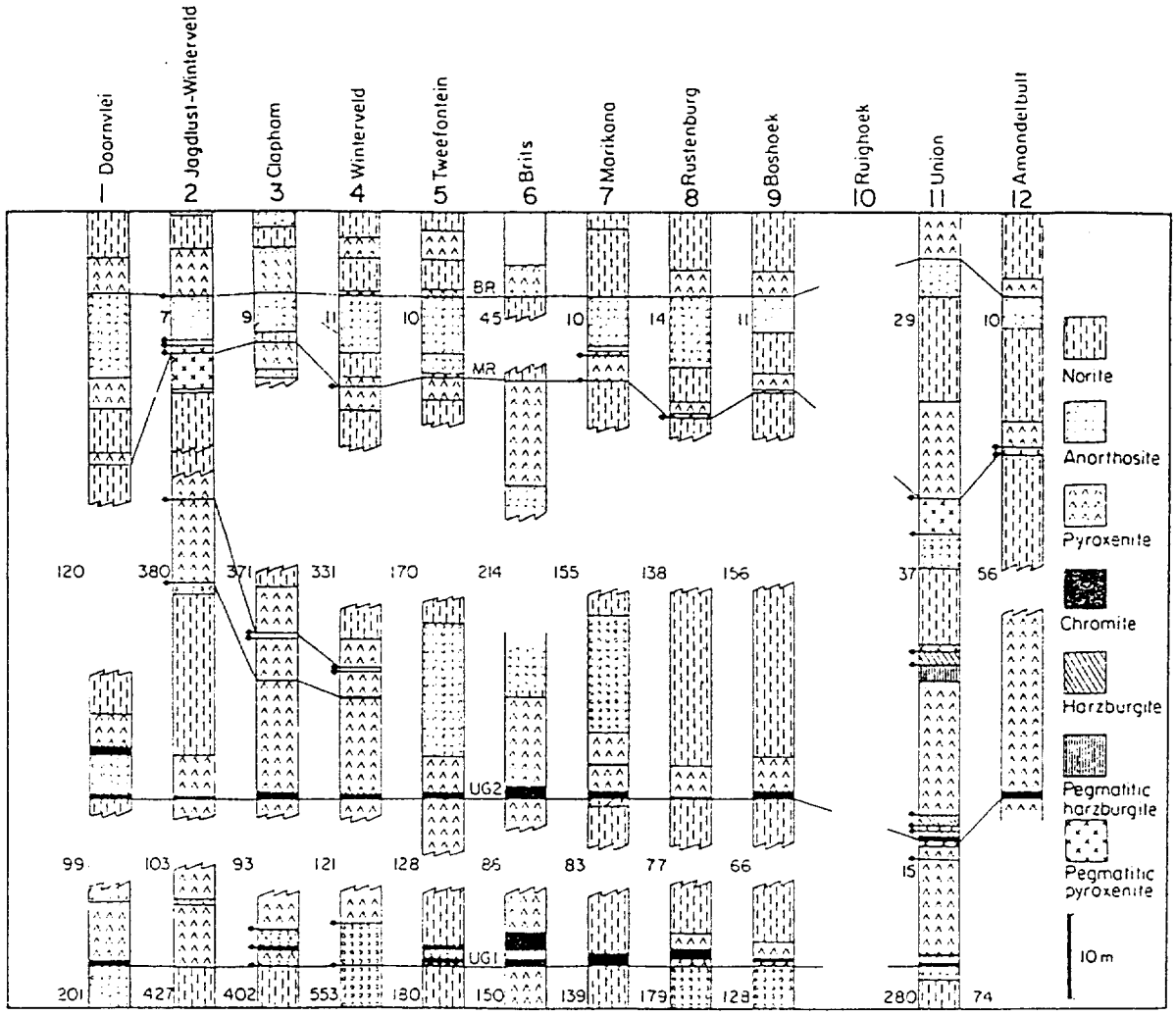

Figure 14: Footwall and hangingwall rock assemblages as associated with the upper group chromitite layers (after Hatton and von Gruenewaldt, 1985). The geographic position of the stratigraphic sections are given in Figure 12.

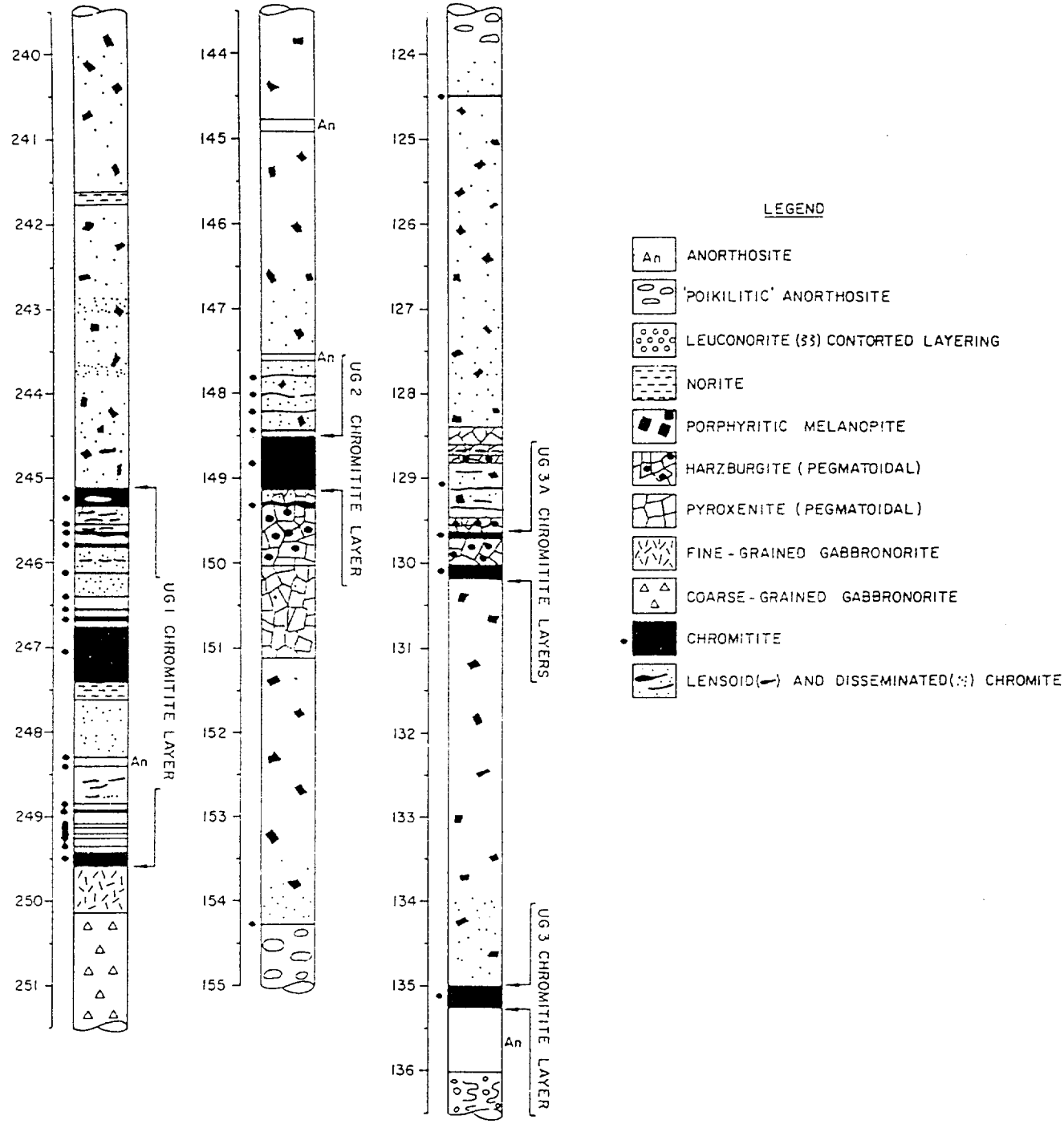

Figure 15: Detailed stratigraphic column delineating the complex assemblage of rock types as associated with the UG1, UG2, UG3 and UG3A of the upper group chromitites (after Gain, 1984).

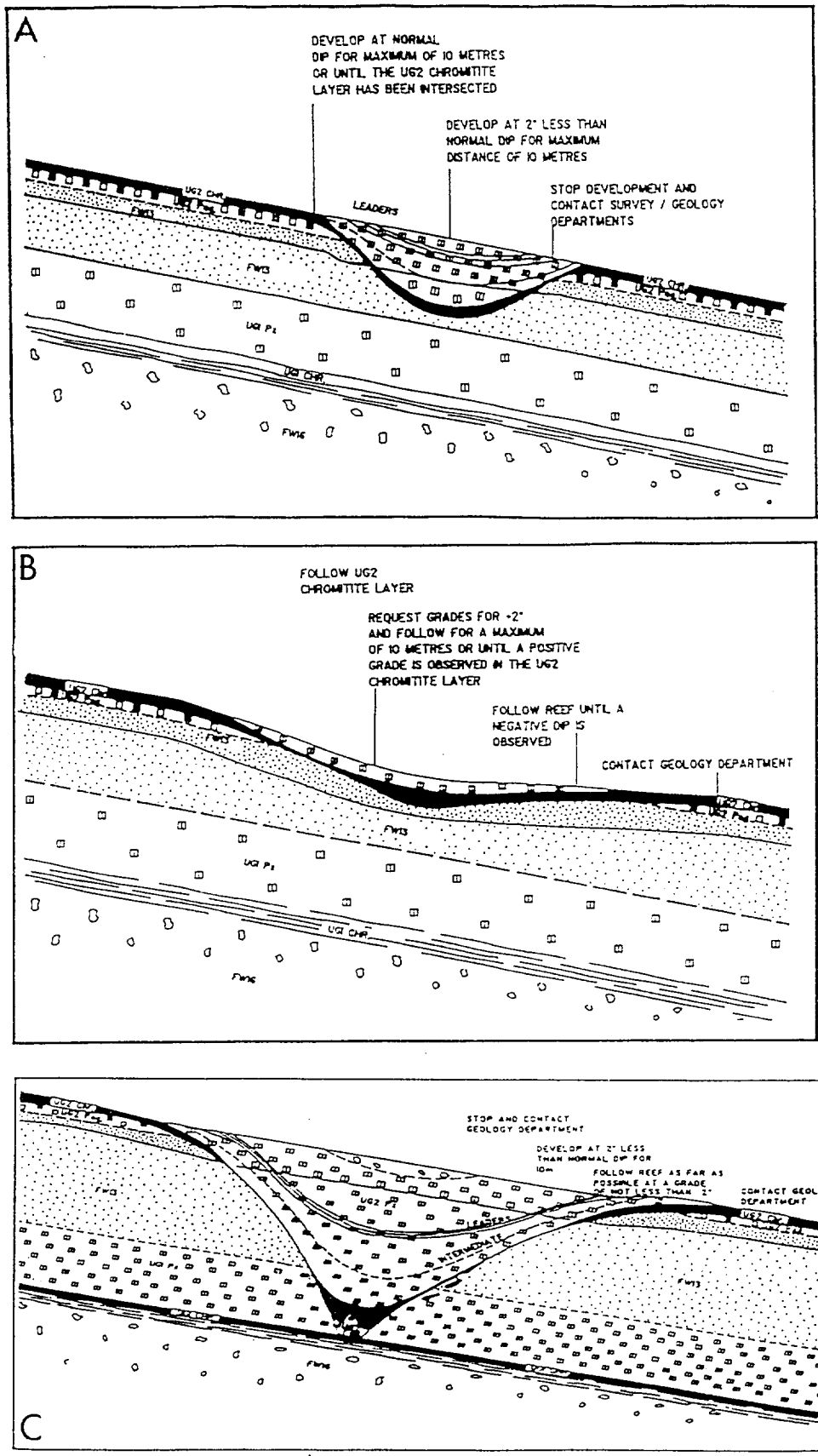

Figures 16a to c: Type 1, 2 and 3 chromitite potholes as associated with the UG2 chromitite layer (after Hahn and Vendale, 1994). Note that the potholes straddle different footwall lithologies.

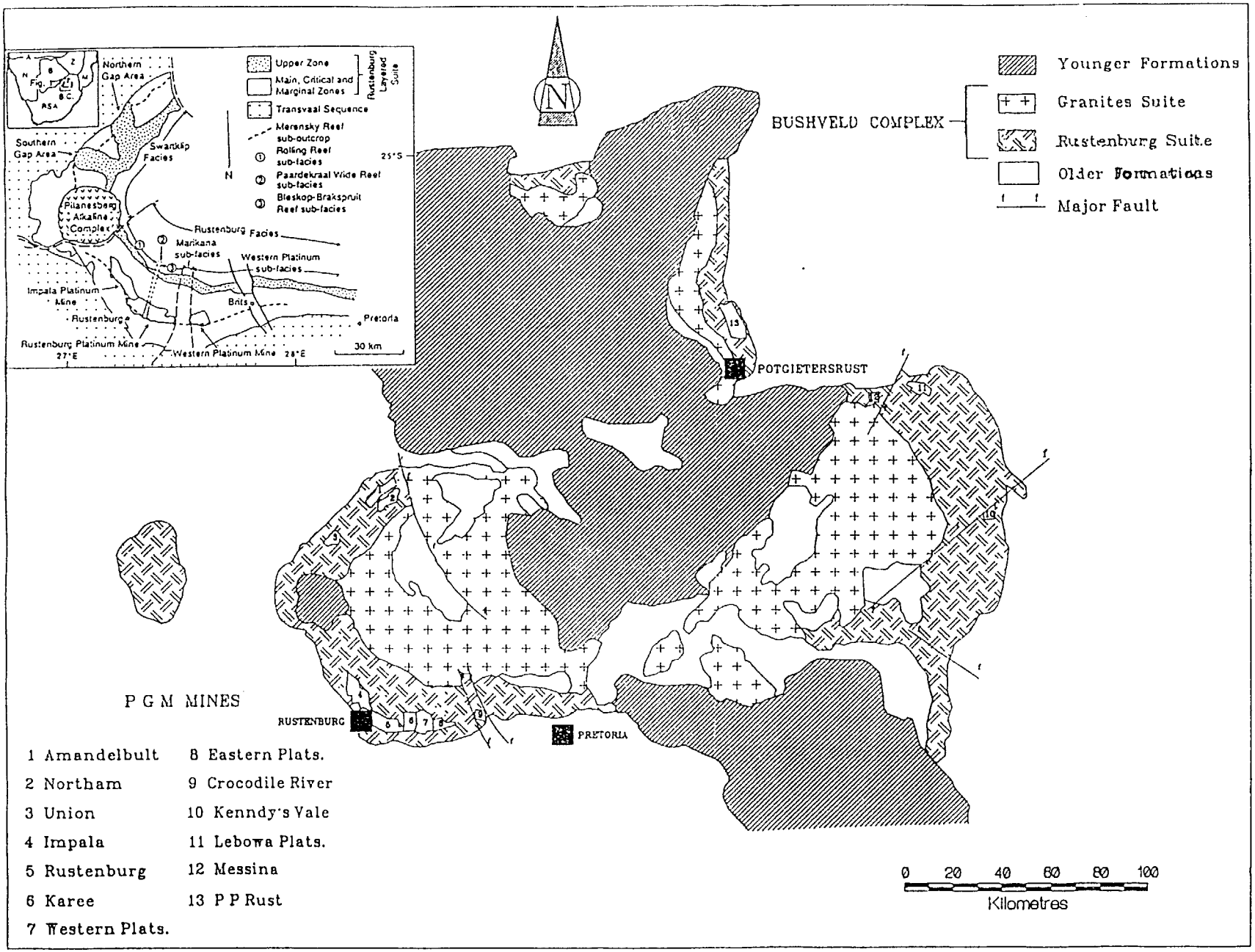

Figure 17: Geographic position of the eastern and western Bushveld platinum ore producers (Barry and Odendaal, 1993). Inset delineates the geographic distribution of the various facies and subfacies as encountered in the western Bushveld Complex (modified after Carr et al., 1994).

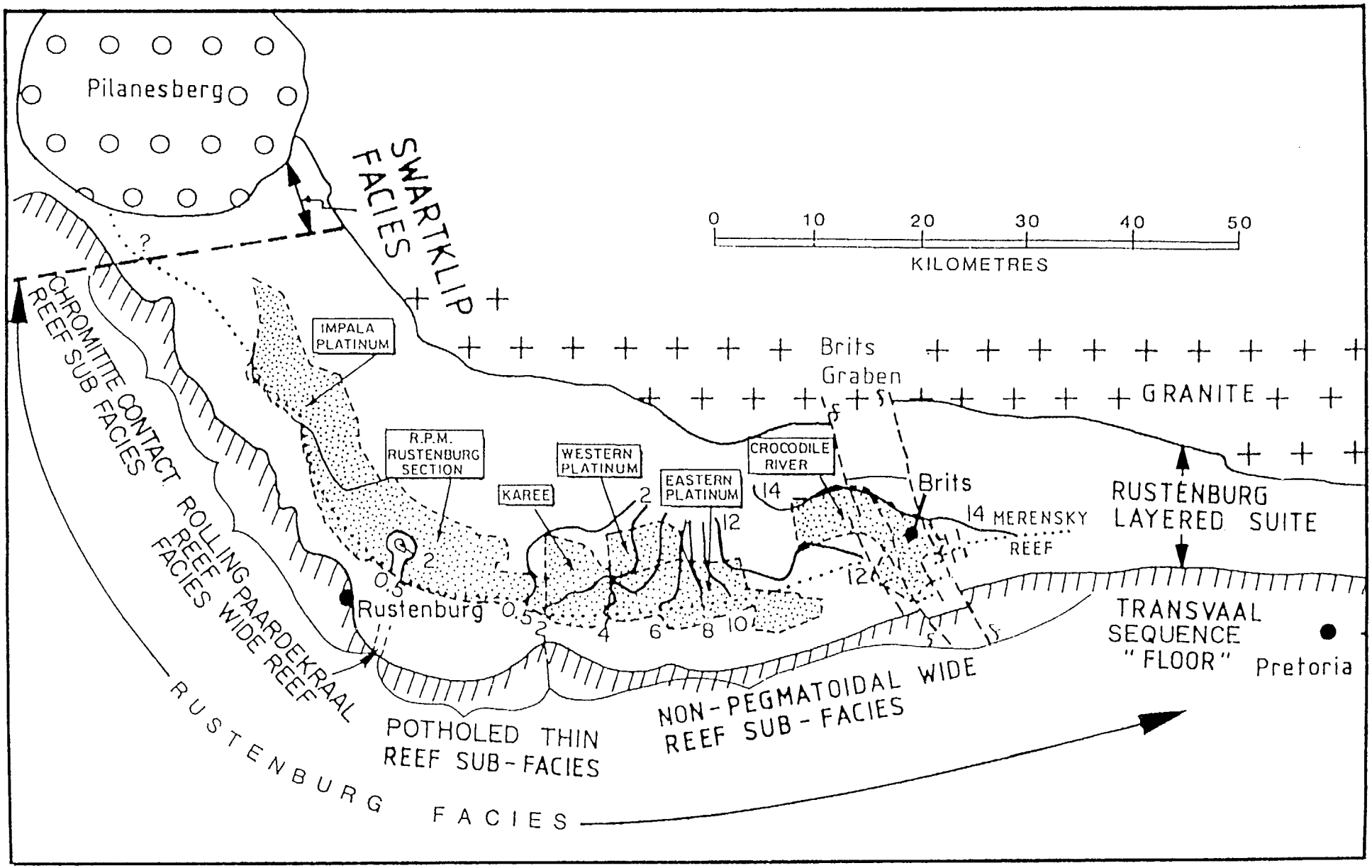

Figure 18: Detailed subdivision of the Rustenburg facies of the Merensky Reef showing distribution of sub-facies and isopachs (in metres) (Viljoen, 1994).

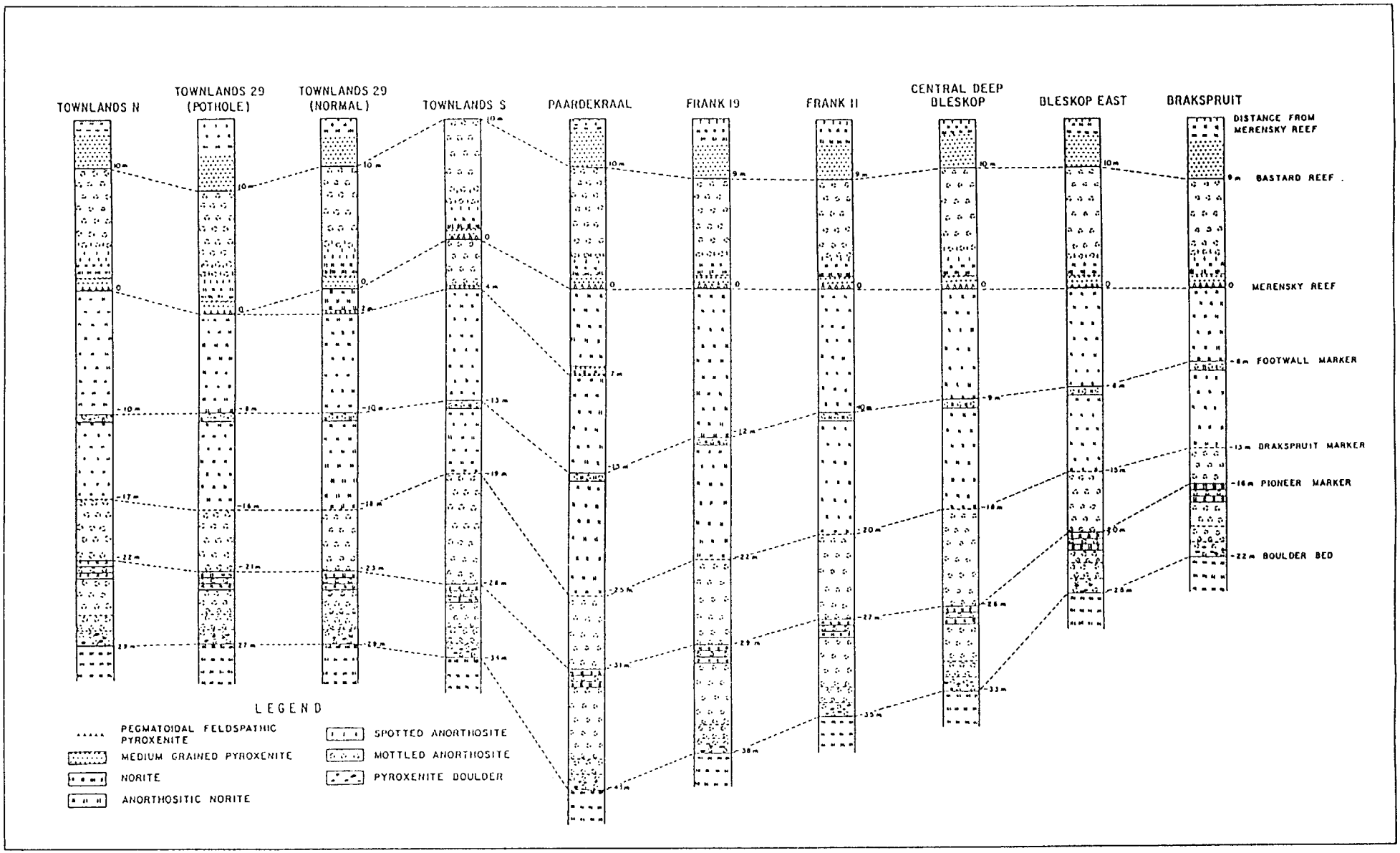

Figure 19: Regional variation in the anorthositic footwall markers relative to the Merensky Reef, across Rustenburg Section (after Viljoen and Hieber, 1986).

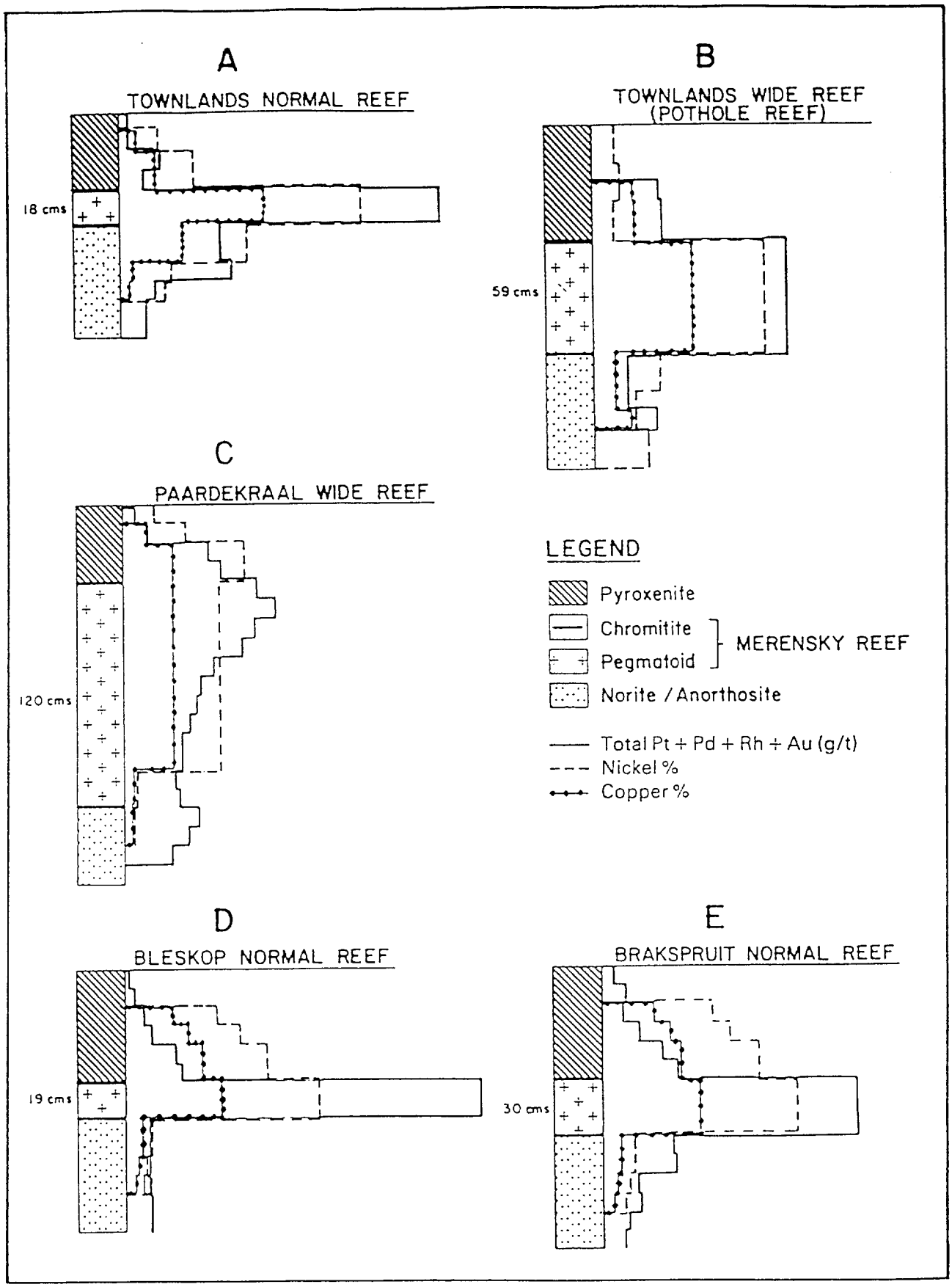

Figure 20: Vertical value distribution considering the Merensky Reef of the Rustenburg section (Viljoen and Hieber, 1986). Note the varying thicknesses of the Merensky Reef package.

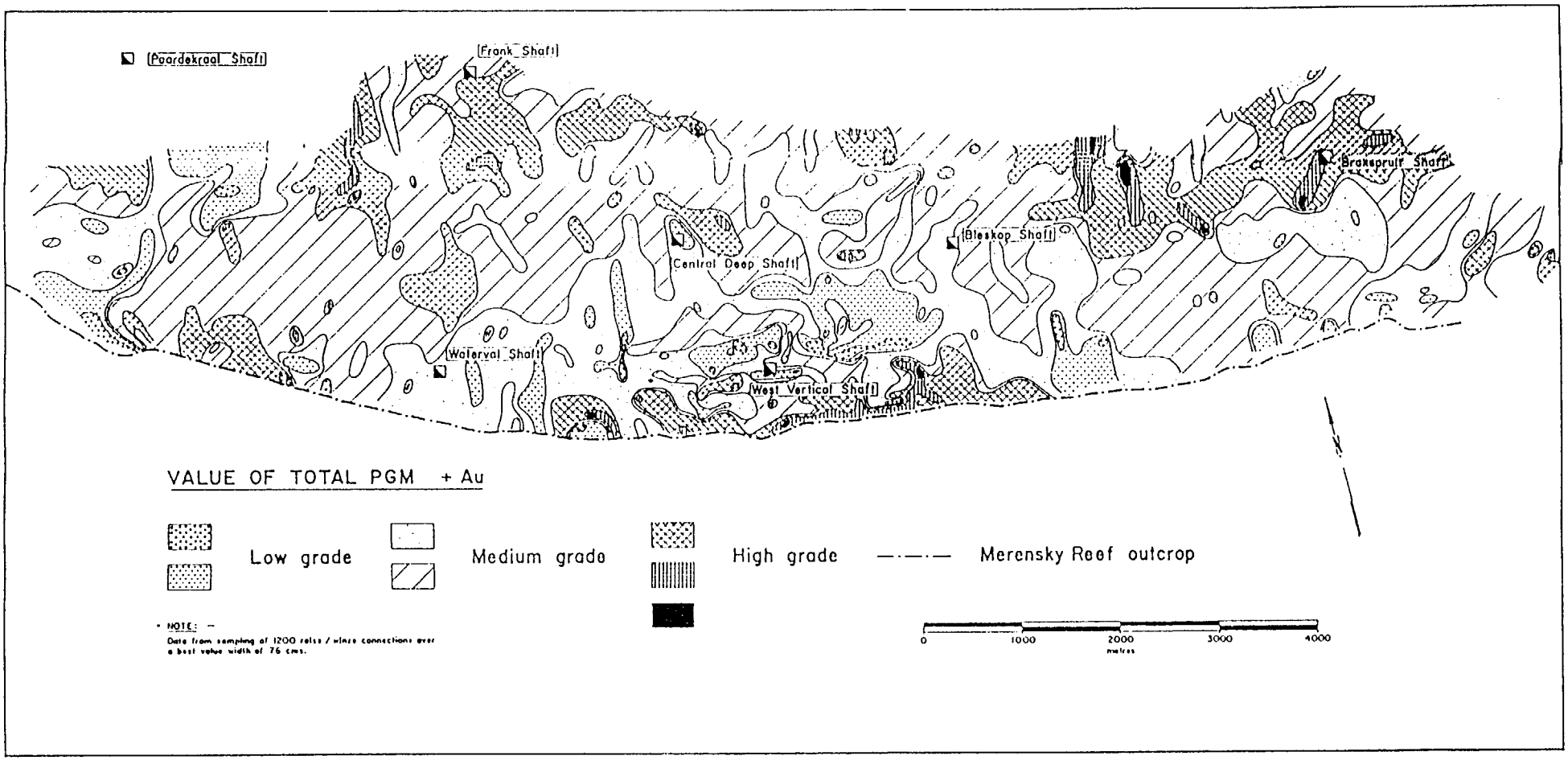

Figure 21: Irregular value distribution in the Merensky Reef as observed at Rustenburg Platinum Mines (Viljoen and Hieber, 1986).

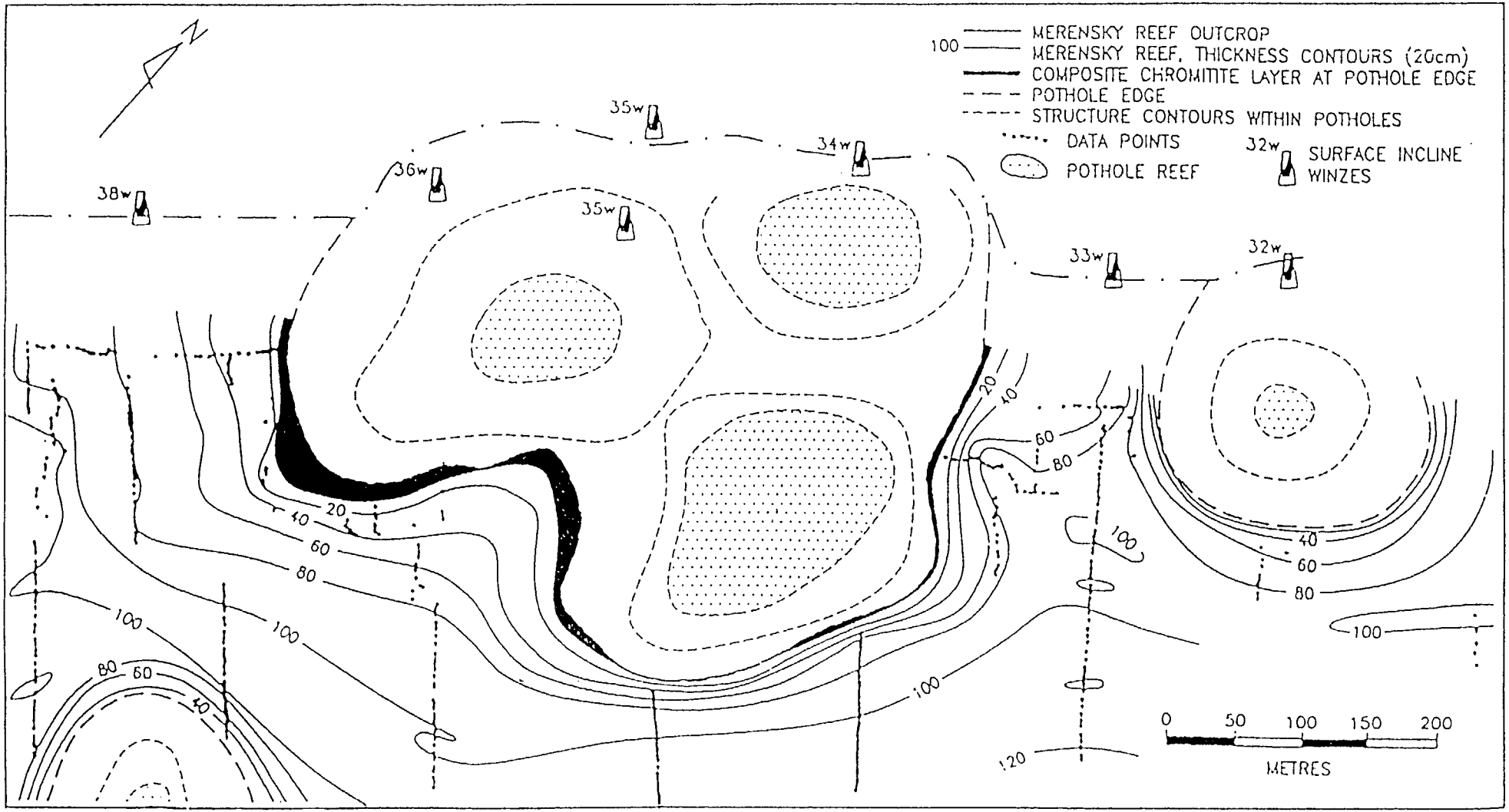

Figure 22: Merensky Reef isopachs, also showing pothole distribution and the varying thicknesses of the orebody (Viljoen, 1994).

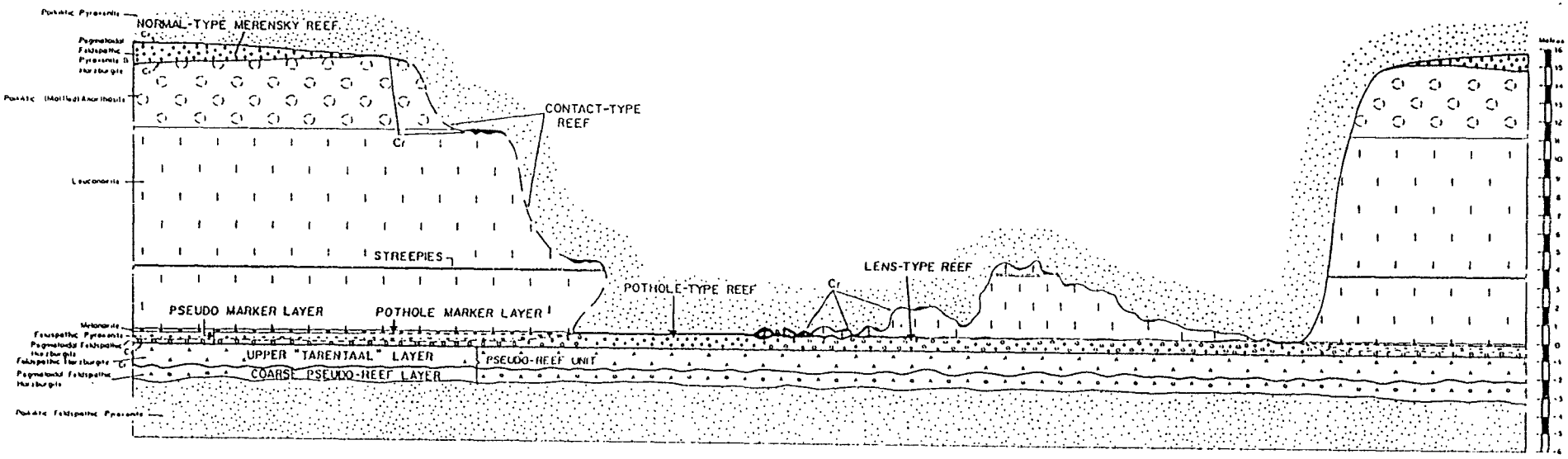

Figure 23: Schematic section through a potholed succession showing normal-, pothole- and lens-type reef development (Viljoen et al., 1986).

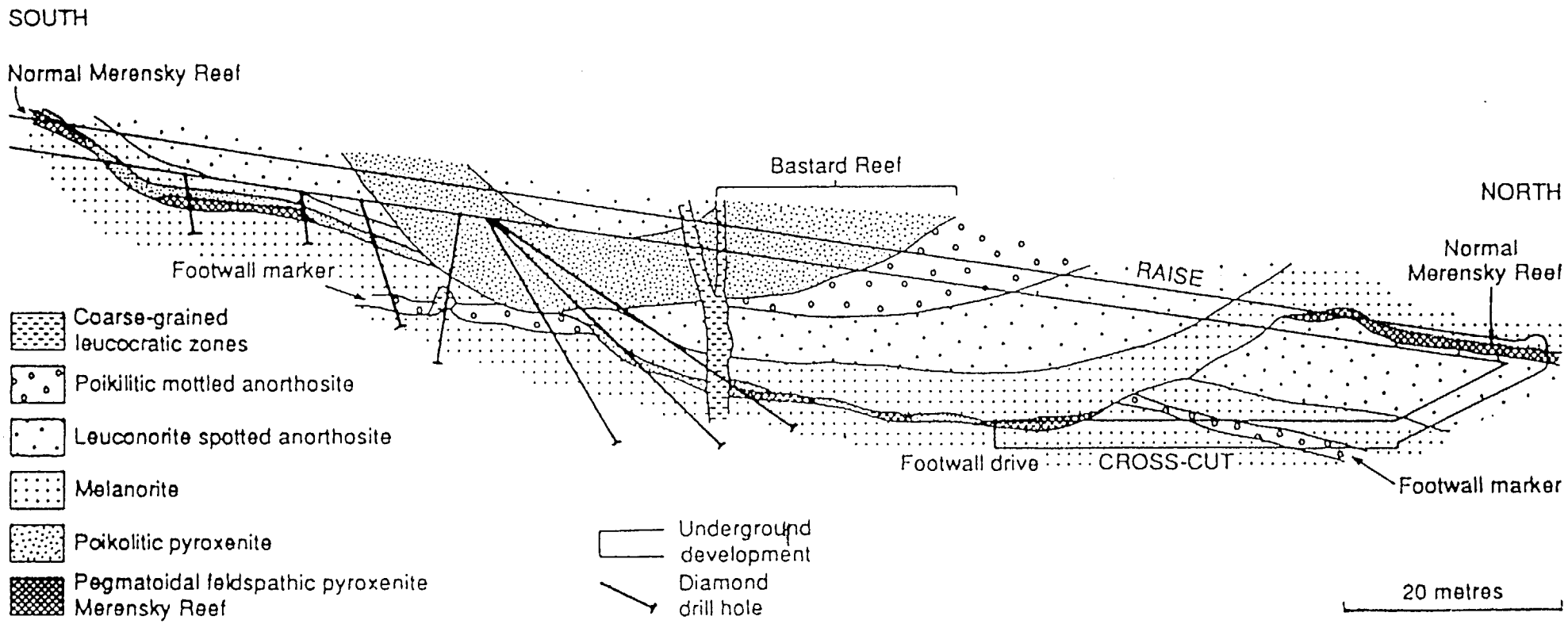

Figure 24: Cross section through a Rustenburg facies pothole (after Carr et al., 1994).

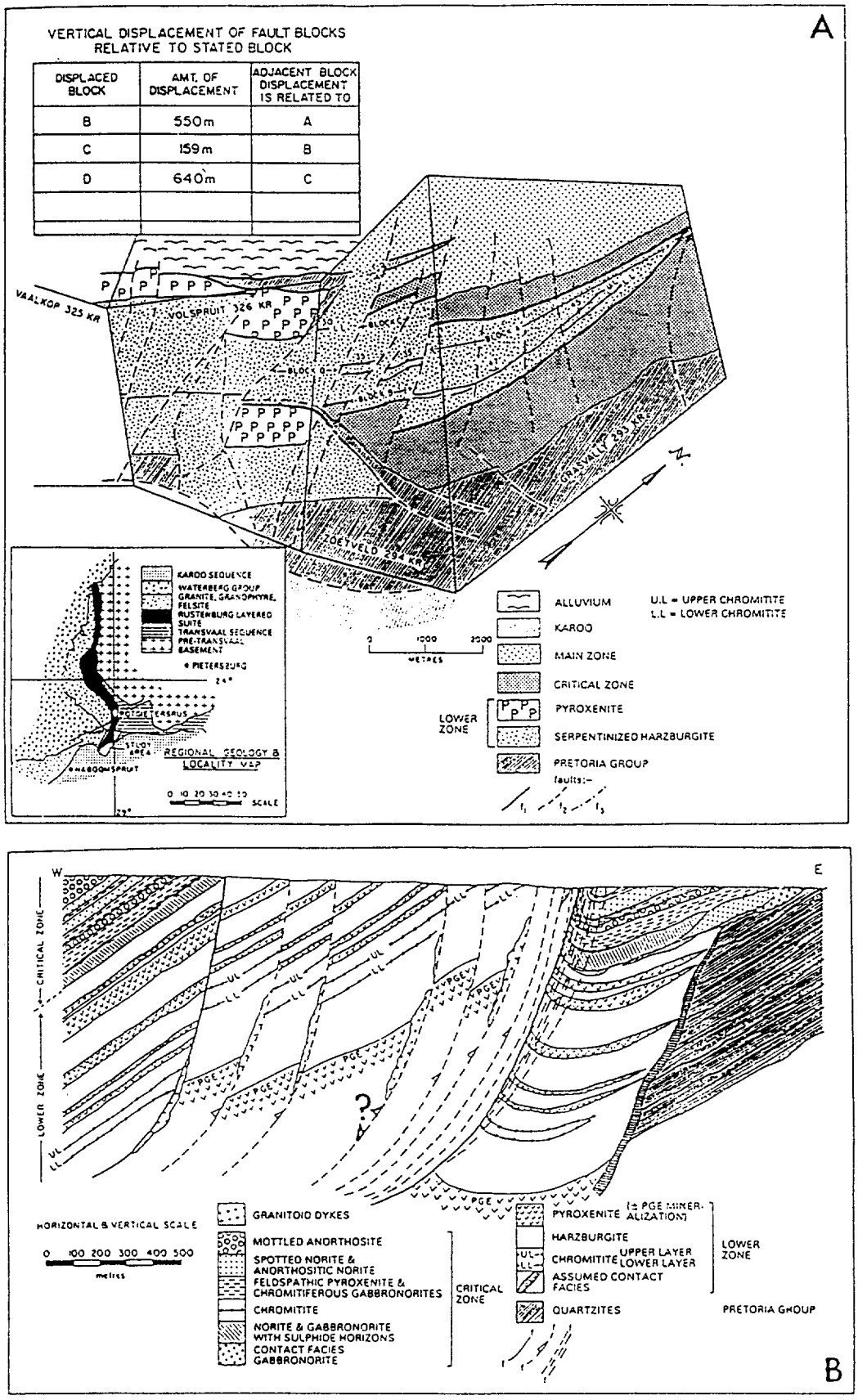

Figures 25 a and b: Different generations of faulting depicted for the Grasvally area, towards the south of Potgietersrus (a, after Mossom, 1986). An idealised cross-section of the same area is shown in Figure 25b.

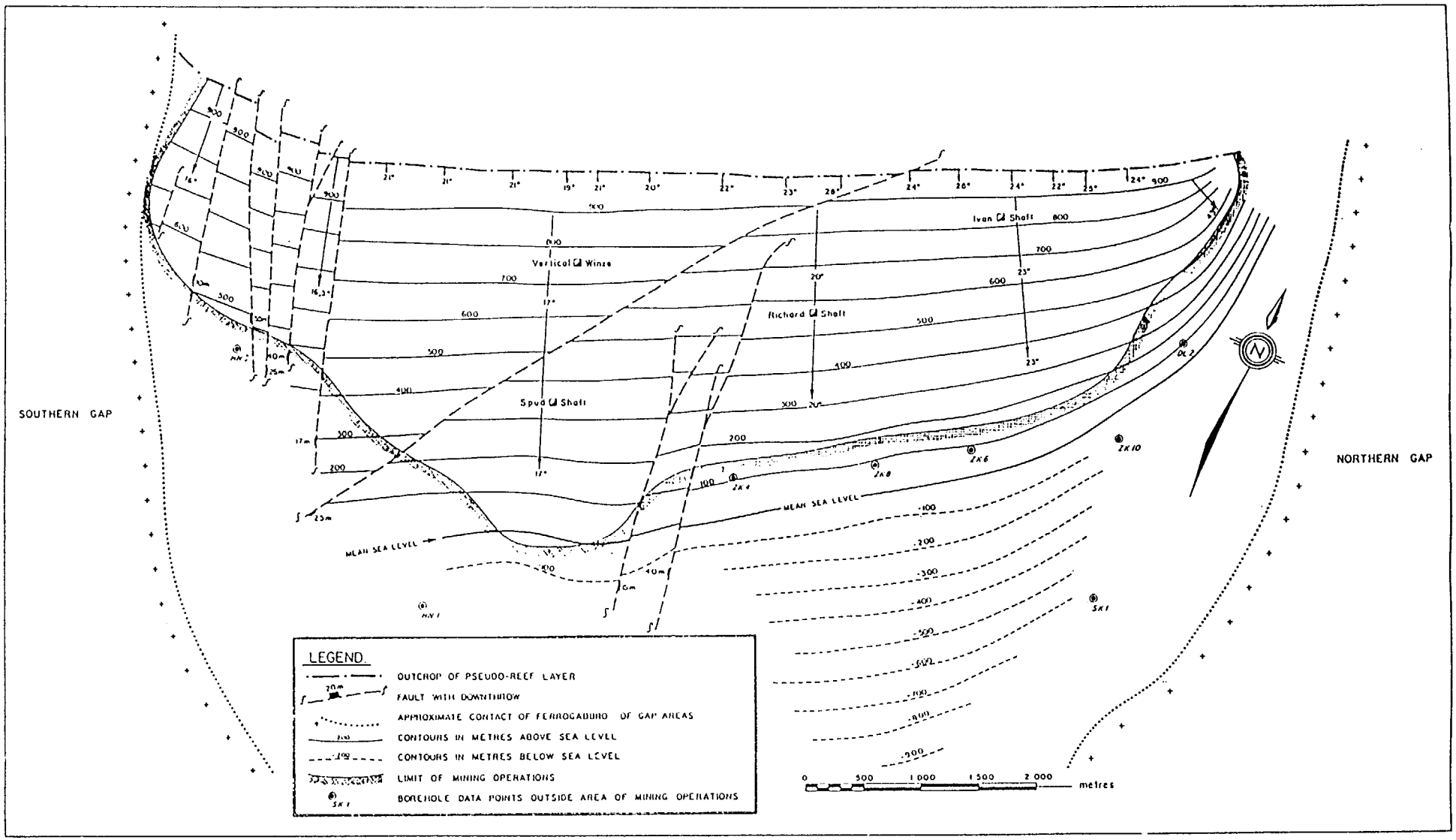

Figure 26: Regional structural features of the Merensky Reef (after Viljoen et al., 1986).

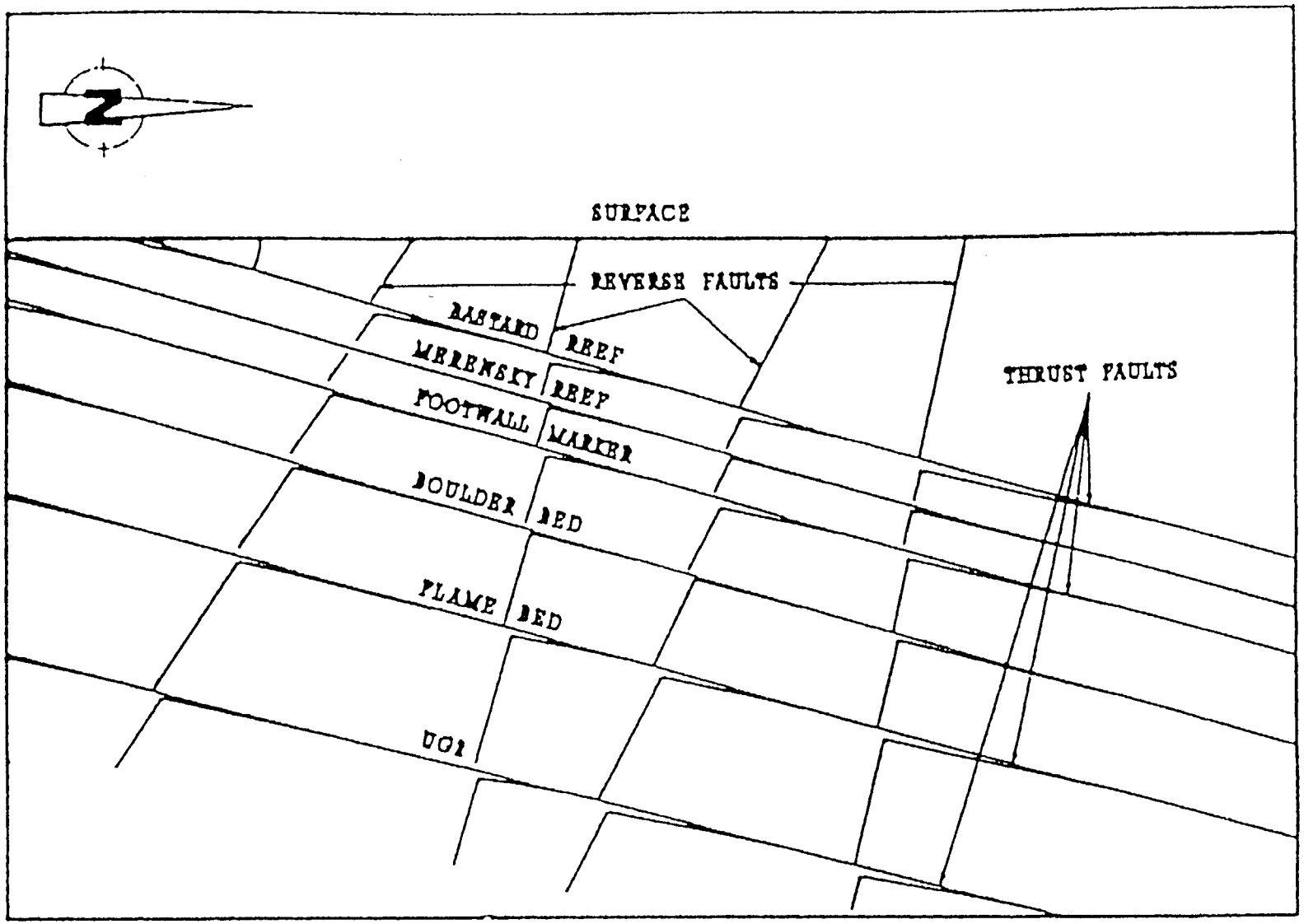

Figure 27: Thrust faulting associated with the Merensky Reef and associated strata (De Maar and Holder, 1994).

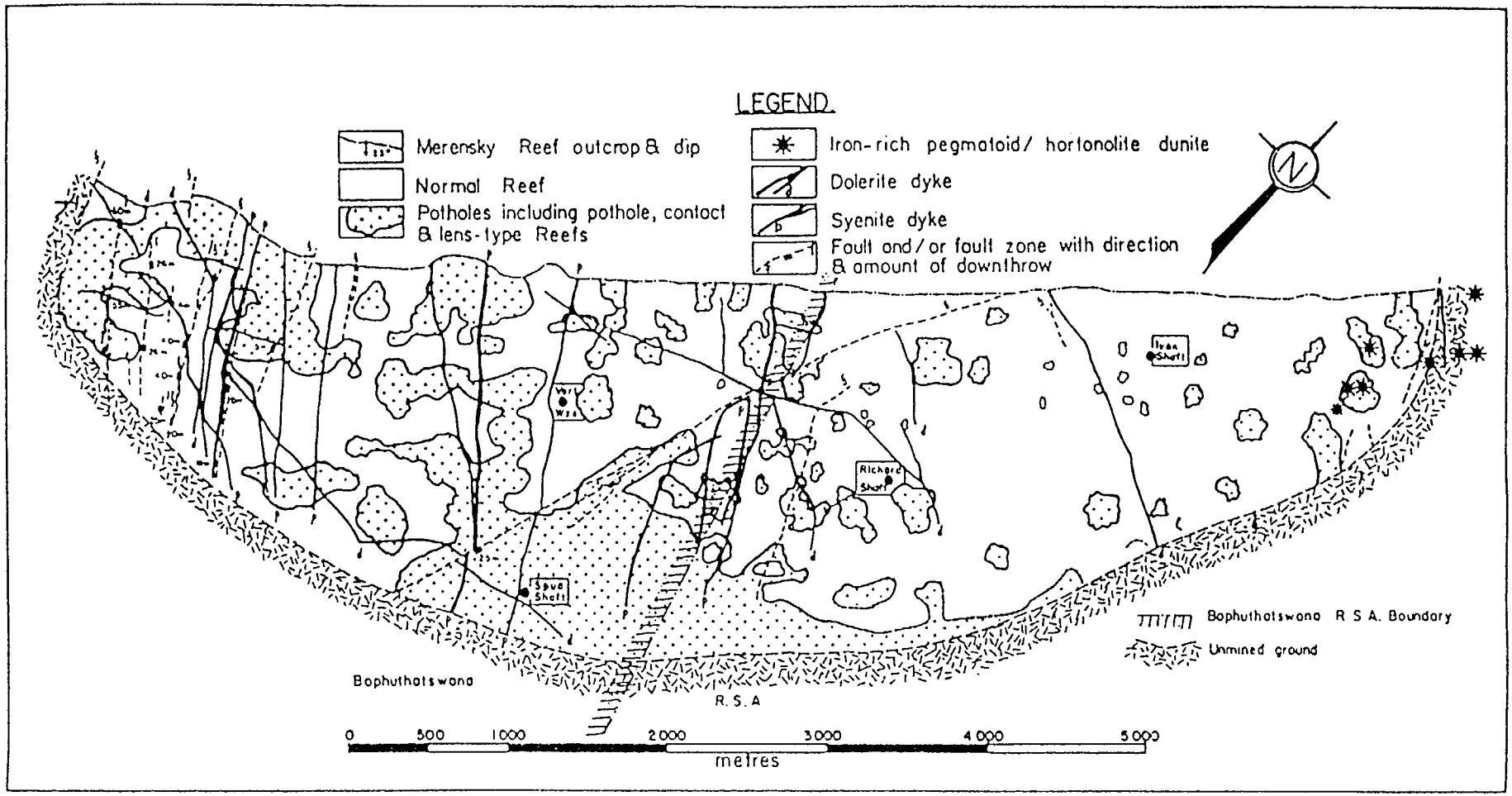

Figure 28: Pothole distribution on the Merensky Reef related to the major dykes and faults (Viljoen et al., 1986).

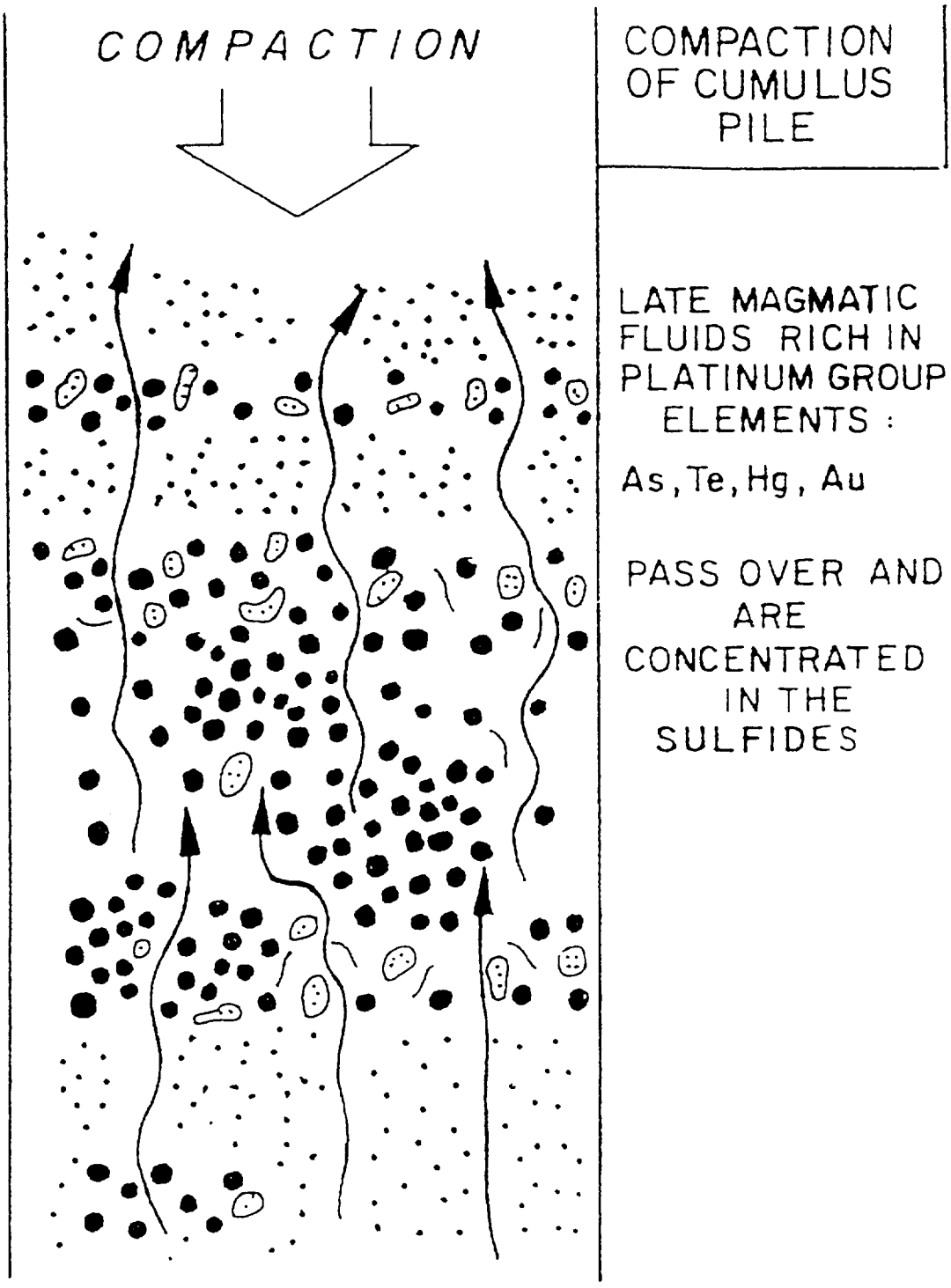

Figure 29: Late magmatic fluids migrate along hydrothermal veinlets through the rock assemblage associated with the UG2 (after Gain, 1984).

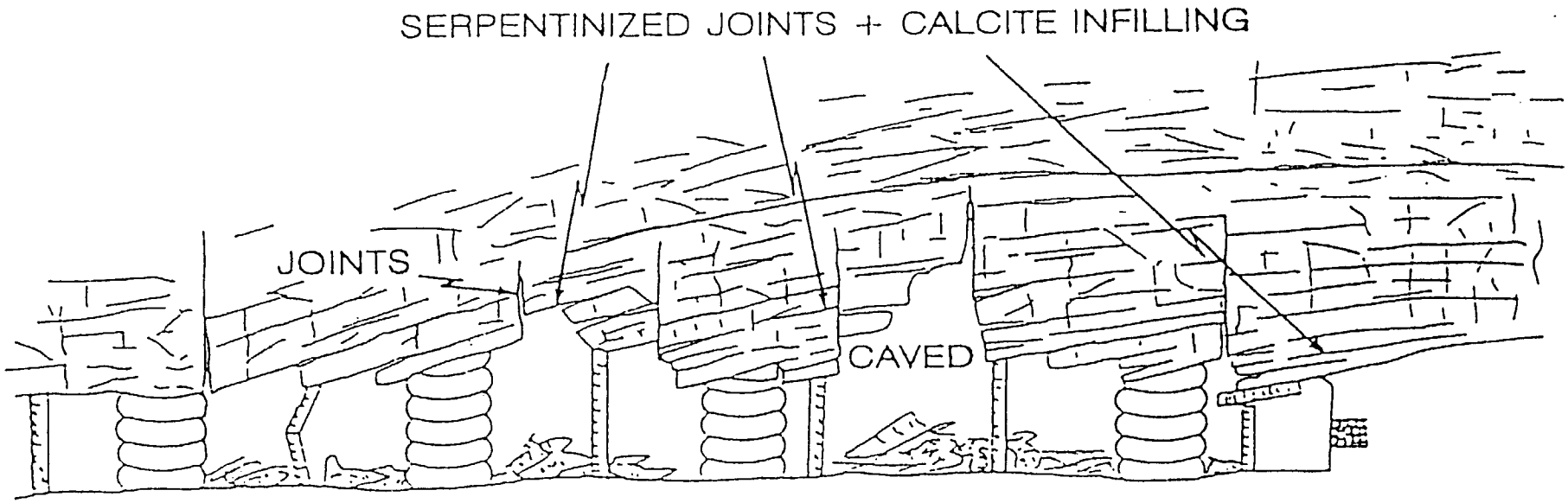

Figure 30: Typical Merensky Reef stops section showing the dome features resulting from calcite and serpentinised joints (De Maar and Holder, 1994).

Appendix B

Joint Mapping in the Bushveld mines

Joint Mapping in the Bushveld mines

During December 1993 and January 1994 a reconnaissance joint mapping survey was undertaken in seven mines around the Bushveld Complex.

These included:

- R.P.M. Rustenburg — Brakspruit Frank 2 Townlands
- Impala — 10 & 12 Shafts
- Union Section — Richard Shaft
- Amandelbult — 15E shaft 16W shaft 44E shaft
- Northam
- ATOK
- Lavino

Reason for the survey

As no records were available of jointing trends in the Bushveld it was decided to visit the mines and undertake a survey. The work was undertaken by three students doing vacation training and a Miningtek technician over the two month period. Due to the huge scope of the undertaking this survey should be regarded as preliminary and a basis for further work.

Methodology

With the assistance of both the Geologists and the Rock Mechanics on each mine, areas in Stopes, Cross-cuts and Haulages were identified where intense, intermediate and light jointing were present and surveys were then conducted in these areas. Typically over a hundred metres of sections of haulages, crosscuts and on reef in the dip and strike directions, mapped at each site. The joints were offset from a tape positioned under survey pegs so that subsequently the bearing of the dip direction could be obtained.

The following were recorded on each joint set present:

* Dip
* Direction
* Consistency
* Roughness — Wavelength Amplitude
* Gouge
* Cohesiveness
* Rock Type
* Structure — Joint Fault Fracture Dyke

Examples of data sheets

1. **ATOK**

Set	1	2	3	4
Dip (degrees)	65	85	75	70
Dip Direction	145	155	275	82
Gouge	no	no	no	no
Cohesiveness	good	good	good	poor
Consistency	good	good	good	good
Roughness	smooth	smooth	smooth	rough
Spacing (joints/m)				
average	,5	,1	,5	,05
maximum	3		3	
Comment	Very little water			

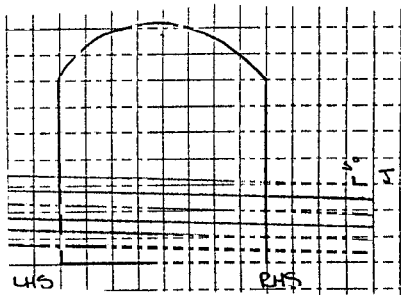

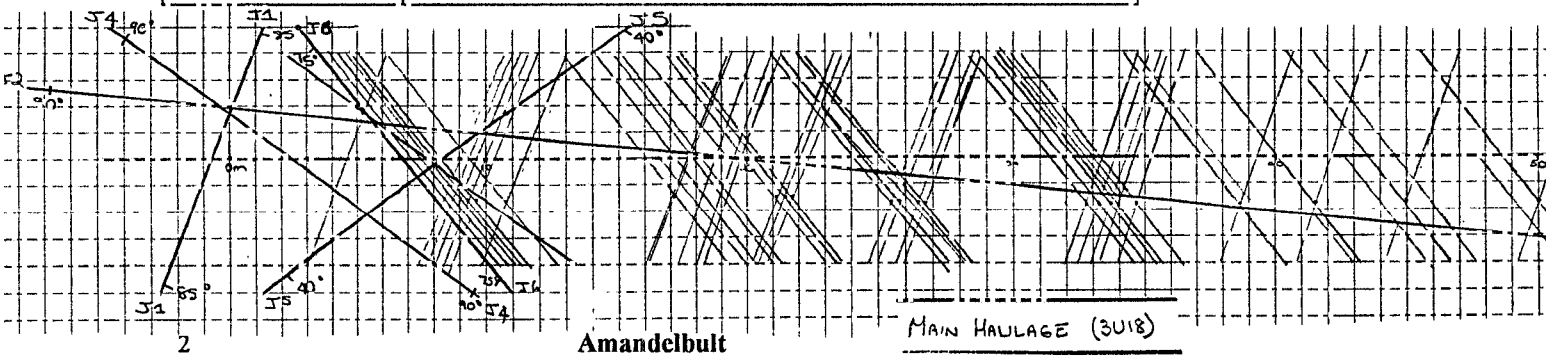

2 **Amandelbult**

Set	1	2	3	4	5
Dip	85	80	80	80	80
Dip direction	20	60	145	270	330
Roughness	medium	smooth	medium	smooth	medium
Gouge	0 - 4 mm	1 - 5 mm	no	no	2 - 4 mm
Cohesiveness	low	serpentine	weathered	serpentine	dome
Consistency	continuous	continuous	continuous	continuous	continuous
Spacing (joints/m)					
average	,5	,08	,33	1 only	
maximum	7	1	2		4
Comment	Domes make for unstable conditions				

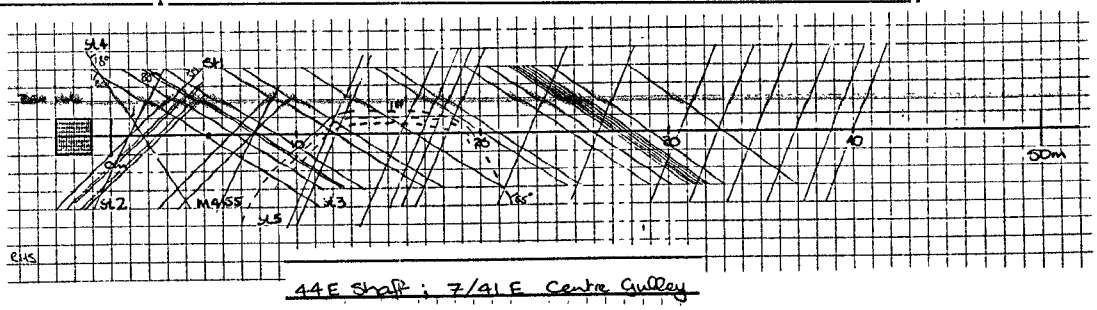

3 **Northam**

Set	1	2	3	4	5
Dip	85	85	60	70	80
Dip direction	84	152	236	293	003
Roughness	medium	smooth	smooth	smooth	open
Gourge	no	no	300 mm	no	no
Cohesiveness	good	good	poor	good	poor
Consistency	continuous	continuous	continuous	continuous	continuous
Spacing (joints/m)					
average	,5	,5	2 only	1 only	1 only
maximum	4	2			
Comment			crushed px		

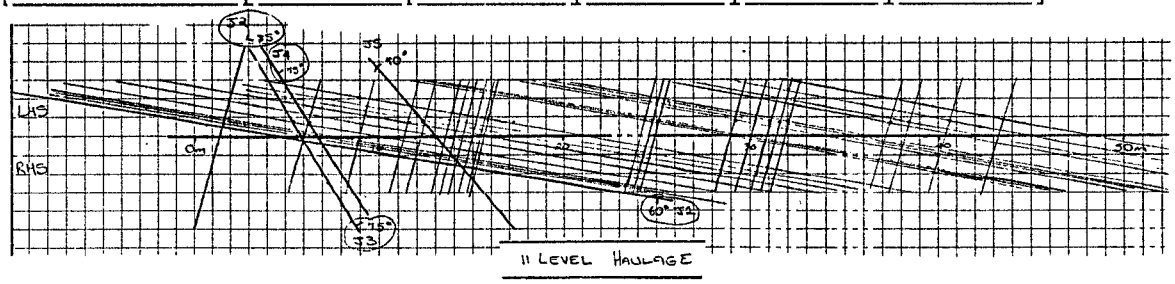

4 **Impala 10 #**

Set	1	2	3	4
Dip	88	90	87	90
Dip direction	186	110	172	241
Roughness	smooth	medium	smooth	smooth
Gouge	no	no	no	no
Cohesiveness	good	good	good	good
Consistency	good	poor	good	poor
Spacing (joints/m)				
average	1,5	1	,12	1 only
maximum	3	2	2	
Comment		slick sided		

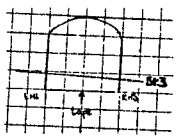

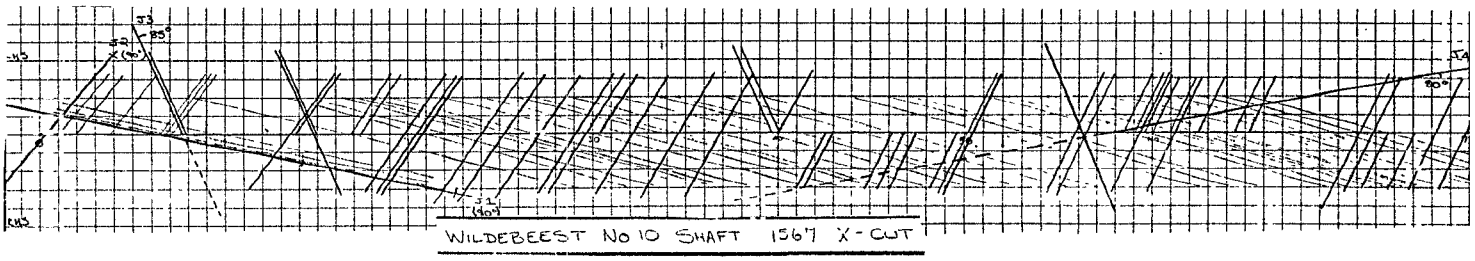

Impala 12 #

Set	1	2	3	4
Dip	85	90	80	80
Dip direction	15	58	75	265
Roughness	smooth	smooth	smooth	smooth
Gouge	2 mm	no	no	no
Cohesiveness	poor	good	good	good
Consistency	poor	good	good	good
Spacing (joints/m)				
average	2	1	1 only	,2
maximum	10	4		1
Comment	area intruded by lamprophrite dykes			

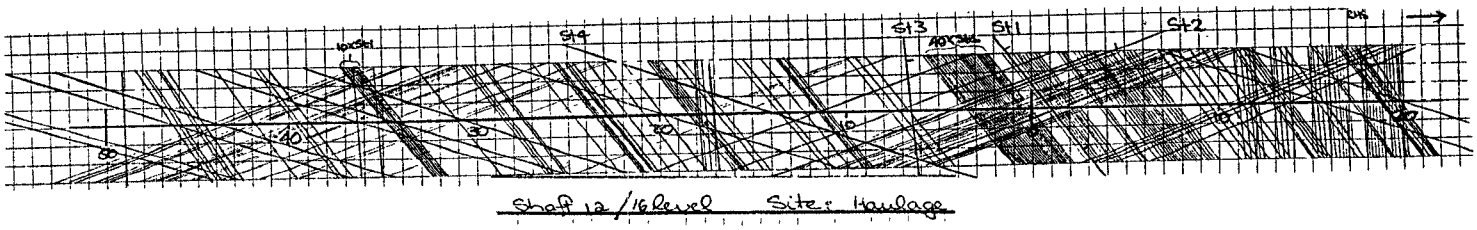

6 **Union Section**

Set	1	2	3	4
Dip	85	90	80	80
Dip direction	15	58	75	265
Roughness	smooth	smooth	smooth	smooth
Gouge	2 - 6 mm	no	no	3 - 6 mm
Cohesiveness	low`	low	low	low
Consistency	continuous	truncates	continuous	continuous
Spacing (joints/m)				
average	1	1	,2	1 only
maximum	3	3	5	
Comment	joints highly serpentinized - heavily supported area			

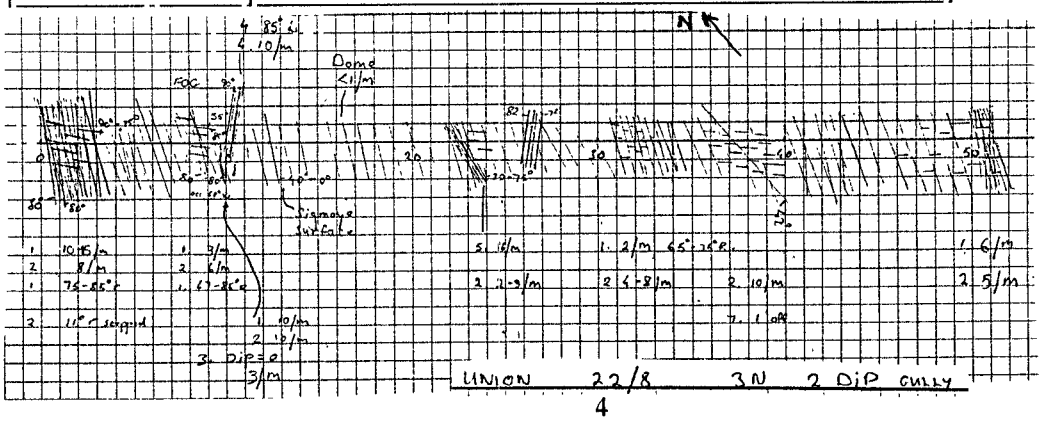

7 **Lavino**

Set	1	2	3	4
Dip	90	70	80	90
Dip direction	180	20	90	150
Roughness	medium	smooth	medium	medium
Gouge	no	no	no	no
Cohesiveness	good	good	low	low
Consistency	continuous	continuous	continuous	continuous
Spacing (joints/m)				
average	,75	,33	occasional	1 only
maximum	3	2		
Comment	falls of ground between sets 2 & 3			

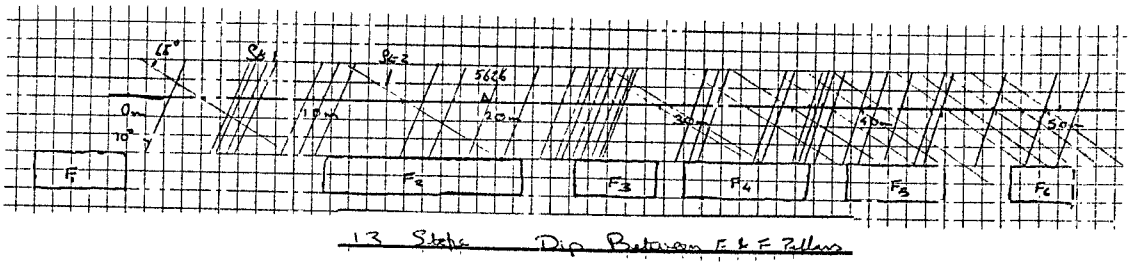

8 **R.P.M. Frank 2**

Set	1	2	3
Dip	70	85	90
Dip direction	30	190	110
Roughness	smooth	rough	rough
Gouge	1 mm	no	1 mm
Cohesiveness	low	high	low
Spacing (joints/m)			
average	,5	,12	1 only
maximum	3	2	
Consistency	continuous	cuts off	continuous
Comment	Gothic arches in E-W haulages		

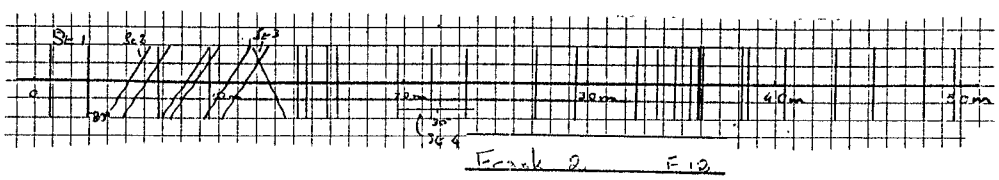

9 **R.P.M. Brakspruit**

Set	1	2	3	4
Dip	90	90	90	20
Dip direction	145	200	225	180
Roughness	smooth	smooth	smooth	smooth
Gourge	no	no	no	no
Cohesiveness	high	low	low	low
Spacing (joints/m)				
average	,5	,1	,33	occasional
maximum	2	2	2	
Consistency	continuous	continuous	continuous	continuous
Comment	Serpentine present on some joints. Some calcite intrusion			

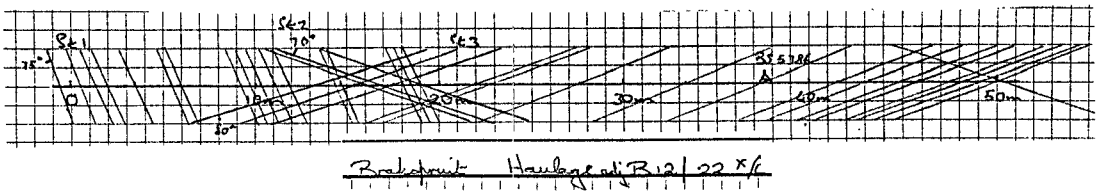

10 **R.P.M. Townlands**

Set	1	2	3
Dip	90	75	75
Dip direction	330	210	30
Roughness	medium	medium	medium
Gourge	0 - 5 mm	0 - 5 mm	0 - 5 mm
Cohesiveness	low	low	low
Consistency	continuous	continuous	continuous
Spacing (joints/m)			
average	,33	occasional	1 only
maximum	1		
Comment	slicken sided		dip opposite to 2

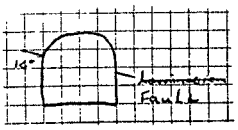

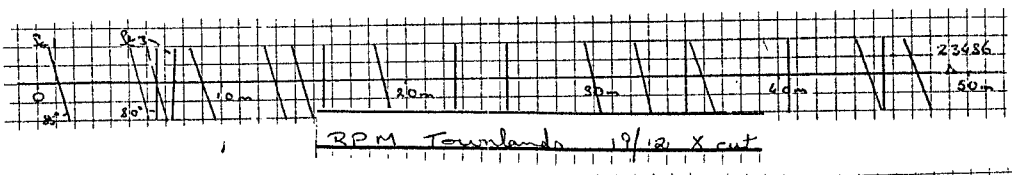

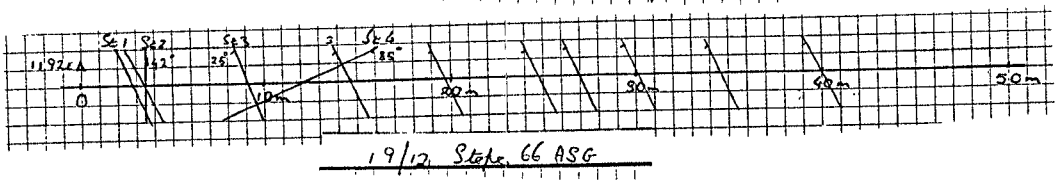

Conclusions

◊ Although joints occur randomly and ubiquitously, sets of joints are often associated with major geological discontinuities in the area, such as for example, the Pilanesberg Dyke set. Assuming that joints occur as a result of stress and stress relief in rock it is reasonable to assume that a secondary and tertiary joint set will occur in the plane of secondary and minor stress fields. This would be evident in joint sets more or less orthogonal to one another been of primary secondary and tertiary significance. This is often found to be the case in the Bushveld.

◊ Jointing forms a plane of weakness through which water can permeate and in so doing leach out or deposit minerals. Movement on joints and deposition from water results in gouge forming on the surfaces and a subsequent week plane.

◊ The pattern of joints which form around and below potholes is potentially useful for the purpose of identifying potholes on the reef from the footwall developments. An unusal joint pattern appears below potholes which extends some meters into the footwall. Generally these are concentric around the dome and often are at variance with existing joint patterns in the area. This phenomenon is under investigation at Northam and further effort should be focused in this direction.

◊ On many of the mines a set of joints was found to exist close to the strike of the reef. This means that a set of joints appears to form a concentric circle around the Bushveld and tends to dip toward the centre.

Appendix C

Analysis of Seismicity at Wildebeestfontein North Mine

SIMRAC PROJECT GAP027 ENABLING OUTPUTS 3, 4 & 5

FINAL REPORT
PART 1

ANALYSIS OF MINING INDUCED SEISMICITY RELATED TO THE PLATINUM MINES OF THE BUSHVELD COMPLEX: No. 10 SHAFT, WILDEBEESTFONTEIN NORTH MINE

A.J. van der Merwe
CSIR Division of Mining Technology
23 November 1995

CSIR
WNNR

CONTENTS

1. Introduction

The monitoring of seismicity on Wildebeestfontein North mine (#10 shaft) forms part of the SIMRAC project ***Rockmass condition, behaviour and seismicity of the Bushveld Igneous Complex*** (GAP 027). As seismicity is expected to increase in the mines of the Bushveld Complex with increasing depth and extent of mining, the objective of this section of the project is to pro-actively develop an understanding of the seismicity and its causes, in order to be in a position to define long-term strategies to minimise seismicity and associated damage. More specifically, this project seeks to understand the mechanisms of the seismic events, and to distinguish events produced by pillar failure from those resulting from other causes. Knowledge of mining-induced seismicity gained in the deep-level gold mines of the Witwatersrand basin cannot be directly applied to the platinum mines of the Bushveld Complex as these mining areas differ with respect to rock types, stress field and mining practice. In the Bushveld Complex mines, small pillars are sometimes used at depths of 1300m. In some cases, these pillars have failed violently.

2. Seismic Monitoring System

The Portable Seismic System (PSS) installed at No.10 Shaft of Wildebeest-fontein North Mine (WN10#), which is part of Impala Platinum Mines, is the first underground seismic network installed in a platinum mine. The selected site is bounded by the footwall drives 14 Level South and 15 Level South, and raises W1566 and W1567, thus including an area of approximately 200 m by 200 m. A three component geophone set (tri-axial) is situated at each corner of the area in the footwall drive, together with a set above the stope in the centre of the area. Each geophone set is grouted in a vertical hole drilled upwards, about 5m in length. The network became fully operational by early September 1993, and stayed so until August 1994, by which time mining has ceased in the immediate vicinity of the network. Electrical noise was prevalent at sites 1 and 4 due to the close proximity of transformer boxes. The resultant 50Hz spikes gave rise to spurious triggers. This noise can be removed efficiently during processing by digital filtering of the data.

2.1. Calibration Blasts

Calibration blasts are used to determine the seismic velocity of the rock and the orientation of the geophones, thereby improving the accuracy of seismic event locations. Three calibration blasts were detonated on 19 November 1993, enabling the calculation of representative P- and S-wave velocities of 6600 ms^{-1} and 3600 ms^{-1} respectively.

2.2. Accuracy of Locations

The P and S velocities calculated from the calibration blasts allowed locational accuracies of better than 3 m in the area of interest, i.e. all events located within a rectangular area described by sides equal to two times the dimension of the network. In addition the orientation of each triaxial site was determined to within 5° by means of a software solution developed by Dr. S. Spottiswoode. Knowledge of the orientation and reliable direction cosines for each sensor is crucial for source mechanism studies.

2.3. Number of Events Recorded

Since commissioning to the end of August, the PSS network was triggered in excess of 20 000 times. The vast majority of these triggers were produced by blasting. In an effort to keep the most significant events, the PSS automatically drops the smallest events from memory when the system is triggered too rapidly. It is very unlikely that any events with a magnitude greater than that produced by a production blast were discarded in this fashion. A total of some 940 waveforms were recorded until the end of August 1994, of which at least 254 were seismic events, the remainder being production blasts.

2.4. Magnitude Discrepancy

Statistical comparison of seismic data recorded earlier by the GENTEL system versus the data recorded later by the PSS showed an order of magnitude difference in the average calculated Richter magnitudes. An investigation of magnitude calculations by the GENTEL code and the PSS code respectively on waveforms recorded by the GENTEL system, provided the first comparison of the results based **on the same data**. Figure 1 (below) indicates that the magnitudes calculated by the GENTEL code are, within realistic limits, exactly one order of magnitude larger than the corresponding PSS results.

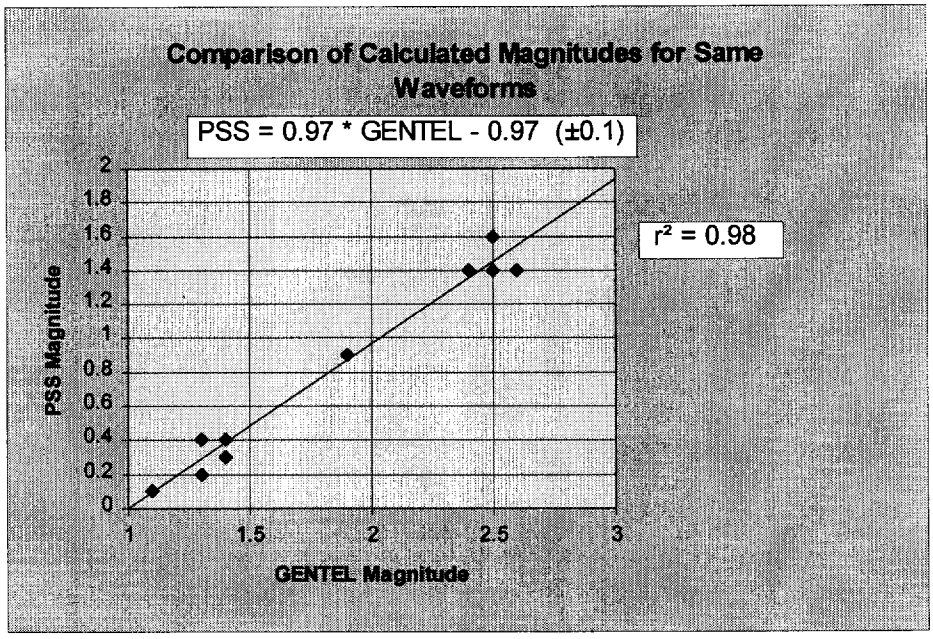

Figure 1. Comparison of magnitude calculations by the GENTEL code vs. the PSS code. Based upon the same waveforms.

Two relatively large seismic events occurred approximately 20 km north-east of the town of Rustenburg during the morning of November 2, 1994. These events were picked up by several of the GENTEL seismic systems located on Impala Platinum Mines and on Rustenburg Platinum Mines. Some of the seismographs of the Council for Geoscience (formerly Geological Survey) also recorded these events. The magnitude results are tabulated overleaf:

	Time	GENTEL Magnitude Range	GENTEL Magnitude Average	Council for Geoscience Magnitude
Event A	4:43	3.9 - 4.8	4.5	3.5
Event B	4:51	3.6	3.6	2.1 *

* Event was too small to allow calculation of magnitude from amplitude; magnitude was estimated from duration.

It is obvious from the above data that the GENTEL magnitudes are exaggerated by roughly an amount of 1 - it follows that since the PSS magnitudes are very nearly one unit of magnitude smaller than the GENTEL values, the PSS magnitudes must be taken as correct. Unfortunately, because the seismogram of this large event had the signature of a distant event and could not be located by the small-scale PSS installation, the waveforms were deleted from the database. Thus no "PSS magnitude" could be directly determined for the event.

3. Spatial Distribution of Seismic Events

The recorded seismograms were each individually inspected, the P- and S-wave arrivals picked manually, and the foci located. The spatial distribution of all events recorded since commissioning of the PSS seismic network until August 1994, is shown in figure 2 overleaf.

From figure 2, four ***general features*** are evident from this regional picture, viz.:

i. a clustering of events at the panels bounded by raises W1566 and W1567, which is in part due to the proximity of the monitoring system and its greater sensitivity to closer events;
ii. a linear scattering of events along a zone sub-parallel to the West 66 raise lines;
iii. a few events located at some new workings at raise W1464; and
iv. some events scattered through the older northern parts of the mine (not shown on figure 2).

Closer inspection of the location of the seismic events in relation to the ***mining geometry*** allows five more observations:

i. The majority (49.5%) of the events located on pillars in mined out areas, indicating that these yield pillars are to some extent failing. Most of the larger events recorded plotted at such locations, and some pillar damage and pillar "punching" into the footwall have been correlated with these events.
ii. Some 35.5% of the recorded events located at active stope faces. These were generally quite small events, but some exceptions have occurred, as in panel 5S at raise W1564 where an event of magnitude +0.8 was correlated with a substantial fall-of-ground.
iii. Some 15% of the events located in the back areas of active and older panels, a number of these could be correlated with falls-of-ground.
iv. The up-dip panels between W1566 and W1567 had an anomalous seismic pattern, with 54% of the events in these panels occurring at the side abutment of the panels (see figure 3).
v. Most events located at or very close to the reef plane (see figure 4).

Only one event could be spatially correlated with any ***geological structure***: this located at the intersection of a northwest - southeast striking dyke with a minor fault (1.3 m throw), some 170 m below the 14 Level Drive South (M_L = -0.24).

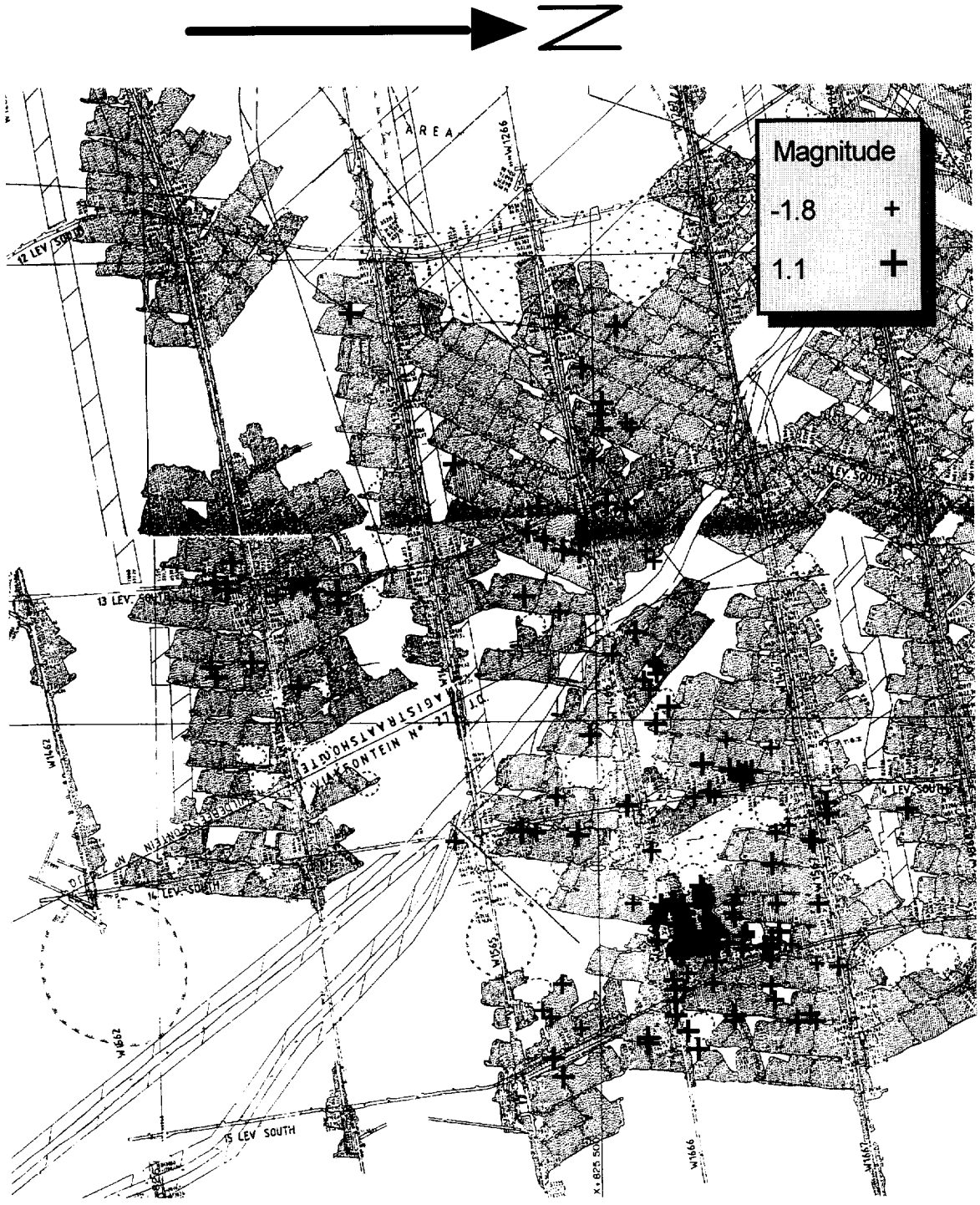

Figure 2. Spatial distribution of seismic events recorded at 10 Shaft, Wildebeestfontein North Mine.

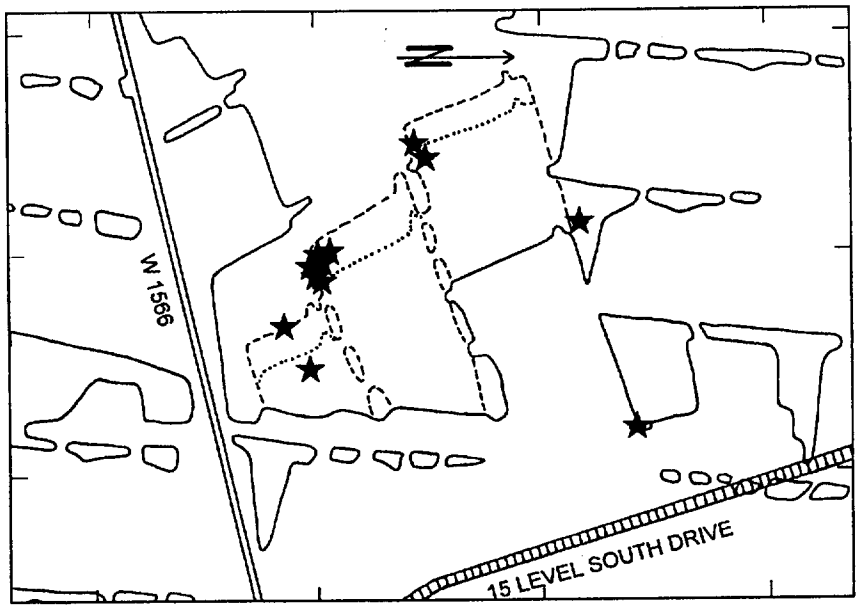

Figure 3. Location of events at the up-dip panels near the W1566 raise line, for the fortnight 13/3/94 to 26/3/94.

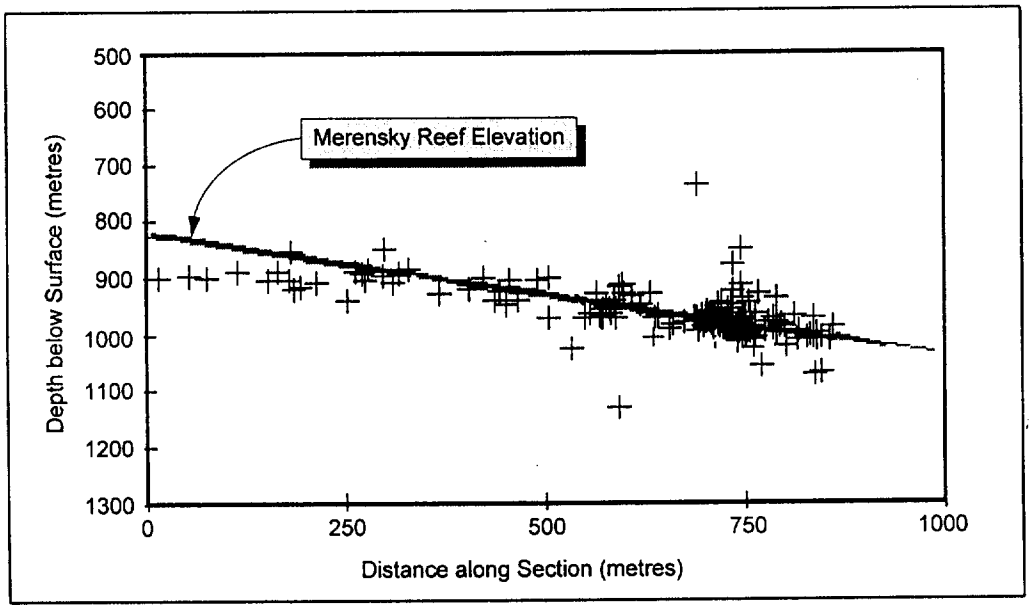

Figure 4. Dip section along raise line W1366 - W1666, showing location of seismic events with respect to Merensky Reef elevation.

4. Temporal Distribution of Seismic Events

The relatively straight slope of the plot of cumulative number of events against time (figure 5, overleaf), shows that the number of events per time unit remained steady over the period from September 1993 to May 1994 (inclusive). However, the graph of the cumulative seismic moment released during the same period shows an increase in the rate of moment release (figure 6, overleaf). This therefore indicates that the average moment released per event increased as mining progressed, which in turn implies a relatively higher risk and perhaps more damage in more mature working areas.

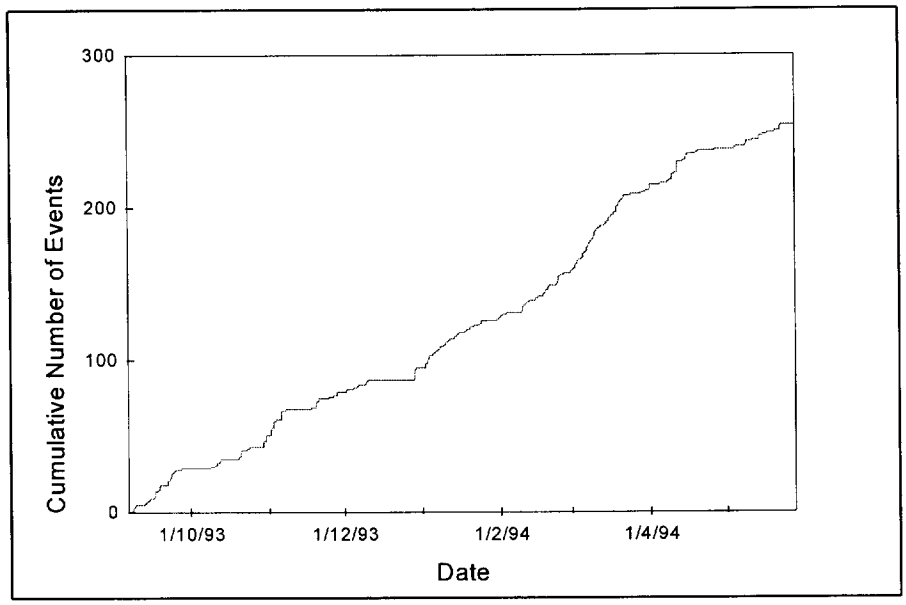

Figure 5. Cumulative number of seismic events during the period 9/93 to 5/94.

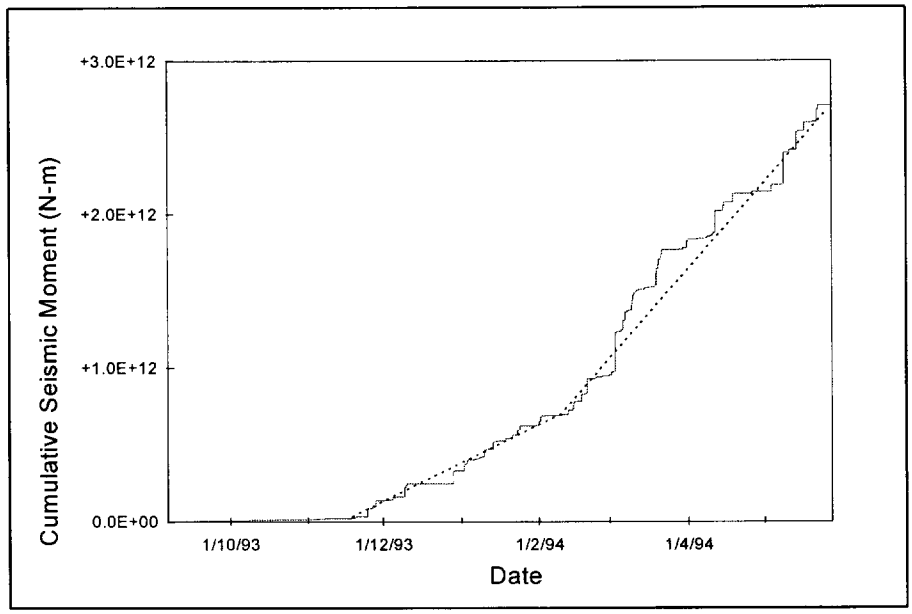

Figure 6. Cumulative seismic moment recorded during the period 9/93 to 5/94.

An analysis of the frequency of occurrence of seismic events with regard to the time of day is shown in figure 7 (overleaf). It is obvious that a large number of events occur during the blasting period, i.e. from 14h00 to 16h00, with some tail-off in the three hours following the blasting period.

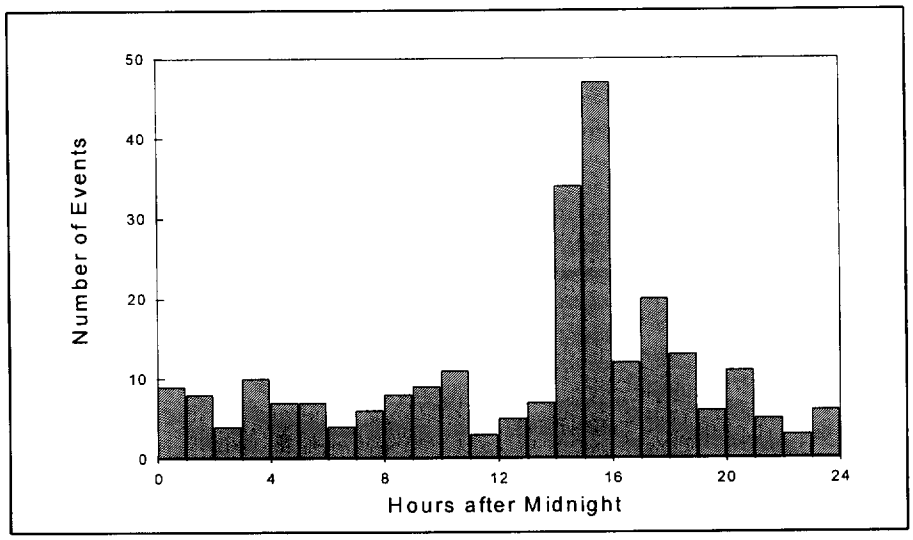

Figure 7. Histogram of the number of seismic events vs. the time-of-day.

5. Magnitude Distribution of Seismic Events

The Richter magnitudes of the recorded seismic events ranged from the smallest event of M_L = -1.8 to the largest event of M_L = +1.1. A graph of the frequency - magnitude distribution (see figure 8 below) does not show a well-defined straight line segment, which contributed to the ±0.09 error in the estimated b-value of 0.66. This relatively low b-value implies that the possibility exists that events larger than magnitude +1.1 could occur, however the sharp near-linear termination of the curve at magnitude +1.1 indicates that the possibility of events with magnitude much larger than M_L = +1.1 is probably low. These larger events would however occur at greater time and spatial intervals, and the relatively short time period (approx. 1 year) and small area covered by the existing data set make it unlikely to have included such a larger event. Due to this bias in space and time, it is felt that the calculated b-value does not allow global comparison with b-values from other areas, and that the projected maximum magnitude of M_L = 2.1 is not indicative of the area under consideration.

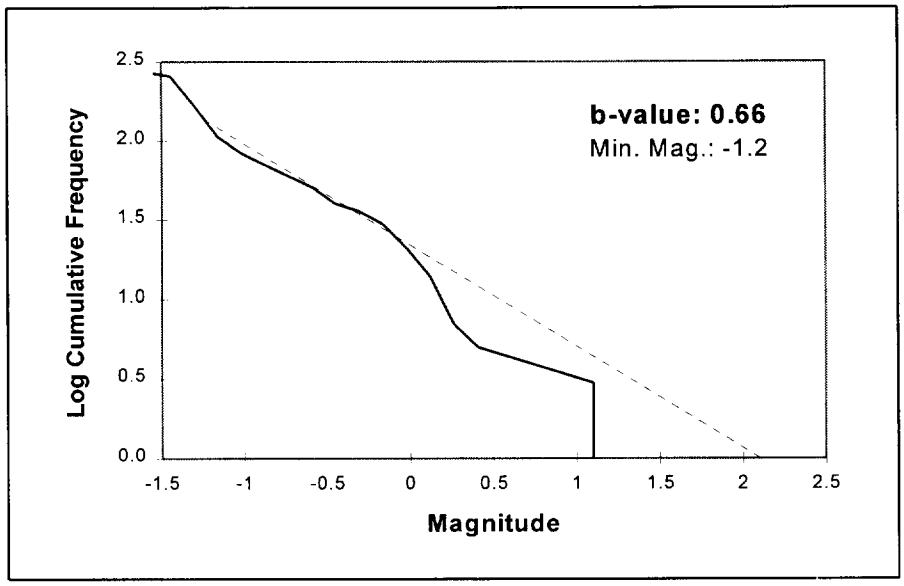

Figure 8. Frequency - magnitude distribution, with b-value indicated.

Comparison of the frequency - magnitude distributions of the events that occurred during blasting time with those that occurred outside the blasting period (see figure 9, below), shows that the events during blasting time tend to be of smaller magnitude. This observation is also reinforced by the relatively lower b-value calculated for the events occurring outside the blasting period, thus indicating a propensity for larger events. Careful investigation of the locations of these events indicate that the majority of blast time events occur near the active working faces, with some scattered events further afield. Conversely, outside of the blasting period, most events tend to locate in or around older / dormant areas. These observations are consistent with that from the previous section, viz.: the larger events tend to occur in the older areas.

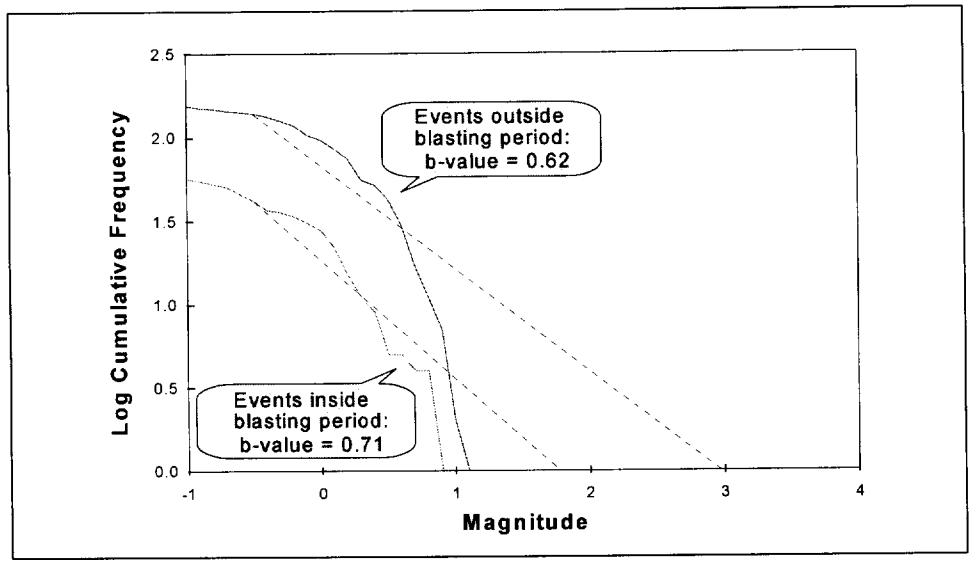

Figure 9. Comparative frequency - magnitude distributions for seismic events occurring inside or outside the blasting period (14h00 to 16h00).

6. Seismic Source Parameters

Two of the seismic source parameters that the PSS suite of software can determine, are the ***stress drop*** ($\Delta\sigma$) and the ***energy index*** (E.I.). The static stress drop as defined by Brune (1970) has a strong correlation with the state of stress in the rockmass, and in general, variations in stress drop (or apparent stress) differentiate regions of different stress state and/or rockmass properties. Energy Index is the ratio of the radiated seismic energy of a given event to the average energy radiated by events of similar seismic moment in the area of interest. It allows the distinction between events which differ in the amount of energy radiated per unit of deformation.

6.1 Stress Drop:

Brune (1970) defined the static drop in stress associated with a seismic event as:

$$\Delta\sigma = \frac{7}{16} \bullet \frac{M_o}{r_0^3} \quad ,$$

where: $M_o = seismic\ moment$

$r_0^3 = source\ radius.$

Following Mendecki (1993), this parameter may be interpreted in the following way:
- consistently higher (lower) values of $\Delta\sigma$ for events of similar moment indicate higher (lower) levels of stress / rock strength, and hence potential for seismicity;
- larger variations in apparent stress associated with seismic events of similar moment in a given area indicate inhomogeneous stress / rock strength, and hence uncertainty about future seismicity.

Figure 10 shows a plot of the calculated stress drops on a mine plan. By comparing the stress drop distribution with the magnitudes (figure 11) it is evident that the two parameters do not correlate well. This apparently random relationship is contrary to the conclusions derived by van Aswegen and Butler (1993) from their work in the gold fields of the Witwatersrand Basin. This category of seismic data could facilitate comparison between areas of similar mining geometry, yet different seismic characteristics, if applied to the wider platinum mining operations. The following discussions are illustrative examples of interpretations of the results from thorough seismic data analysis. One example is the group of five events picked up at the extreme northern range of the PSS (group A on figure 10), which have large magnitudes for the region (average +0.34) yet relatively small stress drops (average ~0.48 MPa), indicating that the region has been largely destressed by the previous mining (some 4 years past) and the subsequent settling of the rockmass. On the other hand the events located at the pillars close to 1366 centre gully (group B) are in a stope which had recently stopped mining. Here the stress drops were relatively high, indicating a fairly violent stress relaxation and redistribution process at this stage of the mining sequence. Since the panels in question were mining up to an already mined-out area, they were in effect mining in what amounts to remnants. This also contrasts markedly with the average magnitudes and stress drops obtained from the central PSS region (group C: $M_{L(ave)}$ = -0.83 and $\Delta\sigma_{ave}$ = 2.91 MPa), and would indicate that at least three different ambient states of stress were detected in the study area.

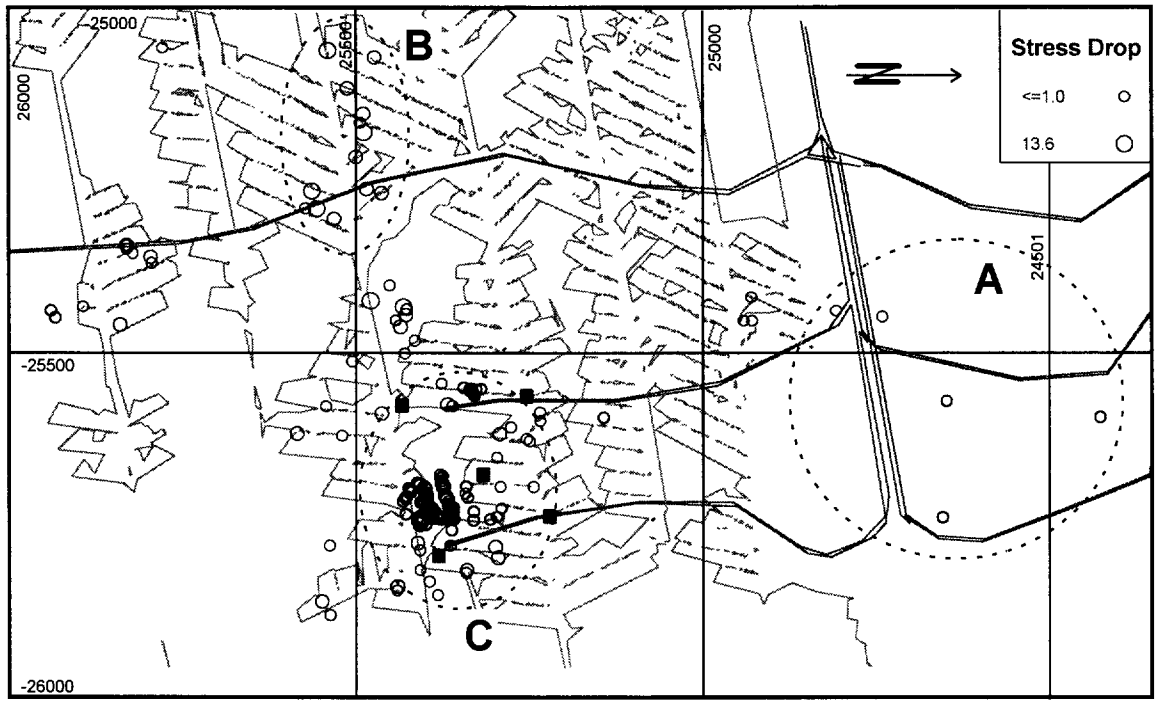

Figure 10. Plan plot of static stress drop associated with seismic events at Wildebeestfontein 10 Shaft.

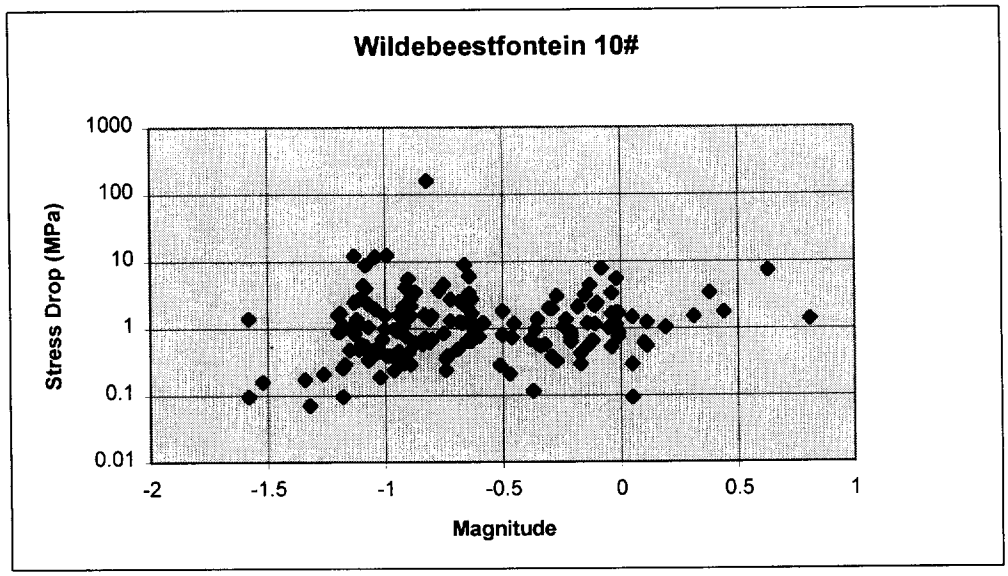

Figure 11. Comparison of Stress Drop values with corresponding Magnitudes.

6.2 Energy Index:

The Energy Index (E.I.) of a specific event is defined as the ratio of the seismic energy radiated by that event, to the average seismic energy radiated by an event of similar magnitude and from the same seismogenic region. The distribution (in magnitude) of the Energy Index (figure 12, below) looks quite similar to that of the stress drop plot. This correlation between energy index and the state of stress despite their different origins, is well demonstrated in figure 13 (overleaf), and has also been commented on by van Aswegen and Meijer (1994). It can simplistically be explained by reasoning that a state of higher ambient stress will result in events radiating higher levels of energy. Closer inspection of the location of the events with higher E.I. and stress drops indicate that these events

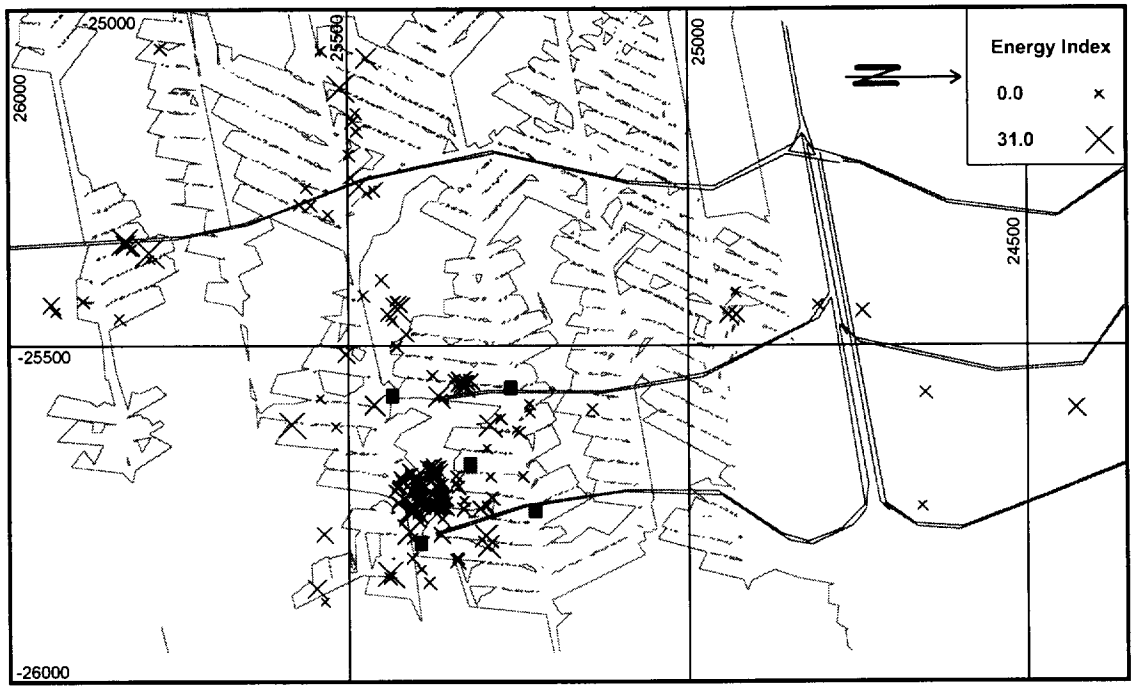

Figure 12. Energy index distribution in the vicinity of the PSS installation.

tend to happen at pillars and the sides of regional pillars and remnants. This phenomenon illustrates the build-up of high stress conditions at these localities .

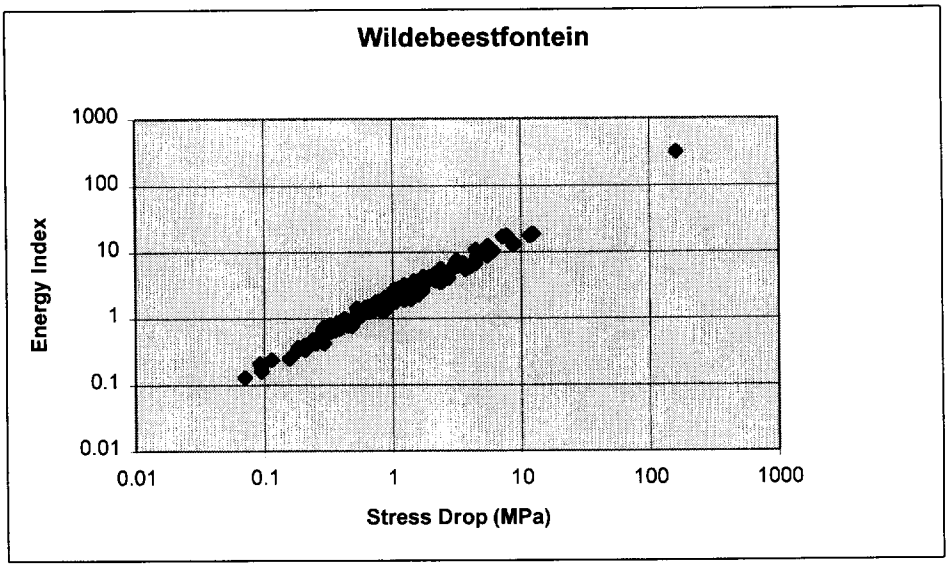

Figure 13. Relationship between Energy Index and Stress Drop.

The usefulness of this parameter in characterising different seismogenic regions can be illustrated by means of the previous example: with the distant northerly region described by $E.I._{ave} = 0.87$, and the central PSS region characterised by $E.I._{ave} = 1.54$. The different states of prevailing stress are thus sharply indicated. The Energy Index is also one of the more useful seismic parameters that lends itself to contouring, thus speeding up the process of identifying areas of different stress states, giving a synoptic view of one aspect of the recorded seismicity.

6.3. Relationship between Energy and Magnitude:

As part of the magnitude discrepancy investigation mentioned earlier, a closer look was taken at the seismic data recorded by the PSS system. The PSS magnitude calculation algorithm determines the magnitude from the energy contained by the seismogram, according to the well-known Gutenberg-Richter equation:

$$\log \text{Energy (J)} = 1.5 \text{ Magnitude} + 4.8$$

The value used for the energy is calculated from the average of:
1. the energy contained in the S-wave portion, and
2. the energy in the P-wave portion, multiplied 15 times (after Boatwright and Fletcher).

Although this supposition of the S-wave containing 15 times the energy of the P-wave has been confirmed by Spottiswoode (pers. comm., 1994), it is strongly challenged by the respective P-wave and S-wave energies determined from the W10 PSS installation, as shown graphically overleaf.

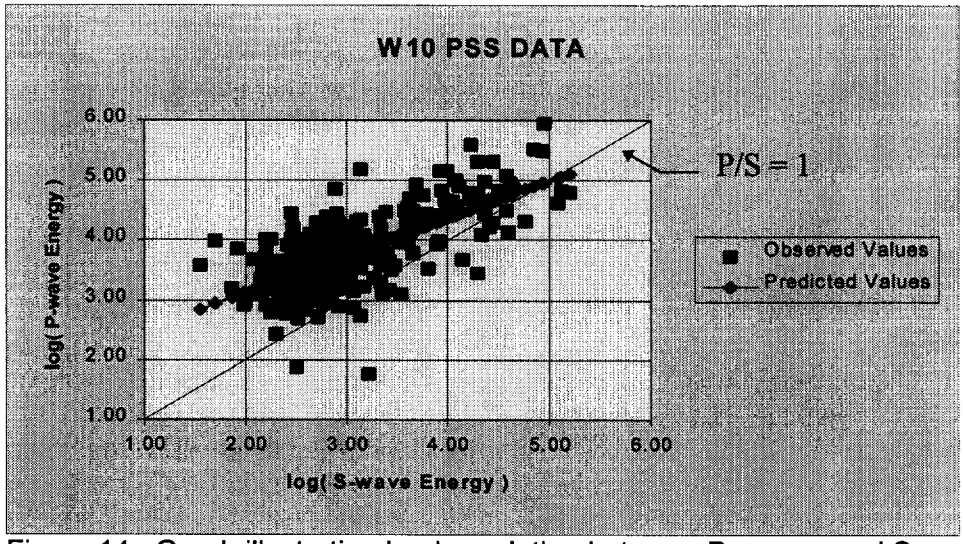

Figure 14. Graph illustrating log-log relation between P-energy and S-energy.

The log-log plot of P- and S-wave energies above shows that a linear relationship exists between the logarithms of P-energy and S-energy, described by the equation:

$$\log \text{P-energy} = 0.62 \log \text{S-energy} + 1.89 \quad .$$

In direct linear terms, this relationship roughly corresponds to:

$$\text{P-energy} = 5 \times \text{S-energy},$$

which is very different from the ratio determined by Boatwright et. al. Whether this phenomenon indicates a fundamentally different rockmass behaviour, or reflects the "crush" type events associated with the yield pillars (see sections 7.1 and 7.2), is not clear at this stage. As a preliminary investigation into the consequences of this observation the regular PSS magnitudes were compared to magnitudes based simply on the sum of the P- and S-wave energies. This comparison indicates that, for the typical event magnitudes recorded by the W10 PSS installation, the "regular" magnitudes were generally under-estimated by a small amount, as shown below.

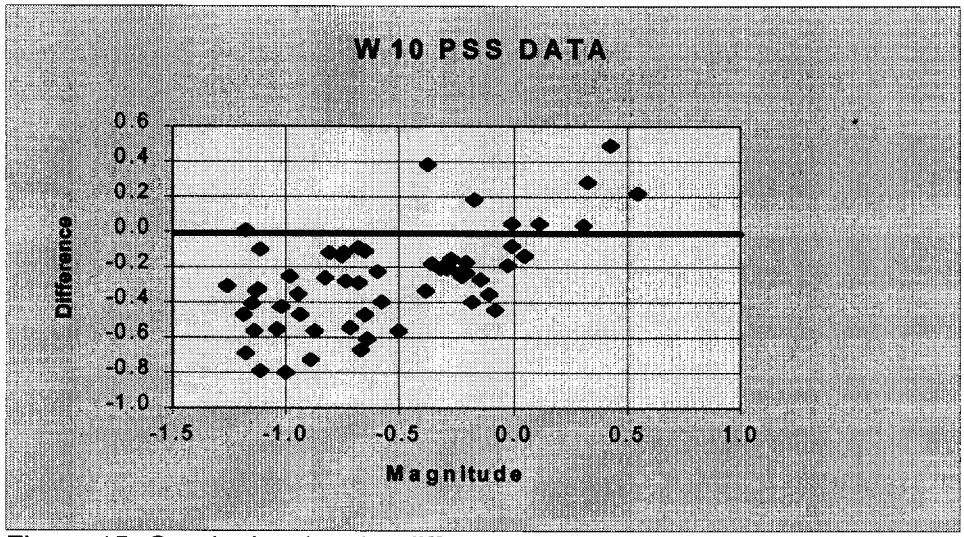

Figure 15. Graph showing the differences between the "regular" PSS event magnitudes and the magnitudes based on the sum of the P and S energies.

Although figure 15 displays quite a bit of scatter, it indicates that the smaller magnitudes are generally under-estimated. Spottiswoode (pers. comm.) attributed this phenomenon to the greater attenuation suffered by the relatively higher frequency content of smaller seismic events.

7. Seismic Source Mechanisms.

7.1. Ratio of P-wave to S-wave:

The ratio of P-wave seismic moment to S-wave moment were plotted against the ratio of P-wave source radius to S-wave source radius. It is possible that this type of diagram can shed some light on the source mechanisms of different seismic events, with seismograms originating from a "crush"-type event having a relatively stronger P-wave moment and source radius than S-wave. For the sake of clarity, the results were split between two charts: figure 16 showing all events closer than 20m to the reef plane, and figure 17 all events more distant from the reef plane. It is worthwhile keeping in mind that the vertical location accuracy is the least reliable (due to the geophones being in a nearly planar configuration), which means that the events that located near to the reef can be regarded as ***at*** the reef plane.

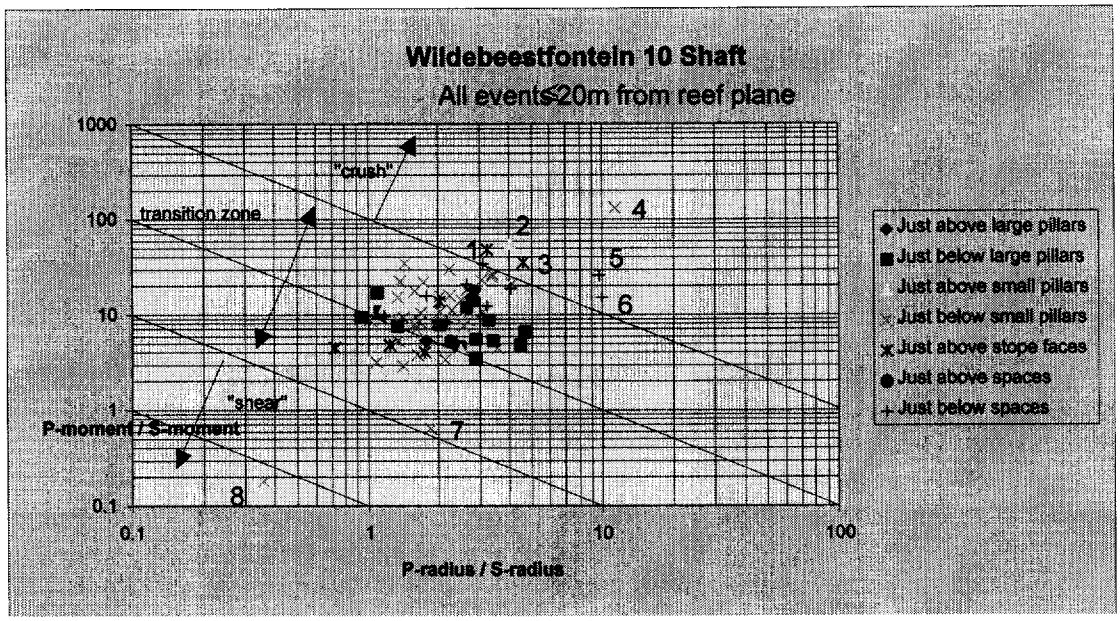

Figure 16. Plot of events at Wildebeestfontein 10 Shaft showing relative propensities for various source mechanisms of events located near the reef plane.

Most of the events plotted on figure 16 fall in the transition zone, making it difficult to comment on the source mechanism at work. There are a number of events which plot at more extreme ranges, and these are more amenable to further interpretation:

1. Events 1 and 3: these events may represent face bursts
2. Events 2 and 4: these events may be due to small support pillars crushing under load
3. Events 5 and 6: may represent buckling up of footwall, a phenomenon which has been observed underground
4. Events 7 and 8: may represent shearing at the edge of the root of a small pillar as it punches into the footwall.

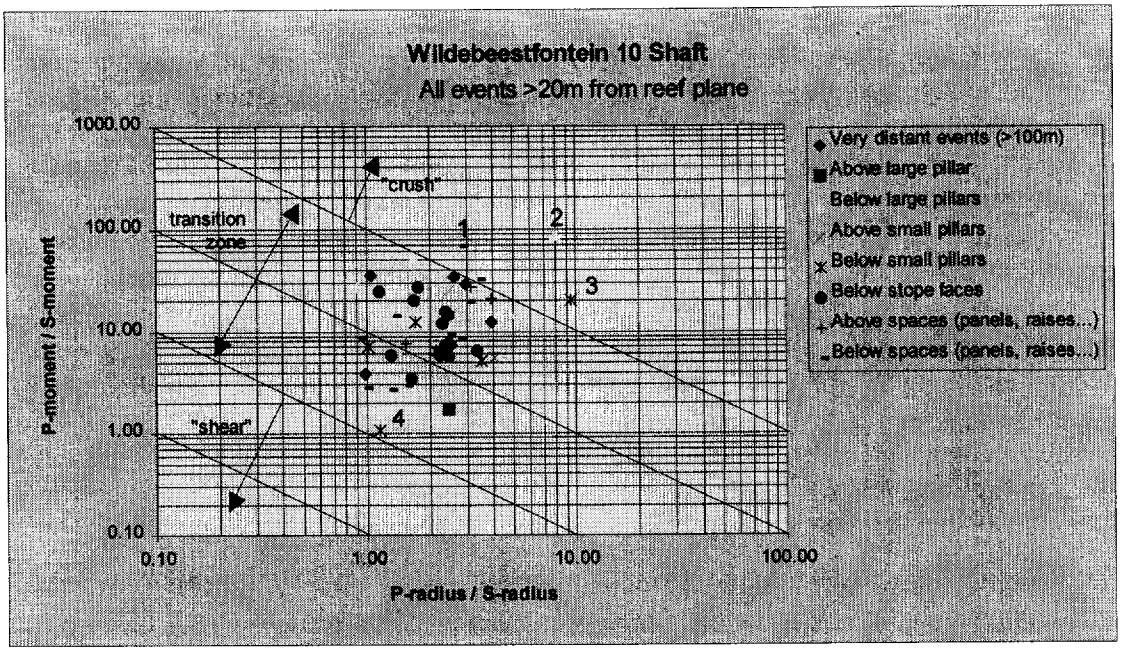

Figure 17. Plot of events at Wildebeestfontein 10 Shaft showing relative propensities for various source mechanisms of events located distant from the reef plane.

The more distant events plotted in figure 17 show a similar picture to figure 16, with few events plotting in the more extreme ranges. Four events were selected for further comment:

1. Event 1: this event located only 27m below a raise (centre gully) and probably represents the footwall buckling up
2. Event 2: this event located an estimated 40m below the edge of a medium-sized triangular pillar (28m x 12m) at some 600m from the network, and taking the inaccuracies for such a configuration into account, probably represents a burst on the sidewall of the pillar, or failure of one of the apexes of the pillar
3. Event 3: may represent the compressional component of a small pillar punching into the footwall
4. Event 4: may be due to the shear component at the edge of the root of a small pillar punching into the footwall.

7.2. Moment tensor inversion:

Various techniques have been proposed in the literature for the inversion of the seismic moment tensor, some with more success and acceptance than others [Jost & Herrmann (1989), Pearce & Rogers (1989) and Koch (1991)]. However, all have proved to be very sensitive to noise contained in the seismic signal (seismogram). A lot of effort was therefore expended in determining the correct direction cosines for the PSS set-up at Wildebeestfontein 10 Shaft. Even so, only 17 successful moment tensor inversions were achieved from a total of some 940 available events, mainly because the moment tensor solution is severely underdetermined for the present 10 Shaft PSS installation. It must also be realised that the inversion technique is still in a development stage and that it will become

more robust with increasing development and experience. Initially the objective was to verify the validity of the technique. Towards this end a coarse approach at interpreting the results was taken, by only looking at the trace of the tensor matrix. It has been shown that the trace of the moment tensor is directly related to the change in volume (volumetric moment) associated with the seismic event. Individual correlation of the volumetric component with the actual seismic event led to the following observations:

- all the events with positive volumetric moments (i.e. "explosive" source) could be correlated with production blasts,
- all events with small moment traces (i.e. small volume component, with mainly shear) were located away from the reef plane in solid rock, and
- close to 80% of the events with negative volumetric components (i.e. "implosive" source) could be correlated with hanging wall collapse, while the remainder may be related to partial failures of stope support yield pillars.

Based on these observations, one can be optimistic and state that the moment tensor inversion technique appears to be reliable, and with some refining should yield specific seismic source mechanisms for individual events. This type of information would be vital in building an understanding of the seismicity encountered in the mining operations in the Bushveld Igneous Complex. Figure 18 (overleaf) shows the distribution of the different source mechanisms on a plot of the ratios of the P source radius to the S source radius versus the P-moment to the S-moment. All the events for which moment tensors were determined plot in the "intermediate zone", and shows why the "P over S" type of representation has had limited success in discriminating between "shear" and "crush" type events since the majority of events tend to fall in the transition zone (i.e. a combination of crush and shear mechanisms).

The relatively high number (approximately 60% of the successful inversions) of events with an "implosive" type source mechanism was initially a source of concern, as conventional wisdom deemed this unlikely. However, Stickney and Sprenke (1993) have found that some 90% of 190 closely observed seismic events in the Coeur d'Alene mining district of northern Idaho showed significant implosive first motions. Although they could not present source models to account for all these events (some of which located several hundreds of metres in solid rock), it was felt that these implosive events generally relate to stope closure. This conclusion is in part supported by the correlation at Wildebeestfontein 10 Shaft of implosive events with falls-of-ground. The crushing and/or (partial) failure of a pillar would also have a component of closure associated with it, and would therefore also be expected to exhibit a significant volumetric moment.

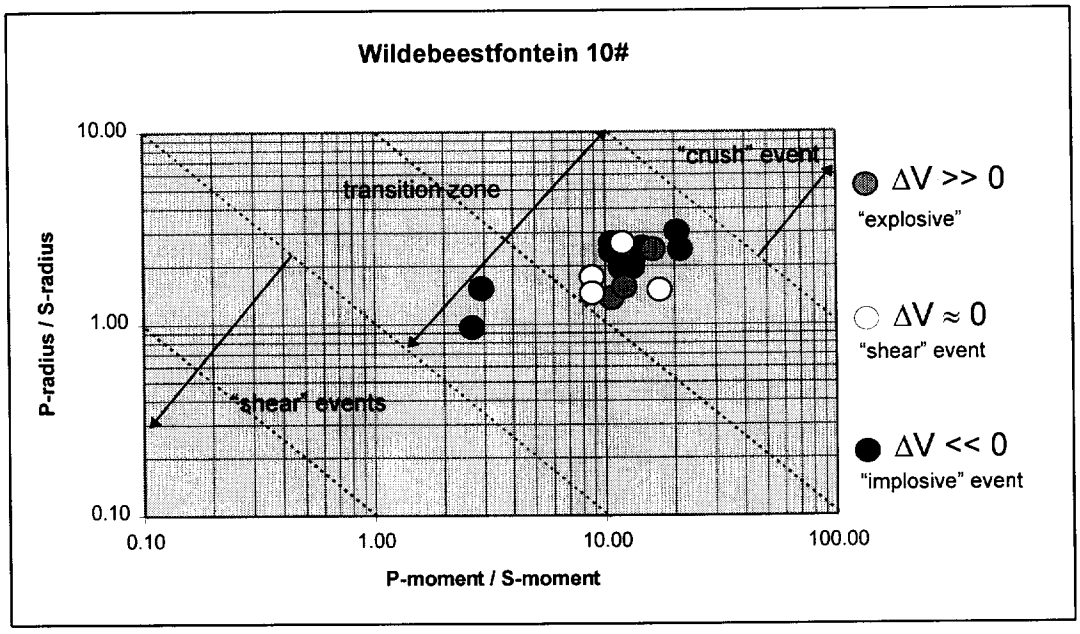

Figure 18. Distribution of the volumetric component of moment tensor solutions on a "P over S" plot.

8. Conclusions

Analysis of the data recorded by the present PSS installation at No.10 Shaft, Wildebeestfontein North Mine afforded the following conclusions to be reached:

- From September 1993 to August 1994 some 254 mining induced seismic events were recorded at the PSS site. The magnitudes of these events ranged from -1.8 to +1.1.
- Frequency - magnitude analysis indicated that the potential for seismic events larger than M_{max} = +1.1 to occur in the study area is limited.
- Although the largest number of events occurred during the blasting period and directly thereafter, the larger magnitude events tend to occur outside this time period.
- The majority of the larger events occurred on the pillars and remnants, probably due to the (partial) failure and / or punching into the footwall of these pillars.
- Some of the larger events occurred in the back areas of stopes, and generally coincided spatially with falls-of-ground.
- Few larger events occurred at active stope faces, but there was at least one instance where it was observed that a M_L = +0.8 event was associated with a significant fall-of-ground in the face working area.
- The up-dip panels between W1566 and W1567 displayed an anomalous seismic pattern, with most events occurring at the side abutments of the panels.

- Most events located at or very close to the reef plane.

- Interpretation of seismic source parameters such as stress drop and energy index demonstrate the build-up of conditions of higher stress at pillars and at the edges of remnants and regional/stabilising pillars.

- Some success was encountered with inversion for the seismic moment tensor, giving information about the seismic source mechanisms:
  - mainly shear type events located some distance from the reef plane in solid rock, and are probably related to geological structures;
  - "explosive" type events were all correlated with production blasts; and
  - "implosive" or "crush" type events could generally be correlated with falls-of-ground or (partial) failure of stope support yield pillars.

9. Recommendations

The comparison of geotechnical and geological factors with the seismic results would enhance the present state of understanding of the behaviour of the rockmass in the Bushveld Complex. In order to allow the widest possible applicability of this work to the platinum mining industry as a whole, it is imperative that the largest possible variety of ground conditions be covered. It is therefore strongly recommended that the present initiative be continued, and that more areas be included in the database.

It will be necessary in future areas covered by a seismic network, to correlate detailed observation of seismic damage underground with seismic source parameters, discussed in this report, of the causative event. In this way a database of knowledge will be developed that will allow interpretation of seismic data to be made with ever increasing confidence and accuracy.

10. References

1. van Aswegen, G. & Butler, A.G., 1993. Applications of quantitative seismology in SA gold mines., in: *Young, R.P. (Ed.) Rockbursts and Seismicity in Mines*, Balkema, Rotterdam.

2. van Aswegen, G. & Meijer, O., 1994. The mechanisms of seismic events around faults in mines., in: *Proceedings: Eurock '94, Delft, The Netherlands*, Balkema, Rotterdam.

3. Boatwright, J. & Fletcher, J.B., 1984. The partition of radiated energy between P and S waves., *Bull. of Seism. Soc. of Am.,* vol.74(2), pp. 361-376.

4. Brune, J.N., 1970. Tectonic stress and the spectra of seismic shear waves from earthquakes., *J. Geophys. Res.*, vol. 75(26), pp. 4997-5009.

5. Jost, M.L. & Herrmann, R.B., 1989. A student's guide to and review of moment tensors., *Seismo. Res. Lett.*, vol. 60(2), pp. 37-57.

6. Koch, K., 1991. Moment tensor inversion of local earthquake data - I. Investigation of the method and its numerical stability with model calculations., *Geophys. J. Int.*, vol. 106, pp. 305-319.

7. Mendecki, A.J., 1993. Keynote address: Real time quantitative seismology in mines., in: *Young, R.P. (Ed.) Rockbursts and Seismicity in Mines*, Balkema, Rotterdam, pp. 287-295.

8. Pearce, R.G. & Rogers, R.M., 1989. Determination of earthquake moment tensors from teleseismic relative amplitude observations., *J. Geophys. Res.*, vol. 94(B1), pp. 775-786.

9. Stickney, M.C. & Sprenke K.F., 1993 seismic events with implosional focal mechanisms in the Coeur d'Alene mining district, northern Idaho., *J. Geophys. Res.*, vol. 98(B4), pp. 6523-6528.

Appendix D

Analysis of Seismicity at Bafokeng North Mine

SIMRAC PROJECT GAP027 ENABLING OUTPUTS 3, 4 & 5

FINAL REPORT
PART 2

ANALYSIS OF MINING INDUCED SEISMICITY RELATED TO THE PLATINUM MINES OF THE BUSHVELD COMPLEX: No. 12 SHAFT, BAFOKENG NORTH MINE

A.J. van der Merwe
CSIR Division of Mining Technology
24 November 1995

CSIR
WNNR

CONTENTS

1. Introduction

During the course of 1992 the stope pillar layout at 12 Shaft Bafokeng North Mine (Impala Platinum Mines) changed from a diamond pattern of 5×5 m stiff pillars with a 30 m spacing, to a pattern of 6×3 m "yield" or "crush" pillars (see figure 1 below), spaced 8 m apart along strike and 31 m along dip. The purpose of investigating the seismicity at Bafokeng 12 Shaft was two-fold: (a) to investigate the effect of different mining techniques on the seismicity, (b) to compare the reputed low seismicity at Bafokeng 12 Shaft to other areas. Historical seismic data covering a four-month period before this change and data covering a similar period some time after this change were analysed in a statistical way to monitor the effect of the change in support layout on the rockmass.

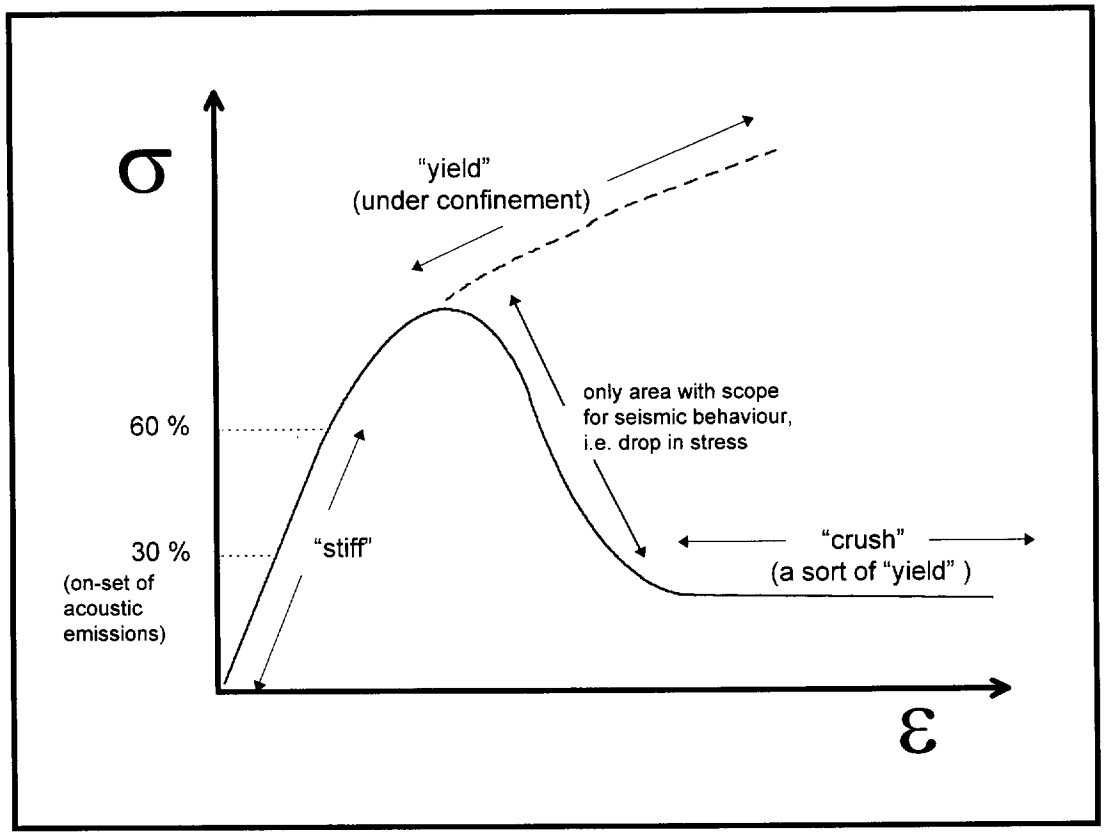

Figure 1. Idealised Pillar behaviour.

2. Seismic Monitoring System

The seismic monitoring system deployed at 12 Shaft Bafokeng North Mine is a GENTEL system comprising a single triaxial geophone set, located down a 50m deep vertical drillhole on surface. Events are located by determining the incoming dip angle and azimuth of the event, and using the P and S wave time separation. If the event is distant enough that the straight-line ray path is closer than 50° to the surface, the waveform is deformed by interference from reflections at the surface. Most of the area analysed in this study falls outside the cone describing the proper operating limit of the

GENTEL system. However, since accurate locations are not necessary for the types of analyses employed, this is not seen as a negation of the results obtained.

The raw waveforms were processed using the PSS analysis software so that the stress drop associated with a seismic event may also be calculated.

3. Spatial Distribution

The general distribution of seismic events at 12 Shaft (see figure 2 below) show a familiar pattern viz.: the majority of seismic events locate in the vicinity of current stoping. There is a concentration of events that occurred during 1993 in an area towards the south. This will be discussed in some detail in paragraph 4.1.

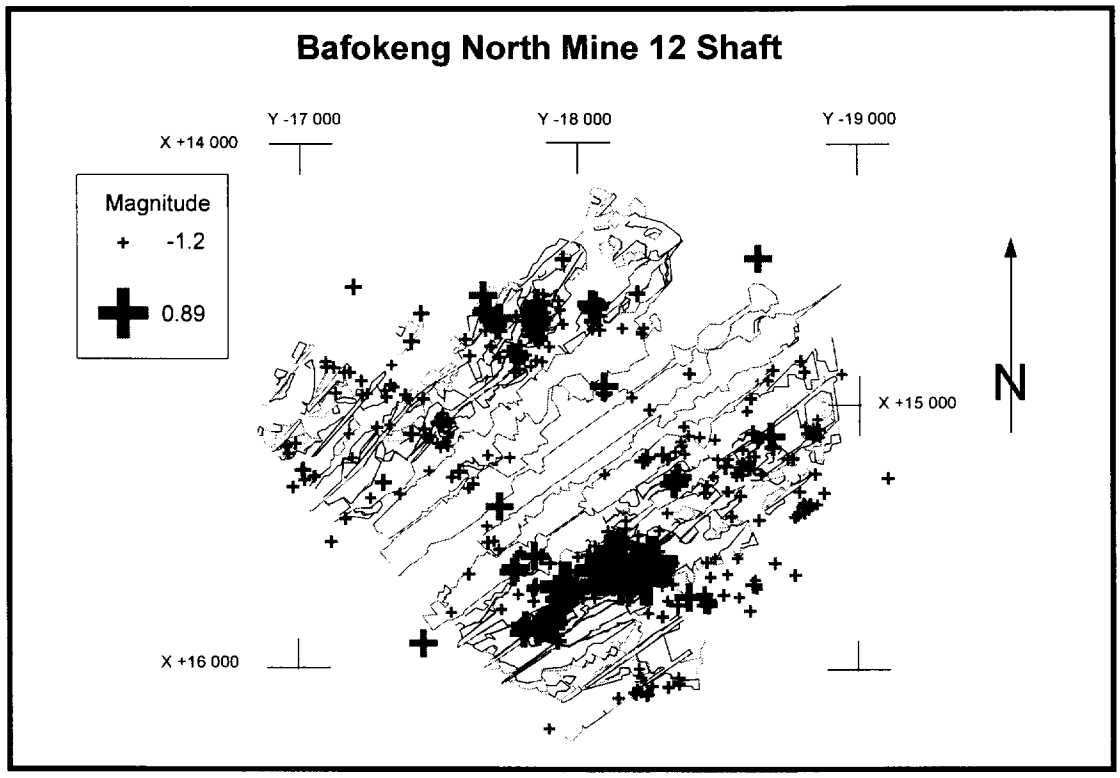

Figure 2. Spatial distribution of seismicity at Bafokeng North 12 Shaft, for the period mid 1991 to mid 1993.

Figure 3 (overleaf) shows the location of events in section: it is clear that the vast majority of events located on or near to the Merensky reef plane. Due to the remoteness of the GENTEL station, and therefore the relative large errors of location particularly in section, it is not possible to comment sensibly on the events located deep in the footwall or hangingwall, although these are more than likely related to geological structures.

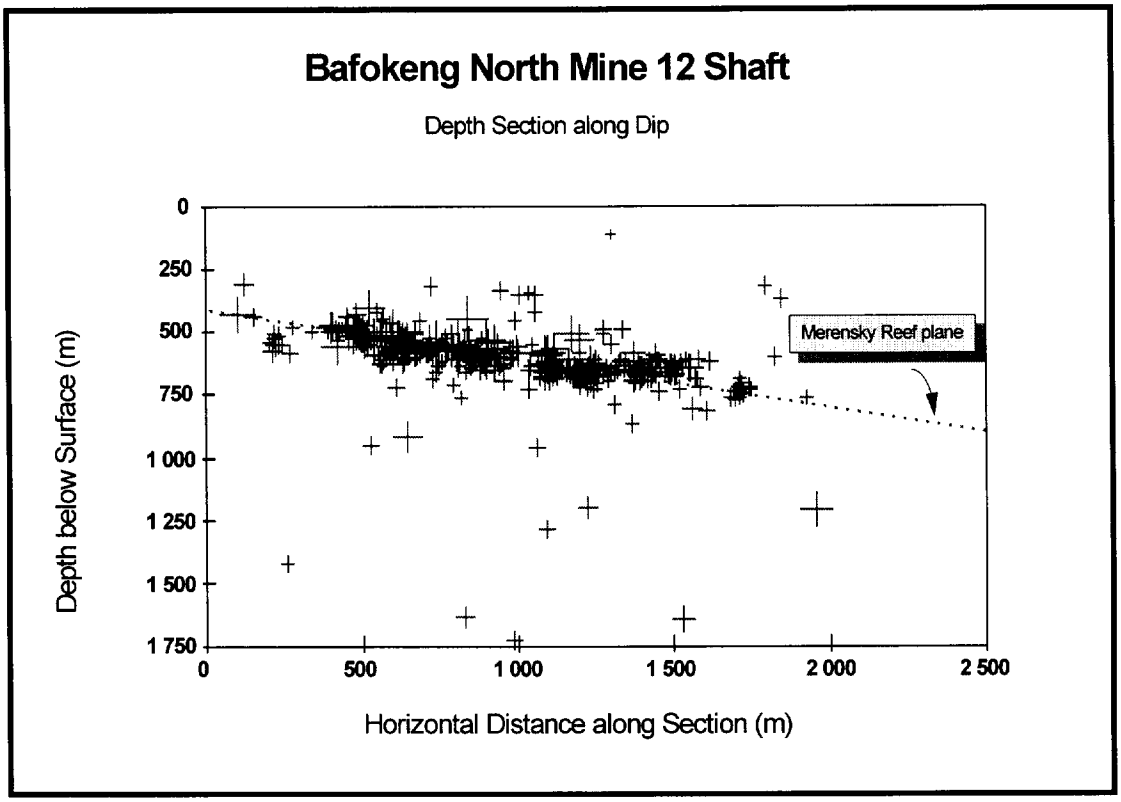

Figure 3. Dip section of seismicity at Bafokeng North 12 Shaft, for the period mid 1991 to mid 1993, showing the location of events relative to the Merensky reef.

4. Comparative Analysis

Several seismic parameters were evaluated to determine the effect that the change in mining layout had on the seismicity.

4.1. Location

The seismic events that occurred during the last four months of 1991 located fairly randomly over the active working areas (see figure 4 overleaf). In contrast, the events that occurred during early 1993 tended to cluster in certain areas (figure 5 overleaf). During this period a large concentration of seismic events occurred near the southern extremity of the mine. Although the events located outside the functional range of the recording system, it is perhaps worth noting that they coincide with a barrier pillar and a dyke. However, these element have existed during previous mining without causing significant seismic activity. It is perhaps worthwhile to note that ***all*** the larger seismic events occurred at this locality.

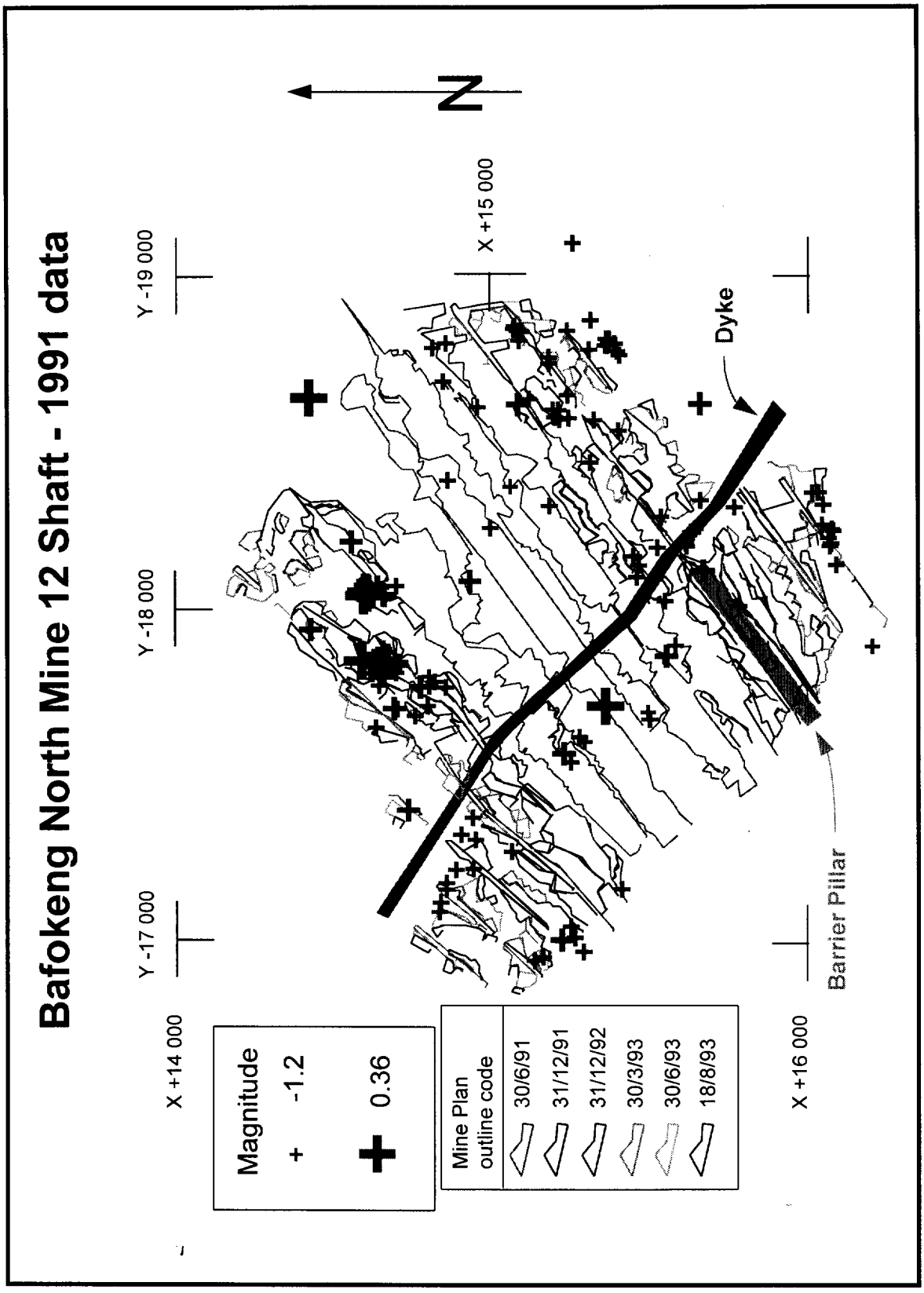

Figure 4. Spatial distribution of seismicity at Bafokeng North 12 Shaft, for the period late 1991.

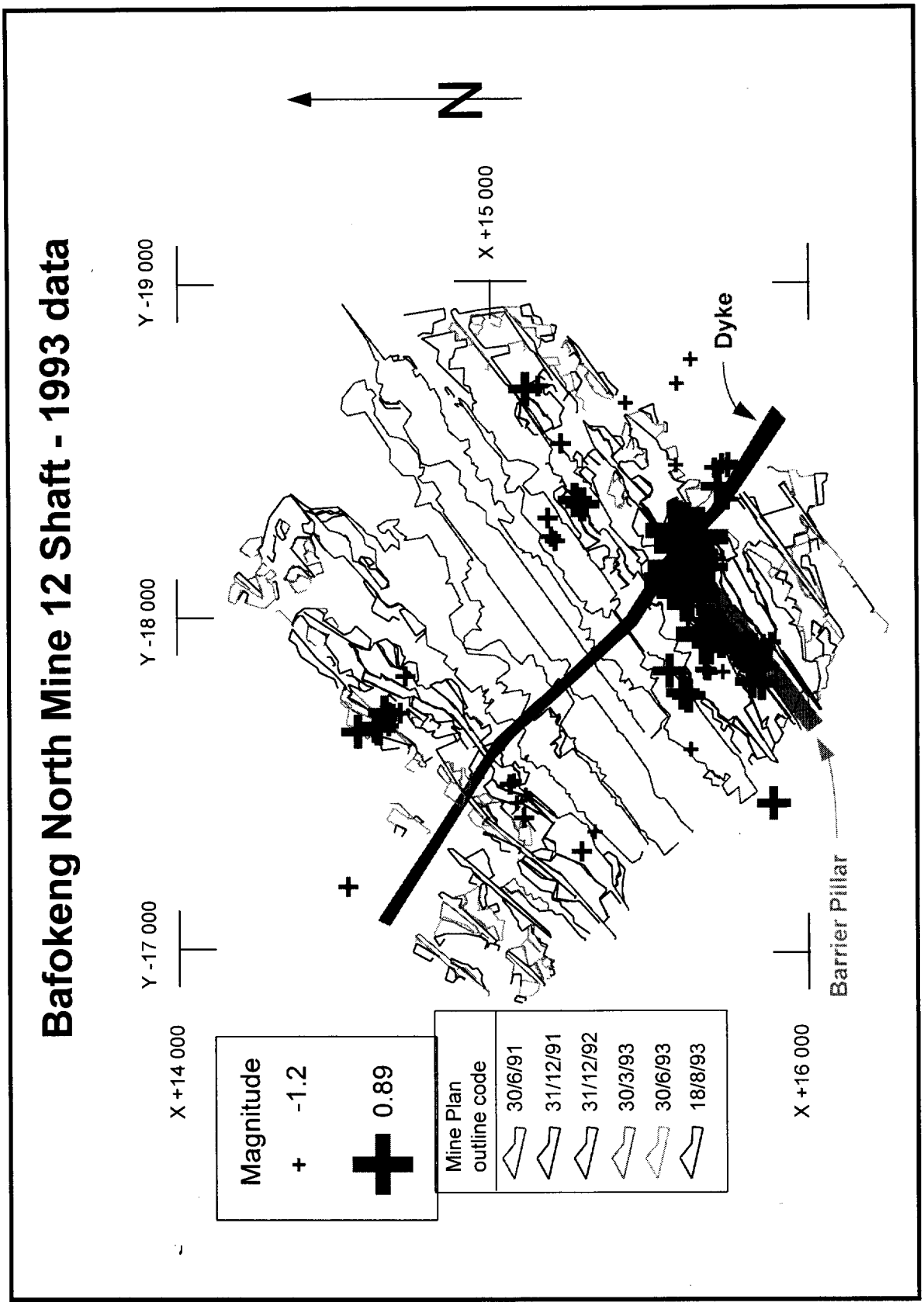

Figure 5. Spatial distribution of seismicity at Bafokeng North 12 Shaft, for the period early 1993.

4.2. Frequency - Magnitude distribution

A total of some 155 events larger than magnitude -1.2 were recorded during the late 1991 period, a large proportion of which were smaller than -0.5 (figure 6 below). The largest event recorded was 0.36. In comparison, the median magnitudes of events recorded at Frank Shaft and Wildebeestfontein (Aref, Jager and Spottiswoode, 1995) were significantly higher (figure 7, below). A high b-value of 1.5 was calculated, also indicating that large magnitude events were uncommon during this period (figure 8 overleaf).

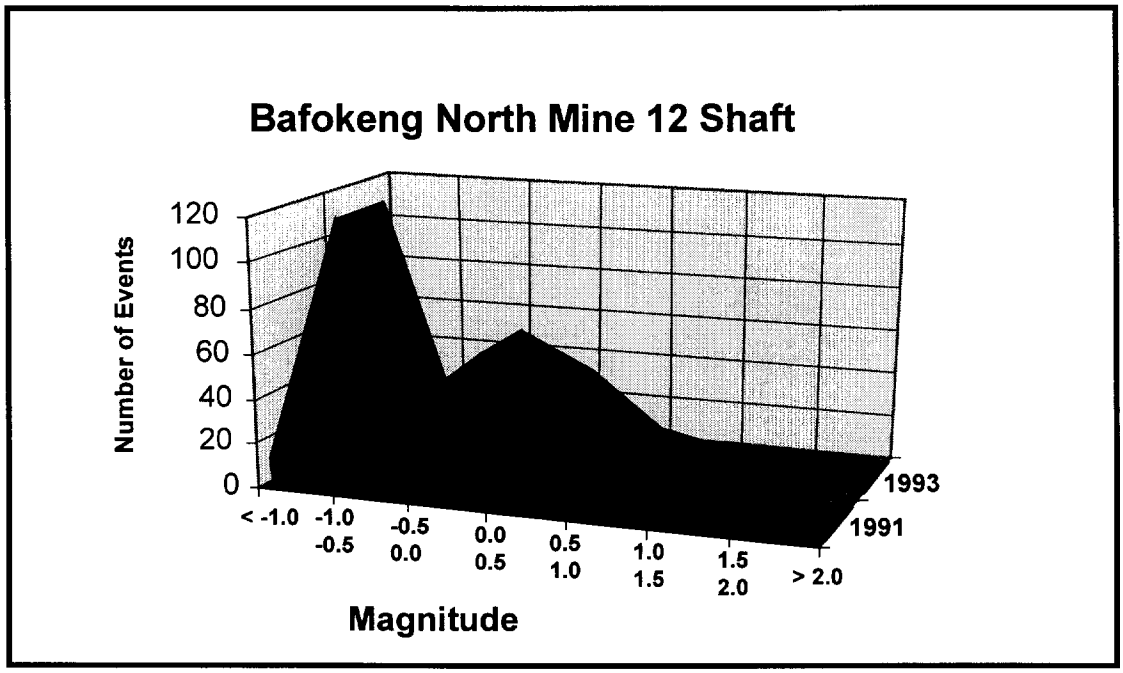

Figure 6. Comparative histogram of number of events.

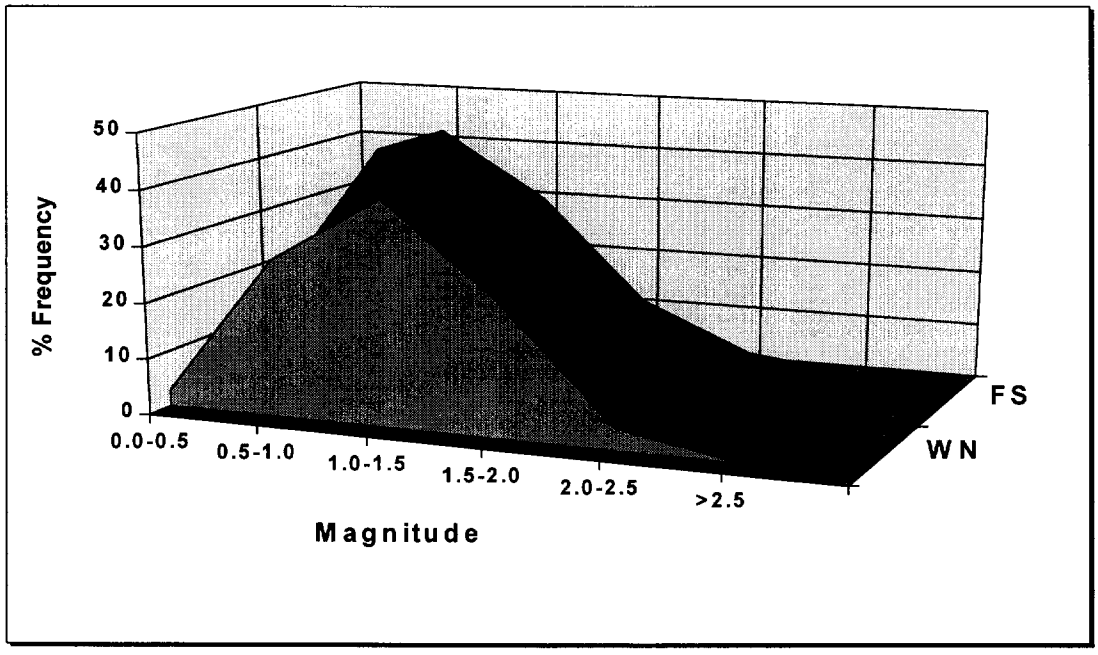

Figure 7. Comparative histogram showing magnitude distributions of seismic events recorded at Frank Shaft (FS) and Wildebeestfontein North 10 Shaft.

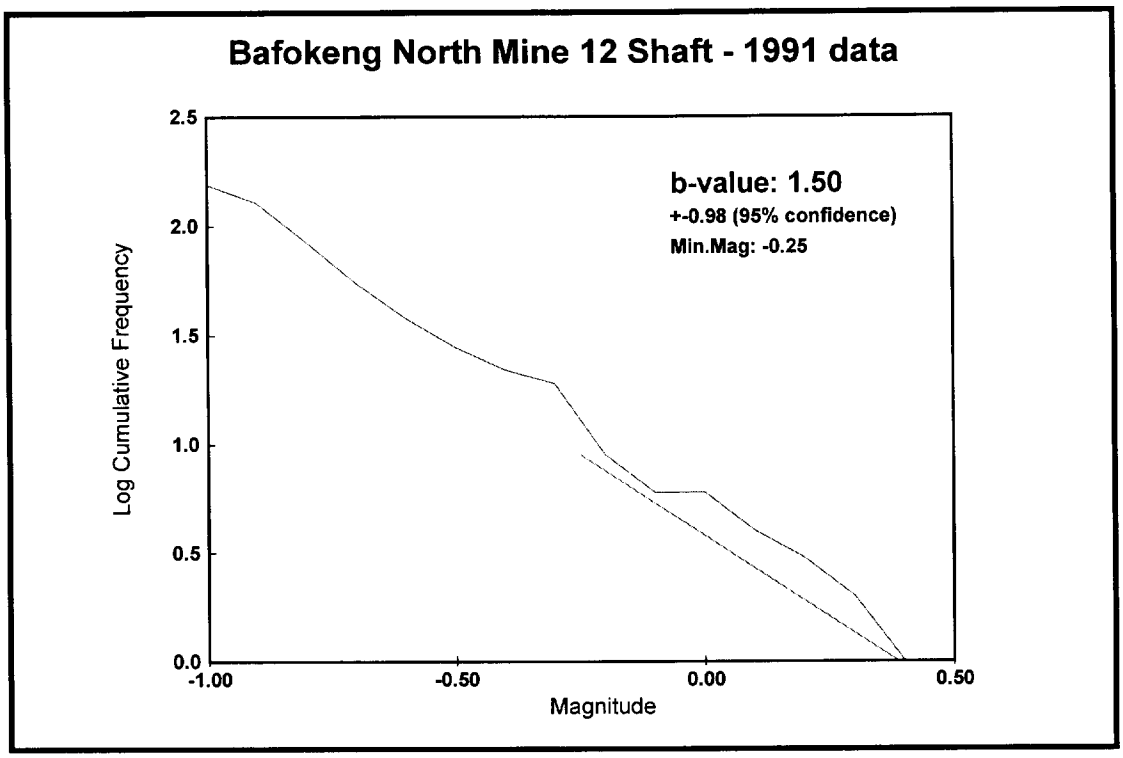

Figure 8. Frequency - Magnitude distribution of events recorded late 1991.

The 1993 data (figure 9) shows a propensity towards slightly larger events than the 1991 data, as evidenced by the somewhat lower b-value (1.25 vs. 1.50). This tendency is reinforced by figure 6, which shows a stronger "tail" of larger events.

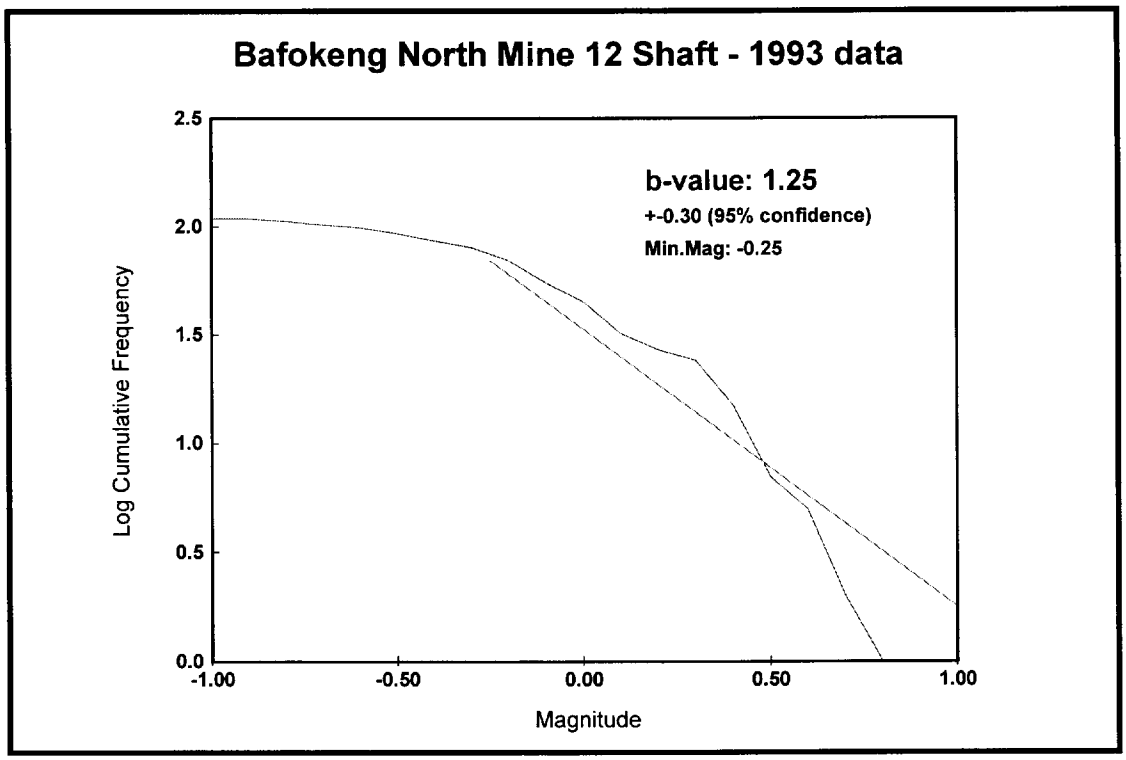

Figure 9. Frequency - Magnitude distribution of events recorded early 1993.

4.3. Static Stress Drop

Unlike the magnitude distribution, the stress drop distribution did not change significantly after the switch over from a stiff pillar system to a yield pillar system (figure 10 below), indicating that the ambient stress field around the workings has stayed the same.

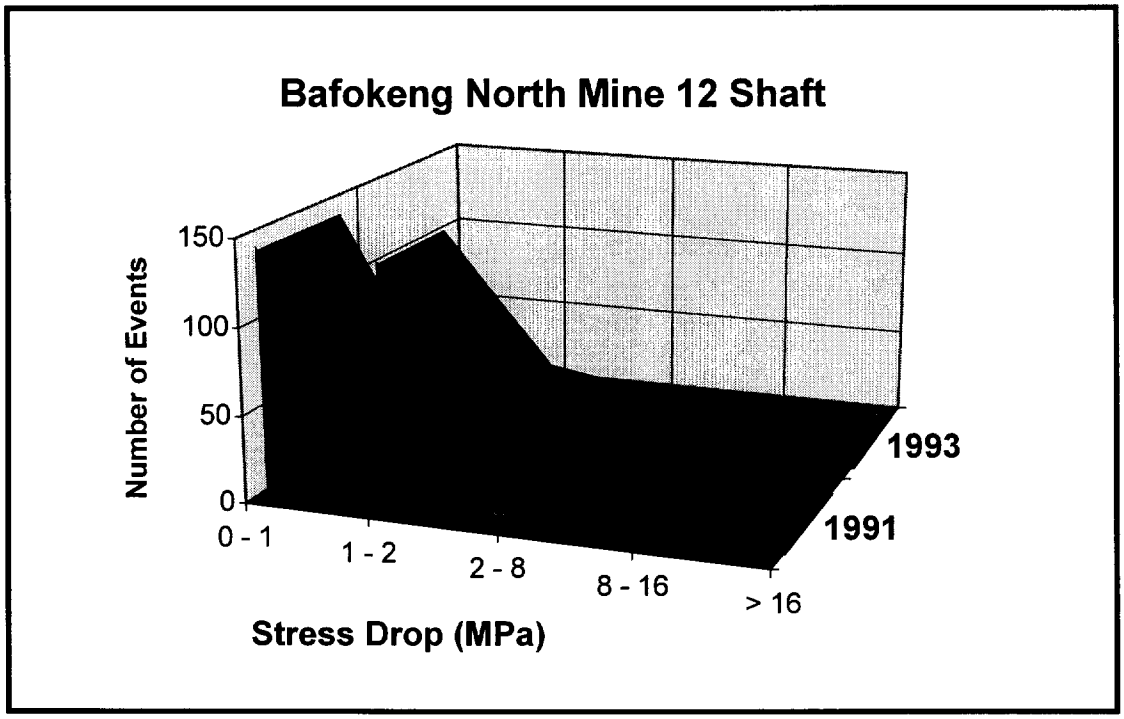

Figure 10. Comparative histogram of Static Stress Drop for "stiff" (1991) and "yield" (1993) pillars.

4.4. Released Energy

The seismic energy released per area mined increased seventeen fold after the introduction of the yield pillars (see Table 2 below). This phenomenon is interpreted as showing that the yield pillars allow at least some energy to be released seismically, whereas with the stiff pillars conditions can be considered seismically stable. However in both cases the amount of seismic energy released is extremely low.

Table 2. Seismic energy released.

	Total Energy (J)	Area Mined (m^2)	Energy per Area Mined (J/m^2)
Stiff Pillars	1.28 E+06	144 650	9
Yield Pillars	1.82 E+07	116 897	156

4.5. Volume change method (Gamma value)

McGarr (1976) has shown that a relationship exists between seismic moment and the rock mass deformation due to mining activities. This relationship can be rearranged and written in the following way:

$$\gamma_c = \frac{\Sigma M_o}{G \cdot \Delta V} \quad ,$$

$$where: \Sigma M_o = Sum\,of\ Seismic\ Moments$$

$$G = Modulus\,of\ Rigidity$$

$$\Delta V = Total\ Volume\,of\ Closure$$

Gamma (γ_c) is an indication of the seismic moment recorded, as a fraction of the volumetric moment induced by mining. It was assumed that the average closure for both pillars layouts was 50 mm (from Aref, Jager and Spottiswoode, 1995). Looking at the γ_c values (Table 3 below), it is obvious that a much larger proportion of the volumetric moment is translated into seismicity by the yield pillar system.

Table 3. Volume change method (Gamma value)

	Σ Mo (N-m)	Area Mined (m^2)	Volume Closure (m^3)	γ_c
Stiff Pillars	3.79 E+12	144 650	7 234	0.02
Yield Pillars	2.19 E+13	116 897	5 845	0.13

4.6. Other Platinum mining areas

The seismic parameters determined for Bafokeng 12 Shaft were compared to results obtained by Aref, Jager and Spottiswoode (1995) for Frank Shaft (Rustenburg Platinum Mines) and Wildebeestfontein North 10 Shaft (Impala Platinum Mines). Table 4 (below) shows that the seismic energy released per area mined is very low at Bafokeng 12 Shaft, while the Gamma value for the 5×5 m pillar system is lower than that for the crush pillar system at Frank Shaft. Comparing the two 6×3 m pillar systems, the gamma value at Wildebeestfontein 10 Shaft is three times that at Bafokeng 12 Shaft. Since Bafokeng 12 Shaft and Wildebeestfontein 10 Shaft employ the same mining layouts, the difference in seismic energy released must be due to some other factor, perhaps related to different geotechnical conditions or to local variations in the stress regime.

Table 4. Comparison of Bafokeng 12 Shaft seismic parameters to other areas.

Mine	Energy Released per Area (J/m^2)	Gamma γ
Frank Shaft	1 300	0.04
Wildebeestftn 10 Shaft	6 600	0.4
Bafokeng 12 Shaft ***5×5***	9	0.02
Bafokeng 12 Shaft ***6×3***	156	0.13

5. Discussion

Table 5 below gives a summary of the seismic characteristics associated with the two different pillar systems.

Table 5. Summary of seismic characteristics of stiff and yield pillar layouts.

	b-value	Energy / area mined (J/m^2)	γ_c
Stiff Pillars (1991)	1.50	9	0.02
Yield Pillars (1993)	1.25	156	0.13

The slight decrease of the b-value indicates that the magnitudes of the seismic events increased somewhat after introduction of the yield pillars, but this shift is not radical (refer to figure 9). Similarly, there was almost no change in the stress drops associated with the seismic events (refer to figure 10), indicating that the ambient stress field around the workings had stayed substantially the same. However, Table 5 shows significant differences in the values for the energy released per area mined, as well as in the gamma factor. These differences show that a much larger proportion of the energy transferred into the rock by the mining process is released by the yield pillar system, whereas the stiff pillars allow more of the energy to be stored in the rockmass.

Since the release of energy through the yield pillars occurs by means of seismic events which are still relatively small (M-0.5 to M+0.5), these pillars are considered to be "working" in the physical sense, and at deeper depths should do more so.

The concentration of seismic events on the barrier pillar during the period after the 6×3 m pillars were introduced demonstrates an increased stress transfer to the barrier pillar. This could be explained either by the supposition that the 6×3 m pillar system is "softer" than the 5×5 m pillar system and was yielding, or by the fact that the mining in the vicinity of the barrier pillar had surpassed some critical span beyond which it may be inevitable that stresses would become high enough to start fracturing the pillar. Concentrated seismic monitoring of an equivalent situation could provide answers and more importantly give improved insight into rockmass behaviour in pillar supported mines.

6. Conclusions

The results of the seismic analysis of two different stope pillar layouts at 12 Shaft, Bafokeng North Mine, show that the "yield" pillar system under the prevailing geological and mining conditions releases some of the energy transferred into the rockmass by the mining process by means of low intensity non-damaging seismicity. However under different geological conditions, but at similar mining depths, at Wildebeestfontein 10 Shaft the same pillar system is associated with significantly different and more severe seismicity, resulting in some damage to excavations and pillars. At the mining depths and spans, and with the geological conditions at Bafokeng 12 Shaft, the 5×5 m pillar system prevented any seismic activity of consequence from occurring. Again it should be noted that under different circumstances 5×5 m pillars have been known to burst and be the direct cause of seismicity and damage. An understanding of the underlying causes for the different seismic responses to different inherent conditions is essential if strategies to ameliorate the expected seismic problems at greater depths in the Bushveld Complex are to be developed. This

research has also illustrated the usefulness of seismic monitoring as a tool to assist the evaluation of different rock engineering approaches, and in understanding rockmass behaviour.

7. References

1. Aref, K., Jager, A.J., & Spottiswoode, S.M., 1995. An Assessment of Seismicity at Wildebeestfontein North Mine and Frank Shaft., SIMRAC Interim Report: Project GAP 027/028, CSIR Mining Technology.

2. McGarr, A., 1976. Seismic Moments and Volume Changes., J. Geophys. Res., vol. 81(8), pp. 1487-1494.

Appendix E

Rock Properties Data Base

Rock Strength Database

Project GAP027
November 1995

1. BACKGROUND

The need for a central computerized database of rock strength properties has been recognized for some time. Many thousands of tests of rock specimens have been carried out over the years, but the information is stored in diverse formats and at scattered locations. Central computerization would readily allow ad hoc extractions and correlations of rock strength data; something which is virtually impossible at present, but which would be extremely useful in many mining and rock engineering applications.

In 1993, Mr A J Jager (COMRO, Rock Engineering) started investigating the creation of such a database. The CSIR were at that time developing an ambitious GIS database which included aspects of detailed geological mapping and rock/soil data storage. However, this database appeared too complex to be suitable for general use in the Mining industry. Consequently Mr Jager, together with Dr J A Ryder and Mr B P Watson, drew up a draft specification of a database tailored specifically for use by the local Mining industry. This document was used as basis for a more detailed specification prepared by Mr T M O'Brian (COMRO, Special Projects).

The database system selected was MS ACCESS. This system is said to be suitable for small/medium scale databases, and is especially good at supporting very flexible ad hoc groupings/queries of the stored data; it is currently the most widely-used system for new database applications in the world. ACCESS is, however, weak at supporting **interactive** graphics; such features are best written in Visual Basic, as linked ("OLE") objects in any main ACCESS system.

The code in its present form was developed by Mr M A V Ryder, with revision and graphical extensions by Dr J A Ryder.

2. DATABASE ORGANIZATION

2.1 Tables of Pre-Set Information

In order to minimize data capture errors and inconsistencies, and to facilitate ad hoc queries out of the database, certain types of information are held in pre-set tables. Out of these tables, a user (whether he is capturing data, or querying the database) can select pre-ordained items of information - e.g. the name "Blyvooruitzicht" for a particular mine, or "MININGTEK" for a particular rock testing facility. [Other information, such as FailureComments, or a description of the detailed Locality from which a particular sample was obtained, can also be captured and retained on the database but are free-form and would therefore be unsuited to later rigorous groupings/queries of the stored data.]

These pre-set tables in their present form (they are capable of being amended, and doubtless many changes and additions will take place in future years) are listed in Appendix I. They are described briefly below.

(a) Districts (20 in all), comprising a DistrictID and a mining District name (8 chs). Used for grouping sets of neighbouring Mines, and for labelling appropriate sets of stratigraphic elements in the geological Members table.
(b) Mines (138 in all), comprising a MineID, DistrictID and a Mine name (16 chs).
(c) Formations (22 in all), comprising a FormationID and a Formation name (16 chs). These are geological names for major groupings of individual Member stratigraphic units. Typical entries are "BC-CriticalZone" (i.e. the platiniferous zone in the Bushveld), and "Wits-Main" (i.e. the Formation containing the MainReefLeader, MainReef and CarbonLeader Members in the Witwatersrand Basin).
(d) Members (typically 40-50 per mining District), comprising a MemberID, FormationID, DistrictID, a "Sequencer" to force correct stratigraphic sequence onto any tabulation presented to a user, and a Member name (32 chs). These are mainly colloquial names and can include synonyms; a typical entry is "Basal/Steyn reef".
(e) RockTypes (currently 60 in all), comprising a RockTypeID and a RockType description (24 chs). These are sorted alphabetically and are ordered by a prefix as follows: C="Coal", D="Dyke/Sill", I="Intrusive/Igneous", L="Lava", S="Sedimentary". A typical entry is "S-Quartzite-Siliceous", meaning a (sedimentary) siliceous/glassy quartzite.
(f) GrainSizes (9 in all), comprising a GrainSizeID and a GrainSize description (8 chs). These include "Fine", "Medium", "Coarse", "Gritty", "Pebbly" (which would apply to most D, I or S type rocks) and "Amygdaloidal", "Porphyritic", "Tuffaceous" (which would apply to most L type rocks).
(g) TestCentres (7 in all), comprising a TestCentreID and a TestCentre name (10 chs). This identifies the facility at which the tests were carried out.
(h) Nature of failure (5 in all), comprising a NatureID and a Nature description (16 chs). This can be used to classify the nature of failure of the specimen in a test - "Controlled", "Uncontrolled", "Violent" or "Type II" (the last signifying a reverse post-failure slope in a servo-controlled testing machine).
(i) Geometry of failure (7 in all), comprising a GeometryID and a Geometry description (8 chs). This can be used to classify the geometry of failure of the specimen - "Shear", "Multiple", "Extension/Splitting", "Conical" or "Crushing".

Where appropriate, all of these pre-set tables include an entry **"U", which signifies "Unknown/Unspecified"**. Hopefully, usage of these "Unknown" fields in the storing of tests in the database can be kept to a minimum. Their use must nevertheless be retained - the capture of tests carried out in say 1985 of "S-Quarzite:Argillaceous/MediumGrained" rock samples may well be of interest, even if the "Formation/Member" or "TestCentre", for example, are Unknown and are stored as such on the database.

2.2 Data Organization and Storage

The primary unit of data stored on the database is called a **Batch**: a collection of tests carried out on a single (more-or-less homogeneous) sample or section of core. Typically, a Batch might comprise a set of Uniaxial/Triaxial tests plus a few Brazil or PointLoad tests, all carried out on a particular sample of the same RockType. At present, complete facilities for only Uniaxial/Triaxial tests have been implemented, but provision has been

made for other tests types (Brazil, PointLoad, Indentation, Extension, Width:Height) to be readily implemented in the future.

Briefly, the storage structure on the database is as follows.

(a) A Batch record which contains information on the source of the sample (Mine, Locality, distance above/below nearest mined horizons, Investigation), the TestCentre and Date tested, and the nature of the sample (RockType within a particular geological Formation/Member). Batches are indexed by a unique system-assigned BatchID field.

(b) The associated collection of records of detailed Test results (moduli, peak strength, stress:strain data, etc.).

(c) A "BatchCalcs" record which summarizes average and standard deviation properties of the Batch (moduli, strength regression data, evolution of cohesion/friction/dilation with plastic strain where available, etc.).

The system also maintains a "BatchFlag" record which controls the performance of Batch Calculations and the printing of Reports, where appropriate - c.f. section 4 below.

All non-required fields (such as Young's Modulus in a Triaxial test), if not captured, are stored on the database as "Null" values (that is, blank), and play no part in subsequent calculations.

2.3 Triaxial Data

Uniaxial tests are treated as merely special cases of Triaxial tests (ones where the confining stress is zero). Figure 1 shows a typical example of Triaxial stress:strain curves. Rather than capturing the full set of detailed stress:strain values (which could amount to hundreds of data points and correspondingly excessive data storage requirements), it was decided rather to focus on a set of just six key points on the curves:

The **t** ("tail") point at which the sample has completed bedding down and linear stress:strain behaviour commences.

The **y** ("yield") point at which deviation from linear elasticity begins.

The **p** ("peak") point marking peak strength.

The **f** point marking the beginning of approximately constant negative-slope post-failure behaviour.

The **k** ("knee") point marking the end of approximately constant negative-slope and initiation into final residual strength behaviour.

The **r** ("residual") point marking residual behaviour at which strength remains substantially constant.

These key points (where known) are stored in the form of Sigma1/Epsilon1/Epsilonr triplets. Certain other properties (where known) are also stored, including sample dimensions, elastic moduli (E and nu), rock density, "Poisson's ratios" at the p and r points (useful for determining dilation angles), characterization of the Geometry and Nature of failure, and "Reliability flags" which express whether the moduli and stress:strain data are considered to be reliable enough to participate in the determination of Batch averages and regressions.

Triaxial tests are stored on the database ordered by a unique "TestReference" identifier within BatchID sequence.

3. MANUAL DATA CAPTURE & VALIDATION

Manual means represent a lowest common denominator in capturing data for any database. Means currently available for capturing Batch and Triaxial data are described below; more automated procedures are described later in section 5.

3.1 Manual Batch Capture

Figure 2a shows a typical completed pro-forma for manual batch capture and Figure 2b the corresponding ACCESS "BatchForm" as it would appear on the screen of a PC.

Apart from the "DateTested" field which is typed in normally, all the "Required" fields on the LHS of the screen are selected from drop-down lists which are drawn from tables of pre-set information - c.f. section 2.1 and Appendix I. The appropriate Formation/ Member that should be selected in Figure 2b is "(Wits-Robinson) SpesBona/BPR-B middling".

Fields on the RHS are not strictly required, but are typed in where known. Prior to storage, the system checks that all the Required fields have in fact been captured.

The "Find Record" bottom serves to provide rapid access, in certain cases, to an existing stored Batch - the user is prompted to type in a string of characters, such as "F.Jones", that he remembers featuring somewhere on an existing Batch record. Failing success of this; more conventional navigation buttons are provided at the bottom of the BatchForm screen. These signify respectively "Go to first existing Batch", "Go to previous Batch", "Delete this Batch", "Create a New Batch so that capturing can start", "Go to next existing Batch", "Go to last existing Batch". The current BatchID is displayed on the top right; the BatchID itself is a system-generated number and can never be altered.

A menu bar at the top of the BatchForm (not displayed in Figure 2b) permits navigation back to the StartupForm (section 4.1), or on to capture Triaxial test data.

3.2 Manual TriaxialTest capture

Figure 3a shows a typical completed pro-forma for manual capture of a triaxial test, and Figure 3b the corresponding ACCESS "TriaxialTestForm" as it would appear on the screen of a PC.

The only strictly required data are the "Test Reference" (an 8 chr text identifier, assigned by the user, and unique within the Batch), the "Confining Stress" field, and the "Peak stress" field. All other fields, if not entered, are stored as "Null" values and play no part in subsequent calculations. Prior to storage, the system checks that all Required fields have in fact been entered and that other fields, where entered, obey reasonable limits (e.g. that $0 < \text{Poisson'sRatio} < 0.5$). In addition, checks are made that any entered stress values ascend up to the peak stress value and descend thereafter, and that both the axial and radial strain values are strictly increasing. Any offending fields are highlighted in colour, and the user is requested to correct them.

Once a new Triaxial test is captured, or an existing one is amended in any way, an entry is made in "BatchFlags" table so that BatchCalcs/Printing (c.f next section) will subsequently take place.

Navigation and menu commands are similar to those on the BatchForm described above.

4. BATCH CALCULATIONS & REPORTS

4.1 The StartupForm & Initiation of BatchCalcs/Reports

The StartupForm presented to the user on system startup (and also available from the menus on the Batch and TriTest Forms) is illustrated in Figure 4. The menu bar (not shown in Figure 4) permits the user to Quit, or to return to the ACCESS development environment (something he might have to do to, for example, to modify little-used pre-set Tables, such as inserting a new entry in the "TestCentres" table).

The command buttons on the StartupForm are as follows.

(a) Go to Batch capture (c.f. section 3.1).

(b) Perform BatchCalcs (all flagged Batches are processed and printed, and the BatchFlags cleared) - c.f. following sections.

(c) Amend the "Members" pre-set table. This function is specially provided to cater for the intricacies involved in updating the "Sequencer" field in the Members table to maintain proper stratigraphic sequence in this table. All other tables are sufficiently simple to be amendable via standard ACCESS "View Tables" procedures.

4.2 Batch Calculations (Triax tests) & Detail Reports

On completion (initiated by pressing the "BatchCalcs" Button described above) of calculations for a particular Batch, results are stored in a BatchCalcs table in the database, and are printed out in the form of Figure 5. The report comprises a header with Batch information (c.f. section 3.1) and BatchCalc information, followed by the detailed Triax test data as described in section 3.2 (only 2 tests out of the set of 19 actually in this particular BatchID=123 are illustrated in Figure 5).

The BatchCalc information is organized in terms of the **Mean**, Std Deviation **SD**, and number **n** of participating data points (tests). The abbreviations in the printout have the following meanings:

E: the Young's Modulus (GPa).

nu: the Poisson's ratio.

del1: the amount by which the axial strain had to be shifted (mm/m) to **standardize** the stress:strain curve so that the linear elastic portion passed through the origin.

UCS: the direct UCS (MPa) determined by the subset of Uniaxial (σ_3=0) tests.

uy-ur: the intercept (MPa) on the straight-line σ_1:σ_3 regression of all tests (the "regressed UCS") for points y-r respectively.

bety-betr: the slope on the straight-line σ_1:σ_3 regression (the "strengthening parameter") for points y-r respectively.

cy-cr: the corresponding cohesion values (MPa).

phiy-phir: the corresponding friction angles (deg).

epy-epr: plastic (shear) strain values (mm/m) for points y-r respectively.

dp, dr: the dilation angles (deg) at the peak & residual points, as estimated from the supplied values of nup and nur.

rd: the rock density.

Some tests may not contain all possible data (i.e. certain fields are "Null"), and some tests may have their ReliabiltyFlags set to "No"; such tests do not participate in the relevant calculations and this accounts for the variability in **n**-counts of certain entries.

The information in the BatchCalc table may appear complex, but it is in fact in a form suitable for statistically meaningful later groupings/queries out of the database. Fields of most common interest will be E, nu, UCS, up (the regressed UCS), phip (the strength friction angle). Other fields will be of potential use in forming the basis for FLAC-type modelling exercises.

Mathematical details of the BatchCalcs are given in Appendix II.

4.3 The TRock Program for Graphical Display/Validation of Triaxial Data

The Trock code was written in the Visual Basic language, which fully supports interaction with ACCESS databases and also provides adequate ranges of interactive graphics and mouse commands (the latter, inexplicably, being not supported by ACCESS itself).

On being called, the program links into the current Batch in the ACCESS database and loads and stores all relevant Batch, BatchCalc and TriaxTest data. It then presents two graphs, each on a separate screen - Figures 6a and 6b.

Figure 6a identifies the BatchID and RockTypes, and illustrates the regressions for the 5 main key points y-r, together with dashed error bound lines (spaced 1 SD from the solid best-fit regression line). The scales of these graphs can be changed by clicking the arrow bars on the left and bottom. Clicking on a particular point gives a small pop-up label identifying the TestRef and ConfiningStress of the test involved. Clicking the R mouse button on a point not only identifies the test (in red), but also permanently displays the test identification as a Memo, for later checking/correction of possibly erroneous data.

The next screen, Figure 6b, first shows thumbnail graphs of E and nu vs confining stress σ_3, together with error bounding lines. This presentation could make visible any possible trend of increase of E with σ_3 (occasionally seen in some Bushveld rocks), and also permits identification of possible outliers which can be recorded with mouse clicks on the offending points. The next graphs illustrate, with error bars, the cohesion C, friction F and dilation D evolutions with plastic (shear) strain, in the notation used by the FLAC SS model. The final graphs replicate the stress:strain behaviour of all tests, superimposed in **standardized** (linear elastic portion passing through origin) form. Each group of confining stresses is displayed in a different colour, and again, clicking on particular points permits identification/recording of offending tests for later verification or correction. Arrow bars can again be used to change scales, where desired.

Menu options (not shown) permit quitting, or printing of the above screens.

At present, TRock has to be run as an independent program. The next version of Visual Basic (4.0, already released overseas) should permit linking TRock as an OLE object directly into the ACCESS BatchCalcs routines; this would significantly simplify and rigorize the validation and data purification aspects of capturing triaxial data into the database.

5. AUTOMATIC CAPTURE OF EXISTING MININGTEK TRIAXIAL DATA

The manual procedures for capture of triaxial data described in section 3.2 are perfectly viable, but involve an onerous amount of effort in transferring stress:strain and slope values onto the pro-forma sheets of Figure 3a - typically more than 10 min per triaxial test captured. Many thousands of tests are stored in DOS files at the MININGTEK test facility at present, and a VBasic program to automate the extraction of data out of these files for direct storage on the database has been specified by Dr J A Ryder, and is currently being coded.

This program ("TexFile") will prompt the user for the appropriate DOS filename(s), will display the stress:strain data (suitably smoothed) on the screen, will display suggested key points t-r, and will permit user adjustment of these points where desired. Radial strain slopes nup and nur will likewise be capable of user adjustment if necessary. Capture of other test information, differing from standard default values, will also be catered for.

The entire process of capturing Uniaxial/Triaxial tests should reduce to no more than 1-2 min per test, thus permitting the bulk capture of existing data by clerical staff.

As a future improvement on the capture of triaxial data for which no computer files of any form exist, the use of a scanner or digitizer to capture existing printouts of stress:strain data should be seriously considered.

6. FUTURE DIRECTIONS

With a concentrated effort by one full-time clerical staff member, and a few hours a month of checking and supervision by MININGTEK staff, the bulk of past tests recorded on computer files could be input into the database in about one year. In the longer term, means to automate the capture of data from other TestCentres, notably the CSIR's EMATEK Division, could be profitably explored. Program extensions to cater for tests other than standard Triaxial need also to be considered.

It is felt that the above level of expenditure of effort on an annual basis would be richly rewarded: the making available on a bulk basis of properly indexed and classified rock strength information, in a form amenable to flexible and ad hoc enquiry.

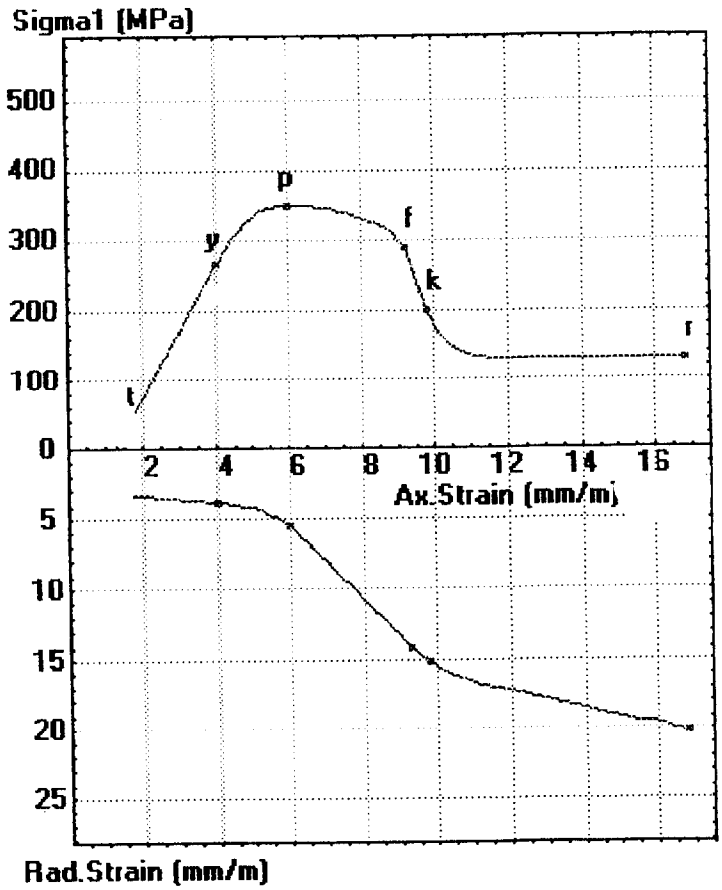

Figure 1 . Typical stress:strain curves for a Triaxial test with confinement $\sigma_3>0$.
The key points are t=tail, y=yield, p=peak, f=f-pt, k=knee, r=residual. On the radial strain graph, the slope t-y is Poisson's ratio nu, the slope at p is nup, the slope at r is nur.

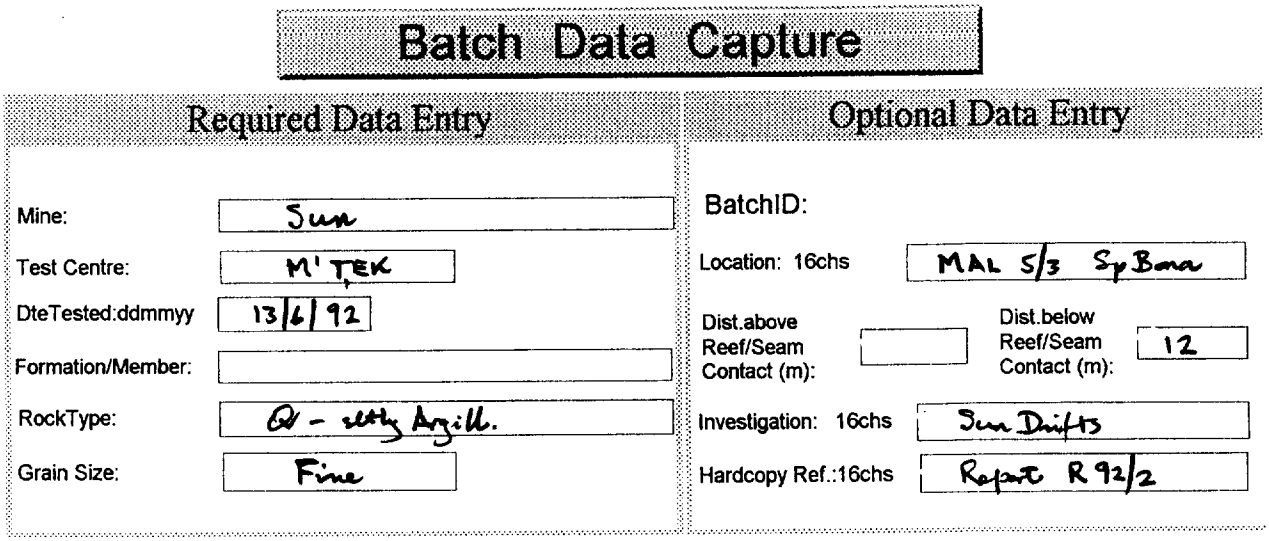

Figure 2a. Typical completed Batch pro-forma.

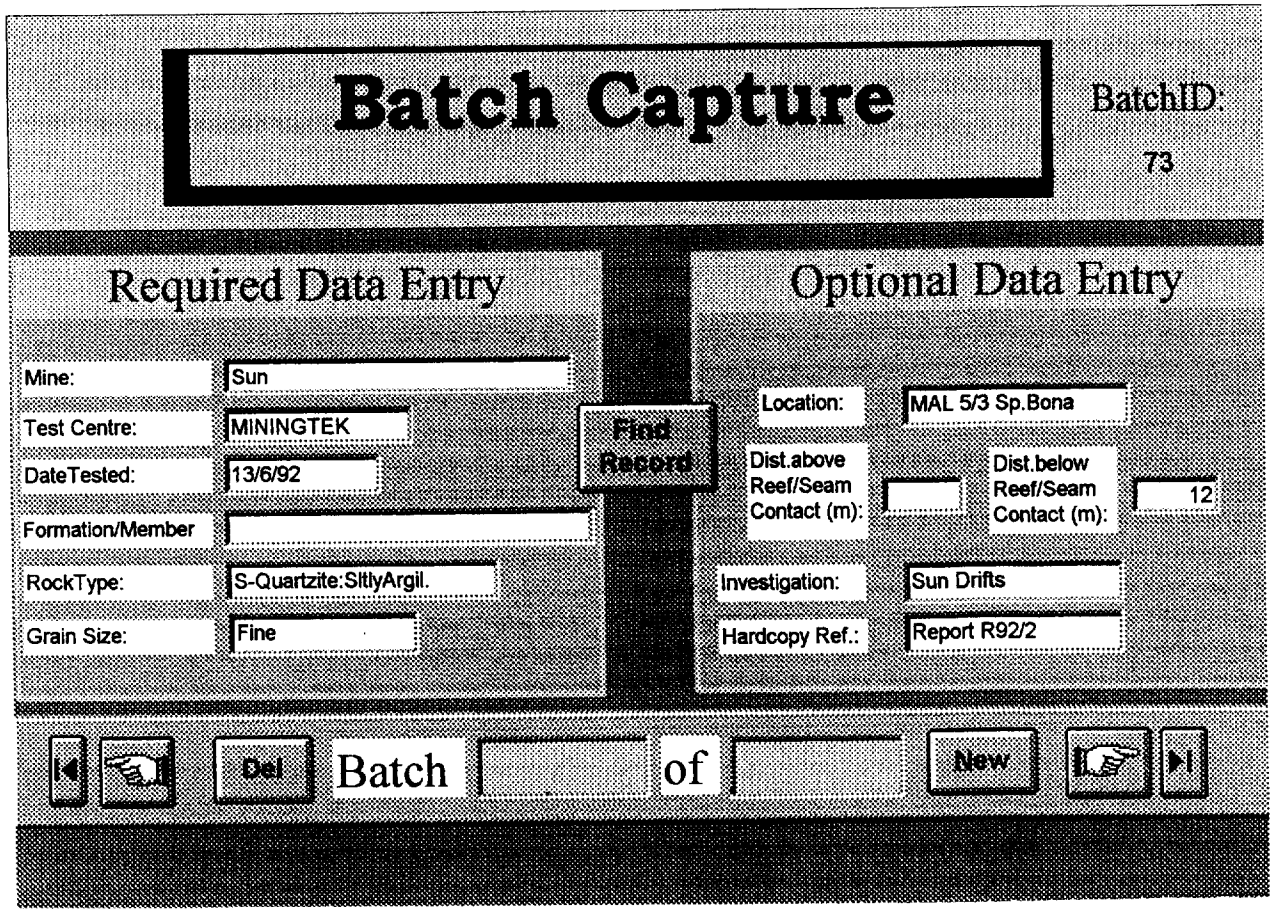

Figure 2b. ACCESS "BatchForm" for manual capture of Batch information.

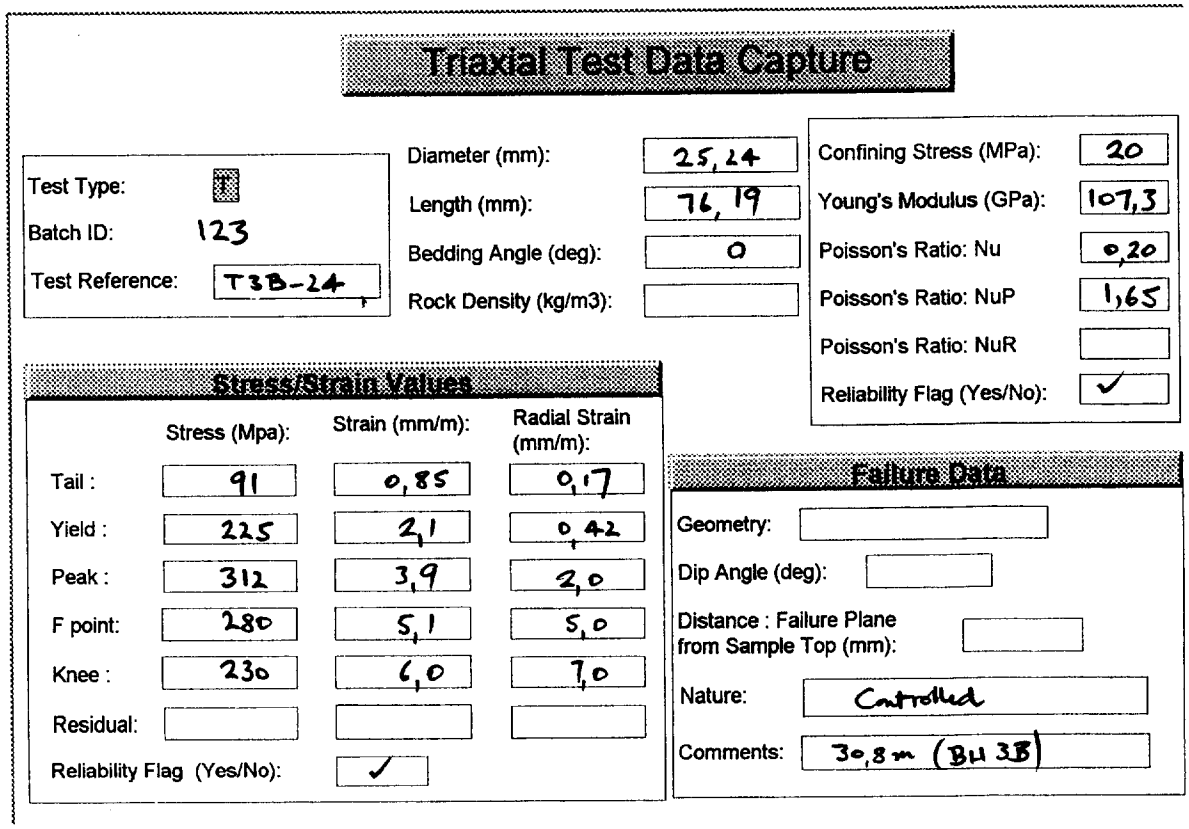

Figure 3a. Typical completed TriTest pro-forma.

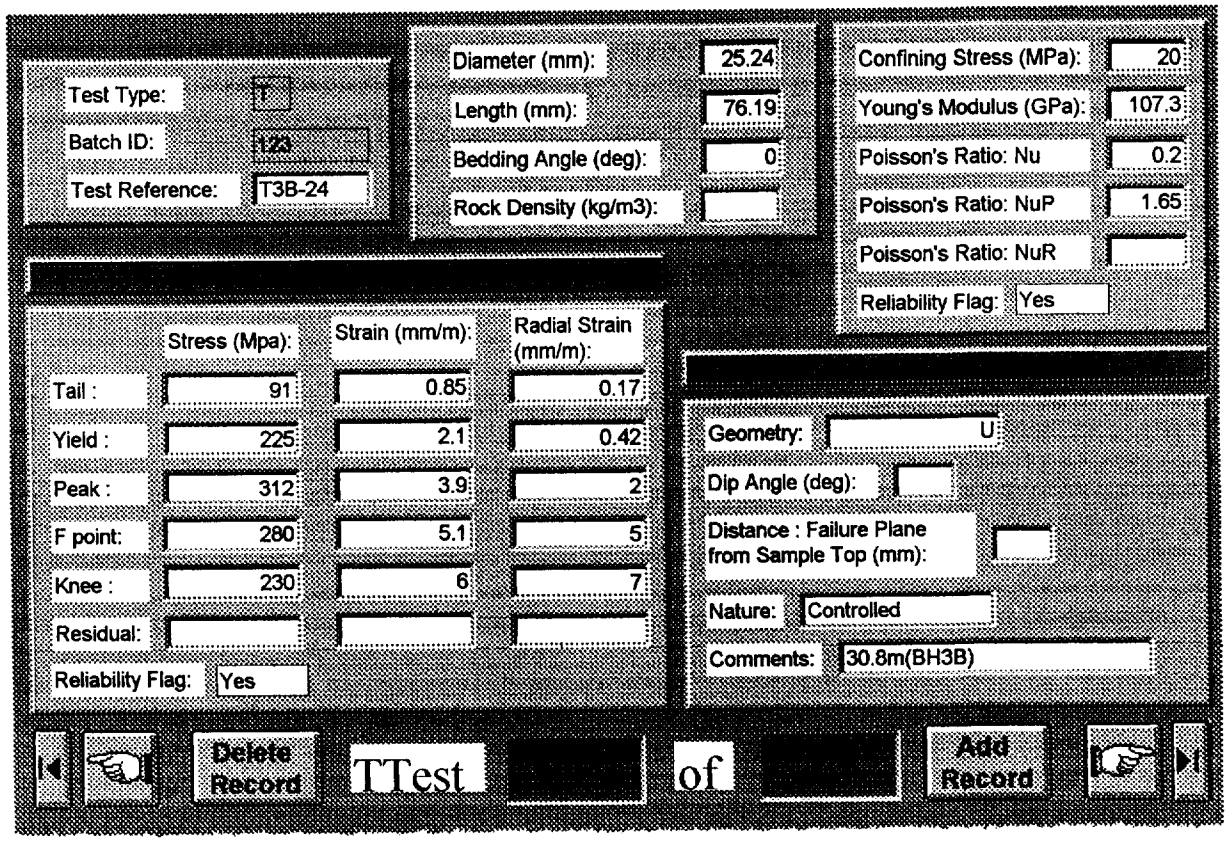

Figure 3b. ACCESS "TriTestForm" for manual capture of Triaxial test information.

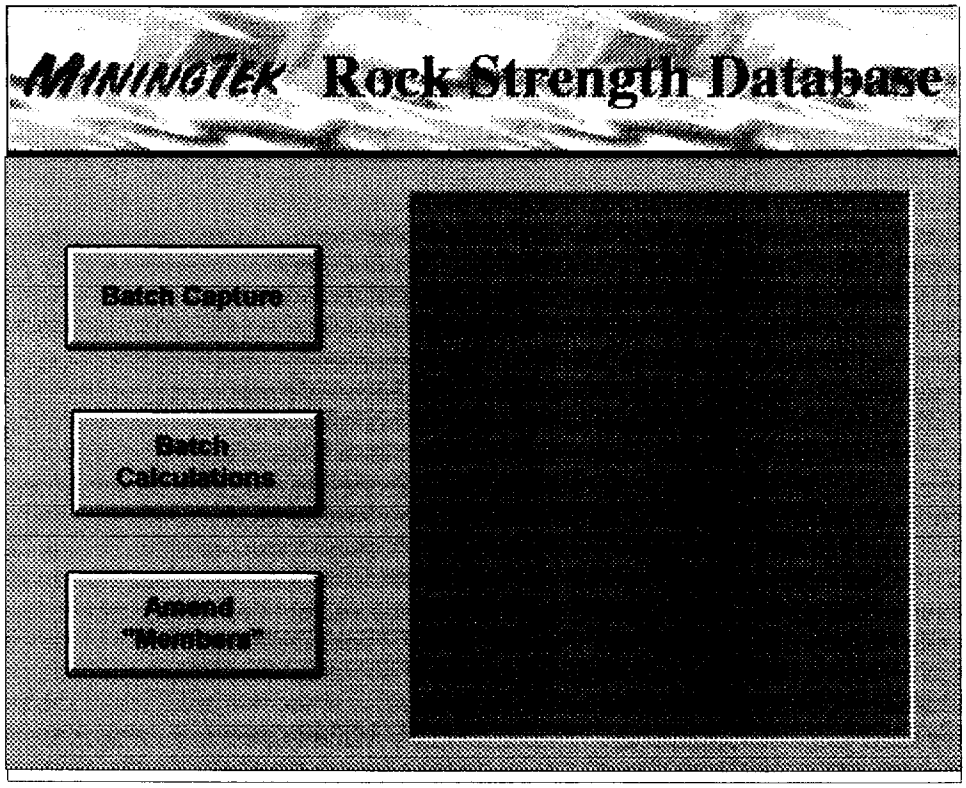

Figure 4. ACCESS "StartupForm".

Batch Detail Report

13-Nov-95 11:47

Batch	Mine	Location	Above Below	TestCentre	DateTested	Investigation
123	RPM Union Sect.	22/8 Richard#	30.0	MININGTEK	22/06/95	Y1024 TestStope

Member	RockType	GrSize	HardcopyRef
Bastard Reef	I-Pyroxenite: U	U	BH3A/3B

TRIAXIAL BATCH CALCULATIONS performed on: 13/11/95

	Mean	S D	n		Mean	S D	n		Mean	S D	n		Mean	S D	n		Mean	S D	n
E:	91.8	21.7	11	nu:	0.25	0.08	4	del1:	-0.01	0.01	11	UCS:	153.9	44.1	7				
uy:	132.6	39.6	11	bety:	4.8		11	cy:	30.2	9.0	11	phiy:	41.1		11	epy:	0.0	0.0	4
up:	153.5	46.37	11	betp:	7.2		11	cp:	28.6	8.7	11	phip:	49.1		11	epp:	2.4	0.8	4
uf:	136.7	41.8	11	betf:	6.7		11	cf:	26.3	8.0	11	phif:	47.9		11	epf:	7.0	3.8	4
uk:	37.7	24.69	11	betk:	7.2		11	ck:	7.0	4.6	11	phik:	49.1		11	epk:	12.2	3.0	4
ur:	21.3	6.2	7	betr:	5.7		7	cr:	4.5	1.3	7	phir:	44.6		7	epr:	19.6	4.2	2
dp:	32.6	3.1	4	dr:	9.3	4.1	2	rd:	0	0	0								

Batch	TestRef	Diam	Length	BA	RDen	S3	E	Nu	NuP	NuR	MRF	SRF
123	T3B-24	25.2	76.2	0		20.0	107.3	0.20	1.65		Yes	Yes

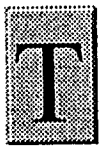

	'Tail'	Yield	Peak	F-pt	Knee	Residual		
s1	91.0	225.0	312.0	280.0	230.0		Delta1	0.00
e1	0.85	2.10	3.90	5.10	6.00		Deltar	0.00
er	0.17	0.42	2.00	5.00	7.00		Strain Ratio	0.34

Failure Comments	Geometry	Nature	FTop	Angle
30.8m(BH3B)	U	Controlled		

Batch	TestRef	Diam	Length	BA	RDen	S3	E	Nu	NuP	NuR	MRF	SRF
123	T3B-25	25.3	76.2	0		10.0	75.9	0.39	2.00	0.80	Yes	Yes

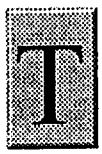

	'Tail'	Yield	Peak	F-pt	Knee	Residual		
s1	43.0	138.0	177.0	175.0	115.0	89.0	Delta1	-0.02
e1	0.50	1.80	3.00	3.40	6.00	9.00	Deltar	-0.01
er	0.20	0.70	2.40	2.60	8.20	12.00	Strain Ratio	0.29

Failure Comments	Geometry	Nature	FTop	Angle
31.2m(BH3B)	U	Controlled		

Figure 5. Sample Batch Calculation Report.

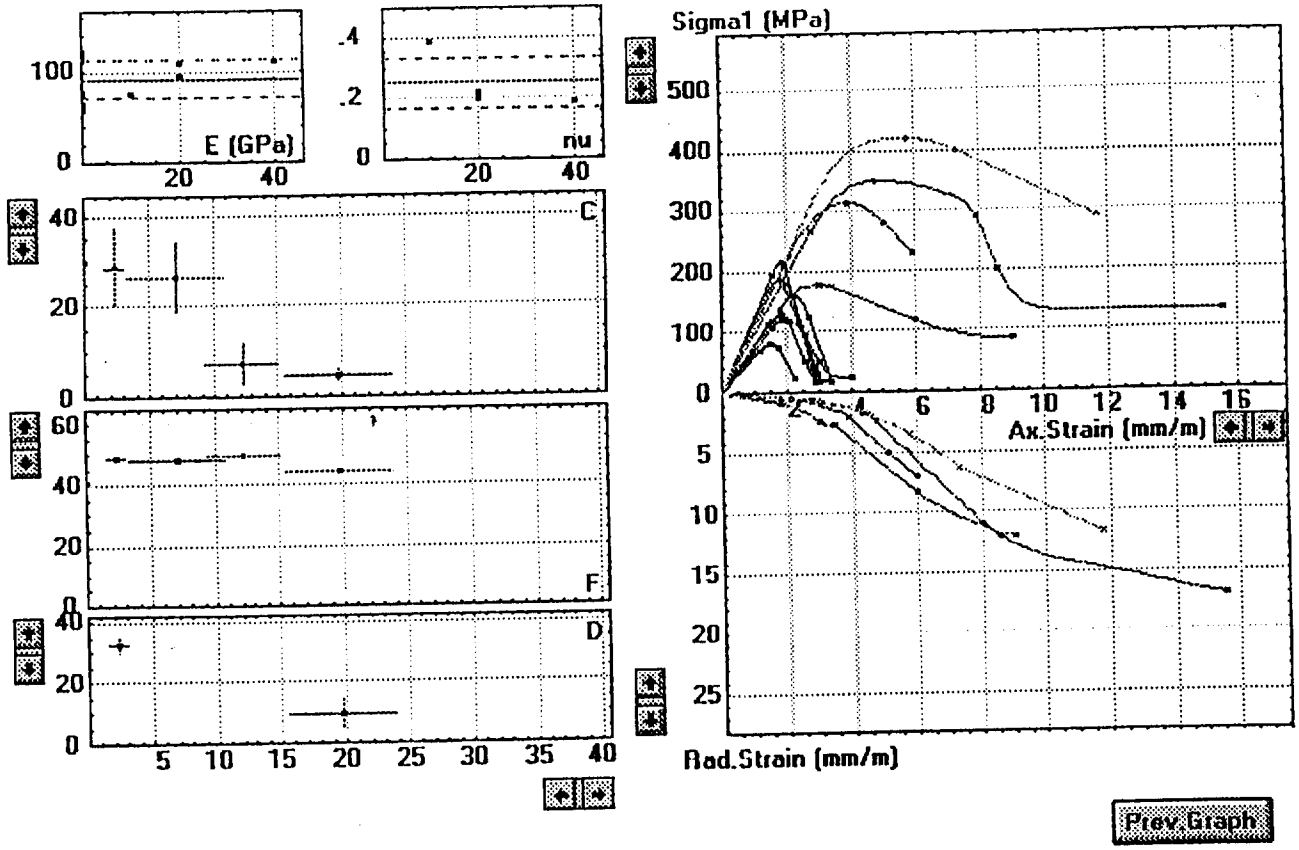

Figure 6b. Screen 2 produced by TRock - E & nu vs σ_3; C/F/D vs ε_p; Stress:Strain.

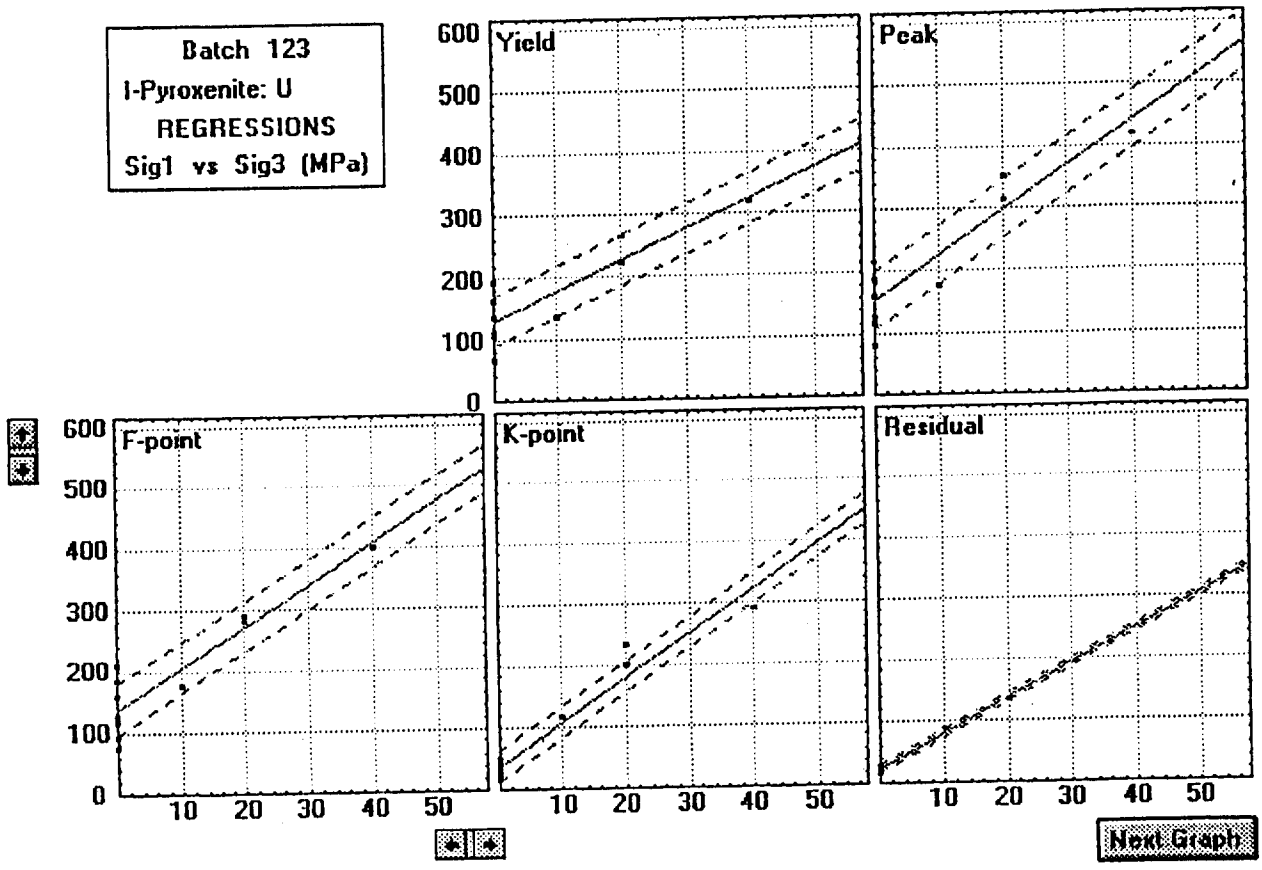

Figure 6a. Screen 1 produced by TRock - Batch regressions on key points.

APPENDIX I - PRE-SET TABLES

The structure and function of these tables is described in section 2.1.

DistrictID	District
1	U
2	Antimony
3	Asbestos
4	Barb'ton
5	Bushveld
6	Copper
7	C.Rand
8	Diamond
9	E.Rand
10	Evander
11	F.W.Rand
12	Iron
13	K'dorp
14	Lead
15	Mang'ese
16	Nat-Coal
17	OFS-Coal
18	OFS-Gold
19	Tvl-Coal
20	W.Rand

(a) Districts

MineID	DistrictID	Mine
1	1	U
2	2	Cons.Murch.
3	3	Griq.Expl.
4	3	Msauli
5	4	Barberton
6	4	Eersteling
7	5	Bafokeng N.
8	5	Bafokeng S.
9	5	Bapong
10	5	Crocodile River
11	5	Dilakong
12	5	Eastern Plats
13	5	Henry Gould
14	5	Impala Granite
15	5	Kudu Granite
16	5	Kielie Granite
17	5	Kennedy's Vale
18	5	Lavino Chrome
19	5	Messina Plat
20	5	Mooinooi
21	5	Northam Plat
22	5	Purity
23	5	RPM Am'bult
24	5	RPM Rust. E.
25	5	RPM Rust. W.
26	5	RPM Union Sect.
27	5	Tweefontein
28	5	Western Plats
29	5	W. Plats Karee
30	5	Wild'fntn N.
31	5	Wild'fntn S.
32	5	Winterveld
33	6	Messina Copper
34	6	O'Okiep Copper
35	6	Palabora
36	7	Durban Deep
37	7	First Wesgold
38	8	De B. Finsch
39	8	De B. Koffief'n
40	8	De B. Premier
41	8	De B. Venetia
42	9	ERPM
43	9	Grootvlei
44	9	Marievale
45	10	Bracken
46	10	Leslie
47	10	Kinross
48	10	Winkelhaak
49	11	Blyvooruitzicht
50	11	Deelkraal
51	11	Doornfontein
52	11	E. Driefontein
53	11	Elandsfontein
54	11	Kloof
55	11	Leeudoorn
56	11	Libanon
57	11	Venterspost
58	11	W.D.L. North
59	11	W.D.L. South
60	11	W. Driefontein

(b) Mines

MineID	DistrictID	Mine
61	12	Sishen
62	12	Thabazimbi
63	13	Afrikander Lease
64	13	Buffelsfontein
65	13	Hartebeestf'tein
66	13	Stilfontein
67	13	Vaal Reefs East
68	13	Vaal Reefs South
69	13	Vaal Reefs West
70	13	Vaal Reefs 11 Sh
71	14	Black Mountain
72	15	Beeshoek
73	15	Blackrock
74	15	Gloria
75	15	Hotazel
76	15	Mamatwan
77	15	Wessels
78	16	Alpha Anthracite
79	16	Durban Navig'n
80	16	Hlobane
81	16	Longridge
82	16	Natal Anthracite
83	16	Springclake
84	16	Vryheid Coron'n
85	16	Welgedacht
86	16	Zululand Anthrac
87	17	New Vaal
88	17	Sigma
89	17	Closed
90	18	Beatrix
91	18	Freddies
92	18	F.S. Geduld
93	18	F.S. Saaiplaas
94	18	H J Joel
95	18	Harmony
96	18	Loraine
97	18	Oryx
98	18	President Brand
99	18	President Steyn
100	18	St. Helena
101	18	Sun
102	18	Target
103	18	Unisel
104	18	Western Holdings
105	19	Arnot
106	19	Arthur Taylor
107	19	Atcom
108	19	Bank
109	19	Delmas
110	19	Douglas
111	19	Duva
112	19	Ermelo Mines
113	19	Goedehoop
114	19	Greenside
115	19	Khutala
116	19	Kleinkopje
117	19	Koornfontein
118	19	Kriel
119	19	Majuba
120	19	Matla
121	19	New Denmark
122	19	Optimum
123	19	Phoenix
124	19	S A Coal Estates
125	19	Savmore
126	19	Secunda Mines
127	19	South Witbank
128	19	Spitzkop
129	19	Strathrae
130	19	Tavistock
131	19	Tshikondeni
132	19	Tweefontein
133	19	Van Dyks Drift
134	19	Witbank Cons
135	19	Wolverpane
136	20	Randfontein Est.
137	20	South Deep
138	20	Western Areas

FormationID	Formation
1	U
2	Dykes/Sills
3	Karoo
4	BC-UpperZones
5	BC-MainZone
6	BC-CriticalZone
7	BC-LowerZones
8	Tvl&Dolomites
9	Wits-Venterspost
10	Wits-Mondeor
11	Wits-Elsburg
12	Wits-GoldEstates
13	Wits-Robinson
14	Wits-Booysens
15	Wits-Krug'dorp
16	Wits-Luip'vlei
17	Wits-Randfontein
18	Wits-Main
19	Wits-Blyvoor.
20	Wits-Maraisburg
21	Wits-Lower
22	Archaean

(c) Formations

MemberID	Member	FormationID	DistrictID	Sequencer
1	U	1	1	1
2	U	1	5	1
3	Dyke-Age1	2	5	2
4	Dyke-Age2	2	5	3
5	Dyke-Age3	2	5	6
6	U	3	5	7
7	U	4	5	8
8	U	5	5	9
9	Bastard Reef	6	5	10
10	Mer.Reef h/w	6	5	11
11	Merensky Reef	6	5	12
12	Mer-UG2 middling	6	5	13
13	UG2 Reef	6	5	14
14	UG2-UG1 middling	6	5	15
15	UG1 Reef	6	5	16
16	UG1-MG4 middling	6	5	17
17	MG4 Reef	6	5	18
18	MG4-MG3 middling	6	5	19
19	MG3 Reef	6	5	20
20	MG3-MG2 middling	6	5	21
21	MG2 Reef	6	5	22
22	MG2-MG1 middling	6	5	23
23	MG1 Reef	6	5	24
24	MG1-LG7 middling	7	5	25
25	LG7 Reef	7	5	26
26	LG7-LG6 middling	7	5	27
27	LG6 Reef	7	5	28
28	LG6-LG5 middling	7	5	29
29	LG5 Reef	7	5	30
30	LG5-LG4 middling	7	5	31
31	LG4 Reef	7	5	32
32	LG4-LG3 middling	7	5	33
33	LG3 Reef	7	5	34
34	LG3-LG2 middling	7	5	35
35	LG2 Reef	7	5	36
36	LG2-LG1 middling	7	5	37
37	LG1 Reef	7	5	38
38	LG1 f/w	7	5	39
39	U	8	5	40
40	U	22	5	41
41	U	1	18	1
42	Dyke-Age1	2	18	2
43	Dyke-Age2	2	18	3
44	Dyke-Age3	2	18	4
45	U	3	18	5
46	U	8	18	6
47	Ventersdorp Lava	9	18	7
48	VCR,Dreyerskraal	9	18	8
49	Vs1a,Uitkyk	10	18	9
50	EA,VS1	11	18	10
51	EB,VS2	11	18	11
52	EC,VS3	11	18	12
53	ED,VS4	11	18	13
54	VS5,RosedaleReef	11	18	14
55	BeatrixReef	11	18	15
56	A'EarlsCrt h/w	12	18	16
57	A/EarlsCrt/Witpan Reef	12	18	17
58	AReef-BPR middling	12	18	18
59	ReworkedBPR,Kalkoenkra	12	18	19
60	BigPebblCong/BPR/BPM	13	18	20
61	SpesBona/BPR-B middling	13	18	21
62	B Reef	13	18	22
63	B Reef f/w,C Reef	13	18	23
64	Doornkop,B/C Reef f/w	14	18	24
65	U Shale Marker,Booysens	14	18	25
66	LeaderReefZone	15	18	26
67	LeaderReef	15	18	27
68	MatureQtzite	15	18	28
69	WaxyQtzite	15	18	29
70	LeaderQtzite,PyriteStringer	15	18	30
71	SaaiplaasReef	15	18	31
72	KhakiShale	15	18	32
73	Basal/SteynReef	15	18	33
74	UF1	16	18	34
75	UF2	16	18	35
76	UF3	16	18	36
77	Int/UF4 Reefs	16	18	37
78	MF1	17	18	38
79	MF2	17	18	39
80	MF3	17	18	40
81	MF4	17	18	41
82	LF1-LF5	18	18	42
83	LF5/Commanage Reef	18	18	43
84	LF6	19	18	44
85	AdaMay/Beisa Reef	19	18	45
86	AdayMay f/w	20	18	46
87	U	21	18	47
88	U	22	18	48

(d) Members
[District 5 (Bushveld) and District 18 (OFS-Gold)]

RockTypeID	RockType
1	C- U
2	C-Anthracite
3	C-Bituminous
4	C-LowRank
5	D- U
6	D-Aplite
7	D-Carbonatite
8	D-Chert
9	D-Diabase
10	D-Diorite
11	D-Dolerite
12	D-Epidiorite
13	D-Lamprophyre
14	I- U
15	I-Anorthosite: U
16	I-Anorthosite:Mottled
17	I-Anorthosite:Spotted
18	I-Bronzitite: U
19	I-CopperOre: U
20	I-Chromitite: U
21	I-Dunite: U
22	I-Gabbro: U
23	I-Gabbro:Anorthositic
24	I-Gabbro:Pyroxenitic
25	I-Gneiss: U
26	I-Granite: U
27	I-Harzburgite: U
28	I-Kimberlite: U
29	I-Norite: U
30	I-Norite:Leuco-
31	I-Norite:Melano-
32	I-Magnetite: U
33	I-Pegmatoid: U
34	I-Pyroxenite: U
35	L-Andesite: U
36	L-Basalt: U
37	L-Dacite: U
38	L-Rhyolite: U
39	S-BandedIronstone: U
40	S-Conglomerate: U
41	S-Dolomite: U
42	S-Grit: U
43	S-Haematite: U
44	S-Limestone: U
45	S-Magnetite: U
46	S-ManganeseOre: U
47	S-Mudstone: U
48	S-Quartzite: U
49	S-Quartzite:Siliceous
50	S-Quartzite:SltlyArgil.
51	S-Quartzite:Argillaceous
52	S-Sandstone: U
53	S-Schist: U
54	S-Shale: U
55	S-Shale:Calcareous
56	S-Shale:Carbonaceous
57	S-Shale:Ferruginous
58	S-Shale:Micaceous
59	S-Shale:Siliceous
60	S-Siltstone: U

(e) RockTypes

GrainSizeID	GrainSize
1	U
2	Fine
3	Medium
4	Coarse
5	Gritty
6	Pebbly
7	Amygd'al
8	Porph'ic
9	Tuff'ous

(f) GrainSizes

TestCentreID	TestCentre
1	U
2	MININGTEK
3	EMATEK
4	Wits
5	AAC-Amcoal
6	AAC-Welkom
7	VKE

(g) TestCentres

Nature	NatureID
U	1
Controlled	2
Uncontrolled	3
Violent	4
Type II	5

(h) Natures of failure

Geometry	GeometryID
U	1
Shear	2
Multiple	3
Xtension	4
Conical	5
Crushing	7

(i) Geometries of failure

APPENDIX II - Specification of Batch Calculations

The following refer to Triax entries within the Batch.

a) Calculate & store in Batch Table the mean, S.D. and no.of items of: E, ν, rock density and $\Delta 1$. [Ignore if item is null, or RF(moduli)='No'].

b) Calculate & store in Batch Table the mean, S.D. and no.of items of: UCS (i.e. the value of s1p for those T tests for which s3=0). [Ignore item if RF(strength)='No']

c) Regress the intercept u* and slope β* independantly for each of the key strength points (*) y p f k r as a function of s3. [Ignore item if null, or RF(strength)='No']
Use the following formulae:
Let $n^*=\Sigma 1$, $A^*=\Sigma s_3$, $B^*=\Sigma s_3^2$, $C^*=\Sigma s_1^*$, $D^*=\Sigma s_3\, s_1^*$, $F^*=\Sigma s^{*2}$, $\Delta^*=n^*B^*-A^{*2}$
(If $n^*<2$ or $\Delta^*=0$, bypass further calculations involving u*, β* or V*).
Then $u^*=(B^*C^*-A^*D^*)/\Delta^*$ $\beta^*=(n^*D^*-A^*C^*)/\Delta^*$ $Var^*=F^*-u^*C^*-\beta^*D^*$
(If now $\beta^*<1$, then $\beta^*=1$ $u^*=(C^*-A^*)/n^*$ $Var^*=E^*-2D^*+B^*-n^*u^{*2}$)
$SD(u^*)=u^*$ If $n^*>2$ Then $SD(u^*)=SQR(Var^*/(n^*-2))$
$\phi^*=\arcsin((\beta^*-1)/(\beta^*+1))$ $C^*=u^*/2SQR(\beta^*)$ $SD(C^*)=SD(u^*)/2SQR(\beta^*)$
Calculate the mean & SD of the plastic strains [ignoring if any item null or RF(strength)='No']: $e^{*p}=er^*+(E\, e1^*-(1+2\nu)s1^*)/(2E)$
For p and r only, calculate the mean & SD of dilation angles [ignoring item if null]:
$D^*=\arcsin(2\nu^*-1)/(2\nu^*+1)$
Store all the above means & SDs in the Batch Table, together with item counts (of which there will in general be 3 distinct values for each key point type: one for the regression, one for the plastic strain, and one for the dilation angle).

d) Record the date on which the Batch Calcs were performed in the Batch Table.

Laboratory Test Results. 22/8 stope Richard shaft

Sample No/	Borehole Depth	σ 3 MPa	σ1 MPa	E Gpa	ν
Anorthosite (mottled)					
UI A -1	24,6	0	161	53,4	
UI A -13	46,9	0	168 *	78,4	
UI A - 14	49,5	0	243	90,6	
TAI - 6	49,1	10	252	115,5	0,13
TAI - 4	49,2	20	156 *	89,7	0,20
TAI - 5	49,4	40	462	121,1	0,16
U2 - 8	22,9	0	219	77,0	
U2 - 9	23,1	0	206	75,1	
U3A - 8	23,8	0	132	53,6	
U3A - 11	25,2	0	167	85,6	
U3B - 12	23,6	0	225	69,2	
U3B - 13	24,6	0	112	41,8	
U3B - 2	49,0	0	240	82,3	
U3B - 20	49,4	0	241	89,0	
U3B - 10	49,9	0	210	79,9	
T3B - 1	24,8	20	214 *	57,4	0,29
T3B - 4	25,1	40	311	61,5	0,23
T3B - 5	50,2	10	297	83,9	0,22
T3B - 16	50,7	10	353	80,6	0,24
T3B - 12	50,9	20	431	85,6	0,20
T3B - 15	50,6	40	569	89,3	0,20
Mean-S.D.			**(11) 196-44**	**(18) 80-19**	**(7) 0,20-0,04**
(Anorthosite (spotted)					
U2 - 6	14,2	0	175	71,9	
U2 - 7	18,5	0	149	58,9	
U3A - 2	17,0	0	198	74,5	
U3A - 7	20,1	0	167	81,0	
U3A - 12	22,6	0	173	61,1	
U3A - 13	22,1	0	127*	75,4	
U3B - 19	18,3	0	195	75,8	
U3B - 15	19,5	0	197	75,2	
U3B - 23	22,1	0	189	81,2	
T3B - 10	19,2	10	312	79,4	0,23
T3B - 14	22,0	10	195	55,7	0,25
T3B - 17	19,3	20	395	86,5	
T3B - 18	19,4	40	540	89,4	0,21
Mean-S.D.			**(8) 180-16**	**(12) 74-12**	**(3) 0,23-0,02**

Sample No/	Borehole Depth	σ 3 Mpa	σ1 MPa	E Gpa	ν
Leuconorite					
U3A -4	7,8	0	100*	39,6	
U2 -5	10,3	0	180	78,3	
U3A - 9	13,8	0	192	84,0	
U3B - 17	11,5	0	87*	65,5	
U3B - 8	14,4	0	196	74,6	
T3B - 11	14,0	10	301	78,9	0,25
T3B - 13	14,1	20	391	82,1	0,21
T3B - 19	14,2	40	534	90,0	0,22
Mean-S.D.			**(3) 189 - 7**	**(6) 81-5**	**(13) 0,23-0,02**
Sample No /	Borehole Depth	σ 3 MPa	σ 1 MPa	E GPa	ν
Melanorite					
U2 - 3	4,0	0	131	81,1	
U3A - 3	5,7	0	112	52,9	
U3B - 5	3,4	0	75*	52,5	
U3B - 16	4,4	0	112	52,4	
U3B - 11	5,0	0	148	66,7	
U3B - 21	6,4	0	123	53,6	
U3B - 18	39,9	0	197	92,5	
T3B - 8	39,6	10	291	86,7	0,25
T3B - 22	4,6	10	224	70,1	0,23
T3B - 21	4,8	20	302	77,6	0,25
T3B - 20	4,7	40	420	84,2	0,21
T3B - 3	39,8	40	496	99,7	0,19
Mean-S.D			**(6) 137-29**	**(11) 74-16**	**(5) 0,23-0,02**
Norite					
UIA - 12	44,0	0	206	102,6	
U2 - 4	7,0	0	175	93,2	
U3A - 5	9,5	0	199	101,0	
U3B - 9	44,7	0	250	89,0	
U3B - 4	45,4	0	215	95,8	
Mean-S.D.			**(5) 209-24**	**(5) 96-5**	

* Failed on discontinuity - not included in averages.

Sample No/	Borehole Depth	σ 3 MPa	σ1 MPa	E Gpa	ν
Pyroxenite (Bastard Reef)					
UIA - 2	25,7	0	141	101,5	
UIA - 3	26,5	0	151	101,6	
UIA - 4	26,9	0	113	66,9	
UIA - 5	28,4	0	182	99,7	
UIA - 6	29,4	0	188	127,8	
UIA - 7	31,3	0	167	127,9	
UIA - 8	31,8	0	253	148,2	
UIA - 9	32,7	0	83*	61,6	
UIA - 10	33,2	0	186	113,7	
UIA - 11	35,3	0	121	100,9	
TAI - 2	35,7	10	240	126,7	0,17
TAI - 1	35,8	10	304	90,9	0,24
TAI - 3	28,0	20	343	118,2	0,18
TAI - 8	29,1	20	274	114,7	0,16
TAI - 7	28,9	40	514	94,3	0,23
TAI - 9	35,6	40	456	123,6	0,14
U3A - 10	28,6	0	128	75,3	
U3A - 15	35,5	0	188	113,8	
U3B - 1	27,8	0	80*	57,3	
U3B - 3	30,7	0	118	65,0	
U3B - 22	32,7	0	216	122,6	
U3B - 14	37,1	0	188	113,0	
U3B - 6	37,8	0	159	74,4	
T3B - 25	31,2	10	177	75,9	0,39
T3B - 24	30,8	20	312	107,3	0,20
T3B - 6	39,5	20	349	95,3	0,22
T3B - 7	31,1	40	419	109,8	0,19
Mean-S.D.			**(15) 167-38**	**(25) 104-21**	**(10) 0,21-0,07**
Pyroxenite (Merensky)					
U2 - 1	0,8	0	147	95,2	
U2 - 2	2,7	0	140	100,2	
U3A - 14	0,1	0	151	113,6	
U3A - 6	1,6	0	114	94,9	
U3A - 1	3,3	0	66*	59,1	
U3B - 7	0,8	0	113	90,7	
U3B - 24	1,8	0	83*	59,5	
T3B - 23	0,4	10	174	111,4	0,22
T3B - 9	0,5	20	239	116,4	0,19
T3B - 2	0,6	40	330	111,2	0,18
Mean-S.D.			**(5) 133-16**	**(8) 104-9**	**(3) 0,20-0,02**

* Failed on discontinuity - not included in averages.

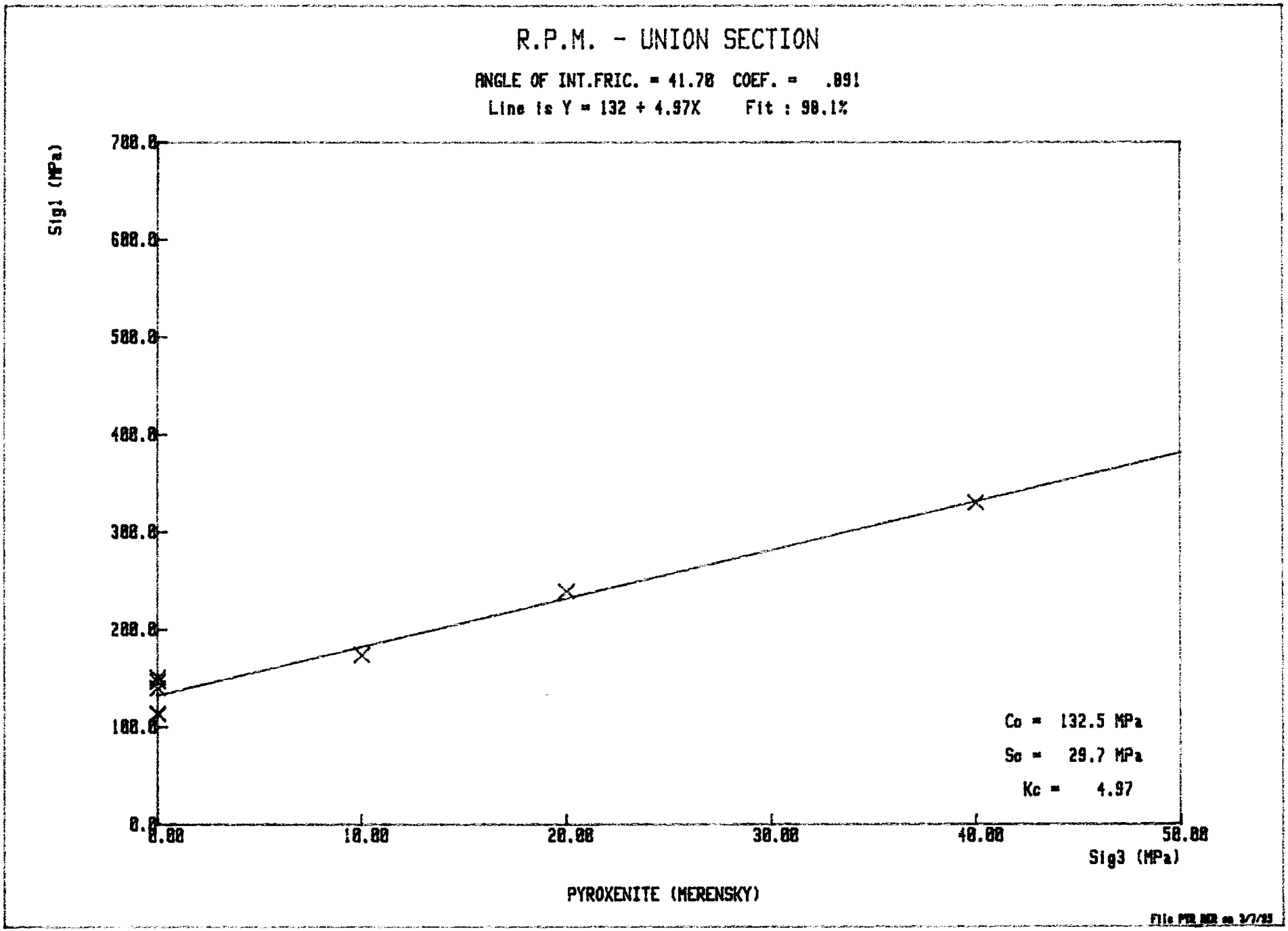
R.P.M. - UNION SECTION
ANGLE OF INT.FRIC. = 41.70 COEF. = .891
Line is Y = 132 + 4.97X Fit : 98.1%
Sig1 (MPa)
700.0
600.0
500.0
400.0
300.0
200.0
100.0
0.0
0.00
10.00
20.00
30.00
40.00
50.00
Sig3 (MPa)
Co = 132.5 MPa
So = 29.7 MPa
Kc = 4.97
PYROXENITE (MERENSKY)

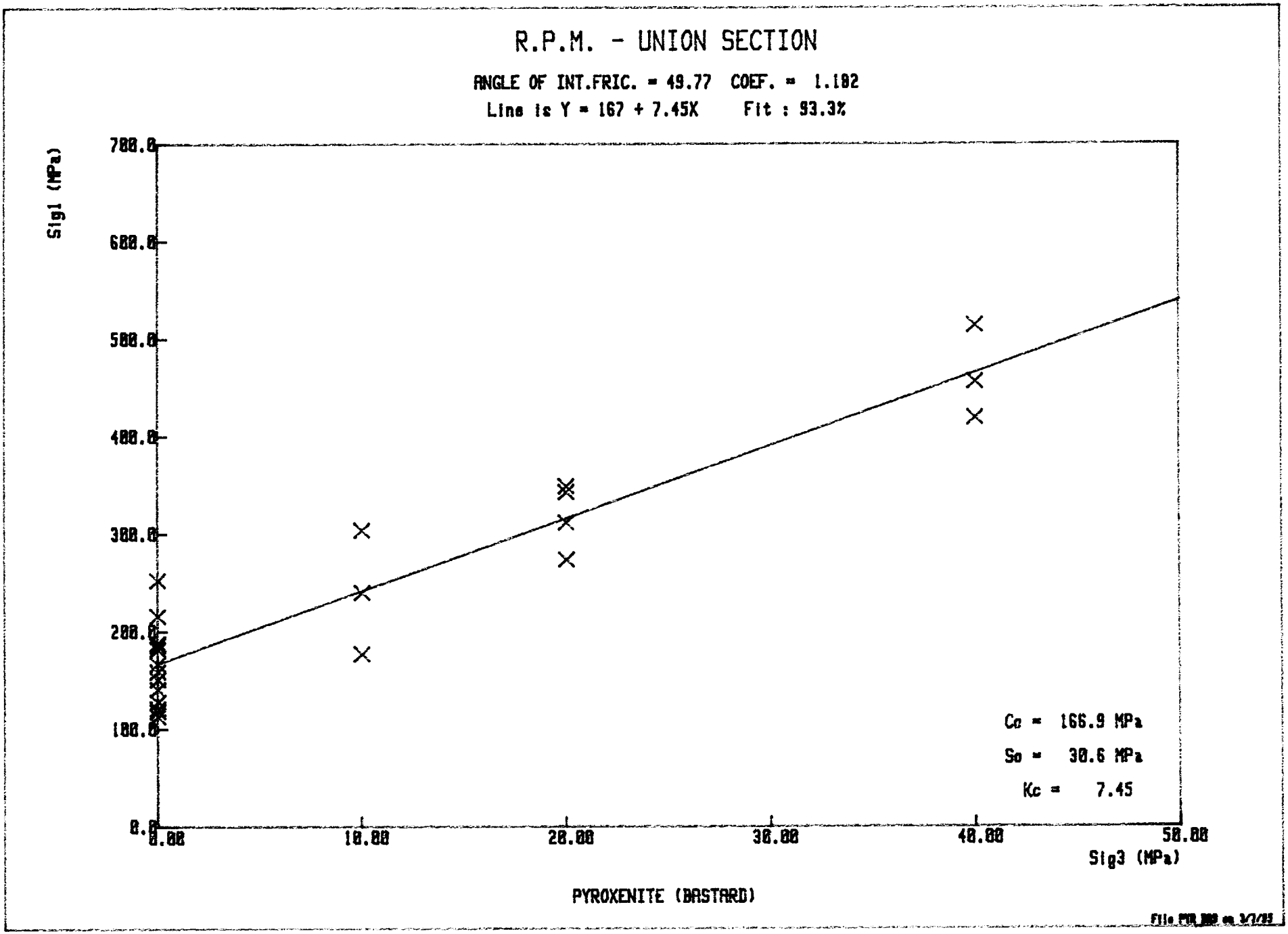
R.P.M. - UNION SECTION
ANGLE OF INT.FRIC. = 49.77 COEF. = 1.182
Line is Y = 167 + 7.45X Fit : 93.3%
Sig1 (MPa)
700.0
600.0
500.0
400.0
300.0
200.0
100.0
0.0
0.00
10.00
20.00
30.00
40.00
50.00
Sig3 (MPa)
Co = 166.9 MPa
So = 30.6 MPa
Kc = 7.45
PYROXENITE (BASTARD)

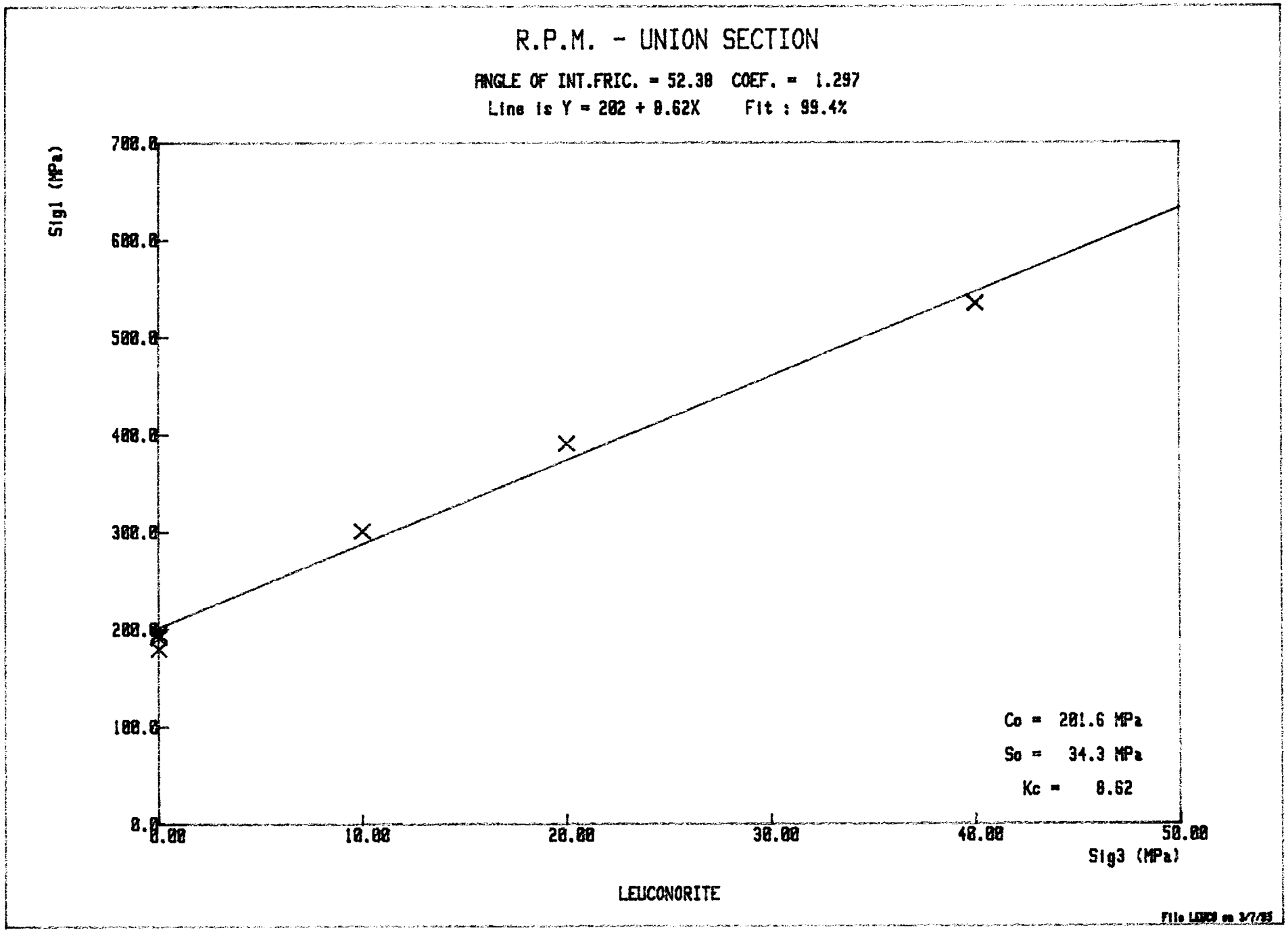
R.P.M. - UNION SECTION
ANGLE OF INT.FRIC. = 52.38 COEF. = 1.297
Line is Y = 202 + 8.62X Fit : 99.4%
Sig1 (MPa)
700.0
600.0
500.0
400.0
300.0
200.0
100.0
0.0
0.00
10.00
20.00
30.00
40.00
50.00
Sig3 (MPa)
Co = 201.6 MPa
So = 34.3 MPa
Kc = 8.62
LEUCONORITE

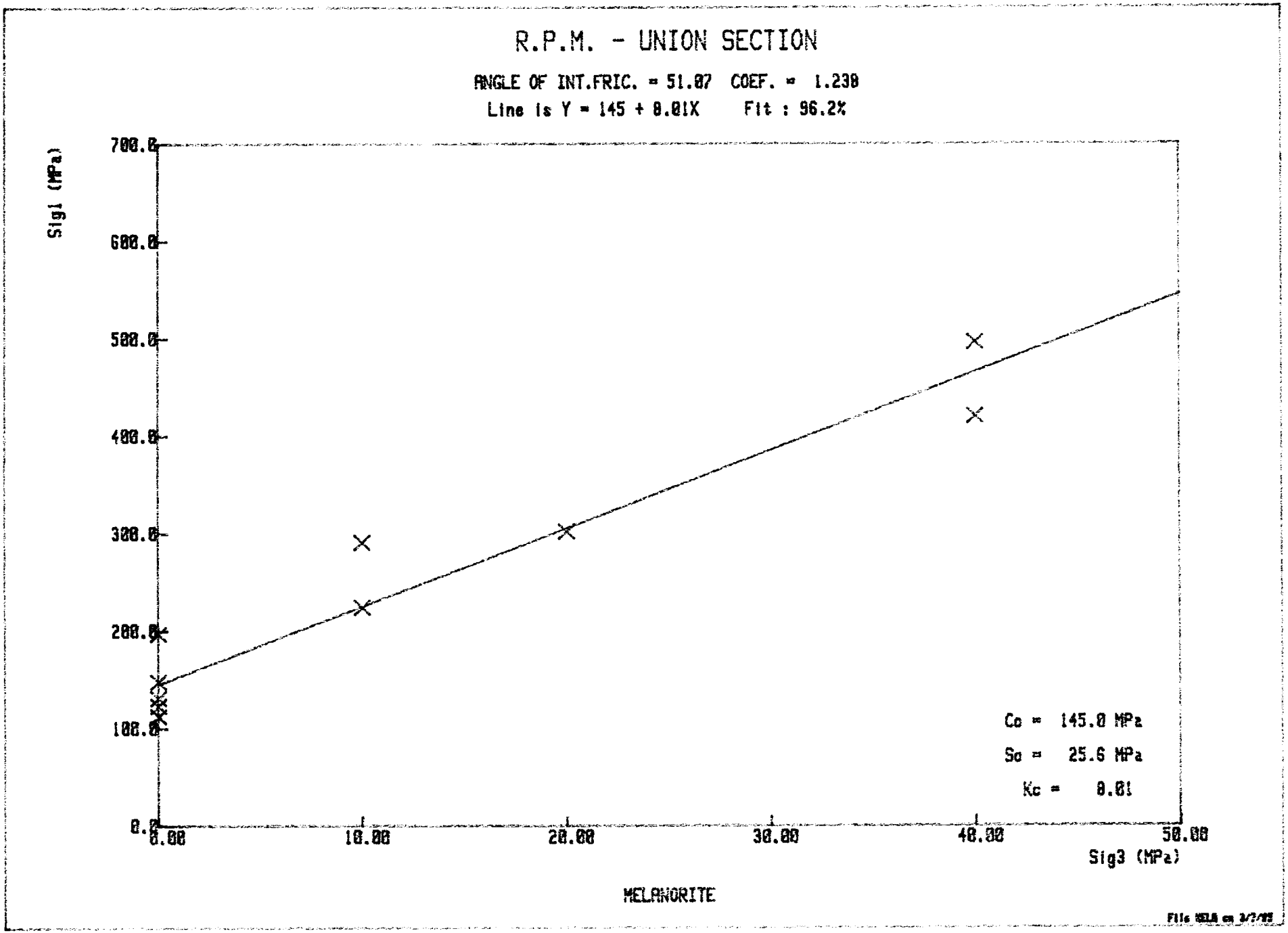
R.P.M. - UNION SECTION
ANGLE OF INT.FRIC. = 51.07 COEF. = 1.238
Line is Y = 145 + 8.01X Fit : 96.2%
Sig1 (MPa)
700.0
600.0
500.0
400.0
300.0
200.0
100.0
0.0
0.00
10.00
20.00
30.00
40.00
50.00
Sig3 (MPa)
Co = 145.0 MPa
So = 25.6 MPa
Kc = 8.01
MELANORITE

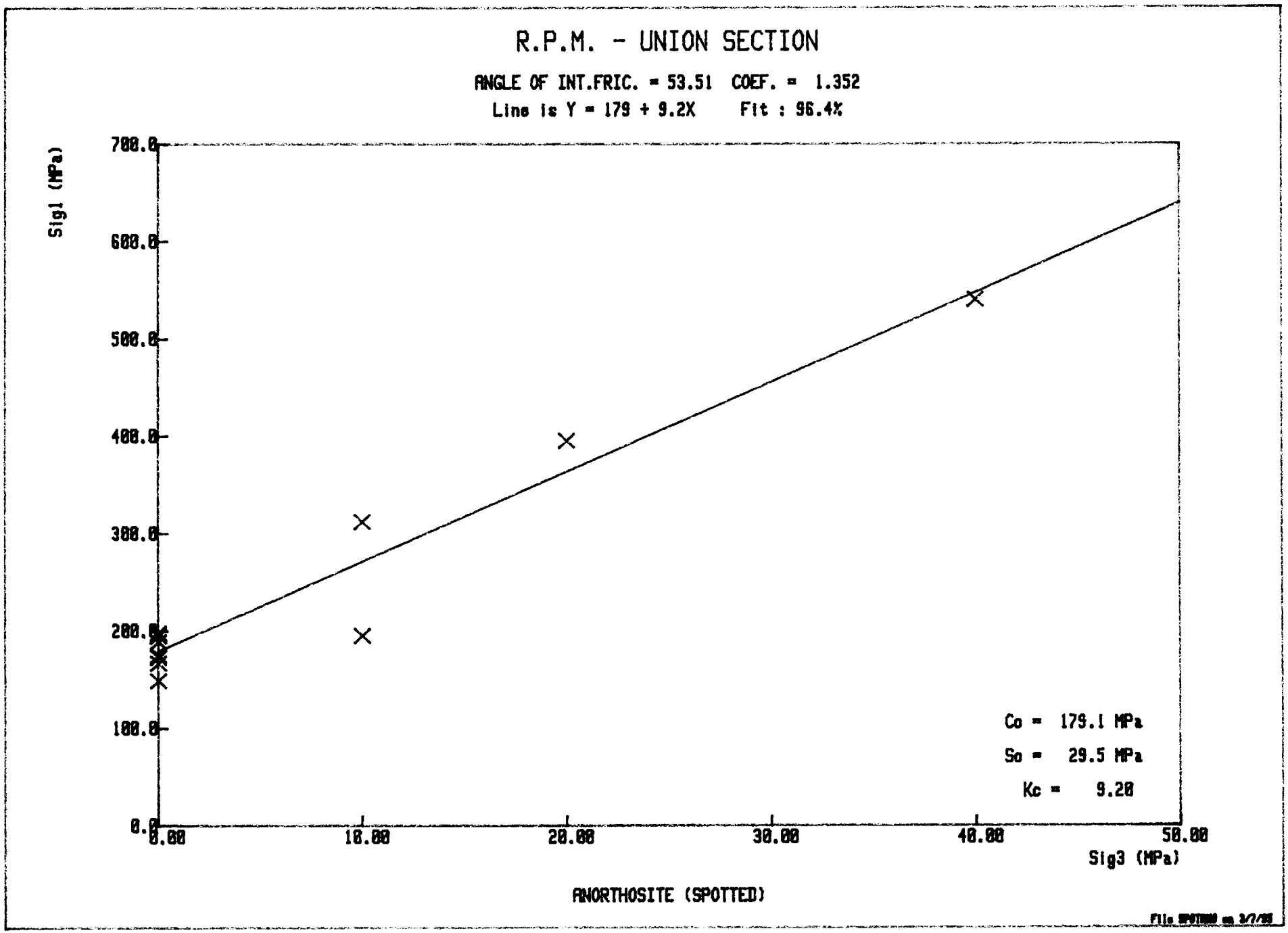
R.P.M. - UNION SECTION
ANGLE OF INT.FRIC. = 53.51 COEF. = 1.352
Line is Y = 179 + 9.2X Fit : 96.4%
Sig1 (MPa)
700.0
600.0
500.0
400.0
300.0
200.0
100.0
0.0
0.00
10.00
20.00
30.00
40.00
50.00
Sig3 (MPa)
Co = 179.1 MPa
So = 29.5 MPa
Kc = 9.20
ANORTHOSITE (SPOTTED)

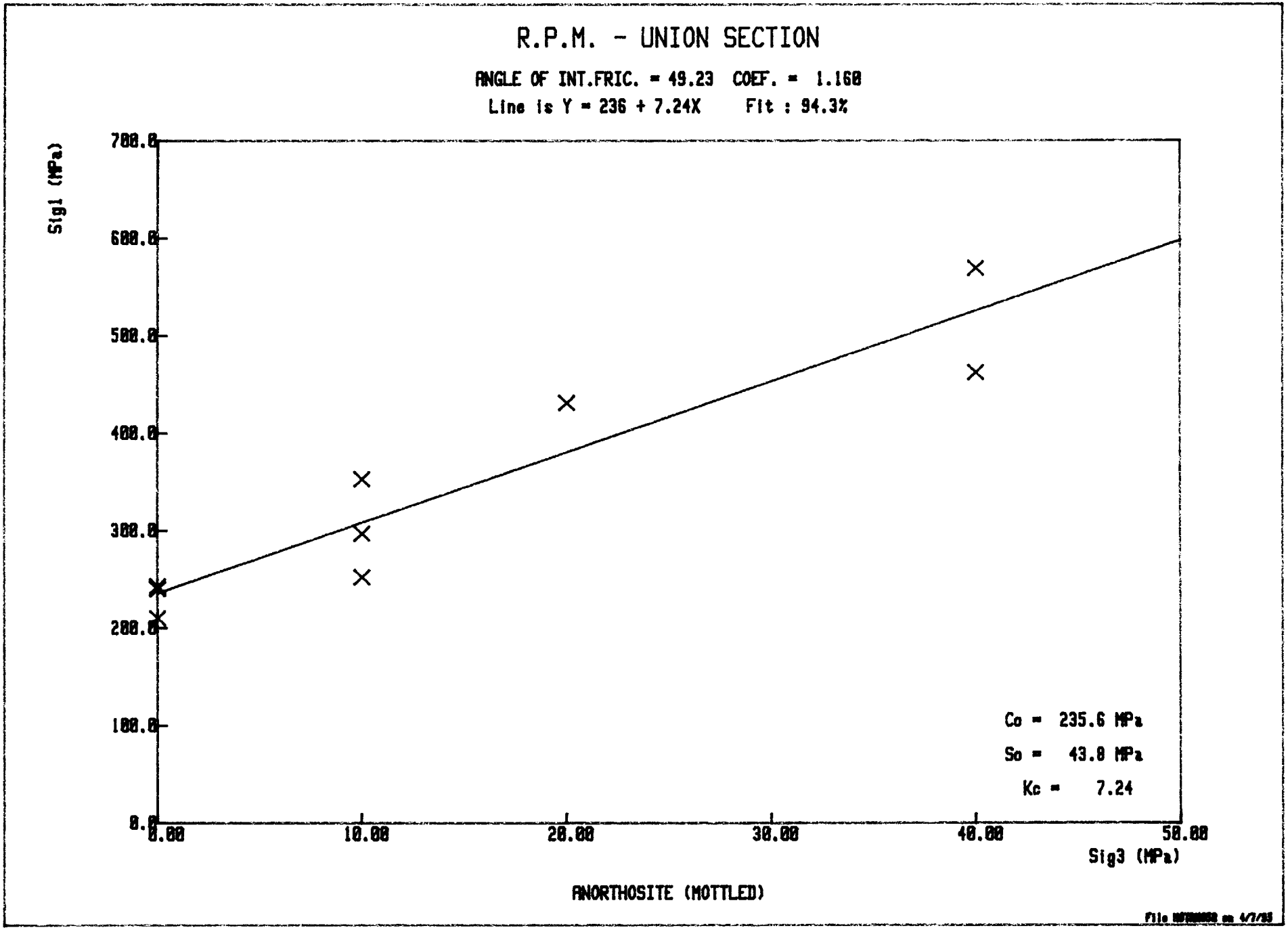
R.P.M. - UNION SECTION
ANGLE OF INT.FRIC. = 49.23 COEF. = 1.160
Line is Y = 236 + 7.24X Fit : 94.3%
Sig1 (MPa)
700.0
600.0
500.0
400.0
300.0
200.0
100.0
0.0
0.00
10.00
20.00
30.00
40.00
50.00
Sig3 (MPa)
Co = 235.6 MPa
So = 43.0 MPa
Kc = 7.24
ANORTHOSITE (MOTTLED)

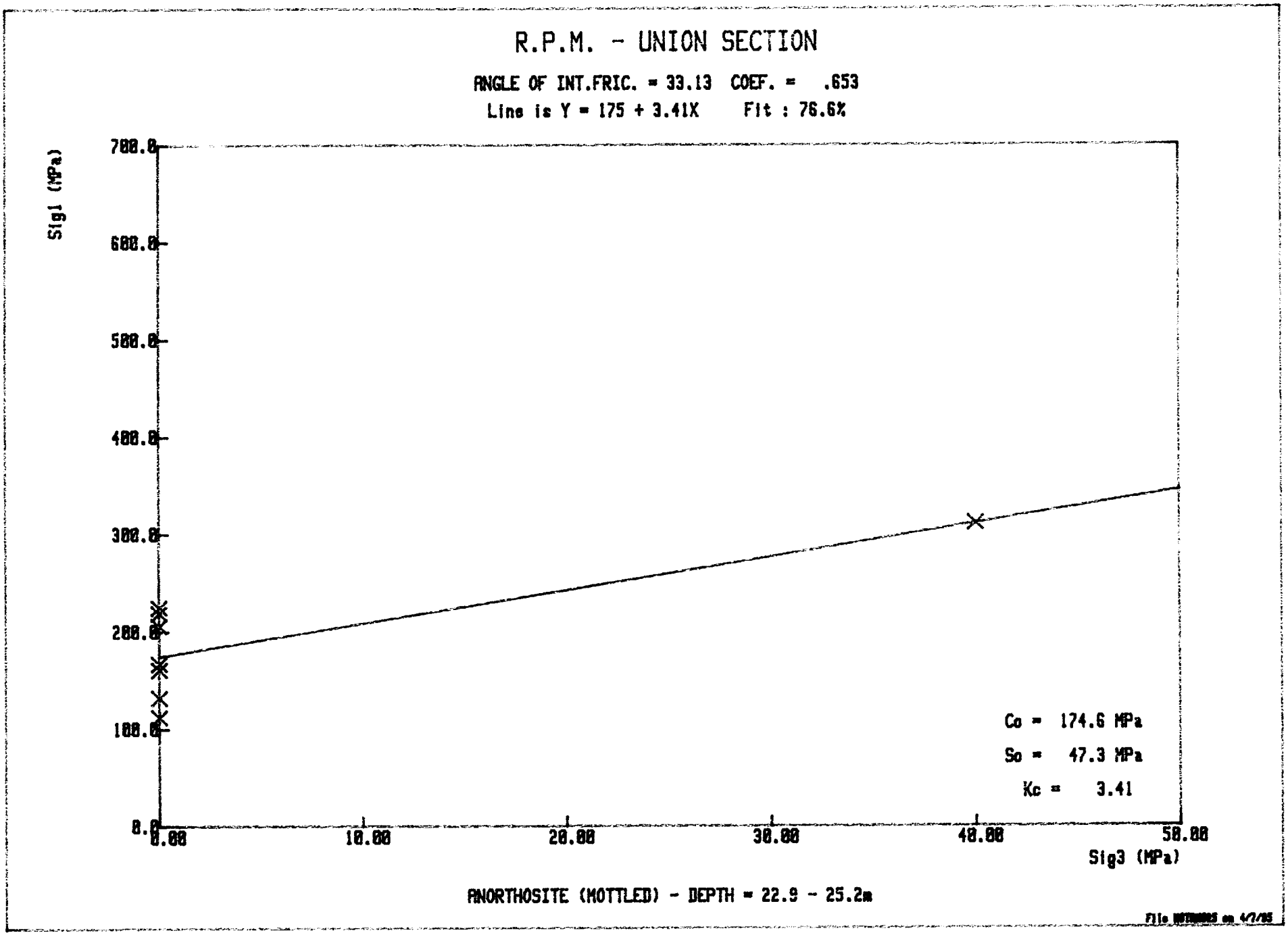
R.P.M. - UNION SECTION
ANGLE OF INT.FRIC. = 33.13 COEF. = .653
Line is Y = 175 + 3.41X Fit : 76.6%
Sig1 (MPa)
700.0
600.0
500.0
400.0
300.0
200.0
100.0
0.0
0.00
10.00
20.00
30.00
40.00
50.00
Sig3 (MPa)
Co = 174.6 MPa
So = 47.3 MPa
Kc = 3.41
ANORTHOSITE (MOTTLED) - DEPTH = 22.9 - 25.2m

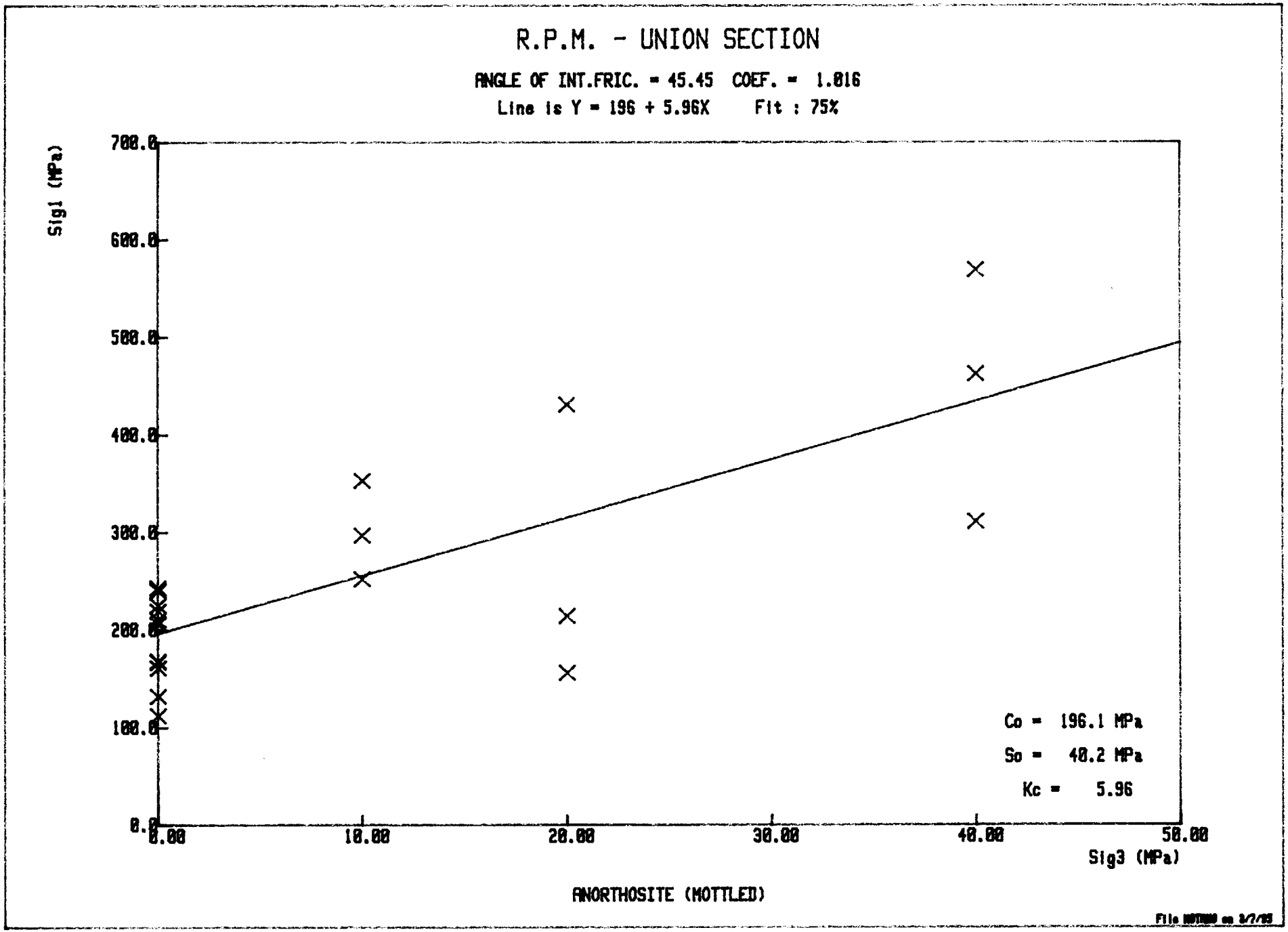
R.P.M. - UNION SECTION
ANGLE OF INT.FRIC. = 45.45 COEF. = 1.016
Line is Y = 196 + 5.96X Fit : 75%
Sig1 (MPa)
700.0
600.0
500.0
400.0
300.0
200.0
100.0
0.0
0.00
10.00
20.00
30.00
40.00
50.00
Sig3 (MPa)
Co = 196.1 MPa
So = 40.2 MPa
Kc = 5.96
ANORTHOSITE (MOTTLED)

KARREE MÉRENSKY UNIAXIAL TESTS

****

SAMPLE NO.		GEOLOGY	UCS (MPa)
KUP1	(B)	FW1b + NORITE	146
	(C)	FW1b + ANORTHOSITE	218
	(D)	FW1a + REEF	213
	(E)	Msky Reef Disc.Cr + pegmatoid	118
	(F)	Msky pyr. Partially replaced by peg.	142
	(G)	Reef Contact + Midl 1/2 H.W.(Norite)	190
KUP4	(A)	Midl 1/2 Norite	182
	(B)	Top Reef Contact	150
	(B)		129
	(C)	Msky Pyroxenite	125
	(C)		80
	(D)	Msky Pyroxenite + middle Cr stringers	75
	(D)		60
	(E)	Msky Pyr	103
	(E)		100
	(H)	1b Norite	179
	(H)		158
	(H)		191
KUP6	(A)	Top Reef + 1/2 Norite	130
	(A)		116
	(C)	Msky Pyroxenite - Anathosite	121
	(C)		86
	(E)	FW 1b. Leuco Norite	194
	(E)		184
	(F)	FW 1b. Leuco Norite	197
	(F)		202
	(H)	FW2 Anorthosite	248
	(H)		251